Understanding growth and development of lucerne crops (*Medicago sativa* L.) with contrasting levels of perennial reserves

---

A thesis
submitted for a degree
of
Doctor of Philosophy
at
Lincoln University
New Zealand

by
Edmar I. Teixeira

Lincoln University
Canterbury, New Zealand
2006

Abstract of a thesis submitted in partial fulfilment of the requirements for a degree of Doctor of philosophy

by

Edmar I. Teixeira

Understanding growth and development of lucerne crops (*Medicago sativa* L.) with contrasting levels of perennial reserves

This research examined seasonal patterns of growth and development of lucerne crops grown with different levels of crown and taproot reserves in a cool temperate environment. The approach required derivation of explanatory mathematical relationships between crop physiological processes and the main environmental variables of temperature, photoperiod and incoming radiation.

To create crops with contrasting levels of perennial reserves (*i.e.* carbon and nitrogen stored in crowns and taproots), four defoliation treatments were applied to an established 'Kaituna' lucerne crop at Lincoln University, Canterbury, New Zealand in the 2002/03 and 2003/04 growth seasons. Treatments consisted of a factorial combination of a (*i*) 28 day (short, S) or (*ii*) 42 days (long, L) regrowth cycle during (*i*) spring/mid-summer and/or (*ii*) mid-summer/autumn. The treatments had acronyms of LL, LS, SL or SS, in which each letter refers to the frequency of defoliation in the first and second period of the season, respectively.

Regardless of defoliation treatment, perennial dry matter (DM_{per}) differed seasonally. In LL crops, DM_{per} increased from <3 t/ha in mid-summer to >5 t/ha in autumn. Frequent defoliations (SS) reduced both the DM_{per} by 20-30% and the concentration and amount of soluble sugars, starch and nitrogen in taproots. As a result, the annual shoot yield ranged from 23 t/ha (LL) to 14 t/ha (SS) in 2003/04. Most of this difference was explained by changes in the weight of each individual shoot. Despite shoot yield differences, plant population declined at similar exponential rates in all crops from 140 plants/m^2 in August 2002 to 60 plants/m^2 in October 2004. Final shoot populations were conservative at ~780 shoots/m^2 in all crops.

Physiologically, yield differences were mostly explained (R^2=0.84) by the accumulated intercepted photosynthetic active radiation ($\sum PAR_i$). The $\sum PAR_i$ was limited in frequently defoliated crops because these crops had lower leaf area index (*LAI*) than LL crops but similar canopy architecture, with an extinction coefficient for diffuse light (k_d) of 0.81. Differences in *LAI* were a direct effect of harvesting before full canopy cover (*i.e.* critical *LAI* of 3.6) in short regrowth cycles. In addition, leaf area expansion rates (*LAER*) in spring were reduced from 0.016 (LL) to 0.011 $m^2/m^2/°Cd$ (SS) as taproot DM declined from 3.0 to 1.5 t/ha, respectively. The reduction in *LAER* was a result of smaller leaves after the 5th main stem-node and a reduction in the leaf area of branches. At the same time the phyllochron was conservative at 34°Cd/leaf (T_b of 5°C) when photoperiod was greater than 12.5 h but increased to 40°Cd (LL and SL) and 60°Cd (LS and SS) at lower photoperiods. All crops had a similar maximum rate of branching of 6.8 leaves/main-stem node and leaf senescence rates at 0.48 leaves/main-stem node.

Shoot radiation use efficiency (RUE_{shoot}) was 1.6 g DM/MJ PAR_i for pooled annual yield. However the seasonal RUE_{shoot} was inconsistent being 1.8 g DM/MJ PAR_i in spring/summer and only 1.0-1.2 g DM/MJ PAR_i in autumn for LL crops. Frequent defoliations decreased RUE_{shoot} by 20% during summer. The average *RUE* for total dry matter (RUE_{total}) was 2.2 g DM/MJ PAR_i but this was affected by defoliation treatments and temperature. Measurements of RUE_{total} from 23 regrowth cycles were then used to validate a previously proposed temperature framework for *RUE*. That framework was used to estimate the RUE_{total} and fractional partitioning of DM to perennial organs (p_{per}). In SS crops, RUE_{total} was 50% of the values of LL crops in four of eight analysed regrowth cycles. This was consistent with the measured reduction of 20% in the saturated photosynthetic rate (P_{max}) of SS crops in the summer/autumn of 2002/03 season. Photosynthetic rates at 1000 μmol photon/m^2/s (Pn_{1000}) were also ~20% lower during the first 150°Cd of regrowth in SS crops in comparison with LL crops. Differences in Pn_{1000} were mostly explained by the specific leaf nitrogen and chlorophyll content of these leaves. The estimated p_{per} increased from <0.05 in winter/early-spring to a maximum of 0.50 in mid-summer and declined slightly to 0.40 in late-autumn for LL crops. Photoperiod (*Pp*) and the ratio between soil and air temperature (T_{soil}/T_{air}) were tested as predictors of p_{per}. A hysterisis model based on increasing and decreasing *Pp* was necessary to relate p_{per} to *Pp* but a single relationship (R^2=0.52) was found between p_{per} and T_{soil}/T_{air}.

The relationships derived from the field experiment were then integrated in a simple computer simulation model. The model accurately predicted seasonal primary leaf appearance, *LAI* and shoot yield of LL crops. Accurate simulation of perennial DM required a seasonal root maintenance respiration (*Rm*) rate of ~0.03 DM/day in spring/summer and <0.01 DM/day in autumn/winter.

In this thesis, the response of lucerne physiological processes to environmental signals and to the level of perennial reserves was quantified and integrated into mathematical relationships. These relationships provided a sound framework to better understand and predict seasonal yield and development of lucerne crops grown in cool temperate climates.

Key words: canopy development, *Medicago sativa*, modelling, partitioning, phyllochron, radiation use efficiency, root reserves, yield components.

List of contents

Page

List of tables

List of figures

List of plates

List of appendices

List of abbreviations

Abbreviation	Description	Units
a.i.	active ingredient	
APSIM	Agricultural Production system SIMulator	
Chl_{a+b}	leaf Chlorophyll a+b	mg/m^2
CP	Crude Protein	% DM
CV	Coefficient of Variation	%
DM	Dry Matter	g/m^2, kg/ha or t/ha
DM_{leaf}	leaf Dry Matter	t/ha
DM_{per}	perennial Dry Matter	t/ha
DM_{root}	taproot Dry Matter	t/ha
DM_{shoot}	shoot Dry Matter	t/ha
DM_{stem}	stem Dry Matter	t/ha
EP	Penman Potential Evapotranspiration	mm
HI	Harvest Index	dimmentionless
IRGA	Infra Red Gas Analyser	
ISM	Individual Shoot Mass	g DM/shoot
k	extinction coefficient	dimmentionless
k_d	extinction coefficient for diffuse light	dimmentionless
LAI	Leaf Area Index	dimmentionless
LAI_{crit}	critical Leaf Area Index	dimmentionless
LGR	Linear growth rate of shoot DM	kg DM/ha/day
LSD	Least Significant Difference	
$N\%_{leaf}$	Nitrogen concentration in leaves	% of leaf DM
$N\%_{root}$	Nitrogen concentration in taptoots	% of taproot DM

P	Probability	
$PAI_{LAI\text{-}2000}$	Plant Area Index taken with canopy analyser	dimmentionless
PAR	Photosynthetically Active Radiation	MJ/m^2
PAR_i	intercepted PAR	MJ/m^2
PAR_i/PAR_o	Fractional PAR interception	dimmentionless
PAR_o	PAR above canopy	MJ/m^2
Pg	gross Photosynthesis	$\mu mol\ CO_2/m^2/s$
$Pmax$	leaf Photosynthetic rate at light saturation	$\mu mol\ CO_2/m^2/s$
Pn	net Photosynthesis	$\mu mol\ CO_2/m^2/s$
Pn'	normalized net Photosynthesis	$\mu mol\ CO_2/m^2/s$
Pn_{1000}	net Photosynthesis at 1000 μmol photon/m^2/s	$\mu mol\ CO_2/m^2/s$
Pp	Photoperiod	h/day
p_{per}	fractional partitioning of DM to perennial organs	dimmentionless
$PPFD$	Photosynthetic Photon Flux Density	$\mu mol\ photon/m^2/s$
R^2	Coeficient of determination	
R_i	total intercepted solar Radiation	MJ/m^2
R_i/R_o	fractional interception of solar Radiation	MJ/m^2
R_o	total solar Radiation above canopy	MJ/m^2
$RMSD$	Root Mean Squared Deviation	
RUE	Radiation Use Efficiency	g DM/MJ PAR_i
RUE_{opt}	RUE_{total} at Optimal temperature	g DM/MJ PAR_i
RUE_{shoot}	Radiation Use Efficiency for shoot DM	g DM/MJ PAR_i
RUE_{total}	Radiation Use efficiency for total DM	g DM/MJ PAR_i
SEM	Standard Error of Mean	
SLN	Specific Leaf Nitrogen	g N/m^2 leaf
SLW	Specific Leaf Weight	g DM/m^2 leaf
$Starch\%$	concentration of Starch in taproots	% of taproot DM
$Sugar\%$	concentration of soluble Sugars in taproots	% of taproot DM
T_{air}	daily mean air temperature (*i.e.* T_{mean})	°C
T_b	base Temperature	°C
T_{max}	daily maximum temperature	°C
T_{mean}	daily mean temperature	°C
T_{min}	daily minimum temperature	°C
T_{soil}	daily mean soil temperature at 100 mm depth	°C
Tt	Thermal-time	°Cd
$Tt_{b1/5}$	Thermal-time with a T_b of 1°C and 5°C	°Cd
Tt_{b5}	Thermal-time with a T_b of 5°C	°Cd
X_0	node position of the largest leaf on main-stem	mm^2

Y_0	area of the largest leaf	mm^2
α	photosynthetic efficiency of light response curve	μmol CO_2/μmol photon
θ	convexity of the light response curve	dimmentionless

1 General introduction

1.1 Overview

Lucerne (*Medicago sativa* L.) is the oldest known cultivated forage crop and is extensively used with over 32 million hectares cultivated worldwide (Irwin *et al.*, 2001; Michaud *et al.*, 1988). In New Zealand, the use of lucerne has been promoted for grazing and conservation since the early 20th century. The area of lucerne in New Zealand peaked at 220,000 ha in the mid 1970's but declined since then, mainly due to the susceptibility of traditional cultivars to pests and diseases (Douglas, 1986). More recently, interest in lucerne has been regained in New Zealand due to the increasing demand for productive forages for dryland environments (Moot *et al.*, 2003) and also due to the introduction of new cultivars resistant to pests and diseases (Purves and Wynn-Williams, 1989). On the east coast of New Zealand, lucerne has been shown to be superior in yield and quality to other grass and legume forage species, under both dryland and irrigated conditions (Brown *et al.*, 2005a; Douglas, 1986). The comparative advantages of lucerne crops can be attributed to (*i*) the potential to produce dry matter yields in excess of 20 t/ha/year (Brown *et al.*, 2000; Douglas, 1986); (*ii*) high protein and energy concentration in the shoot dry matter (Buxton *et al.*, 1985); (*iii*) the ability to symbiotically fix N_2 (Boller and Heichel, 1983); and (*iv*) the capacity to extract water from deeper layers in the soil than other temperate species (Brown, 2004).

To optimize yield and quality of lucerne crops for any given production system it is necessary first to understand the crop responses to environmental and management factors. In lucerne crops that are fully supplied with water, minerals and free from pests and diseases, the rates of plant growth and development are mainly driven by temperature and radiation receipts (Fick *et al.*, 1988). In this context, at non-limiting temperatures, crop yield can be derived from a single linear relationship with cumulative intercepted radiation (Monteith, 1977). This approach has been successfully used to predict yield of annual crops (Sinclair and Muchow, 1999) and can be represented by Equation 1.1.

Equation 1.1

$$Yield = PAR_o \text{ x } (PAR_i / PAR_o) \text{ x } RUE \text{ x } H$$

Where PAR_o is the incident photosynthetic active radiation above canopy, PAR_i/PAR_o is the fractional PAR interception, *RUE* is the radiation use efficiency (g DM/MJ PAR_i) and *H* is the harvest index. For annual crops, where the partitioning of DM to unharvested fractions (*e.g.* roots) is relatively constant throughout each growth cycle, a stable conversion factor of radiant energy to "above ground" dry matter is commonly found (Sinclair and Muchow, 1999) and *H* is implicit in the value of *RUE* for aerial DM.

Previous attempts to develop lucerne simulation models using these principals have been relatively successful but the perennial characteristic of the crop imposes some peculiarities to the traditional approach (Confalonieri and Bechini, 2004; Robertson *et al.*, 2002). Firstly, the partitioning of dry matter to lucerne perennial organs (crown and taproot) is not constant throughout the year (Gosse *et al.*, 1984) which makes the value of shoot *RUE* vary seasonally (Khaiti and Lemaire, 1992). This is the consequence of a seasonal pattern of accumulation and depletion of C and N reserves in taproots (Cunningham and Volenec, 1998) possibly in response to environmental signals such as temperature and photoperiod (Fick *et al.*, 1988; Noquet *et al.*, 2003). Secondly, shoot growth rates are influenced by the level of perennial reserves (C and N) which may affect canopy expansion or *RUE* (Avice *et al.*, 1997a; Justes *et al.*, 2002). The physiological mechanisms involved in these processes are unknown or insufficiently quantified to be predictive.

The construction of more mechanistic and universally applicable lucerne models demands that additional information about crop responses to the seasonal environment and to contrasting levels of perennial reserves is gained.

1.2 Aims and objectives

The aim of this thesis was to quantify the responses of lucerne crops with contrasting levels of perennial reserves to environmental factors and to integrate these relationships in a simple crop model. This was done by assessing the response of crop physiological variables (Equation 1.1) to the seasonal environment during the 2002/03 and 2003/04 growth seasons in the cool temperate climate of Canterbury, New Zealand.

The thesis is structured in nine chapters (Figure 1.1). In Chapter 2 a review of the literature related to lucerne environmental physiology and simulation modelling is presented. In Chapter 3 the details about the experimental design, methods, analysis and the description of the physical environment are given.

The specific objectives of this thesis were related to each one of the five chapters of results:

Objective 1. To describe the effects of the four defoliation treatments on the perennial dry matter (crown and taproot biomass) and the concentrations of carbohydrates and nitrogen of this perennial dry matter (Chapter 4).

Objective 2. To quantify seasonal differences in shoot yield and yield components in response to environmental factors and the levels of perennial reserves (Chapter 5).

Objective 3. To explain differences in shoot yield through the analysis of PAR interception (Chapter 6) and *RUE*, dry matter partitioning and the dynamics of N in leaves and shoots (Chapter 7).

Objective 4. To integrate the relationships derived in Chapters 4 to 7 into a simple lucerne simulation model and test the predictive ability of the model (Chapter 8).

Finally, in Chapter 9 the findings of the experiments and the potential applications for the knowledge gained are discussed.

1.3 Thesis structure

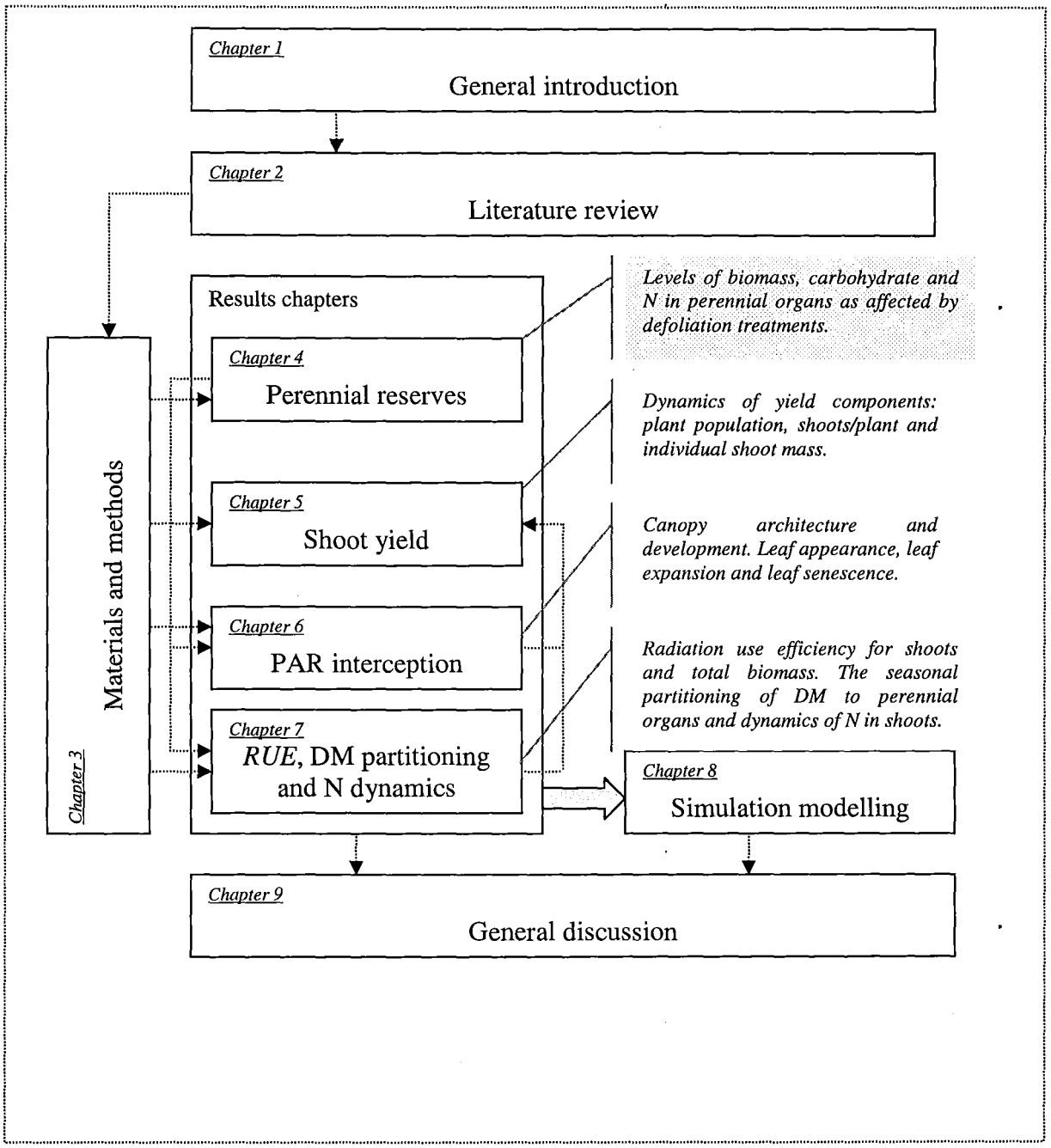

Figure 1.1 Outline of thesis structure and main topics dealt within each results chapter.

2 Review of literature

This chapter reviews current literature on the processes related to biomass production in lucerne. It quantifies the impact of environmental factors and the level of perennial reserves on these processes. Finally it discusses the possibility of integrating functional explanatory relationships to lucerne simulation models.

2.1 A model to study lucerne yield

Lucerne yield forming processes are mainly driven by environmental signals, notably temperature and solar radiation (Fick *et al.*, 1988). These factors modulate the acquisition of carbon dioxide, light, water and mineral nutrients which are the major resources required for plant growth (Monteith, 1994). Understanding the physiological mechanisms by which plants respond to environmental signals permits the integration of those relationships into mathematical functions. These can then be used to examine yield and development of crops in relation to the environment and management practices.

In this thesis the yield model proposed by Monteith (1977) (Equation 1.1) was adapted to explicitly account for the partitioning of DM to perennial organs (*i.e.* crown and taproot). In this adapted model (Equation 2.1) the component yield is termed as the shoot dry matter (DM_{shoot}); the harvest index is assumed as the fractional difference of the partitioning to perennial organs ($1\text{-}p_{per}$) and radiation use efficiency is the conversion factor of PAR_i to "total dry matter" (RUE_{total}).

Equation 2.1

$$DM_{shoot} = PAR_o \times (PAR_i / PAR_o) \times RUE_{total} \times (1 - p_{per})$$

The model in Equation 2.1 was then used as the basic framework to analyse differences in lucerne yield among defoliation treatments and seasons. The following sections will discuss each variable in Equation 2.1 in relation to lucerne yield processes.

2.2 Incident photosynthetic active radiation (PAR_o)

The total amount of incident solar radiation at crop level determines the potential biomass production in a given environment (Monteith, 1981). The intensity ($MJ/m^2/s$) and duration (h/day) of solar radiation varies with latitude and seasons of the year due to the differences in solar angle. These differences define a geographical and seasonal potential of production for crops because photosynthesis is activated by the energy provided by solar radiation, specifically from the spectrum close to the visible wavelengths (Hay and Walker, 1989b). This part of the spectrum (wavelengths from 400-700 nm) is denominated photosynthetic active radiation (PAR) and represents approximately half of the total solar radiation (Szeicz, 1974), although this varies with the proportion of direct to diffuse light and solar angle elevation. At Lincoln, Canterbury, New Zealand (latitude 43.4°S) the solar elevation changes from a maximum of 69° at the summer solstice to a minimum of 23° at the winter solstice. As a consequence, mean total solar radiation ranges from ~4.3 to 23 $MJ/m^2/day$, respectively (Broadfields Meteorological Station, Lincoln, Canterbury).

2.3 Fractional radiation interception by the canopy (PAR_i/PAR_o)

The fraction of incident PAR that is intercepted by a crop (PAR_i/PAR_o) is a function of the crop leaf area index (*LAI*, m^2 leaf/m^2 ground) and canopy architecture. The canopy architecture is characterized by the leaf angles and by the leaf optical properties (reflection and transmission) (Stoskopf, 1981). The relation between *LAI* and PAR_i/PAR_o can be described by an exponential relation of light attenuation through the canopy according to Beer's law (Campbell and van Evert, 1994):

Equation 2.2

$$PAR_i / PAR_o = 1 - \exp(-k \times LAI)$$

Where k is the extinction coefficient (m^2 land/m^2 leaf) that modulates the fraction of PAR intercepted by each unit of *LAI*. The following sections discuss the relevance of each component of Equation 2.2 for a lucerne crop.

2.4 Leaf area index in lucerne

The concept of leaf area index (*LAI*) was first suggested by Watson (1947) and represents the area of leaves per unit of soil area (m^2/m^2). Consequently the processes that regulates the expansion of *LAI* are of major importance in understanding crop responses to the environment because they influence radiation interception (Equation 2.2) and canopy photosynthesis rates (Monteith, 1994).

The *LAI* of a lucerne crop can be conceptually divided into growth components (shoot population and individual leaf area) and development components (number of primary and axillary leaves per shoot) (Brown *et al.*, 2005b) as summarized in Equation 2.3.

Equation 2.3

$$LAI = Shoots/area \times Leaf/shoot \times Area/leaf$$

Where the units are m^2/m^2 (*LAI*), n/m^2 (shoots/area), n/shoot (leaves/shoot) and m^2/leaf (area/leaf).

Dynamically, changes in lucerne *LAI* are also dependent on senescence rates of leaves in the base of the canopy, which together with leaf appearance and leaf expansion rates, will define the daily net expansion of green *LAI* (Brown *et al.*, 2005b).

2.4.1 Development components of *LAI*

Development can be defined as the differentiation of meristematic cells to form vegetative (leaves, stems, branches) or reproductive (flowers) organs (Sharratt *et al.*, 1989). It can be quantified in physical terms by evaluating changes in plant morphology or chronologically by plant phenology (Hodges, 1991). Development affects *LAI* expansion through the rate at which new leaves and branches are produced (Equation 2.3). In crop modelling, development is usually related to environmental variables (*e.g.* temperature and photoperiod) in an empirical form (Charles-Edwards *et al.*, 1986) due to the complex mechanisms involved in cell differentiation at meristematic level (Hay and Walker, 1989b).

2.4.1.1 *Factors that drive crop development*

Temperature is the main factor that drives crop development (Hay and Walker, 1989b). However, for some plants, the effect is modulated by other environmental factors such as photoperiod, vernalisation, and water stress (Hodges, 1991).

Thermal-time sum ($\sum Tt$) has been used widely to quantify the rate of organ initiation (*e.g.* leaf appearance) or differentiation (*e.g.* time to flowering) in lucerne (Fick and Onstad, 1988; Moot *et al.*, 2001; Sanderson *et al.*, 1994) and many other agricultural crops (Hodges, 1991). Simple thermal-time equations assume a linear accumulation of heat-units above a constant crop-specific base temperature (T_b) or temperature threshold (Equation 2.4).

Equation 2.4

$$\sum Tt = \sum (T_{mean} - T_b)$$

The most common models used to calculate thermal-time for lucerne assume a null accumulation of Tt until the T_b of 5°C, a linear increase of Tt from >5°C to an optimum temperature (T_{opt}) of 30°C and a linear decrease to a maximum temperature (T_{max}) of 40°C (Fick *et al.*, 1988). This approach, using three cardinal temperatures has been used to predict leaf development in several crops (Hodges, 1991). Nevertheless, the use of a constant T_b has been found to cause systematic errors in development predictions in lucerne (Sharratt *et al.*, 1989). These authors showed that a variable T_b should be used to minimize the variability in predictions of flowering time, T_b being 3.5°C during spring, 7.5°C in early-summer and 10°C in late-summer. Similarly, leaf appearance rate and time to early-bud in lucerne were more accurately predicted when a T_b =1°C (faster Tt accumulation) was used below 15°C, and a T_b =5°C above 15°C for 'Kaituna' lucerne (Brown *et al.*, 2005b; Moot *et al.*, 2001).

This need to adjust T_b according to the temperature could be justified by the fact that the thermal-time concept is more a functional approach than a mechanistic or explanatory one (Bonhomme, 2000). The approach that relates development rates to $\sum Tt$ considers the response to temperature being always linear (Muchow and Bellamy, 1991). However, this assumption is an over simplification of the parabolic response of enzyme activity to

temperature (Bonhomme, 2000; Taiz and Zeiger, 2002). Additionally, simple thermal-time models ignore other factors like thermo-periodicity and day length effects on development (Hodges, 1991).

In this thesis, the rate of leaf appearance (phyllochron; Section 2.4.1.2) will be used to test the need for a variable T_b to optimize development predictions.

2.4.1.2 Primary leaf appearance rate and phyllochron

Leaf appearance rate is dependant on the rate of differentiation of meristems into leaf primordia and the rate of expansion of these leaves (Hay and Walker, 1989b). In lucerne, leaf appearance rates are considered a central component of *LAI* expansion (Robertson *et al.*, 2002) being controlled mainly by temperature (Moot *et al.*, 2001; Pearson and Hunt, 1972) and modulated by photoperiod (Brown *et al.*, 2005b). The interval between the appearance of successive leaves is denominated the phyllochron and is usually quantified on a $\sum Tt$ basis (Hay and Walker, 1989b). For lucerne, phyllochron (T_b=5°C) has been assumed constant at 34°Cd/leaf in simulation models like APSIM-lucerne (Robertson *et al.*, 2002). In contrast, Brown *et al.*(2005b) showed that although phyllochron (T_b=1/5°C, Section 2.4.1.1) of 'Kaituna' lucerne was 37°Cd during periods of increasing photoperiod (*Pp*), it increased to 60°Cd at decreasing *Pp*>15.7 h. Lucerne phyllochron and its apparent change with *Pp* will be examined in this thesis.

2.4.1.3 Branching and LAI

Branching is the expansion of leaves from axillary buds and the rate of branching is an important component of *LAI* (Stoskopf, 1981). The extent of branching is largely dependant on plant population, cultivar and nitrogen nutrition, factors that can be manipulated by crop management (Hay and Walker, 1989b). Branching capacity is genetically determined and controlled by hormonal signals in the plant. Environmental factors like temperature, light quality and light intensity modulate assimilate supply and hormonal signals that will define the level of branching at vegetative growing points (Charles-Edwards *et al.*, 1986; Stoskopf, 1981). Brown *et al.* (2005b) have shown that branching of 'Kaituna' lucerne started at the appearance of the fifth primary leaf. Branching rates differed seasonally from 2.5 axillary leaves per main-stem node in spring

and autumn to 1.7 axillary leaves per main-stem node in summer. The authors speculated that the sensitivity of branch development to environment signals could be different from the one of phyllochron.

2.4.2 Growth component of *LAI*

2.4.2.1 Shoot population

The shoot population is an important lucerne yield component derived from the product of the number of plants per unit area and the number of shoots per plant (Volenec *et al.*, 1987). The number of lucerne plants in the first year of establishment is a function of the seeding rate, but the population declines in successive years at diminishing rates (Fick *et al.*, 1988). The reasons for a decay in plant population are related to the occurrence of diseases (*e.g.* root rot), pests (*e.g.* aphids); and the susceptibility to those factors can be enhanced by the environment (*e.g.* water logging) and management practices like severe or frequent defoliation (Lodge, 1991). For example, Belesky and Fedders (1997) observed an average decline in lucerne plant population from 400 to 80 plants/m^2 in a 3 year experiment with faster decline in plants grazed intensively.

The decline in plant population is often compensated for by an increase in the number of shoots/plant, a second yield component (Belesky and Fedders, 1997; Gosse *et al.*, 1988). This plasticity of response means that a similar shoot population can be achieved by the product of different combinations of plant populations and shoots/plant in the crop. Interplant competition for light among shoots has been suggested as a major driver of such dynamics (Gosse *et al.*, 1988).

In this thesis, seasonal changes in yield and the effects of perennial reserves on the dynamics of yield components will be evaluated.

2.4.2.2 Leaf area expansion and leaf growth

Leaf growth embraces an initial phase of cell division, when the production of new cell material takes place; and a second phase of cell expansion, when the influx of water into

the cell provides the necessary pressure to expand it (Charles-Edwards *et al.*, 1986). The maximum size that a leaf can attain at each specific node position is genetically determined; however the expression of this genetic potential depends on how environmental factors (*e.g.* temperature, radiation, water and nitrogen) moderate this genetic program during leaf ontogeny (Hay and Walker, 1989b).

Environmental factors affect the final leaf area mainly through changes in daily leaf expansion rate (m^2 leaf/day) rather than the duration of expansion (days/leaf) (Tardieu *et al.*, 1999). Rates of leaf expansion are linearly related to temperature (Hay and Walker, 1989b) as shown by the conservativeness of the time course of leaf expansion and cell division when expressed in thermal-time in non-limiting water and nutrient conditions (Tardieu *et al.*, 1999) (Equation 2.5).

Equation 2.5

$$\frac{1}{d} = b \times (T - T_o)$$

Where $1/d$ is the rate of expansion; d is the period of expansion, T is current temperature, b is the slope and T_o is the intercept of the linear relationship between $1/d$ and T.

When based on Tt accumulation, the leaf area expansion rate (*LAER*, $m^2/m^2/°Cd$) can be used to quantify the effect of other factors on canopy development. In France, Gosse *et al.* (1984) found that lucerne *LAER* was conservative during spring-summer at 0.0092 $m^2/m^2/°Cd$ (T_b=0°C). However *LAER* declined in autumn and these authors suggested that environmental factors other than T_{mean} were involved in regulating *LAER*. Nitrogen availability to shoots also seems to affect *LAER*. Using a T_b of 5°C, lucerne *LAER* was reported to increase from 0.015 to 0.025 $m^2/m^2/°Cd$ as the availability of N reserves increased in the perennial organs (Justes *et al.*, 2002). Nitrogen supply has been shown to have a marked effect on leaf expansion affecting both cell division and cell expansion (Gastal and Lemaire, 2002). Justes *et al.* (2002) found a high correlation between the amount of taproot biomass, the level of soluble proteins and the number of vegetative buds during winter with *LAER* in the subsequent spring regrowth. Therefore, other nutritional and morphological factors seem to influence *LAER* in lucerne.

The effect of contrasting levels of perennial reserves on seasonal differences of *LAER* will be investigated in this thesis.

2.4.2.3 Leaf senescence

Senescence refers to the deteriorative changes that occur in plant tissue before the death of a plant or one of its organs (Charles-Edwards *et al.*, 1986). Lucerne shows a pattern of sequential senescence, leaves senesce progressively from the bottom to the top of the canopy regardless of the ontogenetic state of the leaf. This can be attributed to the increasing shading in leaves at the bottom as the canopy expands. As a consequence there is a decrease in the rate of photosynthesis and exhaustion of the labile materials (mainly C and N) metabolized within these leaves. Brown *et al.* (2005b) have shown senescence in 'Kaituna' lucerne occurred at a rate of 0.3 leaves for each main-stem node. This rate was maintained until the appearance of the ninth main-stem node when senescence increased to 1.08 leaves/main-stem node. The effect of different levels of perennial reserves on the rate of senescence will be evaluated in this thesis.

2.4.3 Canopy architecture and the extinction coefficient (*k*)

The amount of light that is intercepted through the profile of a canopy depends on the leaf area (*i.e. LAI*) and the angular arrangement and optical properties of these leaves (Azam Ali *et al.*, 1994; Monteith, 1994). The value of the extinction coefficient (*k*, Equation 2.2) quantifies the exponential rate of decline by which light is extinguished per *LAI* unit. This approach assumes that light transmission within a canopy follows Beer's law (Monsi and Saeki, 2005) which implies a simplification of the canopy structure: (*i*) leaves are randomly distributed and (*ii*) leaves are opaque (*i.e.* black leaves) (Monteith and Unsworth, 1990).

During the course of each day or a growth season the value of *k* changes according to the canopy architecture (*e.g.* leaf angles) and the zenith angle of incidence of light (Monteith *et al.*, 1994). The zenith angle of incidence of light that reaches a leaf varies within a day and among the seasons of the year while sun inclination changes through time; and this varies with latitude. For crop modelling purposes, it is common to assume a single value of *k* for

a specific cultivar when estimating light interception as this reasonably reflects the integration of the daily changes in k (Christian, 1987).

The physiological importance of k resides mainly on the estimations of light interception of open canopies (incomplete light interception). As a consequence, the value of k defines the critical *LAI* (LAI_{crit}) that is the *LAI* when 95% of the incident light is intercepted (Watson, 1947).

The value of k has been shown to be conservative within a lucerne cultivar throughout different seasons of the year (Gosse *et al.*, 1982b). Values of k for lucerne cultivars have been reported as 0.88 in 'du Puits' (Gosse *et al.*, 1988), 0.86 in 'Dekalb 167' (Whitfield *et al.*, 1986) and 0.91 in 'Aurora' (Evans, 1993). The crop simulation model APSIM-lucerne assumes lucerne k to vary between seedling (k=0.57) and regrowth (k=0.80) stages (Robertson *et al.*, 2002). For 'Kaituna' lucerne, k was shown to be conservative at 0.82 for contrasting water and light environments (Varella, 2002).

There are no reports of the effect of perennial reserves on k of lucerne crops, so this will be investigated in this research.

2.5 Radiation use efficiency (*RUE*)

There is a strong linear relationship between accumulated crop dry matter and intercepted (or absorbed) solar radiation for a variety of plant species grown in non-limiting conditions (Monteith, 1977). The slope of this relationship represents the radiation use efficiency (*RUE*) that quantifies the net efficiency of conversion of radiant energy into crop dry matter (Sinclair and Muchow, 1999).

RUE can be expressed in different forms in regard to (*i*) the band of radiation wavelengths considered (*i.e.* total solar radiation or PAR); (*ii*) absorbed or intercepted radiation; (*iii*) the fraction of plant biomass considered (*i.e.* aerial biomass or total biomass) depending on the purposes of the study (Sinclair and Muchow, 1999). Throughout this thesis, *RUE* will be always referred in an "intercepted" PAR basis (PAR_i, 400-700 nm) and reported as shoot *RUE* (RUE_{shoot}) or total *RUE* (RUE_{total}).

Monteith (1977) brought attention to the stability of *RUE* among different crops and demonstrated that it was relatively constant at ~2.8 g DM/MJ PAR_i for C_3 species. This classical analysis was performed with arable crops and refers to the dry matter accumulation of the aerial part of the plant. When the *RUE* concept is applied to perennial crops, like lucerne, the allocation of dry matter to perennial organs becomes quantitatively important and justifies the inclusion of the whole plant dry matter in the *RUE* calculation (Khaiti and Lemaire, 1992). In this sense, the difference between RUE_{shoot} and RUE_{total} represents the amount of DM allocated to organs other than shoots (*e.g.* crowns and taproots) per MJ of PAR_i. Consequently the fraction RUE_{shoot}/RUE_{total} quantifies the fractional retention of DM in shoots and its reciprocal $[1—(RUE_{shoot}/RUE_{total})]$ the fractional partitioning of DM to perennial organs (Durand *et al.*, 1989). These concepts will serve as the basis for the approach used to quantify *RUE* and fractional partitioning to perennial organs in this thesis.

Several authors reported values for both RUE_{shoot} and RUE_{total} in lucerne grown in temperate climates (Table 2.1). Studying 'du Pois' lucerne in France, Gosse *et al.* (1984) found a conservative RUE_{shoot} of 1.76 g DM/MJ PAR_i during spring and summer but this value was not consistent during the autumn period. These authors speculated that this could be due to a preferential partitioning of assimilates to the root system during autumn driven by environmental signals like shorter photoperiods. Similarly, autumn RUE_{shoot} in 'Kaituna' lucerne has been shown to decline to ~60% of spring values (Varella, 2002). Khaiti and Lemaire (1992) found similar variation in RUE_{shoot} that ranged from 0.79 g DM/MJ PAR for growth at the seeding stage to 1.8 g DM/MJ PAR_i for summer regrowth, with 1.13 g DM/MJ PAR_i as an intermediate value for autumn. There was a consensus among these experiments with regard to slower growth of lucerne shoots during autumn, compared with spring at the same amount of $\sum PAR_i$. However, the seasonal signals responsible for the change were not identified or quantified. For example, crop simulation models that use RUE_{shoot} as a major parameter to predict DM accumulation, like APSIM-lucerne, empirically reduce RUE_{shoot} to 75% of the spring value when accounting for slow vegetative growth in autumn (Dolling *et al.*, 2005). It is also not clear if the pattern of change in RUE_{shoot} occurs abruptly (*e.g.* APSIM-lucerne) or gradually in response to environmental signals.

Table 2.1 Examples of radiation use efficiency (*RUE*) for lucerne shoot (RUE_{shoot}) and total dry matter (RUE_{total}) production.

Reference	RUE_{shoot} g DM/MJ PAR	RUE_{total} g DM/MJ PAR	Cultivar	Location (latitude)
Gosse *et al.* (1984)	1.76	*n.a.*	'du Puis'	France (48°N)
Whitfield *et al* (1986)	1.55-2.15[3]	*n.a.*	'Dekalb-167'	Australia (36°S)
Durand *et al.*(1989)	1.72[5]	2.30[5]	'Europe'	France (46°N)
Khaiti and Lemaire (1992)	1.13-1.76[1]	2.30	'Europe' and 'Beltsvile'	France (46°N)
Duru and Langlet (1995)	~0.50-1.80[1,3]	*n.a.*	'Magali'	France (43°N)
Justes *et al.*(2002)	1.62	0.72-2.14[2]	'Alegro'	France (48°N)
Robertson *et al.*(2002)	2.0[4]	*n.a.*	'Hunter River'	Australia (27°S)
Brown (2004)	1.20-2.00[1]	3.20[2]	'Kaituna'	New Zealand (42°S)
Collino *et al.*(2005)	0.60-1.30[2]	*n.a.*	'Victoria'	Argentina (31°S)

Note: *n.a.* non-available; [1] seasonal differences on *RUE*; [2] temperature effect on *RUE*; [3] drought effect on *RUE*; [4] maximum derived value of shoot *RUE*; [5]*RUE* calculated for absorbed *PAR*.

On the other hand, lucerne total *RUE* (RUE_{total}) has been shown to be conservative during an entire growth season in non-limiting conditions (Khaiti and Lemaire, 1992). These authors demonstrated that when *RUE* was calculated considering total biomass, there was no difference between spring and autumn values and a conservative RUE_{total} of 2.3 g DM/MJ PAR_i could be assumed for lucerne. In this sense, differences in RUE_{shoot} could be mainly attributed to seasonal changes in the fractional partitioning of DM to perennial organs (p_{per}) as calculated in Equation 2.6.

Equation 2.6

$$RUE_{shoot} = RUE_{total} \times (1 - p_{per})$$

The framework of Equation 2.6 will be used as the basis for the estimation of RUE_{total} and the fractional DM partitioning to perennial organs.

Nevertheless, values of RUE_{total} in lucerne crops have been reported to range from 0.7 to 3.2 g/m^2 (Table 2.1). These differences were attributed to changes in the photosynthetic rates of these crops, which is supported by the fact that leaf photosynthesis is strongly related to *RUE* (Sinclair and Horie, 1989).

RUE shows a saturating nature of increase with leaf photosynthesis rates, being consequently sensitive to the same factors that regulate photosynthesis (Sinclair and Muchow, 1999). The main environmental factors that affect leaf photosynthesis are light, temperature, water and nitrogen supply (Moss, 1984; Sands, 1996).

2.5.1.1 Light environment effects on RUE

Differences in the radiation environment affect radiation use efficiency for aerial and total DM. In particular, high values of *RUE* are measured under diffuse radiation (Hammer and Wright, 1994; Sinclair and Muchow, 1999). The responses of *RUE* to irradiance are also dependent on the changes in leaf photosynthetic rates. Lucerne has a C_3 photosynthetic pathway, where ribulose 1,5 biphosphate is carboxylated by the enzyme ribulose 1,5 biphosphate carboxylase/oxigenase (Rubisco) into the chloroplasts of mesophyll cells (Heichel *et al.*, 1988). Photosynthetic rates increase hyperbolically with irradiance, which is mathematically described by a non-rectangular hyperbola (Cannell and Thornley, 1998) whose coefficients P_{max} (μmol CO_2/m^2 leaf/s), α (μmol CO_2/μmol photon), θ (dimensionless) represent the "saturation point", the "light efficiency" and the "curvature" of leaf *Pn* to incident photosynthetic photon flux density (PPFD, μmol photons/m^2/s); and the parameter R_d represents the rate of respiration in the dark.

Average values of P_{max} for non-stressed lucerne leaves range from 32 to 39 μmol CO_2/m^2 leaf/s (Heichel *et al.*, 1988; Varella, 2002). Lucerne leaf photosynthesis increases almost linearly with photosynthetic photon flux densities (PPFD) up ~1000 μmol photon/m^2/s (~half of full sunlight) when it approaches saturation (Gosse *et al.*, 1982a). Any environmental factor that affects P_{max}, α and θ also has an effect on *RUE*. However the responses are not linear because the relationship between *RUE* and photosynthesis is also curvilinear (Sands, 1996).

2.5.1.2 Effects of water availability on RUE

Water stress has been shown to reduce *RUE* for aerial DM in both C_3 and C_4 species (Jamieson *et al.*, 1995). This is attributed to the major influence of water deficits on leaf photosynthesis rates (Sinclair and Muchow, 1999) primarily by inducing stomatal closure

and, under severe deficits, by increasing mesophyll resistance to CO_2 diffusion (Flexas and Medrano, 2002; Gastal and Durand, 2000). Jamieson *et al.* (1995) have shown that *RUE* declined linearly with water deficit (calculated from potential evapotranspiration) but this response varied depending on the timing and duration of drought. In lucerne, drought stress has been shown to primarily affect shoot yield which leads to lower shoot/root ratios (Abdul Jabbar *et al.*, 1982; Durand *et al.*, 1989). In this sense, leaf expansion and the retention of DM in shoots are more sensitive to drought than photosynthesis and RUE_{total} (Durand *et al.*, 1989). A reduction in irrigation frequency has been shown to decrease RUE_{shoot} from 2.15 to 1.56 g DM/MJ PAR_i but shoot/root ratio was not reported, impeding the isolation of water stress effects on photosynthetic capacity and DM partitioning (Whitfield *et al.*, 1986). Similarly, soil moisture deficits >120 mm caused a decline in the RUE_{shoot} of lucerne crops from 1.6 to 1.2 g DM/MJ PAR_i but the authors also could not isolate the effects on photosynthesis or DM partitioning to roots (Duru and Langlet, 1995). Nevertheless, if water potentials decrease enough to affect photosynthesis, RUE_{total} is also expected to decline. Inch (1998), working with lucerne at the same location as the present experiment, observed that shoot production declined when soil moisture deficit at a depth of 2.3 m reached values >200 mm. This threshold will be used in the experiment reported in this thesis as the reference to irrigate and avoid water stress in the lucerne crops.

2.5.1.3 Nitrogen effects on RUE

On average 55% of the nitrogen found in a leaf of a C_3 plant is related to the photosynthetic system, being part of the Calvin-cycle, Rubisco, or the light harvest compounds (Lawlor *et al.*, 2001). In lucerne, Rubisco makes up more than 35% of the leaf total protein pool (Brown *et al.*, 1972). This justifies the high correlation found between leaf photosynthetic capacity and nitrogen concentration per unit area of leaf (*SLN*, specific leaf nitrogen) in C_3 and C_4 species (Sinclair and Horie, 1989) including lucerne (Heichel *et al.*, 1988).

The sensitivity of *RUE* (and leaf photosynthesis) to *SLN* follows a hyperbolic relationship (Muchow and Sinclair, 1994) with greater responses at low levels of *SLN* until an asymptote is reached (Sinclair and Horie, 1989). The time and extent of decline of *RUE* with nitrogen scarcity depends on the trade-off between changes in *LAI* expansion or *SLN* in response to N supply (Bange *et al.*, 1997). This occurs because morphological traits (*e.g.*

leaf area and stem expansion) are more sensitive to the supply of nitrogen than photosynthesis and *RUE* (Justes *et al.*, 2000; Sinclair and Horie, 1989). Nevertheless, Avice *et al.* (1997a) observed a decline in RUE_{shoot} of 'Europe' lucerne from 1.87 to 1.45 g DM/MJ PAR_i in crops with reduced nitrogen reserves in roots, which possibly limited the supply of N to shoots in the early stages of regrowth. The response of leaf photosynthesis and *RUE* will be analysed in relation to the nitrogen status of lucerne crops in this thesis.

2.5.1.4 Temperature effects on RUE

Evidence for an effect of temperature on *RUE* was first suggested for maize (*Zea mays*) grown in temperate climates (Andrade *et al.*, 1993). These authors observed a linear increase in *RUE* at a rate of 0.27 g/MJ/°C from 16 to 20°C. Similarly, Wilson *et al.* (1995) improved predictions of maize yield in Canterbury by assuming a null *RUE* at 8°C and a linear incease until 16°C when maximum *RUE* was achieved. For lucerne grown in the Argentinean pampas (31°S), Collino *et al.* (2005) observed a bilinear response of RUE_{shoot} to temperature from ~0.6 g DM/MJ PAR_i at 13°C to a maximum of ~1.3 g DM/MJ PAR_i when T_{mean} was greater than 21.3°C. However these authors did not quantify RUE_{total} and therefore part of the decline in RUE_{shoot} could be due to differential partitioning of DM to perennial organs in autumn (Section 2.6). In France (48°N), RUE_{total} of 'Alegro' lucerne was 0.72 g DM/MJ PAR_i in the first spring regrowth (T_{mean}=6.4°C) but increased to a maximum of 2.14 g DM/MJ PAR_i in the following two cycles (T_{mean}>11.4°C) suggesting a T_{mean} effect on RUE_{total} (Justes *et al.*, 2002). In Canterbury (42°S), RUE_{total} of 'Kaituna' lucerne increased linearly with T_{mean} at a rate of 0.18 g/MJ/°C from 0 to 18°C, until an optimum RUE_{total} of 3.2 g DM/MJ PAR_i was achieved (Brown, 2004). This framework will be tested in the research reported in this thesis (Figure 2.1).

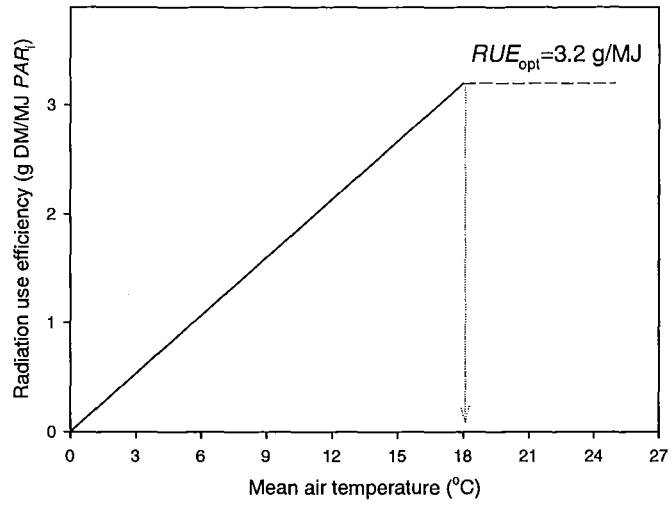

Figure 2.1 Framework of the effect of air temperature on lucerne RUE_{total} as proposed by Brown (2004).

The rationale behind the assumed increase in *RUE* with air temperature relies on the bell shaped response of net photosynthesis to temperature (McAdam and Nelson, 2003). Lucerne photosynthesis rates were maximized at T_{mean} between 20 to 30°C and declined to ~60% at a T_{mean} of ~13°C (Gosse *et al.*, 1982a). Similarly, in controlled conditions, maximum net canopy photosynthesis was 19 μmol $CO_2/m^2/s$ at T_{mean} between 21-34°C but declined to 65% of the maximum at 12°C (Al Hamdani and Todd, 1990). Brown and Radcliffe (1986) showed that lucerne leaf net photosynthesis increased at a rate of ~0.75 μmol $CO_2/m^2/s/°C$ from 10°C to 25°C, maintained a plateau of 22 μmol $CO_2/m^2/s$ until 30°C and declined at rates of ~0.75-1.3 μmol $CO_2/m^2/s/°C$ at T_{mean}>30°C. In C_3 crops as temperature increases there is a reduction in the solubility of CO_2 in relation to O_2 which increases photorespiration (Hay and Walker, 1989b). The Q_{10} value for respiration is higher than for photosynthesis and consequently respiration rates increase relatively faster than photosynthesis rates as temperature rises (Lawlor, 2001).

2.5.2 The measurement of lucerne RUE_{total} in field experiments

The measurement of RUE_{total} depends on accurate quantification of new synthetized DM in shoots and perennial organs (crown and taproots) within each regrowth cycle. The integral assessment of lucerne root system in field conditions is impractical due to the presence of roots at depth greater than 2 m (Abdul Jabbar *et al.*, 1982). Thus taproots are often sampled from a depth of 200-300 mm soil and their weight assumed to represent 80-90% of total

root dry matter (Fornasier *et al.*, 2003; Khaiti and Lemaire, 1992; Lemaire *et al.*, 1992). This procedure is justified by the fact that most of the variation in lucerne root biomass occurs in the top layers of soil (Durand *et al.*, 1989).

Another problem in quantifying the net allocation of newly assimilated DM to crowns and taproots is caused by the fact that these organs are subjected to cycles of depletion and accumulation of DM after each harvest (Luo *et al.*, 1995). In Figure 2.2, a theoretical framework adapted from Durand *et al.* (1989), is used to represent simplified dynamics of lucerne total dry matter accumulation in relation to $\sum PAR_i$ within a regrowth cycle. This framework assumes three phases of crop growth, and was used as a basis for justifying the methodology for RUE_{total} calculations used in this thesis. In phase I, immediately after defoliation, lucerne is mainly composed of non-photosynthesizing tissues (stubble, crown and taproots) remaining from the previous regrowth cycle (Figure 2.2, point A). There is minimal carbon input, as gross photosynthesis (Pg) was impaired or reduced due to defoliation; therefore "perennial DM" (*i.e.* crowns and taproots) decays due to maintenance respiration (R_m). Afterwards, still in "phase I", canopy expansion resumes and new DM is assimilated by recently expanded leaves with a fraction of it partitioned to perennial organs (p_{per}), which minimizes the slope of decline of total biomass. However the crop carbon balance is still negative because $R_m > Pg$. During this phase, RUE_{total} can not be estimated through gravimetric methods in the field because R_m is the major component of the crop carbon balance. However, when photosynthesis is sufficient to offset R_m losses, the crop enters "phase II" that is characterized by a null or positive carbon balance (*i.e.* resume of net dry matter accumulation). In this phase, perennial DM may still decline until $R_m < (Pg \times p_{per})$. In "phase III", the net input of carbon assimilated through photosynthesis is sufficient to offset R_m of perennial DM.

Conceptually only in later stages of phase II and mainly in phase III is it possible to estimate RUE_{total} by gravimetric measurements of shoot and perennial DM. This is because the concept of *RUE* was developed for annual crops and implies that (*i*) respiration rates are proportional to gross photosynthesis and (*ii*) partitioning to roots is constant within the crop cycle (Ritchie *et al.*, 1991). These assumptions are severely invalid in early stages of each lucerne regrowth cycle when remaining non-photosynthesizing tissues make up most of crop DM. However, during later stages of regrowth, particularly when perennial organs show a net accumulation of DM, RUE_{total} can be estimated by sequential measurements of

total dry matter and $\sum PAR_i$. These concepts will be used to define the methodology to calculate RUE_{total} in the experiments reported in this thesis.

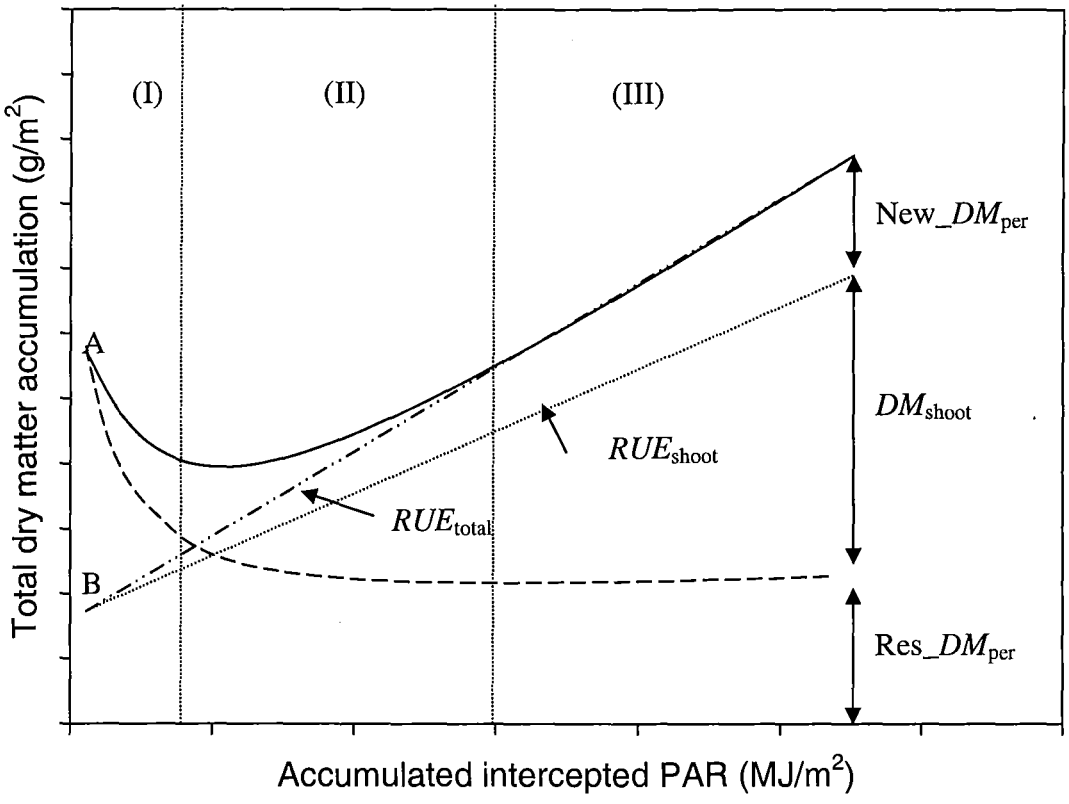

Figure 2.2 Theoretical representation of the relationship between the accumulation of total dry matter (——) and residual dry matter (– – –) as a function of accumulated intercepted *PAR* ($\sum PAR_i$). Adapted from the framework proposed by Durand *et al.* (1989).

Note: Residual perennial DM (Res_DM_{per}) represents the non-harvested material from a previous regrowth cycle. New perennial DM (New_DM_{per}) is the dry matter produced in the actual regrowth cycle. The regressions RUE_{total} (–••–••–) and RUE_{shoot} (·····) indicate the theoretical slope of accumulation of total or shoot dry matter in relation to $\sum PAR_i$. Point A represents initial level of the Res_DM_{per} (non-harvested DM from previous cycle) and point B represents final Res_DM_{per} at the end of the cycle. The difference A-B represents the residual dry matter that was lost (*i.e.* respiration or translocation to shoots) within a regrowth cycle.

2.6 Dry matter partitioning between shoots and perennial organs

Dry matter partitioning encompasses the allocation, distribution, and transport of assimilates (molecules and ions) from their sites of synthesis or storage (sources) to their sites of utilization (sinks) (Heichel *et al.*, 1988). When photosynthesis exceeds the requirements for carbon, imposed by growth respiration, excess carbohydrates are stored in lucerne perennial organs (taproots and crowns) mainly in the form of starch (McAdam and Nelson, 2003). Similarly, excess nitrogen, assimilated through mineral uptake or N_2 atmospheric fixation, is stored in perennial organs mainly in the form of soluble proteins and amino acids (Volenec *et al.*, 1996). These reserves are remobilized from the perennial organs (sources) to growing shoots (sinks) when shoot meristematic activity resumes, mainly following defoliation and at the onset of spring regrowth (Louahlia *et al.*, 1998).

The allocation of carbon and nitrogen to storage organs responds to seasonal environmental conditions (Bouchart *et al.*, 1998). In lucerne, there is a preferential storage of carbon and nitrogen in perennial organs during the autumn period (Cunningham and Volenec, 1998). In contrast, during the spring regrowth, these reserves are depleted and translocated to growing shoots or respired (Hendershot and Volenec, 1993). The partitioning of DM to lucerne roots in 'Kaituna' lucerne grown in Canterbury has been shown to increase from ~10% during spring to ~60% during autumn (Brown, 2004). Similarly, Khaiti and Lemaire (1992) in France, observed that 22% of assimilated DM by 'Beltsvile' and 'Europe' was partitioned to roots during summer but this increased to 65% during autumn. This preferential allocation of DM to storage organs during autumn has been attributed to plant responses to low temperatures and short photoperiod (Fick *et al.*, 1988; Gosse *et al.*, 1984; Noquet *et al.*, 2001). Nevertheless, no quantitative relationships between fractional partitioning of DM to roots and environmental factors have been developed. This thesis aims to assess these relationships by measuring perennial biomass patterns throughout an entire growth season.

The importance of perennial reserves in the regrowth of forages, particularly lucerne, has been long recognized and extensively reviewed in the literature (Avice *et al.*, 2001; Louahlia *et al.*, 1998; Volenec *et al.*, 1996). Despite the plethora of early research that focused on the importance of carbohydrate reserves for lucerne growth and survival

(Nelson and Smith, 1968; Pearse *et al.*, 1969b; Rapoport and Travis, 1984), no unifying relationship between lucerne yield and carbohydrate concentration in perennial organs was established (Louahlia *et al.*, 1998). More recent research has demonstrated that nitrogen reserves in perennial organs have a strong influence on lucerne shoot growth (Volenec *et al.*, 1996). The reason for these differences relies on the fact that carbon and nitrogen reserves have different roles in the physiology of lucerne regrowth (Avice *et al.*, 1996) as discussed in the following sections.

2.6.1 Carbohydrate reserves in perennial organs

Total non structural carbohydrates (*TNC*, *i.e.* starch and soluble sugars) are the most labile fraction of the total carbohydrate content of lucerne perennial organs. Nevertheless, structural carbohydrates (*e.g.* cellulose, hemicellulose and pectins) have also been suggested to be mobilized after defoliation (Avice *et al.*, 1996).

Sucrose is the major form of carbohydrate transported in lucerne (Heichel *et al.*, 1988) making up to 80-90% of soluble sugars in roots (Hall *et al.*, 1988; Morot Gaudry *et al.*, 1987). The most important storage form of carbohydrates in lucerne roots is starch (Heichel *et al.*, 1988); usually composed of 80% amylopectin and 20% amylase (Fankhauser *et al.*, 1989). Starch is mainly found in the bark and in the ray parenchyma cells of wood of taproots (Habben and Volenec, 1990).

After defoliation, the concentration of starch and soluble sugars in lucerne roots goes through a cycle of initial depletion and then accumulation (Habben and Volenec, 1990; Nelson and Smith, 1968; Pearse *et al.*, 1969b). The period to recover or exceed initial *TNC* levels depends on climatic (*e.g.* temperature, radiation receipts) and endogenous (*e.g* previous levels of carbohydrates) factors (Skinner *et al.*, 1999). Nevertheless in general, carbohydrate reserves in taproots decline from early after defoliation until 15-20 days of regrowth (Fankhauser *et al.*, 1989; Kim *et al.*, 1993b; Skinner *et al.*, 1999), from when carbon partitioning from new photosynthetic tissue to roots is sufficient to promote the recover of *TNC* levels. This occurs simultaneously with a flush of cell division in the bark and wood regions of roots and is followed by an increase in cell expansion after 28-35 days of regrowth (Rapoport and Travis, 1984).

There is a seasonal pattern of accumulation and depletion of carbohydrate reserves in lucerne perennial organs when grown in temperate climates (Cunningham and Volenec, 1998). These authors showed that there was a fast accumulation of soluble sugars in lucerne taproots from 7% DM in spring to 16% DM in autumn. This high concentration was maintained throughout winter but declined sharply when growth resumed in the following spring.

Starch concentrations of lucerne taproots increase from mid-spring to summer (Li *et al.*, 1996) when they were shown to reach a maximum of ~27% DM followed by a decline through autumn-winter to levels of ~6% DM (Cunningham and Volenec, 1998). By supplying lucerne plants with marked carbon (^{14}C), Morot Gaudry *et al.* (1987) measured an increase in the partitioning of ^{14}C from shoots to roots from 21% in spring to ~51% in autumn during the initial phases of regrowth. These results suggest that there is a strong environmental control of C partitioning to perennial organs and also mobilization of these reserves in lucerne crops.

In autumn, the two factors that are likely to trigger an increase in partitioning to shoots are low temperature and short photoperiods (Philippot *et al.*, 1991). Nevertheless, reports of experiments that isolated T_{mean} and *Pp* effect on carbon partitioning between lucerne shoot and root are rare. Evidence from an exclusive effect of T_{mean} on shoot growth can be draw from Chen and Chen (1988) who showed that stem extension was limited when T_{mean} declined from 20°C/15°C to 10°C/5°C, the response varying according to the dormancy level of the lucerne genotype. After 42 days of regrowth in controlled conditions (*Pp* of 16 h and 250 μmol photons/m^2/s) stem height at low T_{mean} declined 65% in the dormant 'Beaver', 38% in the semi-dormant 'Lahontan' and only 25% in the non-dormant 'Moapa 69' lucerne. Under controlled conditions, Singh (1974) observed that a decline in light/dark temperature from 30°C/25°C to 20°C/15°C increased the partitioning of marked C (^{14}C) to lucerne roots. The authors stated that carbon partitioning to lucerne roots seemed to be less sensitive to photoperiod than to temperature.

Lucerne plants were compared under contrasting photoperiods (*Pp*) of 9 or 16 h, but at a constant value of PAR which resulted in irradiances of 2.6 and 4.6 MJ PAR/m^2/day respectively (Philippot *et al.*, 1991). These authors found no effect of *Pp* on DM partitioning to roots which averaged ~24% for both treatments. Despite this, field and modelling data from several authors suggest that photoperiod influences the allocation of

photosynthates to lucerne roots (Durand *et al.*, 1991; Gosse *et al.*, 1982a; Khaiti and Lemaire, 1992). It seems likely that this effect was not reproduced in controlled conditions.

The effect of carbohydrate reserves on shoot growth rates was largely accepted by the scientific community until the mid 80's. However evidence for a weak relationship between shoot growth rates and carbohydrate reserves in lucerne has been found in field and controlled conditions (Avice *et al.*, 2001; Hall *et al.*, 1988; Ta *et al.*, 1990; Volenec, 1985). In fact, lucerne genotypes with low concentration of starch yielded twice as much as high starch genotypes after 35 days of regrowth (Boyce and Volenec, 1992). Fankhauser *et al.* (1989) observed no difference in growth rates of lucerne genotypes with root starch concentration differing by up to 3 fold. This lack of response of shoot growth to the levels of carbohydrates in perennial organs was also found in white clover (*Trifolium repens*) (Bouchart *et al.*, 1998). These authors concluded that carbohydrate storage is more important for winter survival than for the promotion of early-spring regrowth. This agrees with the pattern of mobilization of carbohydrates in lucerne roots, that declines throughout winter well before regrowth resumes in early-spring (Cunningham and Volenec, 1998). This decline probably reflects root respiration necessary to supply energy (ATP and reducing power) and carbon skeletons to nitrogenous compounds and protection against freezing as discussed by Bouchart *et al.* (1998).

Avice *et al.*(1996) showed that although 73% of the carbon stored in lucerne perennial organs was mobilized after 30 days regrowth, only 5% of this carbon was recovered in the aerial biomass. The main destination for carbon reserves was the respiration of perennial organs (61% of stored C) and shoots (8% of stored C). Shoot growth and leaf area expansion seemed to rely more heavily on carbon derived from current photosynthesis of neighbouring leaves than from of reserves in perennial organs (Cralle and Heichel, 1988; Hendershot and Volenec, 1993). Singh (1974) observed that ^{14}C translocated from perennial organs made up most of shoot carbon in the first 6 days of regrowth, after that photosynthetic assimilation provided a larger proportion of ^{14}C found in shoots.

2.6.2 Nitrogen reserves in perennial organs

Nitrogen is acquired by lucerne roots through mineral uptake (NH_4^+ and NO_3^-) and also from atmospheric N_2 fixation through symbiosis with *Rhyzobium meliloti* (Kim *et al.*,

1991). Nitrogen reserves are stored mainly in taproots bark tissues, with smaller amounts also found in the wood (Hendershot and Volenec, 1992). The largest pool of N in storage is composed of soluble proteins that are hydrolysed in the more readily available amino acid pool (Avice *et al.*, 2001). Asparagine is the dominant amino acid in lucerne roots (Morot Gaudry *et al.*, 1987) comprising 65-75% of total amino acid transported in lucerne sap (Hendershot and Volenec, 1992; Kim *et al.*, 1993a).

Nitrogen concentration in lucerne perennial organs varies seasonally (Cunningham and Volenec, 1998) with the greatest accumulation occurring in autumn and the lowest levels in early-spring (Hendershot and Volenec, 1992). When adjusted as a percentage of the structural root DM, nitrogen concentration increased from 2.0-2.4% DM in summer to ~4.0% DM in autumn, a level that was maintained until growth resumed in early-spring (Cunningham and Volenec, 1998). Similarly, Li *et al.* (1996) observed a decline in nitrogen concentration of lucerne roots from ~2.5% DM in winter to 1.5% DM in early-spring as growth resumed.

There are specific fractions of soluble proteins that are mobilized to a greater extent in response to seasonal factors and after defoliation (Hendershot and Volenec, 1992). These proteins with molecular masses of 15, 19 and 32 kDa, together with β-amylase (Gana *et al.*, 1998; Li *et al.*, 1996), fit the criteria to be classified as VSP (vegetative storage protein) because they (*i*) are stored at vacuole level, (*ii*) represent a large proportion (>40%) of soluble proteins and (*iii*) are subjected to a cycle of accumulation and depletion in response to defoliation and seasonal signals (Volenec *et al.*, 1996).

The seasonal dynamics of nitrogen in lucerne roots is consistent with the effects of photoperiod and temperature on different N fractions. Low temperatures triggered the accumulation of VSPs in white clover and there was a small synergistic effect of short photoperiods in this accumulation (Bouchart *et al.*, 1998). In lucerne, Noquet *et al.* (2001) found that short photoperiods (8 h vs. 16 h) decreased nitrogen partitioned to shoots from 71 to 61%, with a subsequent increase in the N concentration of taproots from 1.8 to 2.9%, particularly of VSPs. Low temperature (5°C/5°C vs. 20°C/18°C) also induced an increase in nitrogen in roots but with no accumulation of VSPs.

Following defoliation, nitrogen reserves are highly mobilized from lucerne roots and transported to regrowing shoots (Kim *et al.*, 1993b; Volenec *et al.*, 1996). Ourry *et al.*

(1994) showed that after 24 days of regrowth, the amount of nitrogen mobilized from perennial organs was ~75% in taproots, 41% in crowns, and 52% in lateral roots. Taproots being the greatest providers of nitrogen amounts to regrowing shoots (Ourry *et al.*, 1994). Barber *et al.*(1996) found that, after 10 days of regrowth, 34 to 47% of the nitrogen from lucerne roots was recovered in growing shoots. Similarly, Avice *et al.* (1996) showed that 34% of the nitrogen stored in lucerne perennial organs were mobilized after 30 days of regrowth and recovered in growing shoots.

The removal of the photosynthetic tissue with defoliation considerably reduces nitrogen uptake and nitrogen fixation (Kim *et al.*, 1993a; Vance and Heichel, 1981). The capacity for N_2 fixation is negligible in the first week after defoliation (Kim *et al.*, 1993b) which is partially explained by an 80% decline in the activity of the enzyme nitrogenase (Ta *et al.*, 1990). Nitrogenase is responsible for the reduction of atmospheric N in NH_3 and its activity only recovers to normal levels after 14 days of regrowth (Ta *et al.*, 1990). During these early stages of regrowth, lucerne shoot growth is heavily dependent on the supply of nitrogen from perennial reserves. Even at later stages of regrowth (24 days) the contribution of endogenous nitrogen was shown to be >20% of total shoot N (Kim *et al.*, 1993a).

This large dependence of shoots on nitrogen from storage organs justifies the strong relationship found between shoot yield and nitrogen reserves (Avice *et al.*, 2001). Ourry *et al.* (1994) observed that a 4.5 fold increase in the amount of nitrogen in perennial organs at the day of cutting prompted a 10 fold increase in shoot yield after 24 days of regrowth. Avice *et al.* (1997b) showed that shoot yield (35 days of regrowth) was linearly and strongly related to the amount of soluble protein and VSPs on the day of defoliation, however there was no relationship with total nitrogen content in taproots.

Most of the nitrogen mobilized from taproots and lateral roots has been shown to be transferred to growing leaves (Ourry *et al.*, 1994). The highest nitrogen concentrations in growing leaves are found in regions of intense cell division (Schaufele and Schnyder, 2001). This is consistent with the strong relationship between leaf area expansion rates (*LAER*) and soluble proteins, found by Justes *et al.* (2002). The *LAER* increased from ~0.015 $m^2/m^2/°Cd$ (T_b=5°C) at a soluble protein concentration of 1.0% root DM to ~0.028 $m^2/m^2/°Cd$ at 2.5% soluble protein in root DM (Justes *et al.*, 2002).

2.7 Lucerne simulation modelling

The understanding of physiological responses of crops to the environment has achieved a level which allows the integration of this knowledge for predictive purposes (Hammer *et al.*, 2002). Computer simulation models are the means to embody these relationships into mathematical equations which conceptually represent a simplified crop system (Ritchie *et al.*, 1991).

Crop models can be conceptually classified in (*i*) empirical/mechanistic (Monteith, 1996), (*ii*) static/dynamic and (*iii*) deterministic/stochastic (Cheeroo-naymuth, 1999). Empirical models are direct descriptions of observed data without reference to the underlying processes involved (*e.g.* regression equations). In contrast, mechanistic models describe the behaviour of a system based on explicit relationships at lower level attributes. In reality, all models at their lowest level of organization are based on descriptive or empirical functions, however the way by which these functions are used and combined determines if the model is predominately empirical or mechanistic (Christian, 1987). Static models differ from dynamic models by the fact that the latter have time as an independent variable, which allows the integration of systems attributes over a given period. Deterministic models are characterized by definitive predictions while stochastic models provide a measure of uncertainty (*e.g.* variance) of the predicted mean.

The clear statement of the objectives of a crop model is essential to delimit the boundaries by which it will be initially developed and later evaluated (Sinclair and Seligman, 1996). In the past 30 years several crop models have been developed or adapted with the objective of predicting lucerne growth and development (Confalonieri and Bechini, 2004; Fick *et al.*, 1988). Lucerne simulation models can be analysed in relation to three common major components (Marcelis *et al.*, 1998): (*i*) radiation interception, (*ii*) conversion of intercepted radiation into net dry matter (photosynthesis minus respiration), and (*iii*) partitioning of DM among lucerne organs (leaves, stems and perennial DM). The arrangement of these compartments define the structure of the model (Passioura, 1996) and the mathematical equations within them characterize the level of understanding of processes and the model complexity.

At compartment levels, the processes usually assume a rate of growth or development at optimum conditions (*i.e.* genetic potential). The potential rates are then reduced for the

limiting effects of external factors such as sub-optimal temperatures, water deficits and low nitrogen supply (Holt *et al.*, 1975). This is done by multiplying the optimum growth and development rates by coefficients that range from 0 to 1 (multiplicative approach), to give the actual rate at the environment and management condition of the simulated crop (Christian, 1987).

The level of complexity of each process is an important aspect of model development and it has to line up with the proposed objectives (Hammer, 1998). Sinclair and Seligman (1996) stress the importance of a simple model structure in coherence to the organizational level of the problem (*e.g.* tissue, plant or crop) and the use of summary relationships (*e.g. RUE*) whenever possible, in contrast to a reductionist approach.

2.7.1 Modelling of radiation interception in lucerne crops

In most crop models the complex nature of light penetration through crop canopies is dealt with a statistical approach that assumes an exponential decay in radiation intensity with depth (Christian, 1987). For lucerne, the level of sophistication of such models can vary from a multilayer canopy where extinction coefficient (k) is calculated hourly based on the combination of leaf angle and sun inclination (Varella, 2002), to simpler models that work on a daily time step assuming a single value of k (Robertson *et al.*, 2002). Although, Christian (1987) drew attention to the possible errors involved with the oversimplification in the use of a single k, Gosse *et al.* (1982b) demonstrated within a lucerne cultivar, k can be assumed constant throughout seasons allowing accurate estimates of PAR_i/PAR_o once leaf area (*i.e. LAI*) is known.

Leaf area expansion is usually derived from (*i*) plant development, mainly driven by thermal-time accumulation (Equation 2.7); (*ii*) DM partitioning to leaves assuming an area to mass relation (*i.e. SLA*) (Equation 2.8) or (*iii*) a combination of both approaches (Marcelis *et al.*, 1998).

Equation 2.7

$$LAI = \sum_{0}^{n} (LAER \times Tt)$$

Where *LAER* is the leaf area expansion rate ($m^2/m^2/°Cd$) and *Tt* is the thermal-time accumulation (°Cd) from period 0 to n.

Equation 2.8

$$LAI = \sum (DM_{leaf} \times SLA)$$

Where DM_{leaf} is the daily DM partitioned to leaves (g DM/m^2/day) and *SLA* is the specific leaf area (m^2/g DM).

Alternatively, *LAI* can be modelled by considering the individual area of each leaf as a function of node position and therefore expansion is derived from leaf appearance (Dwyer and Stewart, 1986; Robertson *et al.*, 2002). As an example of a simplistic approach, Gosse *et al.* (1984) obtained strong predictions of *LAI* in a non-stressed lucerne crop assuming a linear *LAI* expansion rate of 0.092 m^2/m^2/°C (T_b=0°C) during spring-summer but the model overestimated *LAI* in autumn. These seasonal changes in *LAER* seem to be related to a response of phyllochron and branching to other seasonal signals (*e.g.* photoperiod) (Brown *et al.*, 2005b). These relationships will be explored in this thesis.

2.7.2 Modelling net dry matter accumulation in lucerne crops

Crop dry matter accumulation is ultimately a result of the difference between gross photosynthesis and respiration. In crop models, canopy photosynthesis is commonly calculated by the integration of leaf photosynthesis in time (*e.g.* minute or hourly steps) and space (*e.g.* vertical layers of canopy), by assuming the response of *Pn* to irradiance (*i.e.* PPFD) as a non-rectangular hyperbola (Christian, 1987; Thornley and Johnson, 2000). To account for the CO_2 output, respiration is conceptually divided in growth (R_g) and maintenance (R_m) respiration (McCree, 1974) as in Equation 2.9.

Equation 2.9

$$R_{tot} = a \times Pg + b \times W \times Q_{10}^{(T_{mean} - T_{opt})/10}$$

In this framework growth respiration (a x Pg) is a constant fraction of gross photosynthesis independent of temperature. In contrast, maintenance respiration increases with crop biomass (W) at a rate b at T_{opt} which responds to temperature according to the Q_{10}.

The mechanistic separation of photosynthesis and respiration in crop models has been successfully used for several forage crops (Peri *et al.*, 2003; Sands, 1995; Varella, 2002). However, in predictive models which have the crop as the main organizational level, the use of *RUE* (Section 2.5, Equation 2.1) has been shown to be sufficiently robust to express the underlying physiological processes of photosynthesis and respiration in response to the environment (Sinclair and Seligman, 1996).

The use of *RUE* to estimate DM accumulation is currently part of the framework of lucerne simulation models, like APSIM-lucerne (Robertson *et al.*, 2002) and Cropsyst (Confalonieri and Bechini, 2004). The main problems related to the use of *RUE* to simulate DM yield in perennial crops are (*i*) the violation of the assumed linearity between photosynthesis and respiration (mainly in early stages of regrowth) and (*ii*) the variable partitioning of DM to non-harvestable organs (Section 2.5.2). To overcome some of these limitations APSIM-lucerne (Robertson *et al.*, 2002) assumes a variable *RUE* depending on the development stage of the crop and the season of the year. In the model RUE_{shoot} is 1.2 g DM/MJ PAR_i at the seedling stage, 2.0 g DM/MJ PAR_i at the vegetative growth stage in spring/summer but declines to 1.2 g DM/MJ PAR_i during autumn/winter. RUE_{shoot} is also adjusted for sub/supra-optimal temperatures assuming cardinal temperatures of 0, 8, 25 and 32°C. In contrast, Cropsyst (Confalonieri and Bechini, 2004) assumes an optimum RUE_{shoot} of 3.0 g DM/MJ PAR_i during all stages of regrowth suitable for adjustment at non-optimal temperatures. The high level of empiricism and subjectivity in setting and adjusting *RUE* values in current lucerne models reflect the lack of information about such relationships.

2.7.3 Modelling of dry matter partitioning in lucerne crops

The partitioning of DM at crop level is possibly the weakest point of lucerne simulation models, and most simulation models for other crops, due to the lack of a quantitative understanding of such processes (Confalonieri and Bechini, 2004; Fick, 1977; Ritchie *et al.*, 1991). This situation induces the common use of empirical approaches like descriptive allometry, *i.e.* the relation between growth rates of different organs (Christian, 1987). This approach has been successful in describing partitioning of DM within lucerne shoots by an exponential decline in leaf/stem ratio as shoot yield increases (Lemaire *et al.*, 1992). APSIM-lucerne uses fixed proportions of biomass partitioned to each organ according to

the developmental stage of the crop and the capacity of that organ to accommodate DM. For example, in the vegetative phase 45% of the daily assimilated biomass is partitioned to leaves, the remaining for stems as long as the maximum leaf thickness (*i.e.* minimum specific leaf area) is not achieved (Robertson *et al.*, 2002).

The partitioning of dry matter to/from perennial organs remains ignored or obscured by the majority of lucerne models despite its major importance in terms of total biomass (Section 2.6). Although the seasonality of DM partitioning to perennial organs is well documented (Section 2.6), the mechanisms and stimuli that control such fluxes are rather complex and not sufficiently understood (Farrar and Jones, 2000). This impedes more sophisticated approaches such as the functional equilibrium between shoots and roots (*i.e.* teleonomic models) or sink regulation (Thornley and Johnson, 2000) to be used in lucerne models. For example, to account for increased partitioning of dry matter to roots in autumn (Section 2.6), the model SIMED reduces leaf and stem growth rates at different levels according to the direction of photoperiod (Holt *et al.*, 1975). At a similar level of empiricism, APSIM-lucerne deals with the problem by reducing RUE_{shoot} in autumn-winter to 60% of the summer value (2.0 g DM/MJ PAR) (Robertson *et al.*, 2002).

2.7.4 Improvements in lucerne simulation models

The most effective way of improving lucerne simulation models is by gaining further understanding about the environmental physiology of the crop (Fick *et al.*, 1988). On the other hand, even simulation models that carry known limitations into their code allow the identification of points where knowledge needs to be gained (Hammer, 1998). Based on this review of literature it can be inferred that the major limitations of lucerne models are related to lack of quantitative understanding about the changes in the plant physiology that occur seasonally and also at the onset of regrowth, particularly during the first spring growth. These issues are complicated by the genetic diversity of lucerne which demands cultivar specific parameters, for example related to dormancy responses.

2.8 Conclusions

The main conclusions of this review of literature are:

- Shoot yield and development of lucerne crops respond to environmental factors (*e.g.* temperature, photoperiod and radiation receipts) in a predictable way which permits the construction of simulations models.

- However, in contrast to annual crops, the main physiological variables of *RUE*, $\sum PAR_i$ and p_{per} used in yield models show different responses on a seasonal basis for lucerne. This seems to be related to the perennial characteristic of the crop and the cycles of accumulation and depletion of C and N reserves in crowns and taproots.

- On the other hand, the levels of perennial reserves also influence the response of these physiological variables to the environment and this is not properly described in a seasonal basis.

Based on the information gathered in this literature review the main aim of this thesis was to quantify the seasonal responses of lucerne crops to environmental factors, as affected by the level of perennial reserves. To investigate these relationships, a single field experiment involving four defoliation regimes was implemented. The defoliation regimes aimed to create lucerne crops with contrasting levels of perennial reserves, without affecting other plant characteristics that influence growth potential (*e.g.* number of growing points and residual leaf area). Growth and development of these crops were then quantified during two entire growth seasons based on the yield framework (Equation 2.2) adapted from Monteith (1977). The relationships developed from the field experiment were then integrated in a simple simulation model which was used as an analysis tool to explain lucerne seasonal patterns of growth and development in a cool temperate climate.

3 Materials and Methods

3.1 Site description

3.1.1 Site history

The experiment was located at the Lincoln University Field Service Centre (FSC), Canterbury, New Zealand (43°38'S and 172°28'E) within a 0.56 hectare (140 x 40 m) area of flat land in Block 9 of 'Iversen Field' (Iversen 9, 'I9'). Historically I9 contained a rape crop (*Brassica napus* s.s oleifere) in the 1999/2000 growth season, and green feed oat crop (*Avena strigosa*) from April to September 2000. Oats were grazed and then the area was ploughed on 9 October, roto-crumbled, harrowed and rolled on 9, 16 and 20 October to prepare a fine, firm seedbed. 'Grassland Kaituna' lucerne was established in the spring of 2000 for an experiment involving different sowing dates and irrigation regimes (Brown, 1998). The crops were sown on four dates (24 October, 15 November, 5 December and 27 December 2000) with an Øyjoord cone seeder at a rate of 10 kg/ha (coated seed). After sowing, the area was chain harrowed to ensure seed coverage. Once established, each crop was grazed at approximately 35 day intervals in an experiment involving irrigated and dryland treatments until June 2002 (Brown, 2004). The current experiment commenced on the 14 June 2002.

3.1.2 Soil characteristics

The soil is a 'Wakanui' deep silt loam (USDA Soil Taxonomy: Aquic Ustochrept fine silty, mixed, mesic) classified as 'Pallic' in the New Zealand Soil Classification (Hewitt, 1993; Watt and Burghan, 1992). These soils represent around 12% of New Zealand land area and occur in the seasonally dry eastern parts of the country. They are subjected to water deficits in summer and water surpluses in winter and spring (Molloy, 1988). Wakanui soils usually occur in flat to gently undulating lands where the parent forming materials are silty and sandy alluvium derived from loess or fluvial sediments, from quartzo-feldspathic rocks like schist or greywacke (Hewitt, 1993; Watt and Burghan, 1992). This confers these soils with imperfect drainage but a high base saturation (>50%) and high levels of nutrients with the exception of extractable sulphur. The bulk density

varies from 1,100 kg/m^3 in the top 200 mm, to 1,500 kg/m^3 in lower layers (Watt and Burghan, 1992).

3.2 Meteorological conditions

3.2.1 Long-term meteorological conditions

The climate in Canterbury is characterized by an annual rainfall of ~640 mm, which is slightly higher in winter than other seasons (Table 3.1). The annual mean temperature is 11.4°C varying from a monthly average of 6.4°C in June to 16.6°C in January. The long-term meteorological data for the experimental site (Table 3.1) were measured at Broadfields Meteorological Station (NIWA, National Institute of Water and Atmospheric Research, New Zealand), which is located 2 km North of the Lincoln University campus.

Table 3.1 Monthly long-term means from 1960 to 2003 for total solar radiation (R_o), maximum (T_{max}), minimum (T_{min}) and mean (T_{mean}) air temperatures, potential evapotranspiration (*ETp*), total rainfall and windrun measured in an open field at the Broadfields Meteorological Station.

Month	R_o MJ/m^2/day	T_{max} (°C)	T_{min} (°C)	T_{mean} (°C)	Rainfall (mm)	*ETp* (mm)	Windrun km/day
January	21.92	22.14	11.28	16.60	52.90	153.00	119.02
February	18.94	21.77	11.12	16.33	43.14	117.60	115.65
March	14.04	19.98	9.76	14.79	54.68	96.20	105.36
April	9.55	17.18	6.73	11.93	54.78	62.60	90.21
May	5.89	14.05	4.02	8.99	52.24	43.70	83.39
June	4.30	11.30	1.59	6.40	60.78	33.00	75.55
July	5.05	10.67	1.34	5.95	64.31	37.10	71.42
August	7.74	12.01	2.45	7.18	61.13	50.70	90.51
September	11.99	14.34	4.25	9.24	42.26	68.60	107.94
October	17.10	16.84	6.12	11.40	46.43	104.60	118.44
November	21.04	18.58	7.69	13.05	53.01	123.90	120.68
December	22.88	20.73	9.89	15.22	49.82	142.70	121.66
Annual mean	**13.37**	**16.63**	**6.35**	**11.42**	**635.48**	**1033.70**	**101.65**

3.2.2 Meteorological conditions during the experimental period

3.2.2.1 Solar radiation and air temperature

The monthly values of mean daily total solar radiation (R_o) during the experiment (Figure 3.1) were close to LTM (Table 3.1). The range in the daily R_o was from 0.6 MJ/m^2/day on 17 June 2002 to 38 MJ/m^2/day on 4 October 2002. Extremes of air temperature were -4.5°C on 17 June 2003 and 32°C on 11 February 2003 with the mean daily temperature range from 1.2 to 24°C.

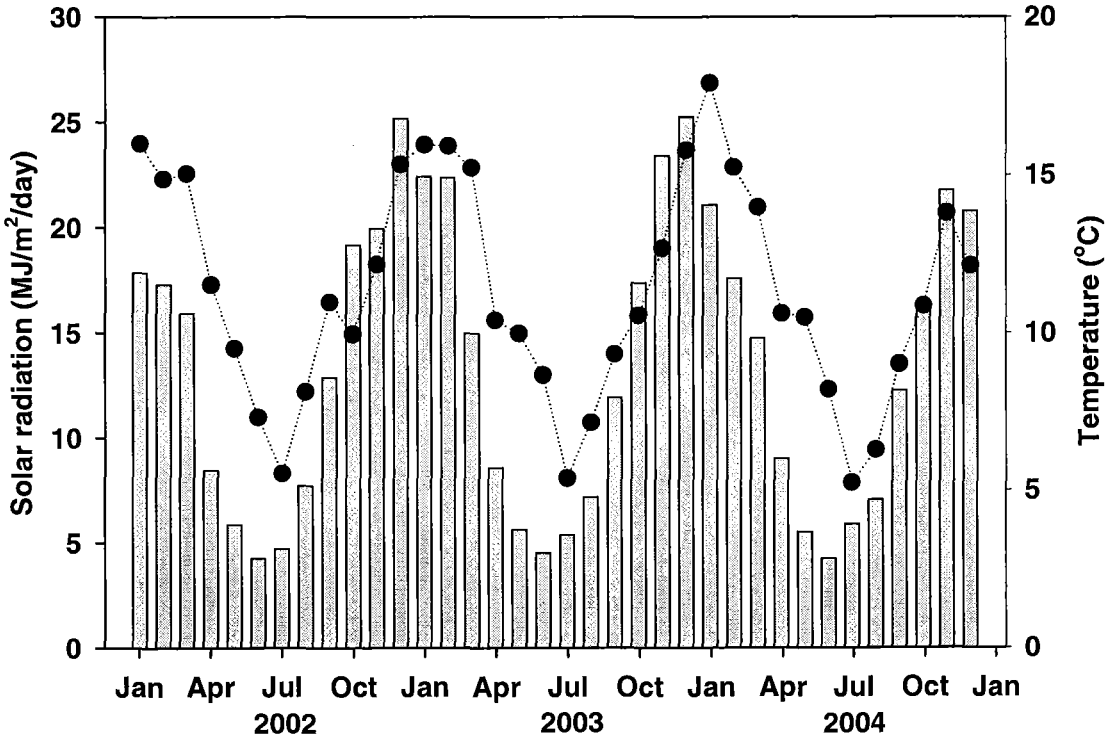

Figure 3.1 Mean daily total solar radiation (grey bars) and mean daily air temperature (•) for monthly periods from 01 January 2002 to 31 December 2004. Data were obtained from Broadfields Meteorological Station, Canterbury, New Zealand.

3.2.2.2 *Rainfall and evapotranspiration*

In 2002 annual rainfall was 675 mm/year and an *ET*p of 1065 mm/year. The year of 2003 was exceptionally dry with only 466 mm rain and *ET*p of 1091 mm/year (Figure 3.2).

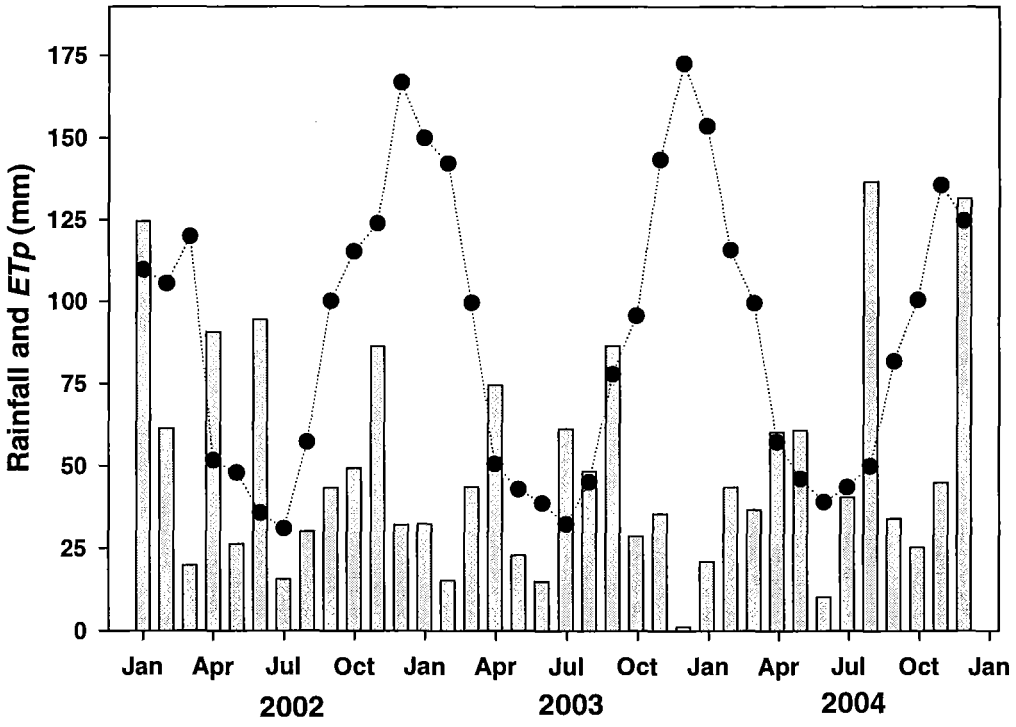

Figure 3.2 Mean rainfall (grey bars) and Penman potential evapotranspiration (*ETp*,•) for monthly intervals from 01 January 2002 to 31 December 2004. Data were obtained from Broadfields Meteorological Station (2 km north of the site), Canterbury, New Zealand.

3.2.2.3 *Vapour pressure deficit and windrun*

In Figure 3.3 the vapour pressure deficit (*VPD*, kPa) and the wind run (*WR*, km/day) are shown. *VPD* ranged from 8 to 15 kPa throughout the period. *WR* averaged 300 km/day and ranged from 280 to 480 km/day.

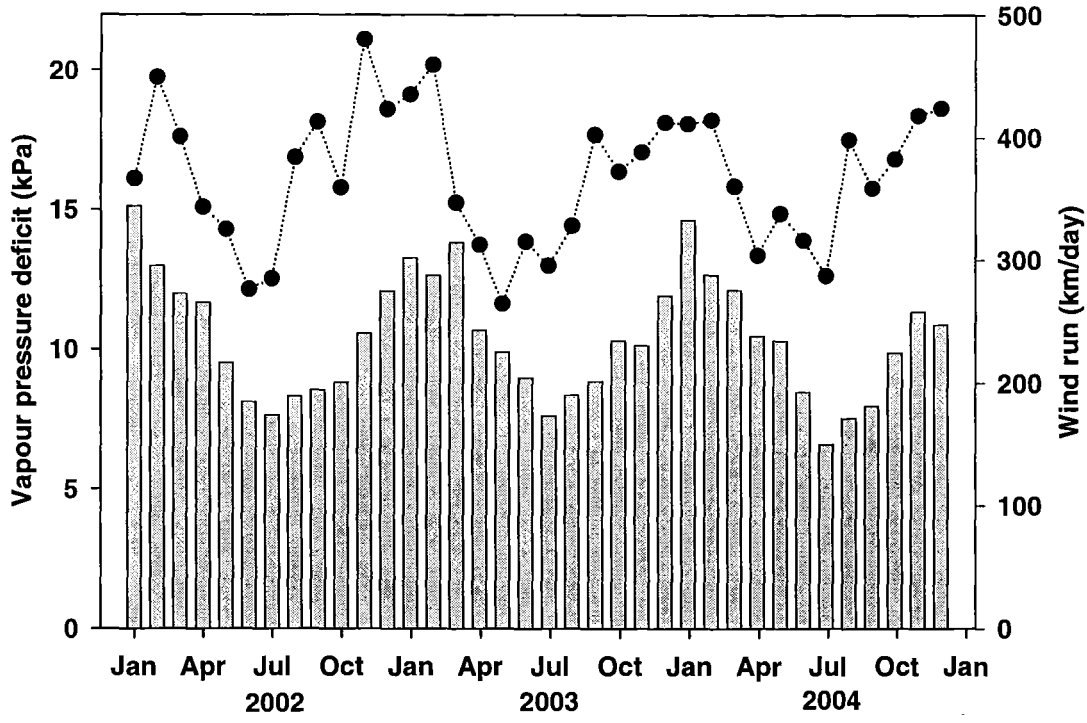

Figure 3.3 Mean vapour pressure deficit (kPa, grey bars) and mean daily windrun (km/day,•) from 01 January 2002 to 31 December 2004. Data were obtained from Broadfields Meteorological Station, Canterbury, New Zealand.

3.3 Experimental design and treatments

The experiment was a 2 x 2 factorial randomised complete block design with 4 replicates. This involved two regrowth cycles: a short (28 days) and a long (42 days) regrowth cycle; and two timings of imposition of regrowth intervals (before and after 4th February). The four treatments were denominated as follows:

(*i*) **Long/Long regrowth cycle (LL):** 42 day cycle (38 days regrowth and 4 days grazing) during the entire growth season. First grazing on 1 October of 2002, 2 October 2003 and 4 October 2004.

(*ii*) **Long/Short regrowth cycle (LS):** 42 day cycle until 4th February and 28 day cycle (25 days regrowth and 3 days grazing) during the remaining of the growth season. First grazing on 1 October of 2002, 2 October 2003 and 4 October 2004.

(*iii*) **Short/Long regrowth cycle (SL):** 28 day cycle until 4th February and 42 day cycle during the remainder of the growth season. First grazing on 15 September 2002, 15 September 2003 and 4 October 2004.

(*iv*) **Short/Short regrowth cycle (SS):** 28 day cycle during the entire growth season. First grazing on 15 September 2002, 15 September 2003 and 4 October 2004.

The criteria to define the dates to start (~15th September and 1st October) and swap or maintain treatments (4th February) were based in the timing when seasonal changes in lucerne DM partitioning between shoots and roots occur (Section 2.6). A schematic representation of treatments is given in Figure 3.4.

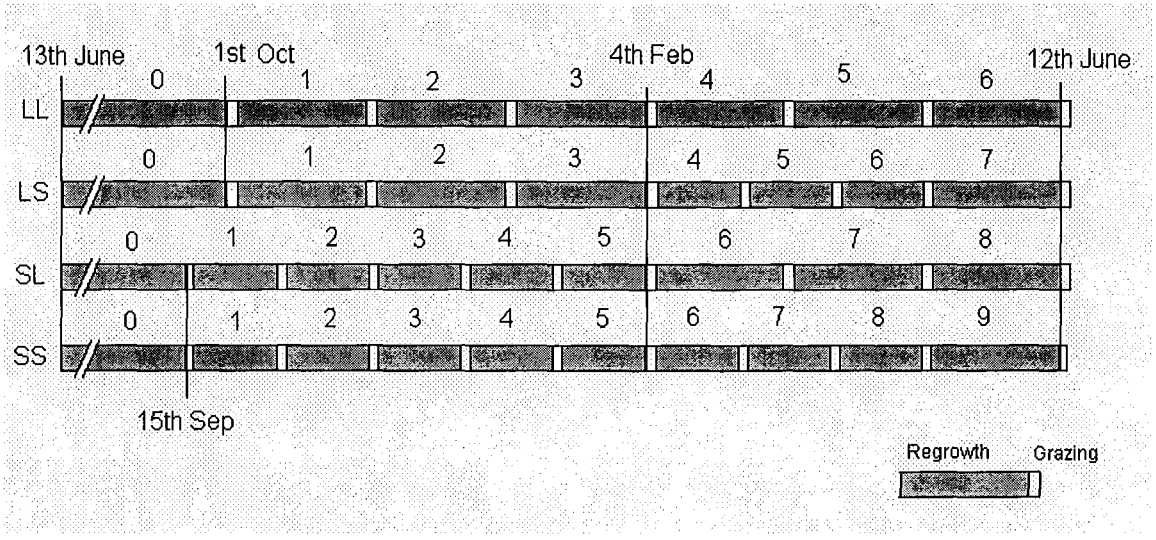

Figure 3.4 Schematic representation of regrowth regimes imposed on lucerne crops with approximated dates of grazing for the 2002/03 and 2003/04 seasons at Lincoln University, Canterbury, New Zealand.

Note: LL, LS, SL and SS are the treatment acronyms as in Table 3.3. Cycle numbers are included for reference (*e.g.* for all crops the winter/early-spring cycle is Cycle 0 and for LL crops the last cycle of the growth season is Cycle 6).

The date of finish of a growth season and start of a new one was set as 13 June ± 1 day, coinciding with the final grazing of all crops (Table 3.2). Therefore from mid-June to early-September all crops were ungrazed.

3.3.1 Experimental period

The experimental period was from 14 June 2002 to 04 October 2004. This period included two full growth seasons (Table 3.2) each separated into halves (before and after 4th February). The season halves were divided in a number of regrowth cycles according to the defoliation treatments. The third spring growth only included the 2004 winter/early-spring regrowth common to all crops (12 June 2004 to 4 October 2004) to examine spring effects of the previous autumn treatments (Table 3.2).

Table 3.2 Experimental seasons for the grazing management of plots in the Iversen 9 experiment at Lincoln University, Canterbury, New Zealand.

Experimental season	Growth season	Actual experimental period
1st growth season	2002/03	From 14 June 2002 to 12 June 2003
2nd growth season	2003/04	From 13 June 2003 to 12 June 2004
3rd spring growth	Spring 2004/05	From 12 June 2004 to 4 October 2004

3.3.2 Definitions and nomenclature

In the result chapters (Chapters 4 to 7) observations will be referred to in text by the treatment acronym (LL, LS, SL or SS, Section 3.3) and when appropriate the growth season (02/03; 03/04 or 04/05) as a subscript (Table 3.3). Specific regrowth cycles are referred to after the acronym separated by a dash sign (*e.g.* $LL_{02/03}$ – Cycle 1). The term "growth season" refers to each annual experimental period (*e.g.* 2002/2003) while the word "season(s)" refers to the recognised seasons of the year (*e.g.* spring, summer, autumn and winter).

Table 3.3 Description of acronyms and symbols used to represent the treatment/growth season combinations throughout the experimental period.

Growing season	Defoliation Treatment	Acronym	Symbol
2002/2003	LL	$LL_{02/03}$	●
	LS	$LS_{02/03}$	○
	SL	$SL_{02/03}$	△
	SS	$SS_{02/03}$	▲
2003/2004 [1]	LL	$LL_{03/04}$	⊕
	LS	$LS_{03/04}$	⊕
	SL	$SL_{03/04}$	⊕
	SS	$SS_{03/04}$	⊕

Note: Includes the early-spring regrowth cycle of 2004/05.

Whenever, for a matter of clarity, data-points from treatments had to be displayed with different symbols from the ones in Table 3.3, the alternative symbols were referred to in the respective figure label. When the distinction between growth seasons in a figure was obvious the treatments were represented with the symbols from 2002/03.

3.3.3 Site and treatments view

The paddock in I9 was divided into 16 plots of 315 m^2 (17.5 x 18 m). A central lane (3.7 x 35 m) was arranged to symmetrically divide the plots and enable sheep to have access to the plots during different grazing dates and to reduce camping effects (Figure 3.5).

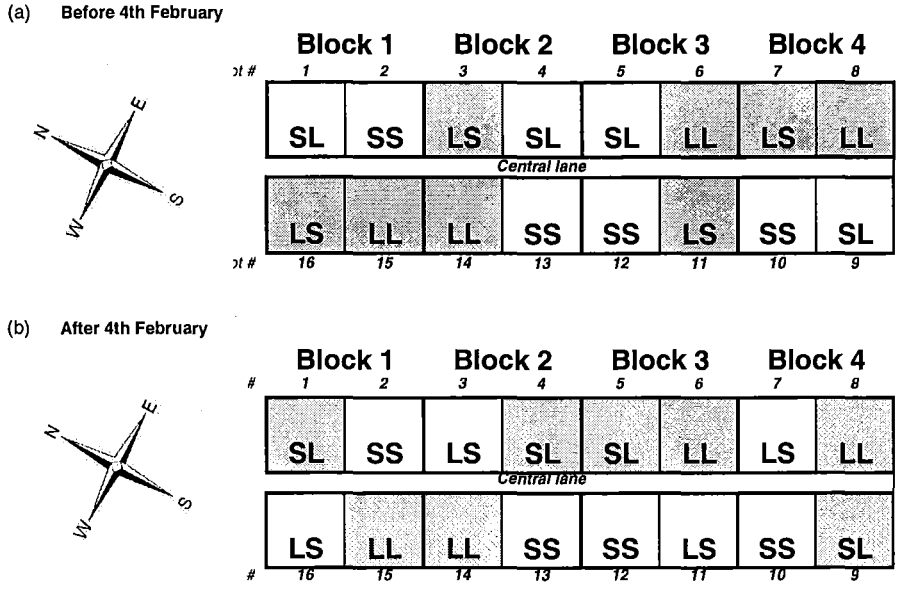

Figure 3.5 Schematic representation of treatments in Field Service Centre (FSC) experiment, Lincoln University, Canterbury, New Zealand.

Note: Plots grazed simultaneously before (a) and after (b) 4th February are filled with the same colour. Plot reference number is displayed near each respective cell outside the figure.

An aerial view of the experimental plots is shown in Plate 3.1.

Plate 3.1 Aerial view of Iversen 9 during a grazing day at Lincoln University, Canterbury, New Zealand.

Note: Note the previously grazed plots and cages of exclusion for recording marked shoots.

3.3.4 Management

3.3.4.1 Grazing management

The plots were grazed according to the defoliation treatments (Section 3.3) with the objective of achieving the regrowth intervals (25 and 38 days) and the grazing durations (3 or 4 days) for short and long regrowth cycles respectively. Effective grazing dates and regrowth durations are shown in Table 3.4.

After each grazing, residual stems were trimmed to ~50 mm above ground using a sickle bar mower. This prevented damage to the crowns but ensured that only new lucerne growth was measured in the subsequent cycles and that no residual leaf area was transferred to the next regrowth period.

Table 3.4 Initial and final dates of regrowth periods and grazing durations of short and long regrowth cycles of a lucerne crop at Lincoln University, Canterbury, New Zealand.

Cycle	Short regrowth cycle				Long regrowth cycle			
	Initial date	Final date	Resting days	Grazing days	Initial date	Final date	Resting days	Grazing days
Growth	season	2002/03						
0	14 Jun	14 Sep	93	5	14 Jun	30 Sep	109	5
1	20 Sep	14 Oct	25	3	06 Oct	12 Nov	38	4
2	18 Oct	09 Nov	23	4	17 Nov	23 Dec	37	4
3	14 Nov	07 Dec	24	4	28 Dec	03 Feb	38	7
4	12 Dec	04 Jan	24	4	11 Feb	17 Mar	35	5
5	09 Jan	06 Feb	29	4	23 Mar	29 Apr	38	5
6	11 Feb	03 Mar	21	4	05 May	11 Jun	38	1
7	08 Mar	01 Apr	25	3				
8	05 Apr	02 May	28	2				
9	05 May	11 Jun	38	1				
Growth	season	2003/04						
0	13 Jun	14 Sep	94	3	13 Jun	01 Oct	111	4
1	18 Sep	16 Oct	29	2	06 Oct	09 Nov	35	3
2	19 Oct	09 Nov	22	3	13 Nov	23 Dec	41	5
3	12 Nov	09 Dec	25	4	29 Dec	02 Feb	36	5
4	13 Dec	04 Jan	23	3	08 Feb	16 Mar	38	3
5	08 Jan	02 Feb	26	5	20 Mar	28 Apr	40	4
6	08 Feb	03 Mar	25	3	03 May	09 Jun	38	2
7	07 Mar	30 Mar	24	4				
8	04 Apr	28 Apr	25	4				
9	03 May	09 Jun	38	2				
Spring	growth	2004/05						
0	12 Jun	4 Oct	116	1	12 Jun	4 Oct	116	1

3.3.4.2 Mineral nutrition management

Soil chemical analysis was done from 20 soil cores (30 mm diameter x 150 mm depth) taken randomly from each half (South and North) of the paddock before the beginning of the experiment in August 2002 (Table 3.5). Levels of all nutrients were adequate, except for sulphate sulphur [$S(SO_4)$], which was slightly below the target of 11 ppm for sedimentary soils in Canterbury (Morton and Roberts, 1999). Therefore, 150 kg/ha extra sulphur super (7% P and 29% S) was applied in I9 in October 2002.

Table 3.5 Soil test results for paddock I9 in the Field Service Centre, Lincoln University, Canterbury, New Zealand from 2002 to 2004. Soil tests were performed using the Ministry of Agriculture and Fisheries Quick Test (MAF QT) procedures.

Site	Ca	K	Mg	Na	P	$S(SO_4)$	pH
		m.e./100 g soil			μg/ml	ppm	
August 2002							
South	5.6	0.92	0.88	0.13	23	9	6.0
North	5.0	0.87	0.88	0.17	31	5	6.3
May 2003							
LL	6.2	1.14	0.83	0.12	20	4	6.2
LS	6.7	1.16	0.83	0.16	21	6	6.2
SL	7.1	1.05	0.91	0.16	20	4	6.3
SS	6.5	1.21	0.83	0.14	23	6	6.1
May 2004							
LL	5.0	1.23	0.80	0.20	28	18	6.1
LS	5.0	1.28	0.84	0.22	31	16	6.1
SL	5.0	1.08	0.84	0.17	32	15	6.2
SS	5.0	1.28	0.84	0.22	30	19	6.0
Lower optima		0.26	0.34		20	11	5.3

Note: Lower optima according to Morton and Roberts (1999)

In late May 2003 another set of 20 soil cores per treatment were taken. Again, only the levels of sulphate sulphur were below that recommended for optimum growth of lucerne, and 250 kg/ha of sulphur super (8% P and 20% S) was broadcast on 18 June 2003. On the final evaluation (May 2004), all levels of nutrients were found adequate for optimum lucerne growth (Table 3.5).

3.3.4.3 Weed control

Herbicides were applied to maintain the crops free of weed competition during the entire experimental period. In the first season herbicides were applied in all crops to control an infestation of twitch (*Agropyron repens*) and twin cress (*Coronopus didymus*). In the first season (2002/03), the herbicide applications (Table 3.6) were over in the entire I9 area, although most of the weeds infested the crops subjected to the short regrowth cycle. During the second season (2003/04), annual weeds invaded mainly SS and SL crops. The main weeds at this time were white clover (*Trifolium repens*) and dock (*Rumex* sp.), and those were controlled with spot spraying to avoid affecting the lucerne crop.

Table 3.6 Herbicide applications to lucerne crops grown at paddock I9 in the Field Service Centre, Lincoln University, Canterbury, New Zealand from 2002 to 2004.

Date	Herbicide (active ingredient concentration)	Commercial dose applied
30/08/2002	Atradex (atrazine 500 g a.i./litre)	1.5 litre/ha
25/11/2002	Gallant (haloxyfop 100 g a.i/ litre)	2.5 litre/ha
19/02/2003	Preside (flumetsulam a.i. 800 g a.i./kg)	50 g/ha
09/06/2003	Gallant (haloxyfop 100 g a.i./ litre)	2.5 l/ha
20/06/2003	2,4 DB (2,4 DB 400 g a.i./ litre)	6.0 l/ha
20/06/2003	Atrazine (atrazine 900 g a.i./ kg)	1.0 kg/ha
21/10/2003	Spinnaker (imazethapyr 240 g a.i./litre)	400 ml/ha
12/03/2004	Spinnaker (imazethapyr 240 g a.i./litre)	400 ml/ha
12/03/2004	Velpar DF (750 g/kg hexazinone)	*Spot spraying
16/06/2004	Nu Triazine 900 DF (atrazine 900 g a.i./kg)	1.0 kg/ha

Note:*Spot praying directed exclusively over invading species (Section 3.3.4.3), all other applications were made over the entire experimental area of Iversen 9.

3.3.4.4 Irrigation

Irrigation was applied to ensure crop growth was not limited by water stress at any time during the experiment. Previous experiments in an adjacent paddock ('Iversen 8') had shown that lucerne yield decreased when soil moisture deficit to 2.3 m soil depth ($SMD_{2.3m}$) was greater than 215 mm (Inch, 1998). Therefore, a target of 200 mm actual $SMD_{2.3m}$ was set as the maximum allowed $SMD_{2.3m}$ to ensure water stress was avoided. Irrigation was applied using a hand shift pipe irrigation system with a rate of water application of 8 mm/h. The amount of irrigated water applied was measured with four rain gauges and details of the irrigation are shown in Table 3.7.

Table 3.7 Irrigation water applied to the paddock I9 in the Field Service Centre, Lincoln University, Canterbury, New Zealand from 2002 to 2004.

Start Date	Finish Date	Amount of irrigation water applied (mm)
First growth season		
11/09/2002	12/09/2002	42
09/10/2002	11/10/2002	40
30/12/2002	31/12/2002	47
18/01/2003	19/01/2003	40
10/02/2003	12/02/2003	45
26/02/2003	28/02/2003	45
12/03/2003	14/032003	50
26/03/2003	27/03/2003	40
Total first growth season		**349**
Second growth season		
25/11/2003	27/11/2003	35
31/12/2003	02/01/2004	40
13/01/2004	14/01/2004	40
12/02/2004	15/02/2004	40
Total second growth season		**155**

The $SMD_{2.3m}$ was measured with Neutron Probe and Time Domain Reflectometer readings (Section 3.4.1.3). The initial measured $SMD_{2.3m}$ at the site was 172 mm on 4 June 2002, prior to the beginning of the experimental season. Irrigation was then applied to bring the $SMD_{2.3m}$ up to ~15 mm from November to December 03. During the following summer, $SMD_{2.3m}$ increased to a maximum of 153 mm by 10 February 2003. From then, $SMD_{2.3m}$ decreased to ~13 mm by 24 April 2003 and stabilized near field capacity by 20 October 2003. In the summer of 2003, $SMD_{2.3m}$ increased to a maximum of ~130 mm by 30 December 2003. Irrigation was applied from this period on and $SMD_{2.3m}$ was maintained < 100 mm throughout 2004 (Figure 3.6).

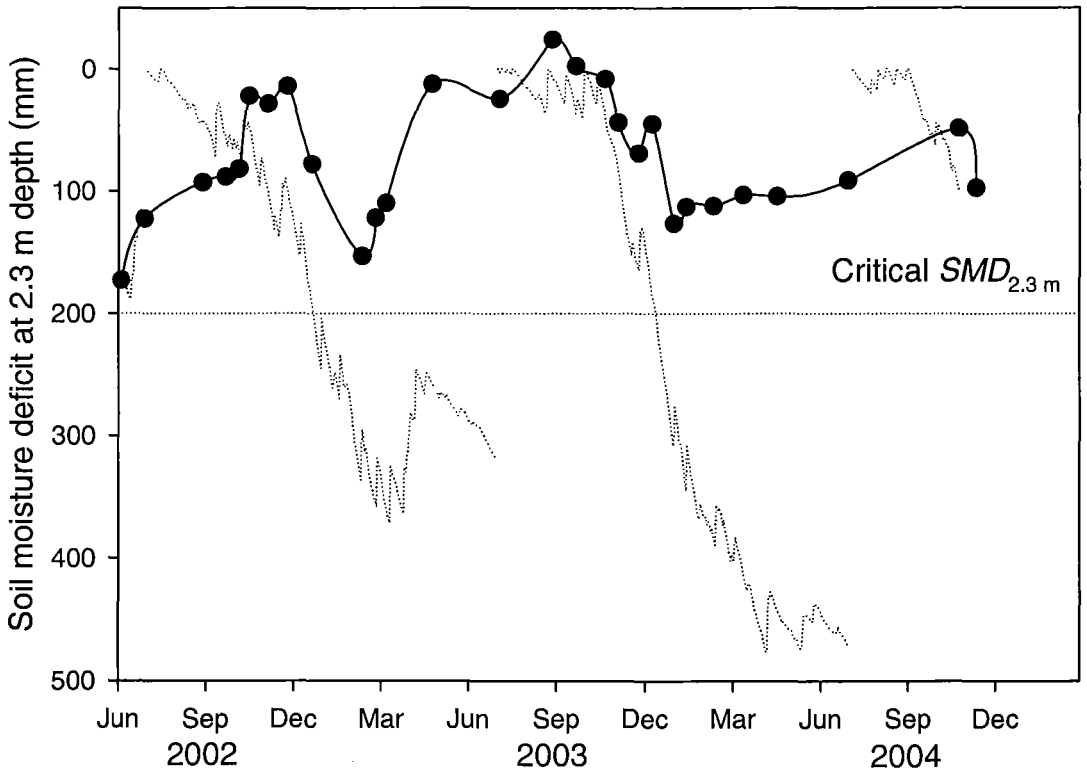

Figure 3.6 Calculated potential (.....) and actual measured (—•—) soil moisture deficit to 2.3 m depth from 4 June 2002 to 23 October 2004 at Lincoln University, Canterbury, New Zealand.

Note: Rainfall data were collected at Broadfields Meteorological Station 2 km North of the experimental site. Potential soil moisture deficit was calculated as Penman potential evapotranspiration - (rain + irrigation) with $SMD_{2.3\ m}$ set to zero when negative and on 1 July each year.

3.4 Measurements

3.4.1 Meteorological measurements

3.4.1.1 Air temperature and solar radiation

During the 2002/03 growth season, solar radiation (R_o, MJ/m^2) was monitored using a pyranometer LI-200SA (LI-COR Inc., Lincoln, Nebrasca, USA) and the air temperature (T_{air}, °C) was measured by a thermistor installed at ~1.50 m above ground, adjacent to plot 5. Both R_o and T_{air} were measured every minute and the average recorded at each 1 hour

interval by a CR10 datalogger (Campbell Scientific, Logan, Utah, USA). The thermistor sensor was installed inside a 0.2 m long polished aluminium tube shelter to remain protected from direct solar radiation and painted black inside to absorb reflected radiation. It was calibrated to a thermometer with 0.1°C precision. During seven days of the experiment, data were not available from I9 loggers due to equipment maintenance or malfunction. Values for those were then substituted with data from "Broadfields Meteorological Station". This represented <1% of daily readings and overall temperature and radiation data from I9 and Broadfields were linearly related (R^2=0.99) with intercept of -0.12±0.1 (P<0.02) and slope=0.99±0.009 (P<0.0001).

During the 2003/04 growth season, a dataTaker logger model 'DT600' (dataTaker Australia Pty Ltd 7, Victoria, Australia) was used. In addition, five tube solarimeters model TSM (Delta-T Devices, Cambridge, UK) were installed at ground level in plots 12, 13, 14 and 15 (2 units) together with one line quantum sensor LI-191SA (LI-COR Inc., Lincoln, Nebrasca, USA) in plot 13. The measurements of solar radiation above canopy were done by the same pyranometer used in the first season (LI-200SA), plus an extra tube solarimeter and one quantum sensor LI-190SA (LI-COR Inc., Lincoln, Nebrasca, USA), all installed 1.8 m above ground. All measurements were taken at 30 second intervals and then averaged and logged at hourly intervals.

3.4.1.2 Soil temperature

Soil temperature was recorded at 150 and 600 mm below ground level in plots 13 and 14. The soil temperatures were recorded at hourly intervals by a 'Hobo 4-channel logger' (Onset Computer Corporation, Bourne, Maryland, USA).

3.4.1.3 Soil water measurements

Water content was measured in the topsoil (0.20 m depth) using a Time Domain Reflectometer (TDR) Trase system, Model 6050X1 (Soil Moisture Equipment Corp., Santa Barbara, USA). From 0.20 m to 2.25 m soil depth, water content was measured using a neutron probe (NP) Troxler model 4300 (Research Triangle Park, NC, USA) at 0.20 m intervals. Measurements were taken at the six points as in a previous experiment at the site (Brown, 2004). These measuring points were located in plots 06, 09, 10, 14 and 15.

Measurements using TDR and NP were taken at around 1 month interval, during the entire experimental period.

Additional measurements related to specific procedures are reported in the relevant chapters.

3.5 Statistical analysis

The experiment was set as a randomized complete block design with four treatments and four replicates (Section 3.3). When comparing growth seasons, results for all variables were analysed as a split-plot design with defoliation regime (LL, LS, SL and SS) as main-plot and growth season (2002/03 and 2003/04) as sub-plots. When necessary, individual regrowth cycles were analysed and compared within each season as a split-plot design with defoliation regime as main-plot and regrowth cycle as sub-plot.

Additionally, linear and non-linear regressions were fitted between dependent and explanatory variables using SIGMAPLOT version 8.02 (SPPSS Inc.) and the regression coefficients and coefficients of determination reported. When appropriate, broken-stick regressions were fitted by the use of a dummy variable to identify the point of breakage (Draper and Smith, 1998) with GENSTAT 7th edition (Lawes Agricultural Trust, IACR, Rothamsted, UK). The accuracy of model simulations was quantified mainly by the value of the root mean squared deviation (*RMSD*) and its components (Section 8.2.7).

The regression coefficients and the results for all evaluated variables were tested using analysis of variance (ANOVA). In all cases, means were compared whenever treatment effects in the ANOVA presented $P<0.05$. Then, a Fisher's protected least significant difference (LSD) was used to separate means at the 5% level ($\alpha=0.05$). The software used for statistical analysis was GENSTAT 7th edition (Lawes Agricultural Trust, IACR, Rothamsted, UK).

4 Perennial dry matter and perennial reserves

4.1 Introduction

The understanding of lucerne yield forming processes involves the quantification of crop physiological responses to environmental (*e.g.* T_{mean}, PAR_i and Pp) and endogenous (*e.g.* C and N reserves) factors (Chapter 2).

To uncouple these two factors, different defoliation regimes were used to create lucerne crops with contrasting levels of perennial reserves (Chapter 2). This involved lucerne crops grazed at different frequencies (regrowth cycle of 28 or 42 days) during different times in the growth season (Chapter 3). Frequent defoliation treatments aimed to limit the acquisition of CO_2 through photosynthesis and nitrogen through mineral uptake (NO_3^-, NH_4^+) or fixation (N_2) in comparison with the 42-day crops. In addition, to enhance differences in the level of perennial reserves, these regrowth cycles were applied interchangeably to two treatments during periods of preferential accumulation (autumn) or depletion (spring/mid-summer) of perennial reserves (Chapter 3).

This chapter reports on the outcomes of this initial procedural requirement. The seasonal patterns of dry matter accumulation of lucerne perennial organs (crowns and taproots) and the concentration of nitrogen and carbohydrate (soluble sugars and starch) of these organs are reported.

4.2 Materials and methods

During each regrowth cycle, crowns and taproots (300 mm depth) were sampled weekly to supply information about the amounts of DM and the concentration of nitrogen, soluble sugars and starch in lucerne perennial organs.

Chemical analysis of nitrogen and carbohydrates was performed exclusively on the taproot fraction of perennial DM. This fraction was used as a reference for chemical composition of perennial DM because: (*i*) taproots are a major storage organ in lucerne (Ourry *et al.*, 1994), (*ii*) the risk of soil contamination in taproot samples is reduced compared with crowns (Fornasier *et al.*, 2003) and (*iii*) taproots are more homogeneous tissues than crowns which can have variable amounts of stem stubble attached. Nevertheless, a set of crown samples were also analysed by wet chemistry to give an indication of the concentration of soluble sugars, starch and nitrogen in relation to the concentration measured in taproots (Appendix 1).

4.2.1 Sampling of perennial dry matter

Samples of perennial DM (crowns and taproots) were collected each 7 days, starting ~10 days after the end of the previous grazing. During winter (June to mid-September), when shoot growth rates were negligible, harvests were extended to every ~30 days. Shoot samples were firstly harvested from a single 0.2 m^2 quadrat, placed randomly in each plot (Section 5.2.1), and then the perennial dry matter was obtained from the same area. To do this, a trench was dug in this area to assess crowns and taproots at a depth of 300 mm. For calculation purposes it was assumed that the sampled tissue represented 80% of total perennial dry matter (Khaiti and Lemaire, 1992).

Crowns and taproots were immediately placed on ice and transported to a cool store (4°C) for further processing. The material was washed free from soil under a stream of cold water and crowns were separated from taproots at the transition zone between tissues. Samples were then frozen at –20°C, freeze dried and weighed. Freeze-dried samples of

crowns and taproots were ground to pass through a 1 mm mesh sieve and stored at room temperature for future chemical analysis.

Samples were collected from 3 replicates during the 2002/03 growth season and 2 replicates during the 2003/04 growth season. The reduction was due to the need to preserve plot area for sampling and the labour intensive and time consuming process of sampling the root system. Therefore, during the 2003/04 season, harvests were alternated in replicates 1-2 and 3-4 at each sampling date. Also, based on the fact that the upper part of taproots is more homogenous in terms of chemical composition (Haagenson *et al.*, 2003a), taproots were split into their upper (<50 mm) and lower (50-300 mm depth) fractions for chemical analysis. This also aimed to quantify the dynamics of reserves in deeper (>50 mm) profiles of taproots.

4.2.2 Total nitrogen analysis

Total nitrogen was analysed from 500 mg samples of plant dry tissue using the Kjeldahl protocol (AOAC, 1995) at the Animal Science facilities, Lincoln University, Canterbury.

4.2.3 Soluble sugars analysis

Sugars were extracted and quantified from a 50 mg DM sample. This was done by incubating samples at 80°C for 30 min with 5 ml of an 80% ethanol solution. Samples were centrifuged for 4 min at 3500 rpm, cooled and the supernatant was transferred to 15 ml glass vials. This procedure was repeated to guarantee total extraction of soluble sugars. The combined supernatants were then placed in a water bath at 70°C and dried with forced air. Ten ml of distilled water was added to dried samples. Three sub-samples of 10 µl were transferred to the wells of a microplate. Two µl of phenol and 100 µl of H_2SO_4 were added to each well. Sucrose standards in 6 dilutions (0 to 800 mg/l) were included with each plate for calibration curves. Absorbance was read at 400 nm wavelength in a microplate reader Model Ceres 900 (Bio-Tek Instruments Inc., Winooski, VT, USA). Concentrations were calculated from standard curves and results reported as a percent of the tissue dry matter.

4.2.4 Starch analysis

The ethanol-insoluble residue of the soluble sugars extraction (Section 4.2.3) was dried free of ethanol in a heating plate at 70°C. Dry pellets were imbibed in 1 ml 2N KOH and placed in a water bath at 100°C for 1 h to gelatinise the starch. After cooling to room temperature, 1 ml of 2N acetic acid was added to each sample to adjust the pH. Starch was digested by adding 2 ml (~50 U) of amyloglucosidase (Sigma Chemical, St. Louis; product A3514) to each tube. Tubes were placed in a water bath at 45°C for 1 h. Samples were then centrifuged at 3500 rpm for 4 min. A 500 µl aliquot was removed, transferred to a new tube and diluted to 10 ml with distilled water. Microplate wells were filled with 20 µl of samples (3 repetitions/sample) and glucose standards (800 mg/l) in 6 dilutions (0 to 800 mg/l). In each well 100 µl of glucose hexokinase (Sigma Chemical, St. Louis; product G2020) was added, plates were then shaken for 1 h at 20°C, and read in a microplate reader Model Ceres 900 (Bio-Tek Instruments Inc., Winooski, VT, USA) at 340 nm wavelength. Readings were calibrated for each plate with glucose standards and results reported as a percent of tissue dry matter.

4.2.5 Total amounts of reserves in taproots

The total amount of reserves of taproots (kg/ha) was calculated from taproot dry matter (t/ha, DM_{root}) multiplied by the fractional concentration of reserves (%DM). This was done for 8 selected final harvests, when treatments were sampled at similar dates. The difference between DM_{root} and the amount of perennial reserves (soluble sugars, starch and crude protein) was termed "structural dry matter". Crude protein was estimated assuming an average concentration of 16% nitrogen (6.25 x $N\%_{root}$) (AOAC, 1995). The assumed proportionality of $N\%_{root}$ and the protein concentration in taproots implies in an oversimplification of the complex dynamics of N in taproot tissues. This adjustment aimed to account for the carbon, hydrogen and oxygen in protein molecules. Structural dry matter was therefore expected to be the taproot fraction composed of mainly of less labile carbohydrates (cellulose, hemicelluloses, pectin), phenols and minerals other than nitrogen but also with the possibility of including labile compounds (*e.g.* amino acids, nitrate, phosphate sugars, organic acids) depending in the level of imprecision of the assumed coefficient of 6.25 x $N\%_{root}$.

4.3 Results

4.3.1 Crown and taproot dry matter

During both growth seasons there was a similar (P<0.32) linear relationship (R^2=0.76, P<0.01) between crown DM and taproot DM for all treatments and defoliation regimes (Figure 4.1). This strong relationship suggested that both organs responded similarly to seasonal signals and defoliation treatments. Therefore, dry matter of both organs were grouped and reported as a single variable denominated perennial dry matter (DM_{per}).

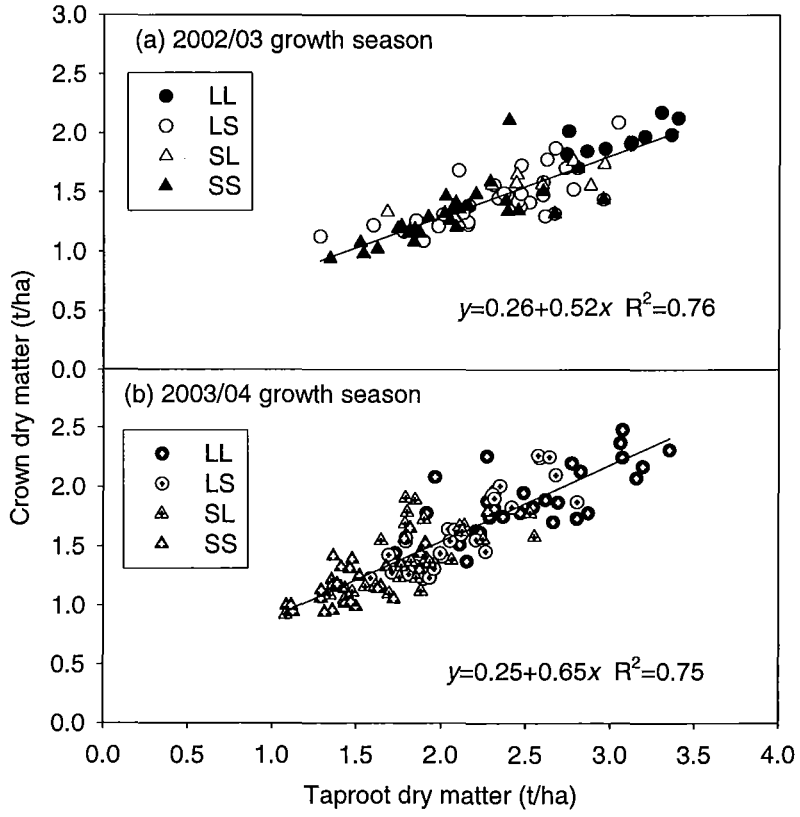

Figure 4.1 Relationship between crown DM and taproot DM (300 mm depth) of lucerne crops subjected to four contrasting defoliation regimes during the 2002/03 and 2003/04 growth seasons at Lincoln University, Canterbury, New Zealand.

Note: Acronyms LL, LS, SL and SS represent defoliation treatments as in Section **3.3.2**

4.3.2 Seasonality and treatment effects on perennial dry matter

Perennial dry matter (DM_{per}) changed ($P<0.01$) throughout each growth season, being greatest ($P<0.05$) during autumn and lowest during summer for all four treatments (Figure 4.2). For example, in August 2002 (winter), prior to treatments being applied, DM_{per} averaged 4.5 t/ha. From this time, DM_{per} decreased ($P<0.05$) in all treatments to a minimum of 2.5-3.0 t/ha in early to mid-summer (Dec 02-Jan 03). From mid-summer to autumn, DM_{per} in LL crops increased to be 5.0 t/ha in mid-autumn (May-June 03). In the 2003/04 growth season, DM_{per} in LL crops showed a similar pattern but at 10-15% higher levels, ranging from 4.0 t/ha in mid-spring (Dec 03) to >5.0 t/ha in mid-summer and autumn (Figure 4.2 *a*).

In contrast, DM_{per} in SS crops was ~2.5 t/ha lower ($P<0.05$) than LL crops from February 2003 onwards (mid-summer, Figure 4.2 *d*). These differences were accentuated in the autumn of 2002/03 and persisted throughout the following regrowth cycles. At this time, $SS_{02/03}$ crops had the lowest ($P<0.05$) DM_{per} of 3.5 t/ha compared with ~4.0 t/ha in $SL_{02/03}$ and $LS_{02/03}$ crops, and 5.0 t/ha in $LL_{02/03}$ crops (Figure 4.2 *b, c*). During the winter 2003, when shoot accumulation was negligible, DM_{per} decreased in all treatments. This decline persisted during the onset of shoot regrowth until September 2003. In the summer period (Jan 04), DM_{per} increased in $LL_{03/04}$ to ~5.0 t/ha but was only 3.0-3.5 t/ha in $SS_{03/04}$ from February to May 2004 (Figure 4.2 *a*). In the autumn 2004, $LS_{03/04}$ and $SL_{03/04}$ crops produced intermediary values of DM_{per} of 4.1 and 4.9 t/ha, respectively. In the third and last spring regrowth, DM_{per} again declined in all the crops to reach values between 3.0 and 4.0 t/ha in October 2004 (Figure 4.2).

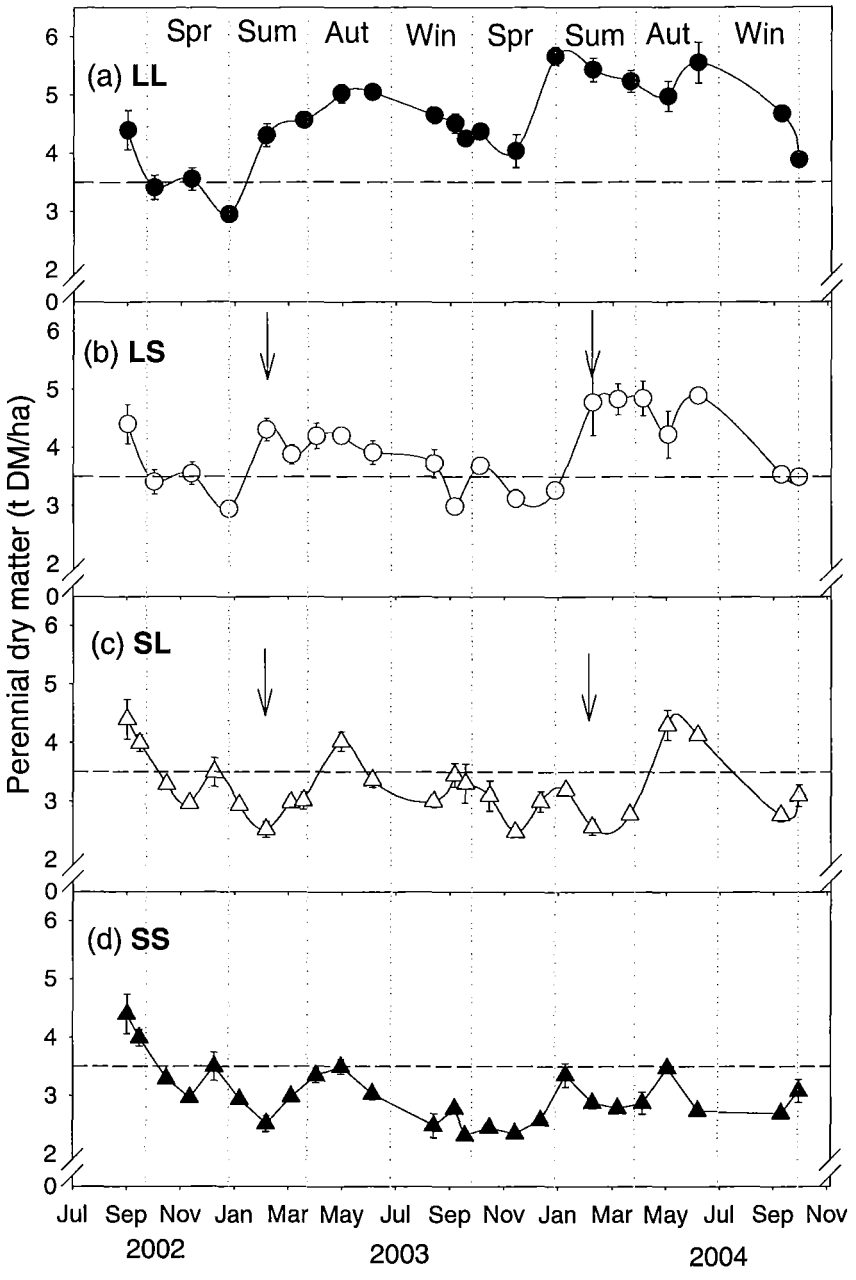

Figure 4.2 Seasonal perennial dry matter (t/ha) at the end of each regrowth cycle of lucerne crops subjected to four contrasting defoliation regimes in the 2002/03 and 2003/04 growth seasons at Lincoln University, Canterbury, New Zealand.

Note: Data-points from samples harvested during winter are also included. Bars represent one SEM for n=3 in the 2002/03 season and n=2 in the 2003/04 season. Dashed line indicates pooled average DM_{per} of 3.5 t/ha. Arrows indicate date of treatment change (4th February).

4.3.3 Soluble sugars concentration in taproots at harvest

The concentration of soluble sugars (*Sugar%*) in taproots during the last harvest of each cycle ranged from 4 to 14% of DM (Figure 4.3). Soluble sugar concentration differed ($P<0.05$) seasonally in all crops. Before treatments were applied (Sep 02), *Sugar%* was ~10% of DM in $LL_{02/03}$ (Figure 4.3 *a*). After that, the *Sugar%* in $LL_{02/03}$ declined to ~6-8% of DM in late summer (Feb 03) and then increased to ~12% of DM in mid-autumn (May 03). In 2003/04 the same seasonal dynamics occurred in $LL_{03/04}$ crops with an even sharper decline in *Sugar%* to ~4% of DM in early-summer (Jan 04), followed by further accumulation in mid-autumn to levels similar to the previous season (11% of DM). This seasonality of response of spring/summer depletion and autumn accumulation of DM was evident in all other treatments but at different levels (Figure 4.3 *b, c, d*).

Frequent defoliations reduced ($P<0.05$) the *Sugar%* of taproots but the response was transient. In $SS_{02/03}$ crops, *Sugar%* declined rapidly once treatments were first applied in September 2002 to ~4-5% of DM (Figure 4.3 *d*). However by mid-summer (Feb 03), the *Sugar%* had recovered to 8% of DM and was then maintained at similar or higher levels to $LL_{02/03}$ following the same seasonal trends throughout the remainder of the experiment.

The response of *Sugar%* to the change in defoliation frequency was more evident in 2002/03, mainly in the crops that had the defoliation treatment changed on 4th February (LS and SL crops). At this time *Sugar%* in $LS_{02/03}$ crops declined sharply from 8 to 4% of DM (Figure 4.3 *b*). These low levels of soluble sugars were maintained until mid-autumn (May 03) when *Sugar%* increased to 11-13% of DM. In the 2003/04 growth season, this response of *Sugar%* to treatments was relatively smaller but the seasonality of response was maintained.

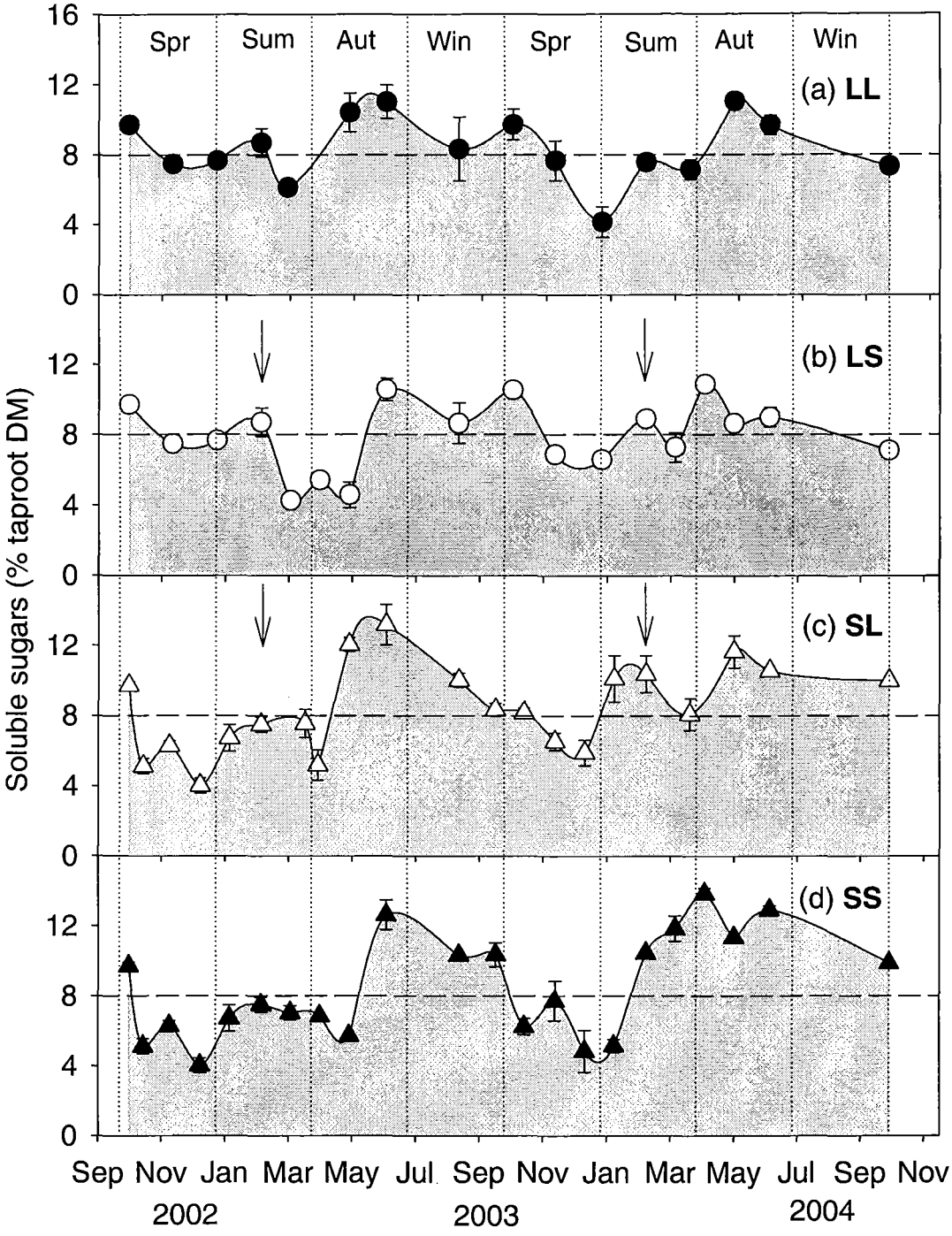

Figure 4.3 Seasonal soluble sugar concentration (%DM) in taproots at the end of each regrowth cycle of lucerne crops subjected to four contrasting defoliation regimes during the 2002/03 and 2003/04 seasons at Lincoln University, Canterbury, New Zealand.

Note: Bars represent one SEM for n=2. Horizontal dashed line represents the *Sugars%* pooled average of 8 % of DM. Arrows indicate date of treatment change (4th February).

4.3.4 Starch concentration in taproots at harvest

The range of changes in taproot starch concentrations (*Starch%*) caused by defoliation regimes was greater than for soluble sugars (Figure 4.4). *Starch%* ranged from a minimum of 2.5% of DM (Figure 4.4 *d*) to a maximum of 28% of DM (Figure 4.4 *a*). In $LL_{02/03}$, *Starch%* increased from 10% of DM in early-spring (Sept 02) to 20% DM in late-summer (Mar 03). *Starch%* then declined sharply to ~13% of DM by mid-autumn (Apr 03) and was maintained close to this level until the following early-spring (Sep 04). From early to late-summer, *Starch%* in LL crops again increased to ~30% of DM by March 04 and then fell throughout the winter period to reach a minimum of 10% of DM in early-spring (Sep 04). This seasonality of accumulation and depletion was again followed by the other crops with a marked effect of defoliation treatments (Figure 4.4).

Defoliation treatments affected *Starch%* in taproots to a greater extent than soluble sugars. For example, at the end of cycles of LL crops, *Starch%* was usually near or greater than the pooled average of 13% of DM (Figure 4.8). In contrast, crops that were subjected to short intervals of defoliation responded rapidly to these treatments with a decrease in *Starch%* in taproots. This caused, for example, SS crops to have lower *Starch%* than the pooled average of 13% of DM throughout the entire experimental period, with the exception of the summer-autumn period of 2003/04, when values for these treatments peaked at 15% of DM (Figure 4.8 *d*). LS and SL crops showed that the response of *Starch%* to defoliation frequency occurred immediately after the shift of regrowth length (4^{th} February). This is highlighted by the sharp increase in taproot *Starch%* of SL crops in late-summer 2003/04 (Mar 04), to levels similar to LL crops at that time (>20% of DM, Figure 4.8 *c*).

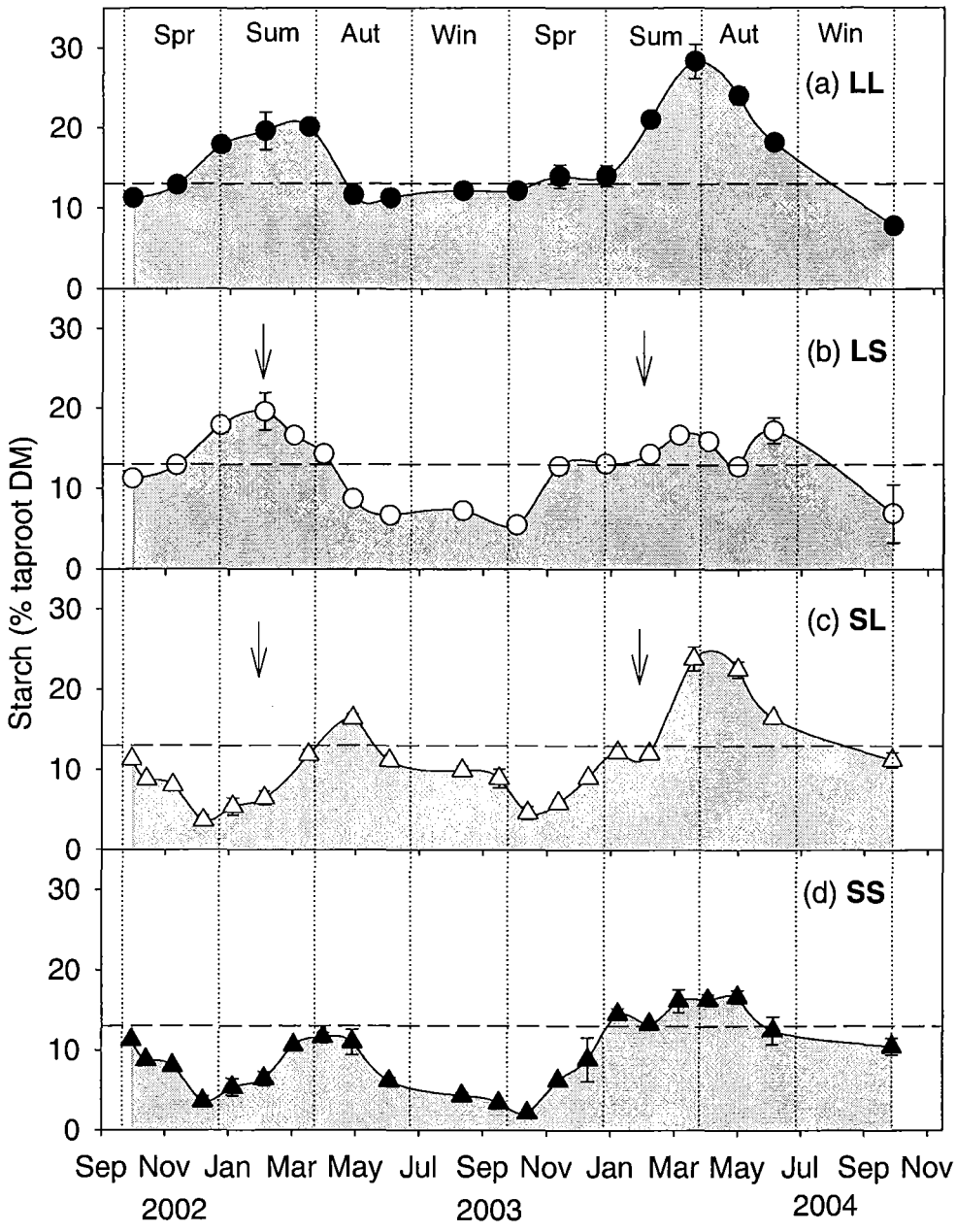

Figure 4.4 Seasonal starch concentration (%DM) in taproots at the end of each regrowth cycle of lucerne crops subjected to four contrasting defoliation regimes during the 2002/03 and 2003/04 seasons at Lincoln University, Canterbury, New Zealand.

Note: Bars represent one SEM for n=2. Horizontal dashed line represents the *Starch%* pooled average of 13% of DM. Arrows indicate date of treatment change (4th February).

4.3.5 Nitrogen concentration in taproots at harvest

The concentration of nitrogen in taproots ($N\%_{root}$) displayed a similar seasonal pattern to carbohydrates (Figure 4.5). In early-spring (Sep 02), before treatments were applied, the nitrogen concentration in taproots was 1.8% of DM. In LL crops this declined to ~1.3% of DM by early-summer (Figure 4.5 *a*). This decline was repeated in 2003/04 and then followed by an increase to ~1.8% of DM in late-autumn of both growth seasons. The seasonal pattern of $N\%_{root}$ was similar in all treatments with greater amplitude in crops grazed with short defoliation intervals. The $SS_{02/03}$ crops displayed a sharp decline in $N\%_{root}$ from mid-spring to late-summer (Dec 02-Mar 03) reaching a minimum of ~1.0% of DM (Figure 4.5 *d*). Over the same period, $N\%_{root}$ in LL crops was >1.3% of DM and reached 1.8% of DM in early-autumn (Figure 4.5 *a*). After the first shift of defoliation treatments (4th February 2003), the $N\%_{root}$ of LS crops declined to similar levels to SS crops (~1.2% of DM) in both growth seasons (Figure 4.5 *d*).

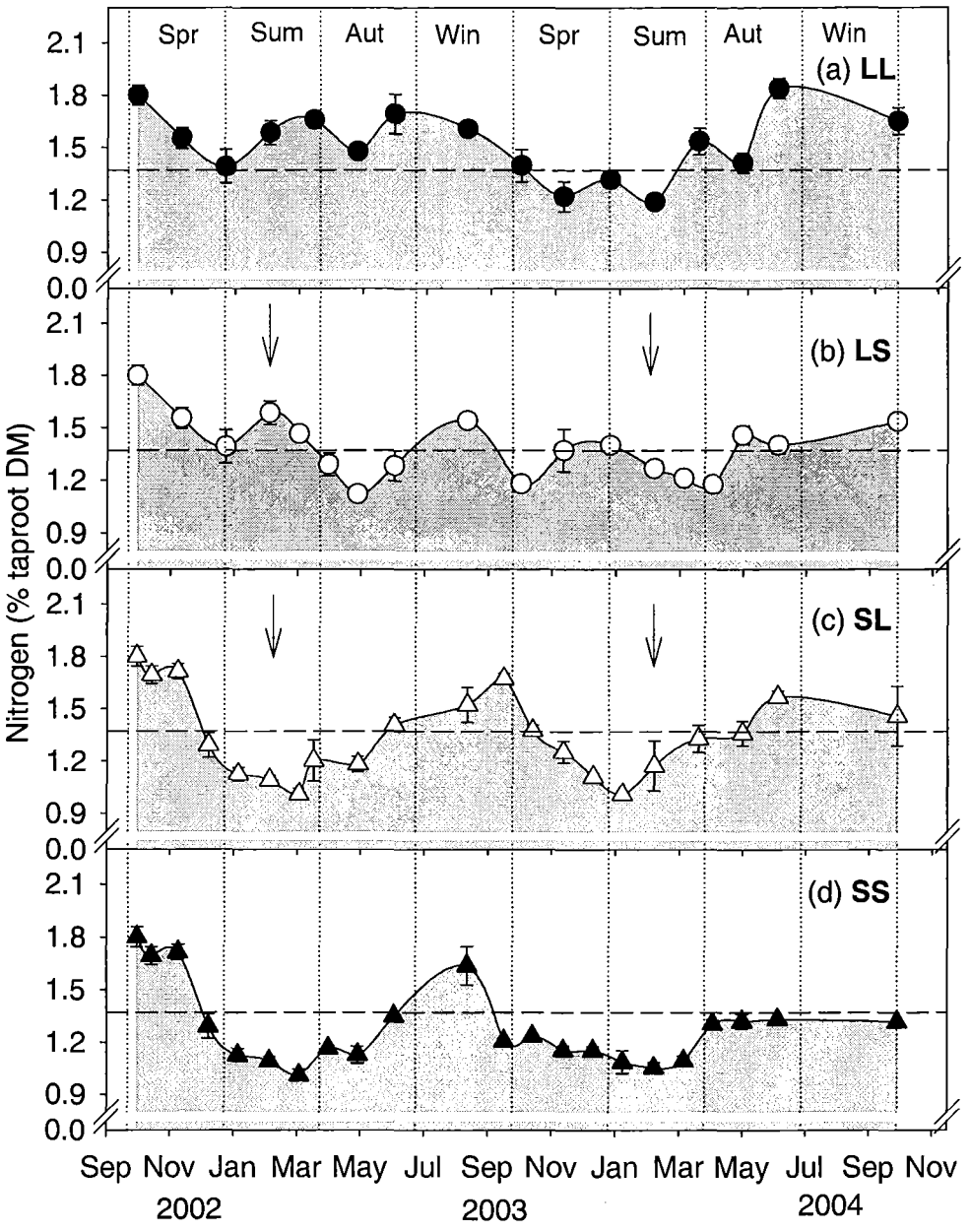

Figure 4.5 Seasonal nitrogen concentration (%DM) in taproots at the end of each regrowth cycle of lucerne crops subjected to four contrasting defoliation regimes during the 2002/03 and 2003/04 seasons at Lincoln University, Canterbury, New Zealand.

Note: Bars represent one SEM for n=2. Horizontal dashed line represents the $N\%_{root}$ pooled average of 1.4% of DM. Arrows indicate date of treatment change (4th February).

4.3.6 Total amount of taproot reserves at harvest

The total amount of carbohydrate and crude protein (6.25 x $N\%_{root}$) in taproots differed seasonally as a function of changes in both taproot dry matter (DM_{root}) and the concentration of reserves (% DM).

The total amount of reserves (kg/ha) accumulated in taproots at the end of a regrowth cycle ranged by ~4 fold for sugars (70 to 300 kg/ha) and crude protein (88 to 350 kg/ha) but up to 8 fold for starch (80 to 650 kg/ha). In most cases these amounts followed the same seasonality observed in perennial dry matter (Figure 4.2) and the concentration of reserves in taproots (Figure 4.3 to Figure 4.5). To illustrate differences the amount of taproot reserves is displayed for pivotal dates of the growing season in the following sub-sections.

4.3.6.1 Taproot reserves prior to defoliation treatments

Prior to the application of defoliation treatments, crops had 2,107 kg/ha of taproot dry matter to 300 mm depth. This dry matter was composed of 238 kg/ha of starch (11% of DM_{root}), 205 kg/ha of soluble sugars (10% of DM_{root}) and 229 kg/ha of crude protein (11% of DM_{root}) leaving 1,435 kg/ha (68% of DM_{root}) of structural dry matter (Figure 4.6).

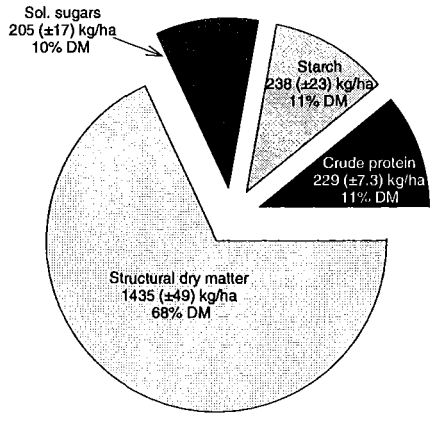

Figure 4.6 Composition of taproots during the early-spring harvest (30 September 2002) of lucerne crops at Lincoln University, Canterbury, New Zealand.

Note: Pie graph includes each mean ± one SEM for n=2.

The ANOVA for comparison of the total amount of reserves among treatments was limited by the sampling and analysis of only two replicates per treatment. For this reason, only the trends in the mean calculated values of amounts of reserves for selected final harvests are presented in the following sections. However, when all selected dates were analysed together (with date as a factor), there was an effect of treatments on the total amount of crude protein ($P<0.05$), sugars ($P<0.02$), starch ($P<0.01$) and to a lesser extent on structural dry matter ($P<0.13$) of crops.

4.3.6.2 Taproot reserves during the late-spring period

By mid-spring (9 November 2003 and 2004), after ~50 days of contrasting defoliation treatments, $LL_{02/03}$ and $SS_{02/03}$ crops were harvested simultaneously and the amount of taproot reserves compared (Figure 4.7). In the 2002/03 growth season, SS crops had 9% less structural dry matter, 37% less soluble sugars, and 53% less starch in taproots than LL crops (Figure 4.7 *a*). Crude protein was ~240 kg/ha in both crops. One year later (9 November 2004), the differences among treatments were accentuated with SS crops having ~50% less crude protein, 76% less starch, 40% less soluble sugars and 40% less structural dry matter than LL crops (Figure 4.7 *b*). By this time, the amount of crude protein in LS crops was similar to LL crops but there was a ~15-20% decline in structural dry matter and soluble sugar amounts and a 30% decline in the amount of starch in taproots. In general $SL_{03/04}$ crops had similar amounts of taproot reserves to $SS_{03/04}$ crops during this period (Figure 4.7 *b*).

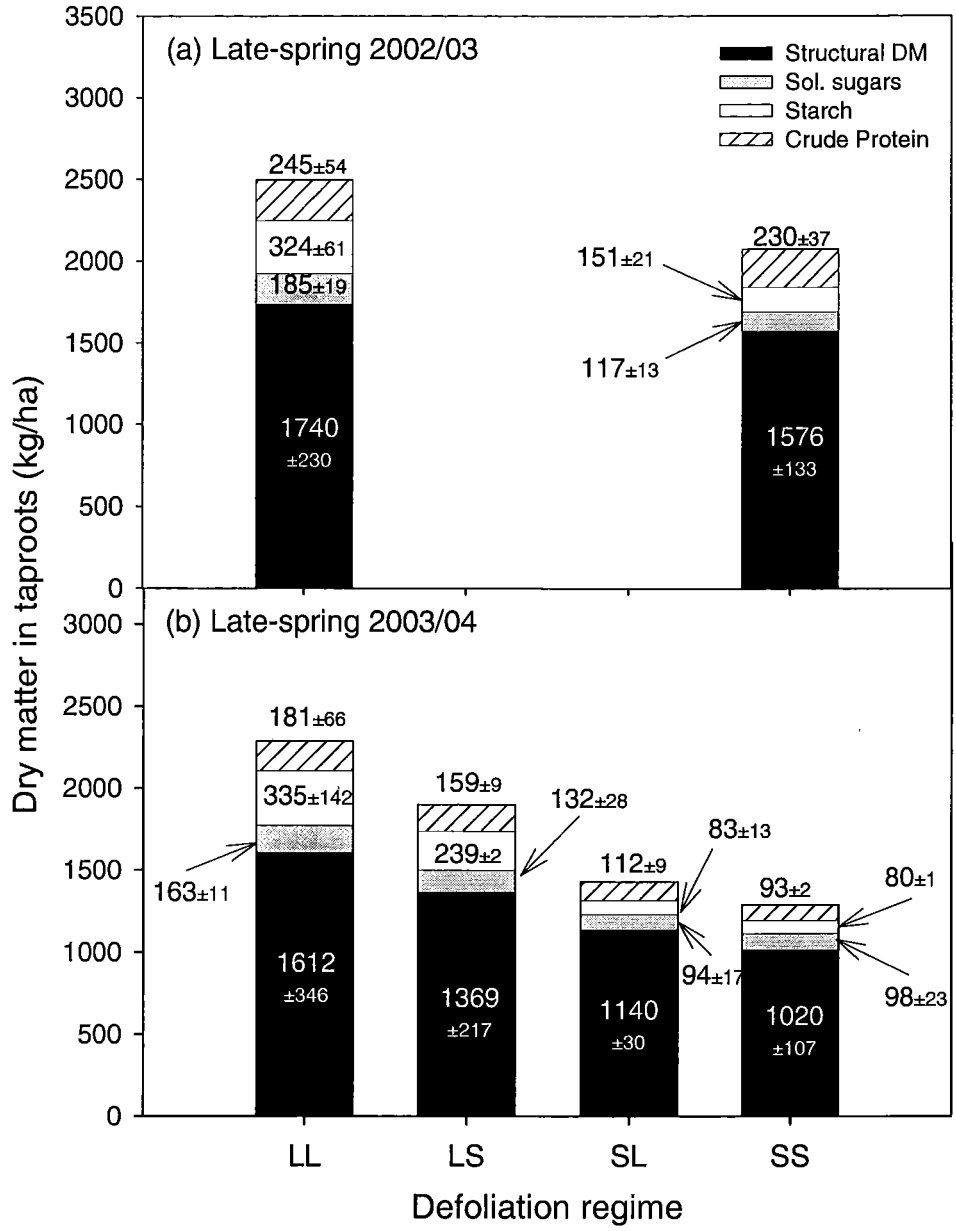

Figure 4.7 Total amount (kg/ha) of structural and reserve components of taproots during the late-spring period of 2002/03 (*a*) and 2003/04 (*b*) in lucerne crops subjected to four contrasting defoliation regimes during the 2002/03 and 2003/04 seasons at Lincoln University, Canterbury, New Zealand.

Note: Late-spring taproot samples refer to harvests at the end of regrowth cycles on 9 November 2003 and 2004. Structural DM was assumed as the difference between total taproot dry matter and perennial reserves (crude protein plus carbohydrates). For each fraction the mean ± one SEM for n=2 is presented.

4.3.6.3 Taproot reserves during the mid-summer period

During the mid-summer harvest (4 February 2003 and 2004) when defoliation treatments where shifted in LS and SL crops, there were marked differences between LL and SS crops with regard to the amount of taproot reserves (Figure 4.8). In the 2002/03 growth season (Figure 4.8 *a*), SS crops had ~57% less crude protein, 78% less starch, 30% less soluble sugars and 22% less structural dry matter than LL crops.

On 4 February 2004 (Figure 4.8 *b*), LL and LS crops had similar amounts of taproot crude protein (~220 kg/ha), soluble sugars (~235 kg/ha), and structural dry matter (~1,900 kg/ha). In contrast, the amount of starch in LS crops was 60% of the LL crop (385 vs. 651 kg/ha). At this time, the amount of crude protein and structural dry matter (107 and ~1,100 kg/ha, respectively) were also similar in SL and SS crops, however both were only 50% of LL crop levels (Figure 4.8 *b*). Similarly, the amount of starch in SL and SS crops was ~70% less than in LL crops taproots. During this time, soluble sugars were 60% (SL crops) and 73% (SS crops) of that in LL crops (Figure 4.8 *b*).

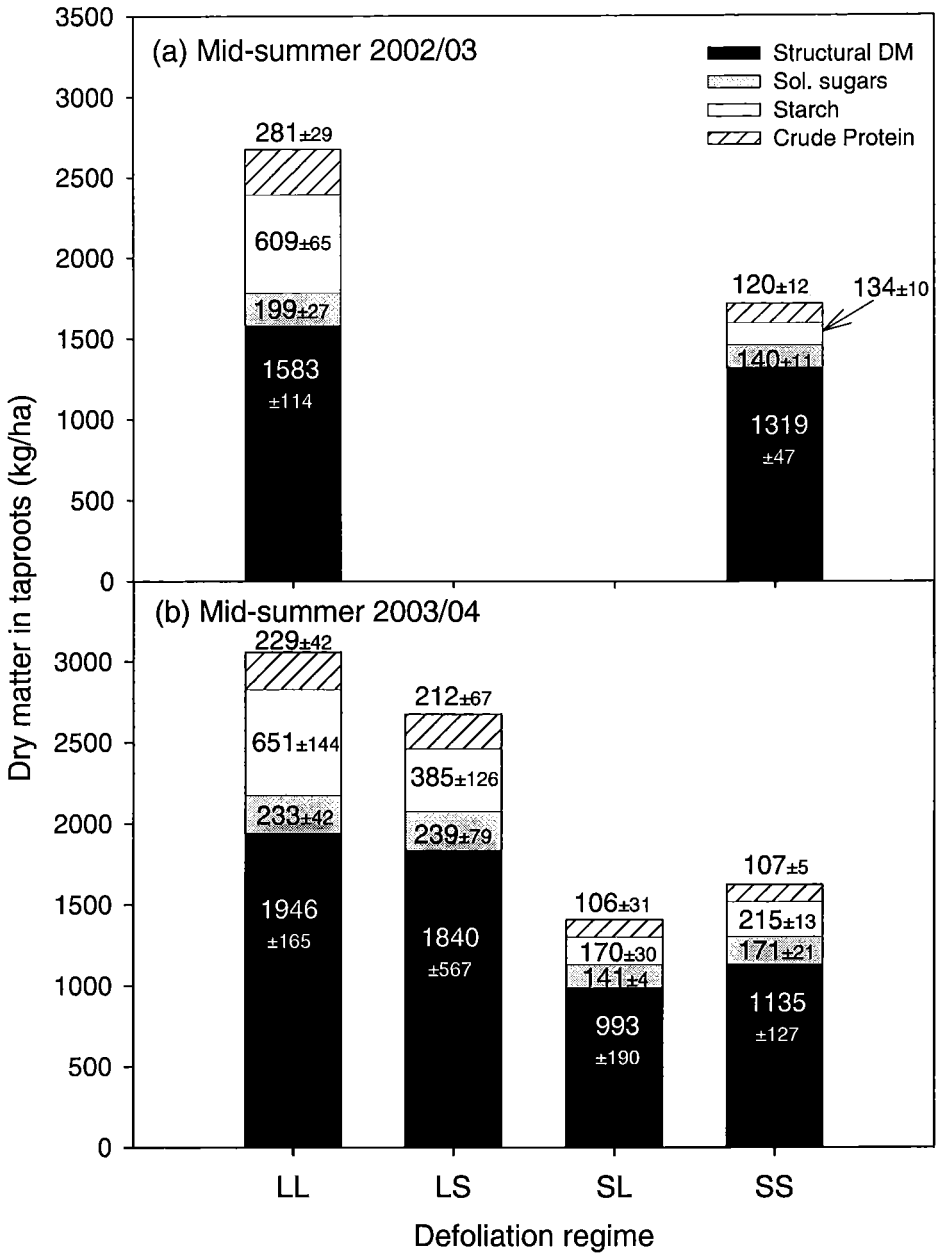

Figure 4.8 Total amount (kg/ha) of structural and reserve components of taproots during the mid-summer period of 2002/03 (*a*) and 2003/04 (*b*) in lucerne crops subjected to four contrasting defoliation regimes during the 2002/03 and 2003/04 seasons at Lincoln University, Canterbury, New Zealand.

Note: Mid-summer taproot samples refer to harvests at the end of regrowth cycles on 4 Feb 03 and 04. Structural DM was assumed to be the difference between total taproot dry matter and perennial reserves (crude protein plus carbohydrates). For each fraction the mean ± one SEM for n=2 is presented.

4.3.6.4 Taproot reserves during the late-autumn period

During late-autumn harvests LL crops had 40% more crude protein than the other treatments, that were similar at 160 kg/ha (Figure 4.9 *a*). Also, in both years there was a recovery of the amount of starch in SL crops in relation to mid-summer levels (Figure 4.8 *b*). Specifically, the autumn starch level in SL crops was 70-90% of the level of LL crops (Figure 4.9) compared with <30% in the previous mid-summer sampling (Figure 4.8 *b*).

This trend of recovery in the reserves of SL crops was most evident in the 2003/04 growth season (Figure 4.9 *b*). The amounts of crude protein (250 kg/ha), starch (505 kg/ha) and soluble sugars (255 kg/ha) in SL crops were 85-90% of LL crops. These levels were all similar to LS crops. The SS crops had only ~30% of the nitrogen and starch, 60% of the soluble sugars and ~50% of the structural dry matter amount of LL crops taproots in 2003/04 (Figure 4.9 *b*).

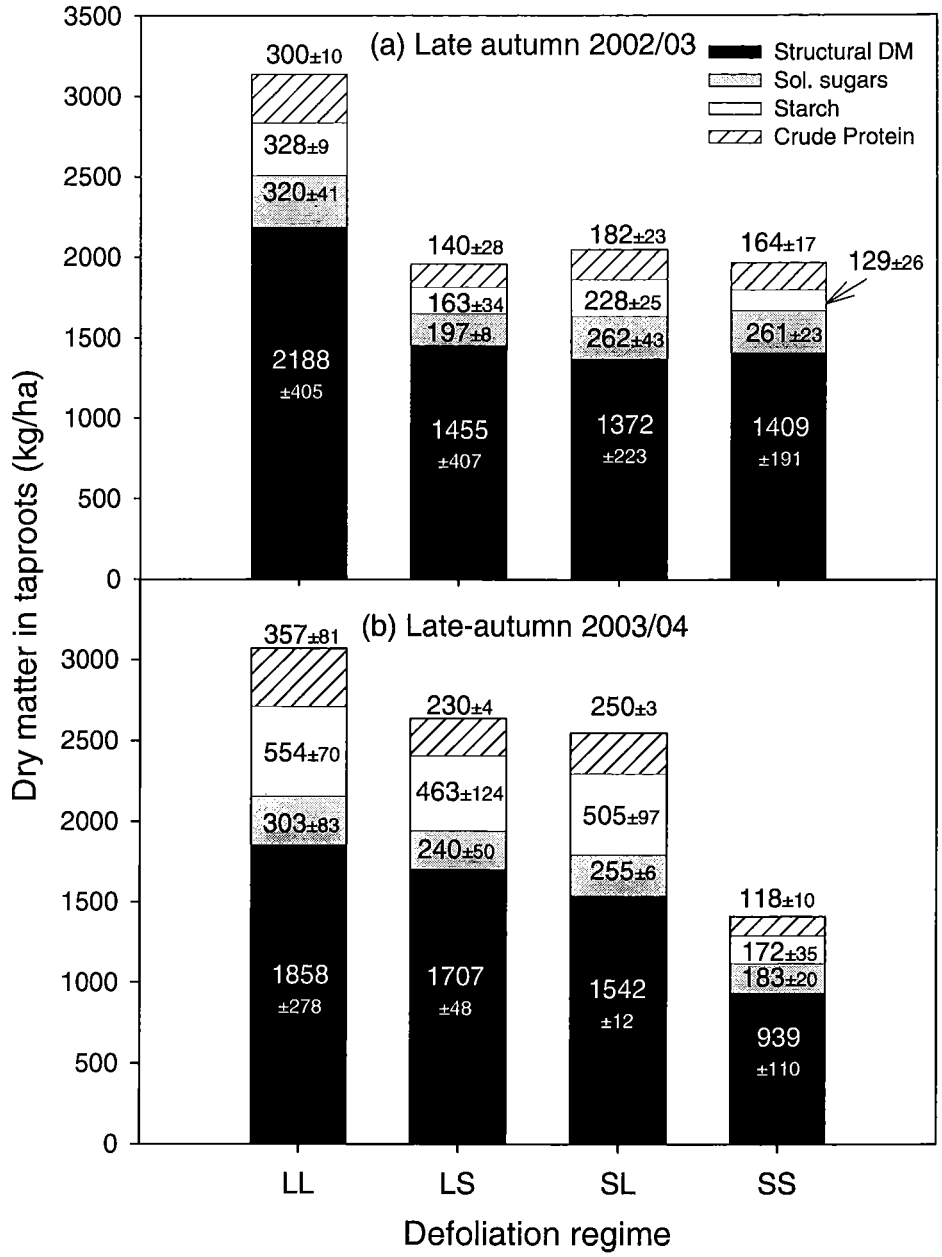

Figure 4.9 Total amount (kg/ha) of structural and reserve components of taproots during the late-autumn period of 2002/03 (*a*) and 2003/04 (*b*) in lucerne crops subjected to four contrasting defoliation regimes during the 2002/03 and 2003/04 seasons at Lincoln University, Canterbury, New Zealand.

Note: Late-autumn taproot samples refer to harvests at the end of regrowth cycles on 2 June 2003 and 31 May 2004. Structural DM was assumed to be the difference between total taproot dry matter and perennial reserves (nitrogen plus carbohydrates). For each fraction the mean ± one SEM for n=2 is presented.

4.3.6.5 Taproot reserves during the early-spring period

During the early-spring harvests, at the onset of the new season regrowth, the relationship among treatments shown in the previous autumn period (Figure 4.9) was relatively maintained (Figure 4.10). In the spring of the 2003/04 growth season (Figure 4.10 *a*), the amount of crude protein in SL and LS crops was 70-100% of LL crops, which highlights the fast recovery of SL crops throughout mid-summer and autumn. Similarly, the amounts of soluble sugar and structural dry matter in these crops were 70 to 90% of LL crops. In contrast, SS crops had only 47% of the crude protein (100 vs. 212 kg/ha), 15% of the starch (45 vs. 293 kg/ha), 60% of the soluble sugar amount (138 vs. 232 kg/ha) and 62% of the structural dry matter amounts of LL crops during this period (Figure 4.10 *a*).

In the spring of the 2004/05 growth season, LL crops had a marked decline in the amount of taproot reserves (Figure 4.10 *b*) when compared with the late-autumn levels (Figure 4.9 *b*). In the first 95 days of regrowth throughout winter and early-spring there was a reduction of 144 kg/ha of crude protein, 393 kg/ha of starch, 155 kg/ha of soluble sugars and 330 kg/ha of taproot structural dry matter. The level of recovery of crude protein amounts, previously observed in SL crops (Figure 4.9 and Figure 4.10), was not evident in the 2004/05 season. However, the amounts of soluble sugars and starch were similar to LL crops. By this time, LL crops had 15-30% more crude protein than the other crops. Starch (~150-185 kg/ha) and soluble sugar (~140-170 kg/ha) amounts were similar among all crops at this period (Figure 4.10 *b*). The amount of structural dry matter was 1,528 kg/ha in LL crops but just 1,042 kg/ha in SL crops with intermediary values observed in SS and LS crops (Figure 4.10 *b*).

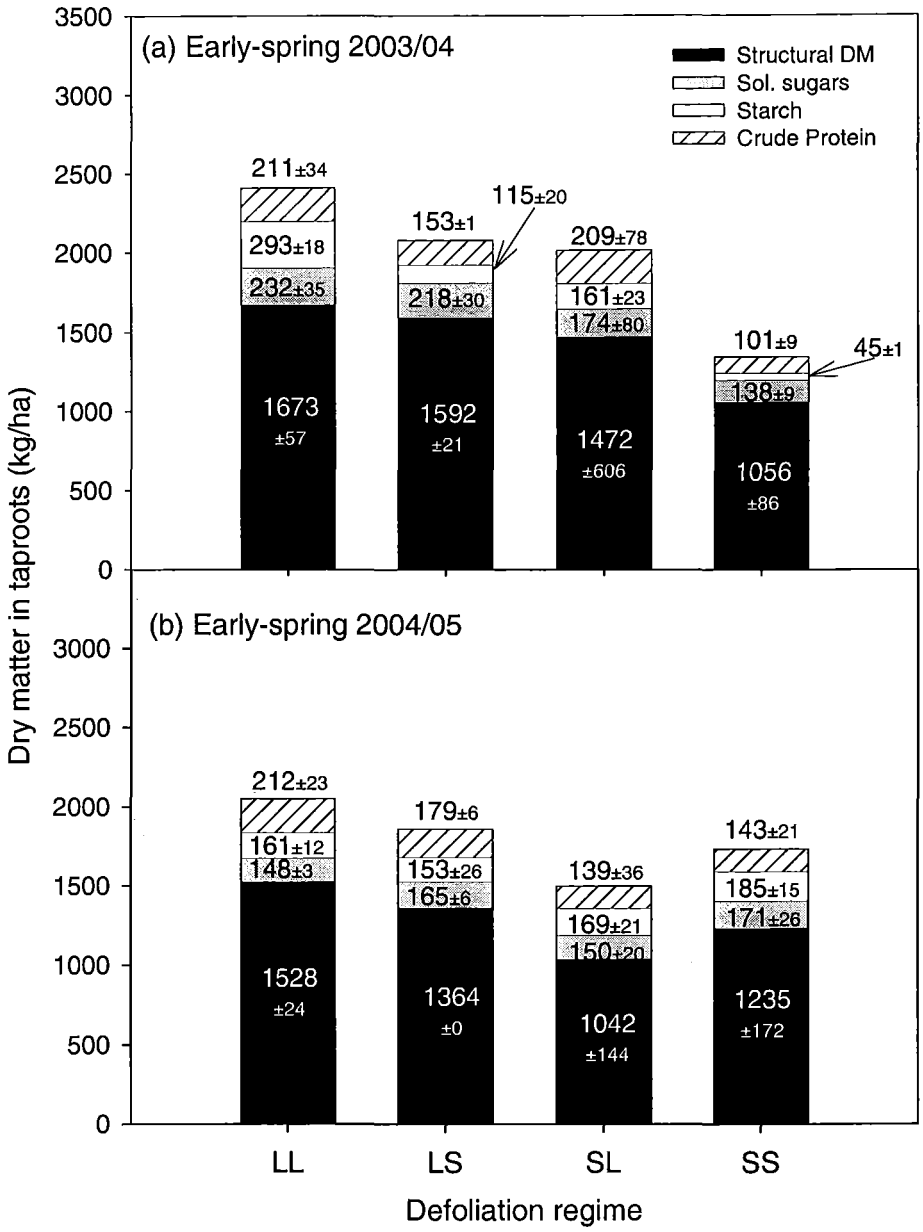

Figure 4.10 Total amount (kg/ha) of structural and reserve components of taproots during the early-spring period of 2003/04 (*a*) and 2004/05 (*b*) in lucerne crops subjected to four contrasting defoliation regimes during the 2002/03 and 2003/04 seasons at Lincoln University, Canterbury, New Zealand.

Note: Early-spring taproot samples refer to harvest at the end of regrowth cycles on 14 Sep 03 (SS and SL crops); 30 Sep 03 (LL and LS crops); and 22 Sep 04 (all crops). Structural DM was assumed to be the difference between total taproot dry matter and perennial reserves (nitrogen plus carbohydrates). For each fraction the mean ± one SEM for n=2 is presented.

4.3.6.6 Dynamics of perennial reserves within a regrowth cycle

The amount of dry matter (DM_{root}, t/ha) and the concentration of organic reserves (% DM) was compared in the upper (<50 mm) and lower (50-300 mm) part of taproots during the late-summer regrowth cycle from 4 February 2004 to 16 March 2004.

Taproot dry matter

In all crops the upper portion of taproots represented ~50% of total taproot dry matter (Figure 4.11). This implies a five fold greater density of dry matter (g DM/mm soil depth) in the first 50 mm horizon of soil when compared with the lower 250 mm.

In the upper part of taproots of LL crops, dry matter was 1.5 t/ha at Day 0 but decreased to 1.0 t/ha at Day 20 (~180°Cd). After that, DM_{root} increased and reached similar levels to those at the beginning of regrowth (Figure 4.11 *a*). The lower part of taproots (50-300 mm depth) showed a similar dynamic, reaching a minimum of 1.0 t/ha at 30 days of regrowth (~280°Cd) and recovering after that to >1.5 t/ha (Figure 4.11 *b*). The SS crops displayed a less pronounced oscillation in DM_{root} being always ≥0.5 t/ha lower than LL crop level in both upper and lower portion of taproots. In general, LS crops followed the trends observed in LL crops but, because they were harvested at Day 28, there was not a complete replenishment of DM_{root} in the lower part of the taproots (Figure 4.11 *b*). Interestingly, SL crops showed a fast recovery of DM_{root} in both parts of taproots until Day 30 (250°Cd) but declined after that to a level of ~0.7 t/ha.

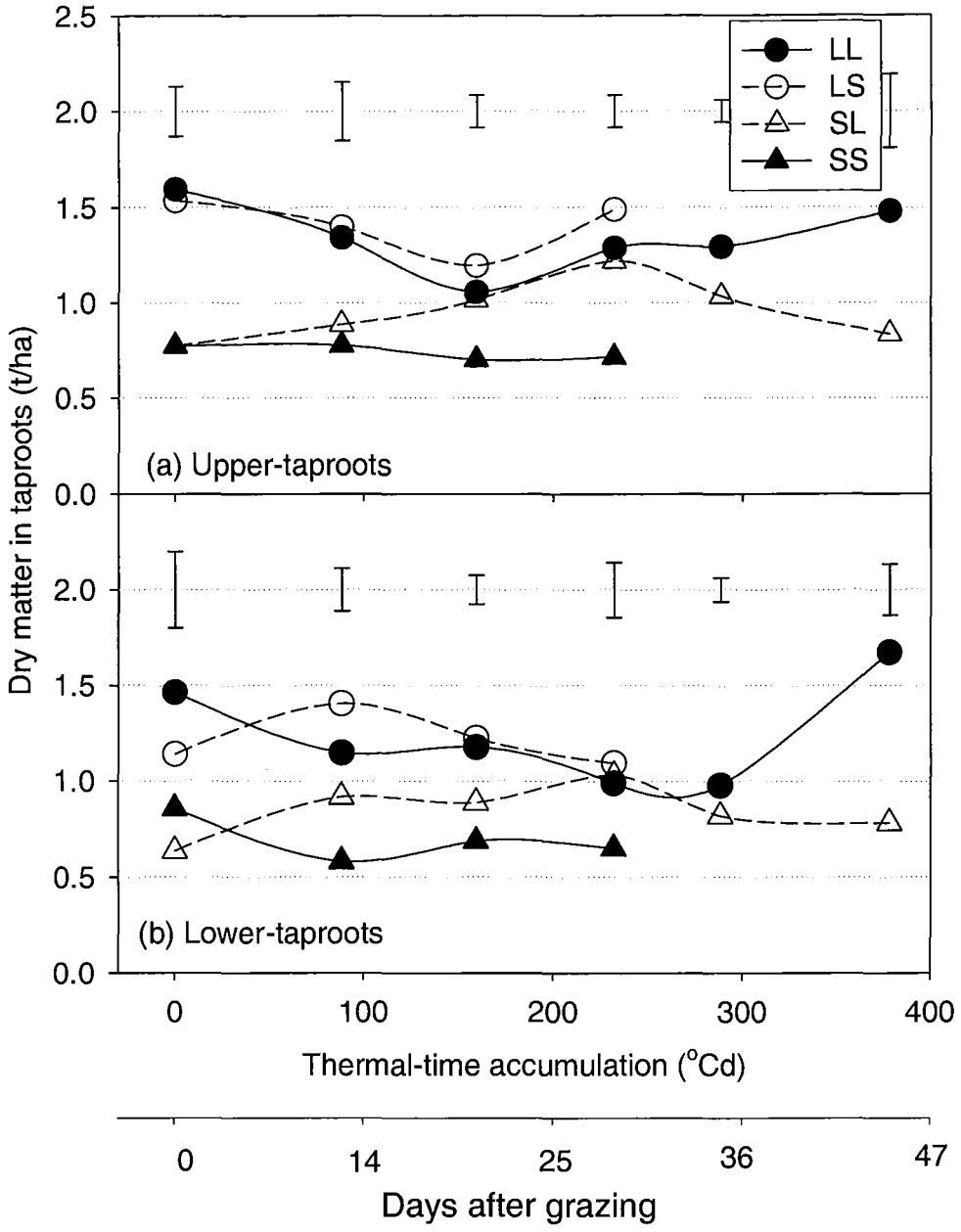

Figure 4.11 The dynamics of taproot dry matter in the (a) upper (0-50 mm) and (b) lower (51-300 mm) part of taproots during the summer regrowth cycle from 4 February 2004 to 16 March 2004 of lucerne crops subjected to four contrasting defoliation regimes during the 2002/03 and 2003/04 seasons at Lincoln University, Canterbury, New Zealand.

Note: Bars represent one SEM for each harvest date, n=2. Upper taproot is the portion of taproot dry matter <50 mm depth and lower taproot from 50 to 300 mm depth.

Soluble sugars concentration in taproots

The concentration of soluble sugars (*Sugar%*) in all defoliation regimes declined in the first 20 days (~150°Cd) but accumulated after that (Figure 4.12). The LL crops had an

initial *Sugars%* of 6-8% of DM at Day 0 but, similarly to the other crops, these dropped to ~4% of DM at Days 15-20 and then increased to 12% at Day 36 (~300°Cd). The *Sugar%* in the upper taproots of SS crops was ~10% of DM at Day 0 but decreased to 4% of DM on Day 20. By Day 28 (~250°Cd), *Sugars%* returned to the initial level of 10% in both taproot depths (Figure 4.12). Both LL and SL crops displayed a rapid decay in *Sugars%* from Day 36 to 42 (300-380°Cd) in both upper and lower taproot after reaching maximum levels of 12% of DM on Day 36 (Figure 4.12 *b*).

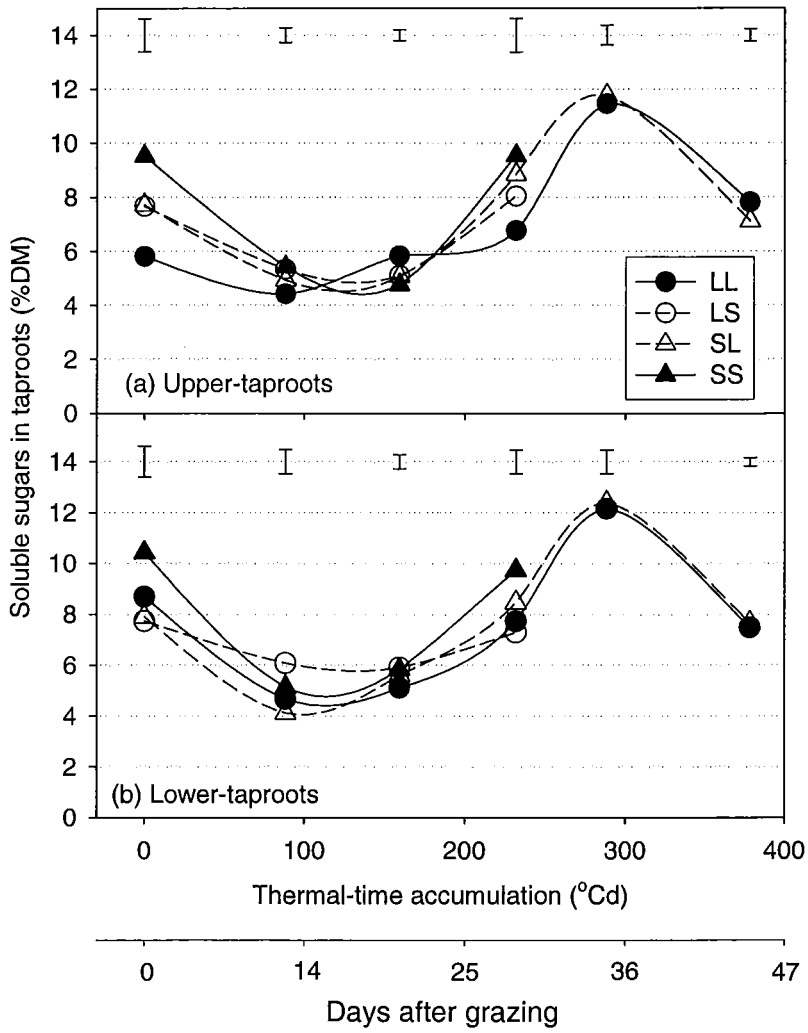

Figure 4.12 Taproot concentration of soluble sugars (%DM) during the summer regrowth cycle from 4 February 2004 to 16 March 2004 of lucerne crops subjected to four contrasting defoliation regimes during the 2002/03 and 2003/04 seasons at Lincoln University, Canterbury, New Zealand.

Note: Bars represent one SEM for each harvest date, n=2. Upper taproot is the portion of taproot dry matter <50 mm depth and lower taproot from 50 to 300 mm depth.

Starch concentration in taproots

The concentration of starch in taproots (*Starch%*) ranged from 10 to 25% of DM depending on the treatment and the period of regrowth. In LL crops, *Starch%* declined from ~20% on Day 0 to ~10% of DM on Day 30 (~250°Cd), this happened earlier in the upper than the lower taproot (Figure 4.13). From then, *Starch%* increased to 13% of DM in the upper and 25% of DM in the lower part of the taproots. In SS crops, *Starch%* was similar to LL crops in the upper taproot but ~50% lower in the lower taproot during the first 20 days (~150°Cd). The longer regrowth (42 days or 380°Cd) for SL crops allowed these crops to reach *Starch%* levels similar to LL crops at the end of the cycle in the upper and lower fraction of taproots (Figure 4.13).

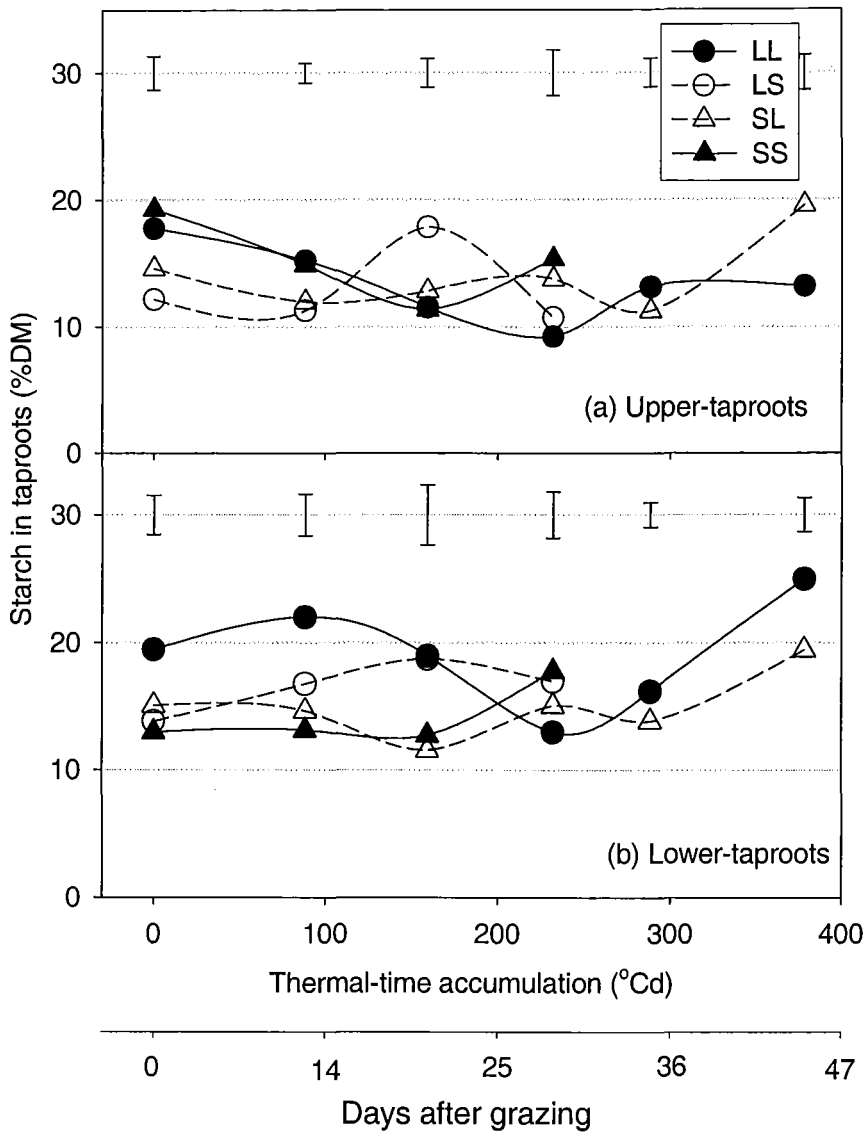

Figure 4.13 Taproot concentration of starch (%DM) during the summer regrowth cycle from 4 February 2004 to 16 March 2004 of lucerne crops subjected to four contrasting defoliation regimes during the 2002/03 and 2003/04 seasons at Lincoln University, Canterbury, New Zealand.

Note: Bars represent one SEM for each harvest date, n=2. Upper taproot is the portion of taproot dry matter <50 mm depth and lower taproot from 50 to 300 mm depth.

Nitrogen concentration in taproots

Nitrogen concentration in taproots ($N\%_{root}$) tended to be maintained or slightly increased from Day 0 to 14 (~100°Cd) in both upper and lower taproots (Figure 4.14). From 14 to 30 days (100-250°Cd) there was a trend of decline in $N\%_{root}$ in all crops with the exception of

LS crops (Figure 4.14). From 30 to 42 days, after LS and SS crops were grazed, both LL and SL crops showed an accumulation of $N\%_{root}$ to levels near 1.5% of DM.

Although differences among treatments were not statistically significant at most of the harvest dates, there was a trend of SL and SS crops having $N\%_{root}$ consistently lower than LL crops throughout the regrowth cycle. The extra 13 days of regrowth for LL and SL allowed these crops to reach $N\%_{root}$ >1.5% of DM in the upper-taproot at Day 42 compared with 1.3% of DM in SS and LS crops at 28 days of regrowth (Figure 4.14).

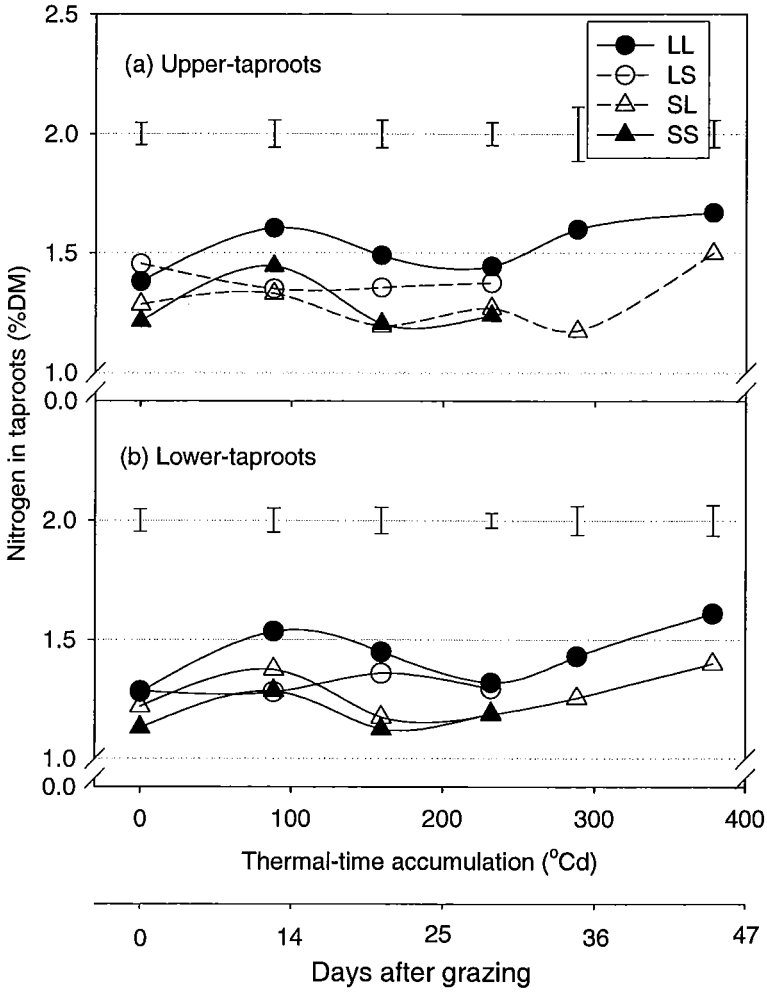

Figure 4.14 Taproot concentration of nitrogen (%DM) during the summer regrowth cycle from 4 February 2004 to 16 March 2004 of lucerne crops subjected to four contrasting defoliation regimes during the 2002/03 and 2003/04 seasons at Lincoln University, Canterbury, New Zealand.

Note: Bars represent one SEM for each harvest date, n=2. Upper taproot is the portion of taproot dry matter <50 mm depth and lower taproot from 50 to 300 mm depth.

4.4 Discussion

The use of the defoliation regimes (Section 3.3) effectively created differences in the amounts and levels of perennial reserves among lucerne crops. Therefore the first objective of this experiment (Section 1.2) was achieved by setting a framework where the effect of perennial reserves on the seasonal yield and development of lucerne crops may be quantified (Chapters 5 to 7).

4.4.1 Perennial dry matter

The partitioning of dry matter to taproots and crowns responded similarly to treatments and seasonal signals (Figure 4.1). On average, taproot dry matter increased at twice the rate observed in crowns. These results suggest that both organs are important as storage compartments of perennial reserves, but taproots (300 mm depth) represent a larger fraction of perennial DM, as previously observed by Fornasier *et al.* (2003).

During the first five months after the application of defoliation treatments (Sep-Jan 03) there was no difference in DM_{per} among treatments (Figure 4.2). This implies that defoliation frequency had a minimal influence on the partitioning of dry matter to perennial organs during spring and mid-summer. At this time, dry matter partitioning to crowns and taproots was insufficient to compensate for losses in DM_{per}, which led to a consistent decline of ~10 kg DM/ha/day in all treatments. A similar seasonal depletion of lucerne fine roots in spring-summer was reported by Luo *et al.* (1995), who observed a 45% decline in root dry weight during this period. The insensitivity of DM_{per} to defoliation regimes in spring-summer suggests that dry matter allocation prioritized shoot growth ahead of perennial organs at this period. The decline in DM_{per} during spring-summer can be seen as a negative carbon balance in perennial organs with demand (*e.g.* maintenance respiration and mobilization to shoots) being greater than supply (*e.g.* C flux from shoots) leading to the need to use glucidic reserves. The low allocation of C to perennial organs in spring-summer could be a response to environmental stimuli (Section 2.6).

From mid-summer to autumn there was an increase in the allocation of dry matter to perennial organs at ~20 kg DM/ha/day in both $LL_{02/03}$ and $SS_{02/03}$ crops (Figure 4.2 *a, d*).

Similarly, Dhont *et al.* (2002) observed an increase in lucerne root weight from ~2.0 g/plant in summer to 4.5 g/plant during autumn in Canada (~46°N). The direction of DM allocation to perennial organs in mid-summer/autumn was also not influenced by defoliation treatments, and mimicked the seasonal accumulation of carbohydrates and nitrogen in taproots described by Cunningham and Volenec (1998).

Overall the seasonal pattern of DM partitioning to perennial organs was unaffected by defoliation treatments but short regrowth cycles reduced DM_{per}. Frequent defoliations reduce the photosynthetic activity of crops and consequently the supply of carbon to perennial organs (Richards, 1993). The average 13 less days in the cycle length for SS crops reduced DM_{per} by ~35-45% in relation to LL crops. Similarly, Gramshaw *et al.* (1993) observed a 20% reduction in taproot reserves when cutting interval was shifted from 35 to 21 days. This confirms that most of the allocation of DM to storage organs, within each regrowth cycle, occurred after 15-20 days from defoliation, as previously demonstrated by other authors (Habben and Volenec, 1990; Heichel *et al.*, 1988).

The amount of DM_{per} declined throughout both winters at ~5-10 kg DM/ha/day in all crops. Considering that growth is negligible during this period (Section 5.3.2), most of the decline in DM_{per} can be attributed to root maintenance respiration (R_m). The root *Rm* at 20°C is commonly reported to be in the range of 1.0-3.0%/day for lucerne (Durand *et al.*, 1991) and cereal crops (Hay and Walker, 1989b). The reduction in DM_{per} from May to September averaged 0.35% DM/day (~0.10-0.75%). It is possible that the low rates of decline in DM_{per} during winter resulted from a temperature effect on R_m. Rates of root R_m respond exponentially to temperature by a Q_{10} of ~1.1-2.9 (Atkin *et al.*, 2000). Soil temperatures in Canterbury during winter were ~7°C, which should bring R_m to less than 0.5% depending on the values of R_m, Q_{10} at 20°C. There is great uncertainty about these parameters and a general lack of understanding of root respiration (Atkin *et al.*, 2000). The consistency of the patterns of accumulation and depletion of DM_{root} however gives an important insight into the possibility to model these processes. A lucerne simulation model will be used to test hypotheses about root R_m patterns in Chapter 8.

The LS and SL crops offer a framework to investigate the sensitivity of DM_{per} to defoliation treatments. Treatments limited the accumulation of DM_{per} to a greater extent than the growth of shoots in autumn. By June 2003, DM_{per} of $LS_{02/03}$ was 20% lower (Figure 4.2) than $LL_{02/03}$ but the shoot yield of both treatments was similar (Section 5.3.2).

This high sensitivity of perennial dry matter to autumn defoliations was also observed by Dhont *et al.* (2004), who reported a decline of 30% in lucerne root dry matter when an extra harvest was applied in autumn (400°Cd after the last summer cut) compared with undefoliated crops.

In the same way, the long autumn defoliation interval of the SL crop restored part of the DM_{per} lost during spring-summer (Figure 4.2 *c*). These results support the suggestion that long periods of regrowth (*e.g.*>35 days) in mid-summer/autumn are required to recover DM_{per} (Moot *et al.*, 2003).

4.4.2 Concentration of perennial reserves in taproots

The concentration of nitrogen, soluble sugars and starch in taproots also differed seasonally. The overall results suggest a strong environmental control of the mobilization of reserves in lucerne taproots, which agrees with previous research (Avice *et al.*, 2001; Louahlia *et al.*, 1998). The physiological mechanisms that drive such processes are not fully quantified (Section 2.6), but gene activation and morphogenetic responses to photoperiod and temperature were suggested to be involved in the control of DM partitioning in lucerne (Gosse *et al.*, 1984; Noquet *et al.*, 2001).

4.4.2.1 Concentration of soluble sugars in taproots

Regardless of defoliation treatment, the concentration of soluble sugars in taproots tended to an adjustment to similar seasonal values in all treatments (Figure 4.3). This suggests a homeostatic regulation of *Sugar%* to an equilibrium possibly controlled by external signals. The largest changes in *Sugar%* were observed in the first half of the 2002/03 growth season, as a short-term response to first imposition of frequent defoliations. At this time, *Sugar%* declined in SL and SS crops from 8% DM in September to 4% DM by December 02 (Figure 4.3 *c, d*). The same short-term response was observed in LS crops on 4th February 2003, when these crops were first subjected to short regrowth cycles. After that, notably in the 2003/04 growth season, the *Sugar%* returned to similar levels in all crops following almost exclusively the common seasonal patterns. The short-term decline of *Sugar%*, when short cycles were initially applied, indicates that this fraction was rapidly mobilized to meet the post-harvest demand for carbon (*e.g.* respiration, translocation and

growth) of lucerne shoots and roots. The implication is that, in the long-term, *Sugar%* in taproots was not a strong predictor of the carbohydrate status of lucerne crops. The maintenance of high levels of *Sugar%* during winter (Figure 4.3), while *Starch%* was declining (Figure 4.4), suggests that during this period starch was hydrolysed into soluble sugars (Li *et al.*, 1996) which were not consumed due to slow metabolism at low temperatures (Haagenson *et al.*, 2003b). The level of specific soluble sugars (*e.g.* raffinose and stachyose) was shown to increase during winter and this may be related with cryoprotective processes in lucerne plants (Dhont *et al.*, 2002).

Nevertheless, seasonal signals influenced *Sugar%*, as demonstrated by the consistently greater levels (~10-12% DM) during mid-autumn/winter than spring-summer (~4-6% DM) despite differences in taproot biomass. Morot Gaudry *et al.* (1987) quantified a ~2.4 fold greater partitioning of ^{14}C to lucerne roots in autumn than spring, 40-80% of this being recovered as soluble sugars (~85% as sucrose). This seasonal pattern also agrees with the observations of Cunningham and Volenec (1998), who reported that *Sugar%* levels increased from 7% DM in summer to 16% DM in autumn in field grown lucerne.

4.4.2.2 Concentration of starch in taproots

The concentration of starch in taproots (*Starch%*) was consistently reduced by short regrowth cycles (Figure 4.4). This can be highlighted by the range of variation of *Starch%* in LL crops (~10-30% DM, Figure 4.4 *a*) in comparison with SS crops (~3-15% DM, Figure 4.4 *b*). Other authors also reported variations greater than 5 fold in *Starch%* (Avice *et al.*, 2001). For example, Avice *et al.* (1997a) observed *Starch%* decline from 11.5% DM in crops defoliated each 45 days to 4.5% DM in crops defoliated each 30 days, but the level of response differed between lucerne cultivars. Starch is the main form of carbon storage in lucerne (Heichel *et al.*, 1988) and it is cyclically consumed after defoliation (Nelson and Smith, 1968; Pearse *et al.*, 1969b). The storage of starch is an active process as energy is needed to transport carbohydrates across membranes (Lemaire and Millard, 1999). This together with the resistances of C transport from a distant source (*i.e.* leaves) makes starch storage only occur when other sinks are satisfied (Lemaire and Millard, 1999). Therefore *Starch%* declines when the regrowth length is too short to allow sufficient carbon assimilation to compensate for losses from respiration, translocation to shoots, exudation and decay of perennial organs.

The levels of *Starch%* differed seasonally with the lowest levels observed in mid-spring and the highest in early-autumn (Figure 4.4). This agrees with Cunningham and Volenec (1998) who showed that starch accumulation resumed in mid-spring reaching 27% DM by summer and declining through autumn-winter to less than 6% DM by the following early-spring. These changes are partially explained by the seasonal activity of endoamylases in lucerne roots (Li *et al.*, 1996). The implication in terms of lucerne management is that, frequent defoliations in a period of intense accumulation of starch, reduce the level of reserves available for the following spring. This was the case for *Starch%* that was ~25-30% lower in LS crops than in LL crops during April of both growth seasons (Figure 4.4 *a, b*). Haagenson *et al.* (2003b) also observed that defoliation in early-autumn caused a decline of 30% in *Starch%*, but this effect was diminished as the date of harvest advanced to near winter. In the current experiment, the critical period for starch accumulation started in mid-spring/summer (Figure 4.4), and therefore it can be expected that frequent defoliations at any stage of this period will limit starch accumulation.

4.4.2.3 Concentration of nitrogen in taproots

Frequent defoliations (SS crops) reduced $N\%_{root}$ by up to 30% compared with LL crops (Figure 4.5 *a, c*). Similarly, Avice *et al.* (1997a) observed a decline in $N\%_{root}$ when crops were defoliated each 30 days rather than 45 days. The reduction was probably caused by limited N assimilation through a decline in the rate of mineral N uptake and N_2 fixation (Section 2.6.2). This was particularly apparent in the first two weeks after harvest, which represented relatively more time in the 28 day (short) than in the 42 day (long) crop. Therefore, long cycle crops had more time to restore the levels of N in perennial organs.

Regardless of defoliation regime, all crops showed a marked seasonality in $N\%_{root}$ (Figure 4.5) which suggests a strong environmental control. Low temperatures and short photoperiods were shown to increase the allocation of nitrogen to lucerne roots (Noquet *et al.*, 2001). Under controlled conditions, a reduction in the photoperiod from 16 h to 8 h resulted in a 3 fold increase in the concentration of nitrogen in taproots (Noquet *et al.*, 2003). These authors suggested that the phytochome system may be involved in the process because an interruption of 15 min in the dark period at short *Pp* cancelled the accumulation of 32 and 57 kDa VSPs.

4.4.3 Total amounts of reserves in lucerne taproots

The total amount of reserves in taproots was more sensitive to defoliation treatments then the concentration of nitrogen and carbohydrates. Explanatory relationships between physiological traits of lucerne and perennial reserves can be improved when reserves are expressed as total amounts instead of concentration (Dhont *et al.*, 2002; Nelson and Smith, 1968). For example, while $N\%_{root}$ changed by 2 fold (~1.0 to 2.0% of DM) throughout treatments and seasons, the actual amount of nitrogen (*i.e.* 0.16 x crude protein) changed by 4 fold (~90 to 350 kg/ha).

Starch and crude protein were the most sensitive fractions to defoliation treatments as their concentrations were also affected by treatments (Section 4.3). Changes in the soluble sugars amounts in general followed the changes in taproot biomass (DM_{root}) because *Sugar%* was relatively insensitive to treatments (Section 4.3.3).

Structural dry matter ranged 2 fold among treatments and seasons from 1,000 to 2,100 kg/ha. The structural dry matter was also affected by treatments but declined slower than reserves concentration (*e.g.* SS crop in Figure 4.7). This indicates a slow consumption and decay of the poor labile components of taproots. Data from Avice *et al.* (1996) suggests that less labile carbohydrates, such as hemicellulose, can also be mobilized after defoliation which would contribute to the decline in taproot structural DM. This was possibly the case for SS crops that often had the lowest amounts of structural DM (Figure 4.7 to Figure 4.10). Nevertheless, the uncertainty about the actual amount of crude proteins in taproots, due to the simple assumption of proportionality between crude protein and $N\%_{root}$ (Section 4.2.5), would affect the estimation of structural DM. The protein content of taproots (mainly soluble proteins) is known to fluctuate independently of the level of N in taproots (Li *et al.*, 1996). Therefore part of the differences in the structural dry matter could be caused by the mobilization of labile compounds (*e.g.* amino acids, nitrate) that were included in this fraction as an artefact of the calculation method, which assumed a proportionality between crude protein and $N\%_{root}$.

The analysis of amounts of reserves was particularly useful to quantify the changes observed in LS and SL crops. The shift of defoliation frequency on 4th February was

sufficient to deplete LS reserves and enhance SL crop reserves through late-autumn (Figure 4.9). Several authors have shown that autumn defoliations cause depletion of reserves in lucerne taproots (Section 2.6). This effect was more pronounced in LS and SL crops after the shift of treatment (Figure 4.2) which is consistent with previous results (Dhont *et al.*, 2002).

4.4.4 Dynamics of taproot reserves within cycles

The total amount of taproot at 300 mm depth ranged from 0.5 to 1.8 t/ha which is close to values reported for field grown lucerne (Lemaire *et al.*, 1992; Nelson and Smith, 1968). The cyclic mobilization of reserves after harvest was observed in both strata (<50 mm and 50-300 mm depth) of taproots (Figure 4.11 to Figure 4.14). This indicates that the patterns of respiration (*e.g.* carbohydrate dynamic) and translocation of matter (*e.g.* nitrogen dynamic) to shoots were similar throughout the 300 mm profile. Nevertheless, the first 50 mm of soil contained ~50% of the taproots dry matter from the 300 mm profile (Figure 4.11) which gives a 5 fold greater root DM density for this upper profile.

After defoliation, the soluble sugar fraction (*Sugar%*) showed the clearest pattern of mobilization, which was similar regardless of defoliation regime (Figure 4.12). This indicates the transient nature of soluble sugars in taproots, which reflects the balance between supply and demand of carbon among plant organs. In this sense, *Sugar%* represents the net result of the equilibrium among physiological processes (*i*) photosynthesis, (*ii*) carbon partitioning to perennial organs, (*iii*) starch degradation and accumulation, and (*iv*) taproot respiration. This explains the trend of *Sugar%* to return to equilibrium (Figure 4.3) after an initial response to imbalances in source/ sink relationships (*e.g.* defoliation event).

In general, regardless of defoliation treatment, the maximum mobilization of starch from taproots occurred with a delay of 10-15 days in relation to *Sugars%*. It seems likely that soluble sugars were immediately consumed to supply carbon skeletons and energy for metabolic processes after photosynthesis ceased with defoliation. Once used, the degradation of starch followed to restore *Sugars%* in taproots. For example, at 250°Cd, when *Starch%* reached minimum values (Figure 4.13), the *Sugar%* was already increasing to similar levels as before defoliation (Figure 4.12).

The concentration of nitrogen in taproots ($N\%_{root}$) tended to increase in most crops during the first sampling date after defoliation (Figure 4.14). This reflected the relative accumulation of this fraction in taproot DM due to the rapid mobilization of soluble sugars in the early stages of regrowth.

The changes in the concentration and the amounts of perennial reserves in these crops are expected to influence shoot growth and development (Section 2.6). The following chapter explores the agronomic aspects of shoot yield and its components as related to defoliation treatments and levels of perennial reserves.

4.5 Conclusions

The results of this chapter permit the following conclusions:

- The use of the defoliation treatments was effective in creating contrasting levels of dry matter (~2.5 to 5.5 t/ha) and different concentrations of nitrogen and carbohydrates in perennial organs.

- Frequent defoliations (28-day cycle) reduced the absolute amounts of perennial DM and the amounts and concentrations of nitrogen and starch in taproots.

- The concentration of soluble sugars was similar among treatments, apart from a short-term decline immediately after the application of short regrowth cycles.

- The defoliation frequency imposed specifically during mid-summer/autumn (*e.g.* LS and SL crops) was important in defining the level of reserves for the following spring growth.

- Total amounts of perennial dry matter and the concentrations of carbohydrates and nitrogen in perennial organs followed a seasonal pattern in all crops. In general, perennial reserves declined during winter to mid-summer and increased from mid-summer to late-autumn. However, specific patterns differed as influenced by defoliation treatments.

- The seasonal patterns and treatment effects on perennial DM were more evident in the absolute amounts of reserves rather than their concentrations. This was because structural DM also differed with seasons and defoliation treatments.

5 Lucerne yield and yield components

5.1 Introduction

Appropriate management practices for lucerne crops depend on an understanding of how crop growth and development respond to environmental (*e.g.* temperature, radiation and photoperiod) and endogenous (*e.g.* perennial reserves) factors. To uncouple these factors requires crops with different levels of reserves but similar morphological characteristics (*e.g.* residual *LAI*, meristem number) grown in a changing environment (Chapter 2). This was achieved through the use of the four different defoliation regimes (Chapter 3) which created crops with contrasting levels of perennial reserves (Chapter 4).

The impact of these treatments and consequent levels of perennial reserves on shoot yield were assessed by quantifying the composition of leaves, stems and senesced material for each regrowth cycle/treatment combination. Additionally, shoot yield was segmented into yield components of plants/m^2, shoots/plant and individual shoot mass (Volenec *et al.*, 1987). Limiting levels of perennial reserves can affect one or more of the lucerne yield components by (*i*) accelerating the rate of plant death (Davies and Peoples, 2003); (*ii*) limiting crown bud initiation (Berg *et al.*, 2005); or (*iii*) by limiting the allocation of assimilates to individual shoots (Volenec *et al.*, 1987).

This chapter quantifies the agronomic aspects of the field experiment in relation to aerial biomass production. Initially, annual and seasonal shoot yield are reported in relation to the effects of defoliation treatments. Any differences in shoot yield are then analysed by the seasonal pattern of each yield component.

5.2 Materials and methods

A detailed description of the experimental design and layout is given in Section 3.3. In this chapter, methods specific to the measurement of shoots are reported.

5.2.1 Shoot dry matter yield

Shoot dry matter (DM_{shoot}, t/ha) was measured from samples collected at 7 day intervals starting 7-10 days after grazing. Samples were taken from a single 0.2 m^2 quadrat placed randomly in each plot. Shoots were cut above crown level with a set of hand shears and the number of shoots counted. During the first year, a sub-sample of ~20 shoots was separated in three size classes based on the tallest shoot (H_{max}). The three classes were nominated (*i*) 'suppressed shoots' (shoot height <1/3 of H_{max}); (*ii*) 'intermediate shoots' (shoot height between 1/3 and 2/3 H_{max}), and (*iii*) 'dominant shoots' (shoot height > 2/3 H_{max}).

From each class sub-sample, shoots were separated into leaf (leaflets), stem (stem plus petioles) and senesced material. Main samples (bulk) and sub-samples were dried in a forced air draft oven at 65°C for at least 48 hours to a constant weight. Values of DM_{shoot}, number of stems (stems/m^2), and leaf to stem ratio (*LSR*) were then calculated for each stem class. During the 2003/04 growth season, the DM_{shoot} sub-sample was not split into height categories but the remaining measurements were performed on the whole sample. Final harvests for each regrowth cycle were taken within the 24 hours preceding commencement of grazing.

5.2.2 Yield components

Lucerne shoot yield was analysed through its yield components (Volenec *et al.*, 1987) as shown in Equation 5.1:

Equation 5.1

DM_{shoot} = (plants/m^2 x shoot/plant x *ISM*) x 100

Where the unit of DM_{shoot} is t DM/ha and individual shoot mass (*ISM*) is in g DM/shoot.

Plant population (plants/m^2) was measured by counting the number of individual plants from the single 0.2 m^2 quadrat sample per plot used to assess perennial dry matter (Section 4.2.1).

5.2.3 Calculations

5.2.3.1 Yield components

Values of plant population were reported as the mean of each regrowth cycle (3-4 consecutive sampling dates). Values of shoots/plant were calculated by dividing shoot population (shoots/m^2) by plant population (plants/m^2) for each plot and sampling date. Individual shoot mass (g DM/shoot) was calculated by dividing DM_{shoot} yield (converted to g DM/m^2) by shoot population (shoots/m^2) for each plot and sampling date.

5.2.3.2 Linear growth rates

Linear growth rates (*LGR*, kg DM_{shoot}/ha/day) were calculated for each plot and regrowth cycle. It was not possible to fit growth logistic curves to the data because there was no clear indication of the initial lag phase, nor an obvious occurrence of an asymptotic (*i.e.* ceiling) yield during the regrowth cycles. Therefore, *LGR* was calculated by fitting a linear regression between regrowth period (days) and shoot dry matter accumulation using all data-points within the range of 5 to 95% of the maximum observed yield for each regrowth cycle (Brown, 2004).

5.2.3.3 Proportion of leaves

Leaf:stem ratio (*LSR*) and leaf proportion (*LP*) are two common ways to refer to the relationship between leaves and stems in a sward (Fick *et al.*, 1994; Lemaire *et al.*, 1992). *LSR* was calculated by dividing leaf dry matter (DM_{leaf}) by stem dry matter (DM_{stem}). Leaf proportion represented the fractional contribution of DM_{leaf} per unit of DM_{shoot}. Both *LSR* and *LP* were calculated and related to predictors such as thermal-time and DM_{shoot}. *LSR*

and *LP* were not measured during the winter/early-spring regrowth (Cycle 0) when leaf and stem separation was difficult to perform because shoots were less than 20 mm in height and first leaves were often frost damaged and tightly folded.

5.2.3.4 Thermal-time calculation

Thermal-time (Tt_{b5},°Cd) was derived from mean air temperature (T_{mean}) using a broken-stick framework (Section 6.2.4) with four cardinal temperatures (Fick *et al.*, 1988). This framework has a base temperature of 5°C, which was validated for 'Kaituna' lucerne in the current experiment (Section 6.3.4).

5.3 Results

5.3.1 Total annual shoot dry matter yield

Total annual accumulated DM_{shoot} increased through a sigmoid pattern ($P<0.01$, $R^2>0.99$) over time for all treatment/season combinations (Figure 5.1). Analysis of parameters of these curves allowed the overall annual pattern of growth of the crops to be compared (Table 5.1). The sigmoid curves were described by (*i*) the asymptote or maximum shoot yield ($Yield_{max}$, t/ha), (*ii*) the maximum annual growth rate (GR_{max}, kg/ha/day), (*iii*) the lag phase defined as the number of days required to achieve 5% of $Yield_{max}$ (D_{lag}, days), and (*iv*) the number of days required to achieve 95% of $Yield_{max}$ (D_{max}, days). The difference between D_{max} and D_{lag} indicates the approximate number of days of growth at GR_{max} of each crop.

LL crops produced the highest ($P<0.001$) annual $Yield_{max}$ of ~24 t/ha during both growth seasons. This was followed by LS at 22 t/ha, SL at 15 t/ha and SS at 13 t/ha in the 2002/03 growth season. There was no interaction ($P<0.37$) between treatment and growth season although, during the 2003/04 growth season, LS and SS crops had ~13% lower ($P<0.05$) $Yield_{max}$ than in 2002/03.

During the 2002/03 season, the GR_{max} was 82 kg/ha/day for LL and LS crops but was 40% lower for SL and SS crops (Figure 5.1). SL crops yielded more than SS crops due to 26 days longer growth (D_{max}) at a similar GR_{max} (~49 kg/ha/day) (Table 5.1).

The effects of the defoliation regimes in 2002/03 were carried to the following season. In 2003/04, LL crops yielded similarly to 2002/03 (24.0 t/ha) but LS crops yielded 3.6 t/ha less than the previous season. This difference was not due to a change in GR_{max}, which was 86 kg/ha/day for both crops, but caused by 26 days less of linear regrowth (*i.e.* D_{max}–D_{lag}) in LS crops (Table 5.1).

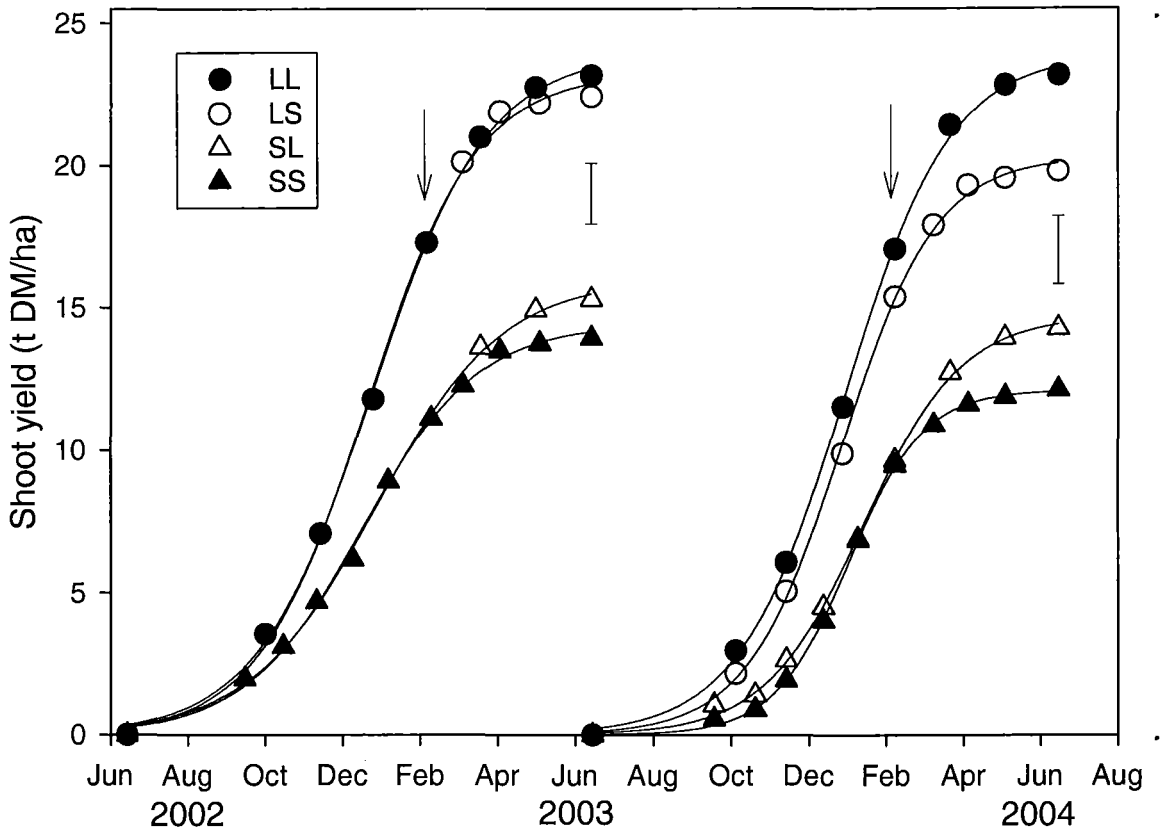

Figure 5.1 Cumulative shoot yield of lucerne crops subjected to four contrasting defoliation regimes in the 2002/03 and 2003/04 growth seasons at Lincoln University, Canterbury, New Zealand.

Note: Solid lines represent sigmoid curves ($y=a/1+\exp(-(x-x0)/b)$, $R^2>0.99$. Parameters are displayed in Table 5.1. Bars represent one SEM at the end of each regrowth season, $n=4$. Arrows indicate the day when treatments were shifted (4th February).

In 2003/04 SL and SS crops yielded 40-45% less than LL crops. This was mainly due to the GR_{max} being 60 kg/ha/day compared with 89 kg/ha/day for LL crops. SL crops yielded ~2 t/ha more than SS crops in 2003/04, due to 38 days longer duration of regrowth at GR_{max} (Table 5.1, Figure 5.1).

Table 5.1 Parameters of sigmoid curves displayed in Figure 5.1 that represent the accumulated growth of lucerne crops subjected to four contrasting defoliation regimes in the 2002/03 and 2003/04 growth seasons at Lincoln University, Canterbury, New Zealand.

Treatment	$Yield_{max}$	GR_{max}	D_{lag}	D_{max}	D_{max}-D_{lag}
2002/03	(t/ha)	(kg/ha/day)	(days)	(days)	(days)
LL	24.2_a	80_a	68_{ab}	339_b	271_b
LS	23.8_a	83_a	74_a	326_b	252_b
SL	16.5_b	49_b	59_b	358_a	299_a
SS	14.4_c	48_b	60_b	332_b	272_b
Significance	*<0.01*	*<0.01*	*<0.06*	*<0.01*	*<0.01*
SEM	*0.3*	*1.0*	*3.7*	*3.8*	*7.0*
2003/04					
LL	23.9_a	89_a	85_c	329_a	244_a
LS	20.3_b	84_a	$95b_c$	313_b	218_a
SL	14.7_c	58_b	108_b	334_a	226_a
SS	12.8_d	63_b	124_a	296_c	172_b
Significance	*<0.01*	*<0.01*	*<0.01*	*<0.01*	*<0.01*
SEM	*0.9*	*5.0*	*4.7*	*4.9*	*8.2*

Note: Within regrowth seasons, means in a column followed by similar letters are not different at a significance level of α=0.05.

5.3.2 Seasonal shoot dry matter yield

The seasonal pattern of lucerne DM_{shoot} accumulation is displayed in Figure 5.2. The study of individual regrowth cycles enabled the analysis of two distinct aspects of shoot growth: (*i*) the seasonal pattern of DM_{shoot} accumulation and (*ii*) the impact of defoliation regimes on individual regrowth cycles.

During both seasons, ~70% of annual DM_{shoot} was produced before treatments were shifted (4th February) in all crops. During this period, each 42 day regrowth cycle of LL and LS produced yields in excess of 3 t/ha (Figure 5.2 *a, b*). In contrast, SL and SS crops, on the 28 day regrowth cycle, rarely exceeded 3 t/ha, the exception being $SL_{03/04}$-Cycle 6 (Figure

5.2 *c*). For all crops, DM_{shoot} was negligible during May-July and, by the following early-spring regrowths (Cycle 0), only the $LL_{03/04}$ crop exceeded 3 t/ha (Figure 5.2 *a*).

Also of note, was the impact of the previous spring-summer defoliation on the regrowth cycles immediately after the shift of treatments (denoted with arrows in Figure 5.2) when comparable crops were growing at the same time and environmental conditions. For example, DM_{shoot} in $LS_{03/04}$-Cycle 4 was 1.1 t/ha greater ($P<0.004$) than the comparable $SS_{03/04}$-Cycle 6 over the 28-day regrowth cycle. Similarly, over the 42-day regrowth cycle, the DM_{shoot} of LL-Cycle 4 was ~30% greater ($P<0.05$) than the comparable SL-Cycle 6 in both growth seasons.

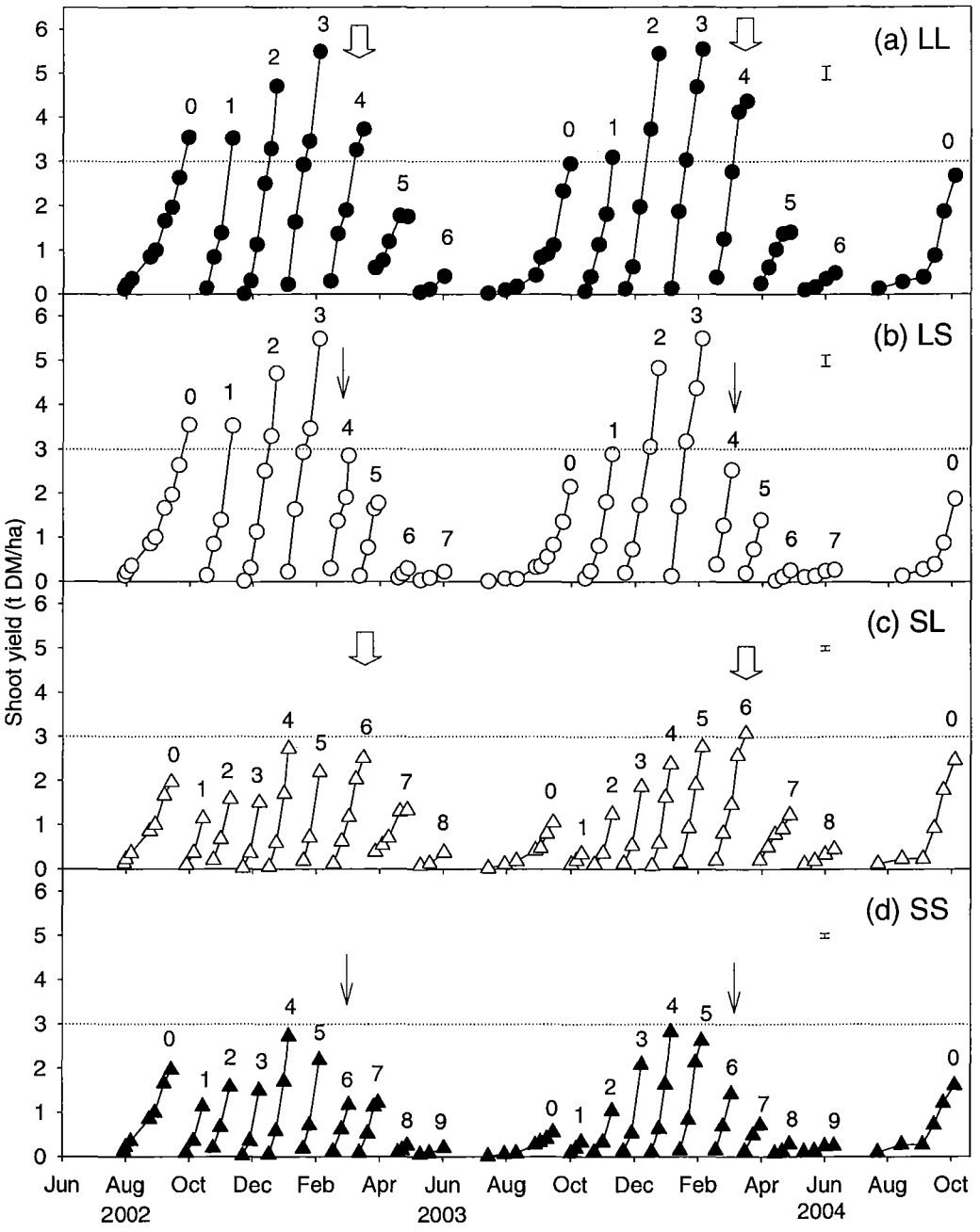

Figure 5.2 Seasonal shoot dry matter yield of lucerne crops subjected to contrasting defoliation regimes in the 2002/03 and 2003/04 growth seasons at Lincoln University, Canterbury, New Zealand.

Note: Dotted line represents yield of 3 t DM/ha for reference. Bars are SEM for comparison of regrowth cycles within each treatment, n=4. Regrowth cycles are numbered (0-9). Arrows indicate first regrowth cycle immediately post treatments shift of for comparison between (*i*) LL and SL crops (↓) and (*ii*) LS and SS crops (⇩).

5.3.2.1 Shoot linear growth rates (LGR)

The mean linear growth rate (*LGR*) of each regrowth cycle is displayed in Figure 5.3. During the winter, DM_{shoot} was minimal and the first data-points considered in *LGR* calculations were from mid-August. During both growth seasons, LL crops had an initial *LGR* of 75 kg/ha/day in early-spring. This increased to a maximum of ~170 kg/ha/day in summer (December-February). From late February to June, the *LGR* declined and reached a minimum of less than 10 kg/ha/day during the final autumn defoliation.

LL crops always had greater ($P<0.05$) *LGR* than SS during spring-summer. In most cases, crops defoliated with a long rotation during spring-summer (LL and LS) grew at 20-50 kg/ha/day faster than SL and SS crops during both 2002/03 and 2003/04 seasons.

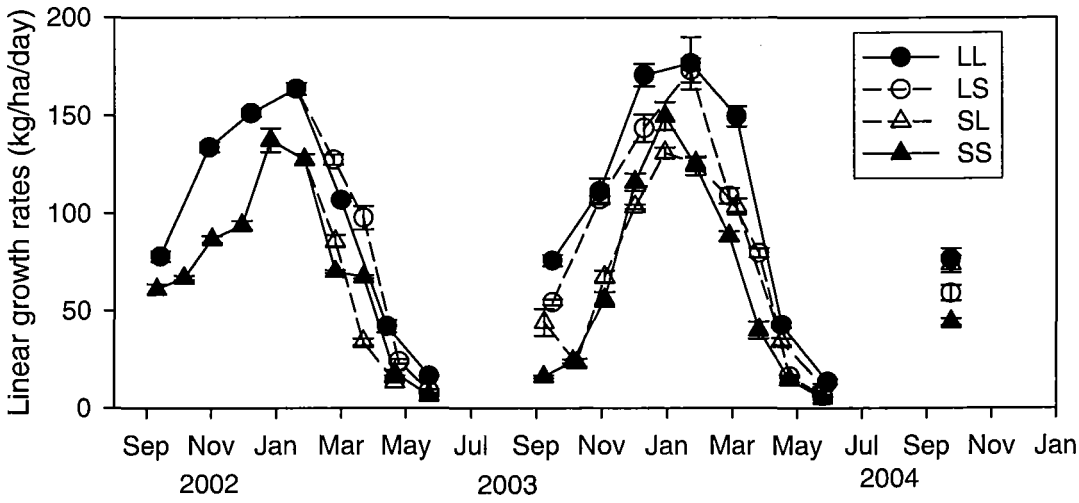

Figure 5.3 Linear growth rates (kg/ha/day) of lucerne crops subjected to contrasting defoliation regimes in the 2002/03 and 2003/04 growth seasons at Lincoln University, Canterbury, New Zealand.

Note: Bars represent one SEM of a given growth cycle, $n=4$. Data points were positioned in the average date of the range analysed in a regrowth cycle.

5.3.2.2 Early-spring regrowth

The two early-spring regrowth cycles, when all crops grew simultaneously (Cycle 0 in 2003/04 and 2004/05), were compared at a common thermal-time accumulation (Figure

5.4). During this period, the only contrasting factors affecting DM_{shoot} accumulation were the amounts and concentration of perennial reserves of each crop, as a result of the previous defoliation regimes (Chapter 4). By the 2004/05 spring harvest, when crops had accumulated ~370°Cd (T_b=5°C), LL and SL crops had a similar DM_{shoot} of 2.5 t/ha. This yield was greater (P<0.01) than for LS (2.0 t/ha) and SS (1.6 t/ha) crops (Figure 5.4).

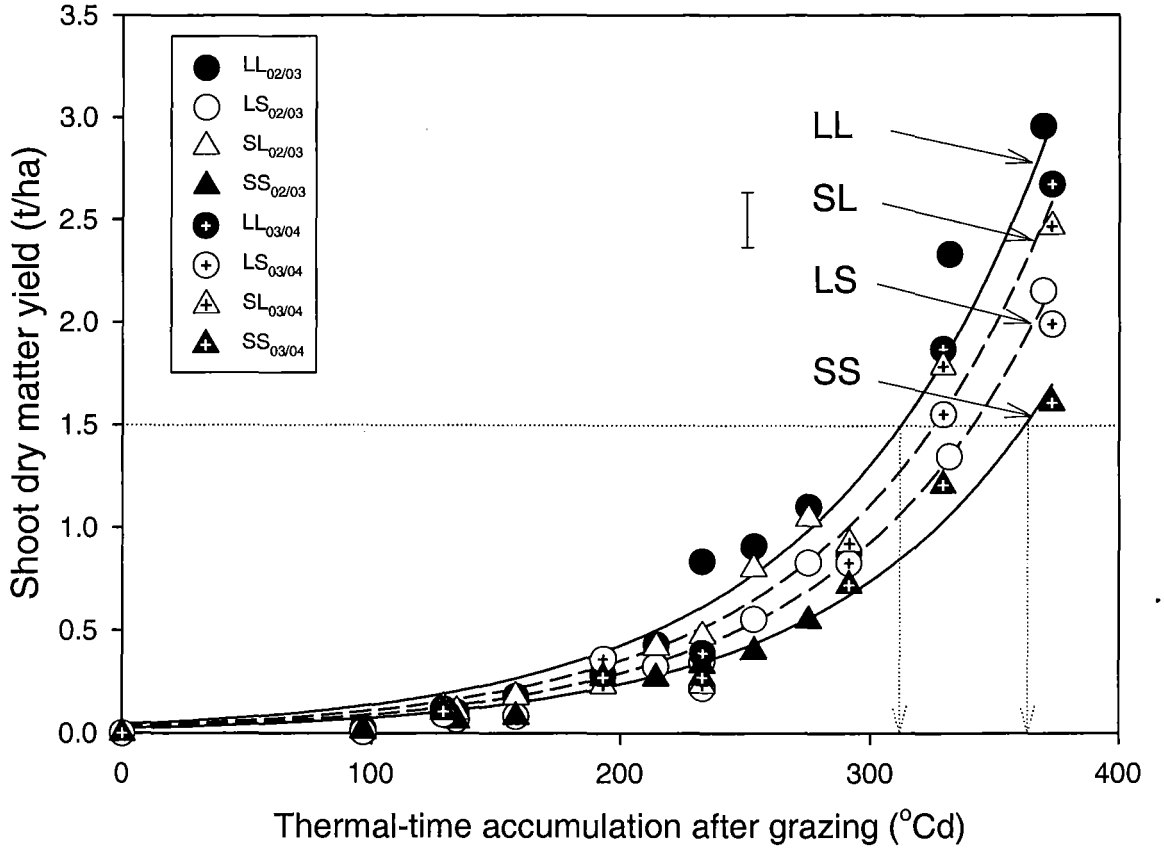

Figure 5.4 Shoot yield during two winter/early-spring regrowth periods in relation to thermal-time accumulation of lucerne crops subjected to contrasting defoliation regimes in the 2002/03 and 2003/04 growth seasons at Lincoln University, Canterbury, New Zealand.

Note: Data refer to regrowths from ~14 June to 1 October. Dotted arrows indicate estimated $\sum Tt_{b5}$ when shoot yield was 1.5 t/ha for reference. The parameters of exponential models are displayed in Table 5.2. All R^2>0.95. Regressions were fitted to data-points combined from both growth seasons for each treatment.

Exponential regressions (Figure 5.4) indicated that LL crops grew at faster rates (P<0.06) than SS crops during early-spring (Table 5.2). LS and SL crops were similar at intermediate growth rates, but there was a trend of SL crops having faster growth as reflected by the greater yield at the final harvest (~370°Cd after grazing).

Table 5.2 Comparison of parameters of exponential regressions (Figure 5.4) relating shoot yield during early-spring regrowth and thermal-time accumulation after grazing of lucerne crops subjected to contrasting defoliation regimes in the 2002/03 and 2003/04 growth seasons at Lincoln University, Canterbury, New Zealand.

Parameter	LL	LS	SL	SS	Significance	SEM
a	0.0716_a	0.0485_{ab}	0.0516_{ab}	0.0224_b	$P<0.06$	0.000829
b	0.01043	0.01045	0.01248	0.01255	$P<0.16$	0.000819

Note: Exponential model was y= *a* x exp(*b* x *x*). Means followed by the same small letters in lines are not significantly different at $\alpha=0.05$.

5.3.2.3 The effect of taproot reserves on LGR during the early-spring regrowth

There was a moderate relationship ($R^2=0.58$) between *LGR* and taproot nitrogen concentration ($N\%_{root}$) (Figure 5.5 *a*). Shoot linear growth rates increased ($P<0.05$) at 63 kg/ha/day/%N as $N\%_{root}$ increased from ~1.2 to 1.8% DM (Figure 5.5 *a*). Total winter nitrogen amounts were strongly ($R^2=0.76$) related to spring *LGR* (Figure 5.5 *d*) which increased ($P<0.01$) at 1.1 kg/ha/day for each additional 1 kg/ha of taproot nitrogen.

The relationship between *LGR* and the amounts and concentrations of carbohydrates in taproots (Figure 5.5 *b, c, e, f*) were not significant ($0.07<P<0.36$) but there was a trend ($0.41<R^2<0.52$; $0.07<P<0.12$) of increased *LGR* with greater winter amounts of starch and soluble sugars in taproots (Figure 5.5 *e, f*).

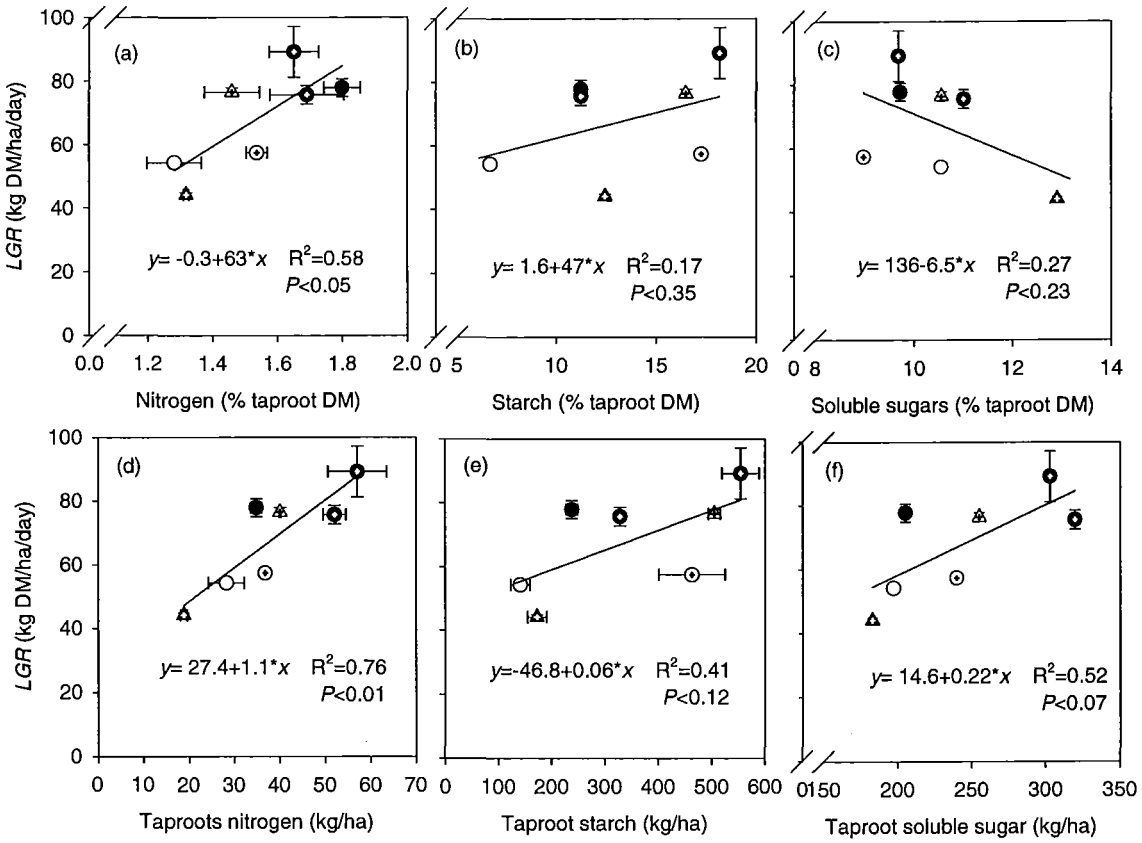

Figure 5.5 Relationship between linear growth rates (kg/ha/day) of shoot dry matter during the first spring regrowth and the percentage (*a*, *b* and *c*) and total amounts (*d*, *e* and *f*) of taproot reserves from samples harvested in the previous winter period from lucerne crops subjected to four contrasting defoliation regimes in the 2002/03 and 2003/04 growth seasons at Lincoln University, Canterbury, New Zealand.

Note: Bars represent one SEM for n=2. Symbols referring to treatment/growth season are displayed in Table 3.3 .

5.3.3 Shoot components

Shoot samples were separated into leaves, stems and senesced material (Section 5.2.1). Annual leaf yield was 9 t/ha for LL and LS crops, which was greater (P<0.001) than the 7.4 t/ha for SL and 6.7 t/ha for SS crops (Figure 5.6). The stem yield was the shoot component that contributed the most to differences in annual DM_{shoot}. Annual stem DM was greatest (P<0.001) in $LL_{02/03}$ crops (13.6 t/ha) followed by $LS_{02/03}$ (12.1 t/ha), $SL_{02/03}$ (7.2 t/ha) and $SS_{02/03}$ (6.2 t/ha). Senesced material represented <3% of total annual DM_{shoot}

in any crop. In general, LL and LS had a similar annual senesced DM yield of 300 kg DM/ha compared with ~100 kg/ha for SL and SS crops.

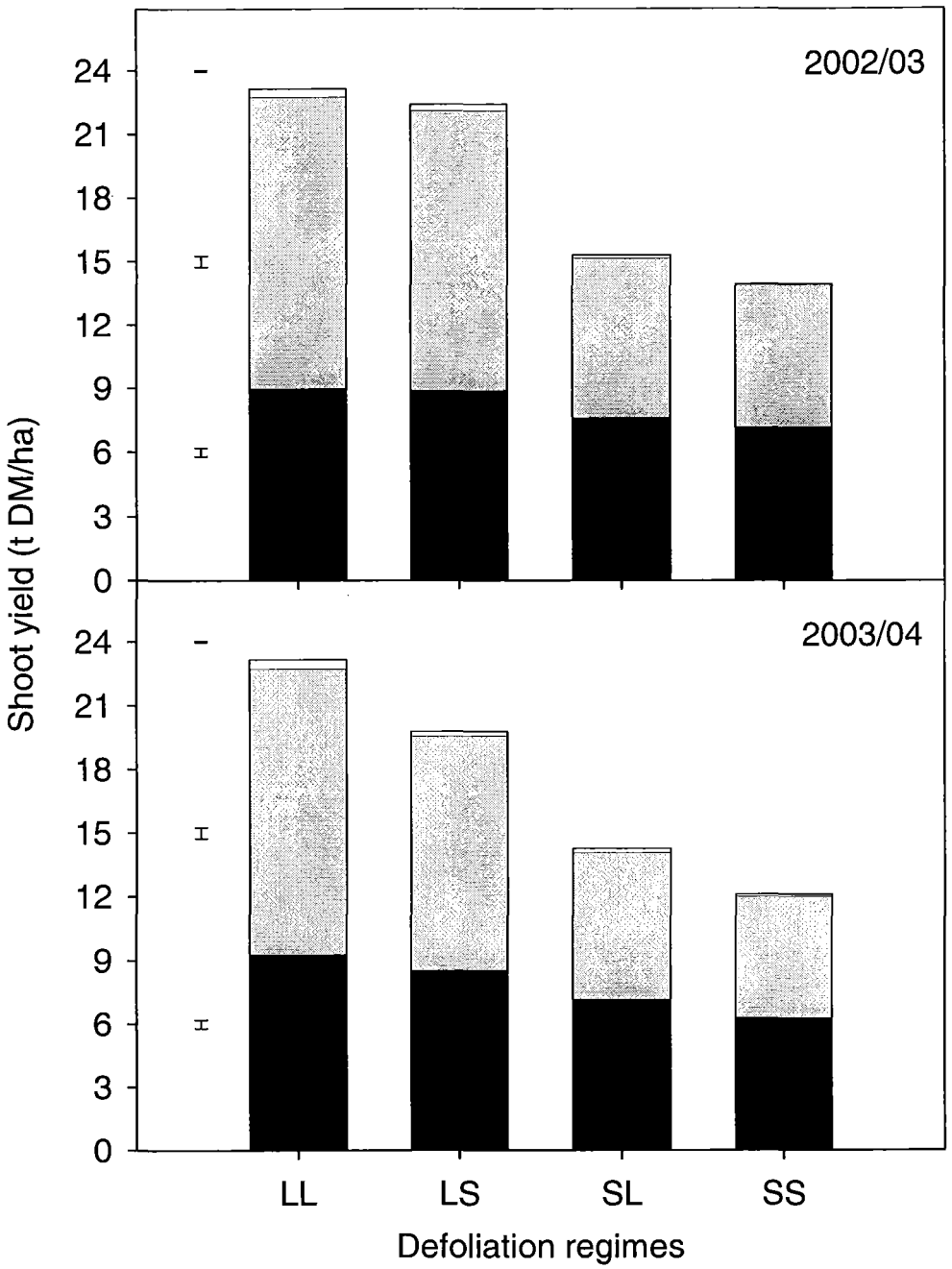

Figure 5.6 Annual yields of leaves (■); stems (▒); and senesced DM (□) of lucerne crops subjected to four contrasting defoliation regimes in the 2002/03 and 2003/04 growth seasons at Lincoln University, Canterbury, New Zealand.

Note: Bars represent one standard error of the mean (SEM) for comparison of shoot fractions within each growth season/shoot component combination.

5.3.3.1 *Leaf:stem ratio and leaf proportion*

The contribution of leaves in DM_{shoot} was quantified by the use of leaf:stem ratio (*LSR*) and leaf proportion (*LP*) (Section 5.2.3.3). The *LSR* measured at the end of each regrowth cycle, ranged from 0.5 to 2.0 (Figure 5.7). As expected, *LSR* was lower in periods of intense growth (*e.g.* summer) and in treatments that accumulated more DM_{shoot} (*e.g.* long regrowth cycles).

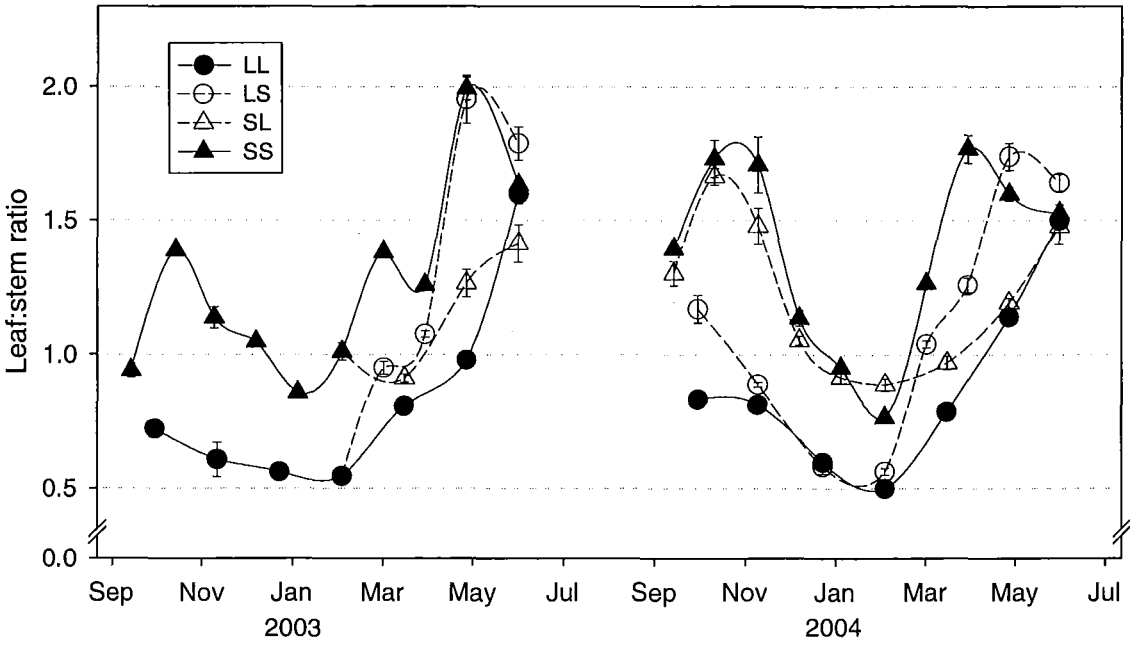

Figure 5.7 Leaf:stem ratio at the end of each regrowth cycle of lucerne crops subjected to four contrasting defoliation regimes in the 2002/03 and 2003/04 growth seasons at Lincoln University, Canterbury, New Zealand.

To understand the mechanisms behind the changes in *LSR* or *LP*, two prediction bases were tested. Firstly, as proposed by Onstad and Fick (1983), *LP* was plotted as a function of thermal-time accumulation ($\sum Tt_{b5}$, °Cd) from grazing day. There was a linear decrease ($P<0.01$, $R^2=0.65$) in *LP* with $\sum Tt_{b5}$ accumulation at a rate of -7×10^{-4} units/°Cd from 0.70 (*i.e.* 70% of leaves in DM_{shoot}) in early stages of regrowth to 0.40 at 400°Cd (Figure 5.8). One of the models proposed by Onstad and Fick (1983) is plotted in Figure 5.8 for reference.

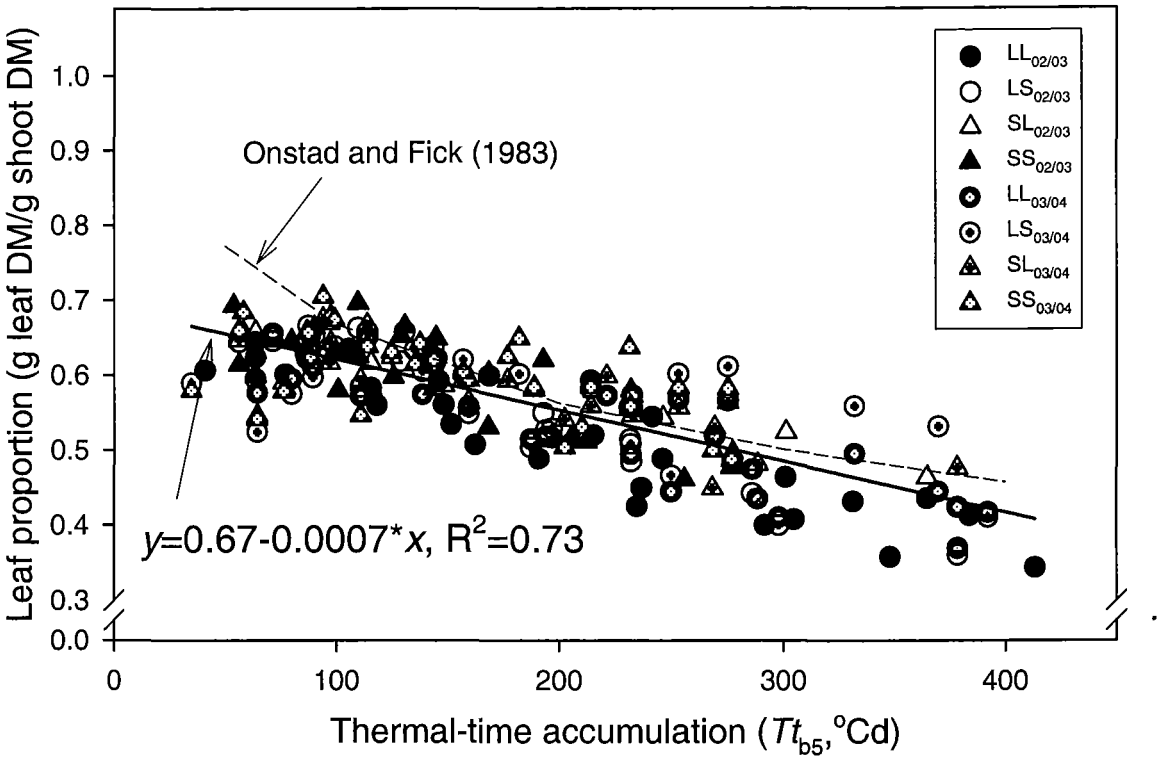

Figure 5.8 Relationship between leaf proportion (g leaf/g shoot) and thermal-time accumulation from the last grazing day (°Cd) of lucerne crops subjected to four contrasting defoliation regimes in the 2002/03 and 2003/04 growth seasons at Lincoln University, Canterbury, New Zealand.

Note: Dashed lines (-----) represent model y=1.37-0.15 x ln(x+1), proposed by Onstad and Fick (1983) for early-spring regrowth.

The second approach was based on results from Lemaire *et al.* (1992), where DM_{shoot} was tested to predict *LSR* at several stages of regrowth. The *LSR* was strongly related (R^2=0.77) to DM_{shoot} and decreased (P<0.01) exponentially from ~1.9 at the beginning of each regrowth cycle to an estimated minimum of 0.3 when DM_{shoot} was greater than 5.5 t/ha (Figure 5.9).

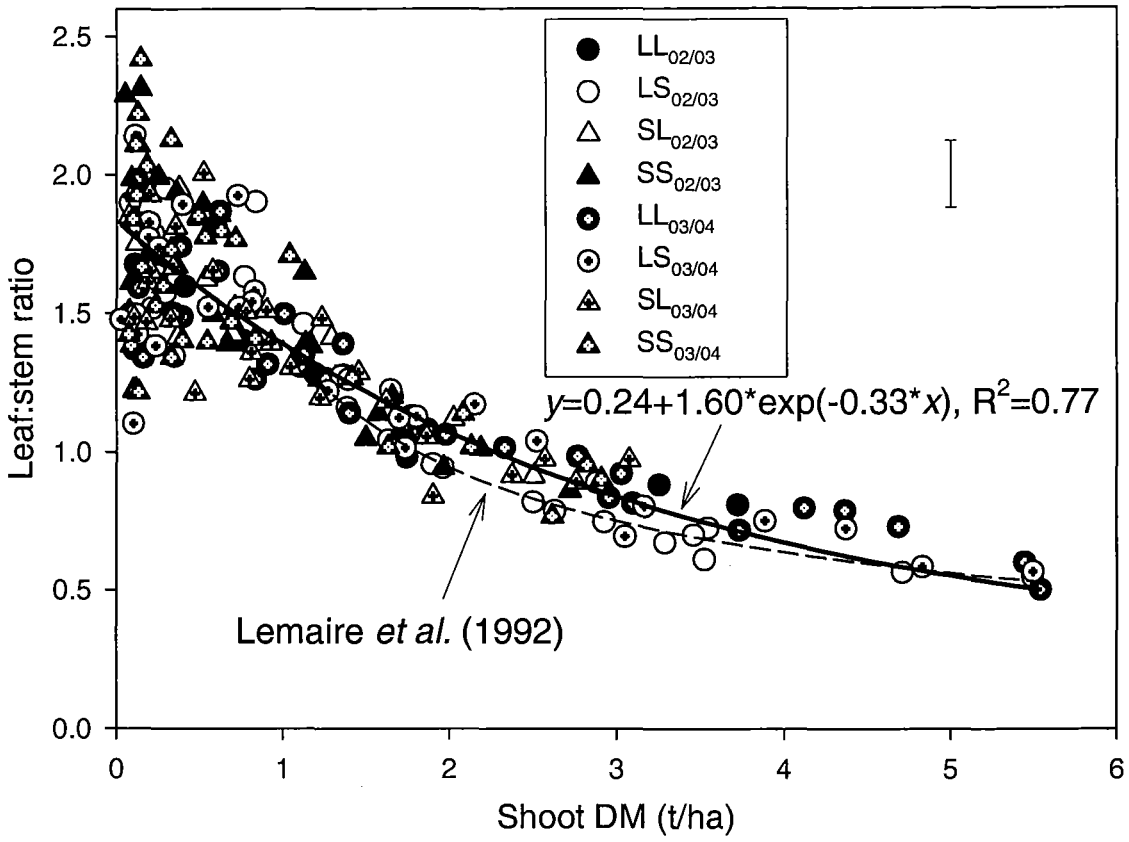

Figure 5.9 Leaf to stem ratio in relation to shoot dry matter (DM) yield of lucerne crops subjected to four contrasting defoliation regimes in the 2002/03 and 2003/04 growth seasons at Lincoln University, Canterbury, New Zealand.

Note: Dotted line represents model $y=1.43(DM_{shoot})^{-0.57}$ proposed by Lemaire *et al.* (1992) for DM_{shoot} >1 t/ha. Bar represents one polled SEM.

Although *LSR* followed the same pattern of change with DM_{shoot} in all treatments, this relationship was more variable at DM_{shoot}<1t/ha. For example, at the lowest measured DM_{shoot}, *LSR* ranged from 1.2 to 2.4. This was possibly an artefact of greater measurement bias at low yields, as there was a strong (R^2=0.99) allometric relationship between each individual shoot fraction (leaf and stem) and DM_{shoot} (Figure 5.10). The exponents of the equations in Figure 5.10 indicated that the rate of accumulation of stem DM increased at rates ~25% greater than for leaf DM and, at DM_{shoot} of 1 t/ha, DM_{shoot} was 57% leaves and 43% of stems regardless of treatment or season.

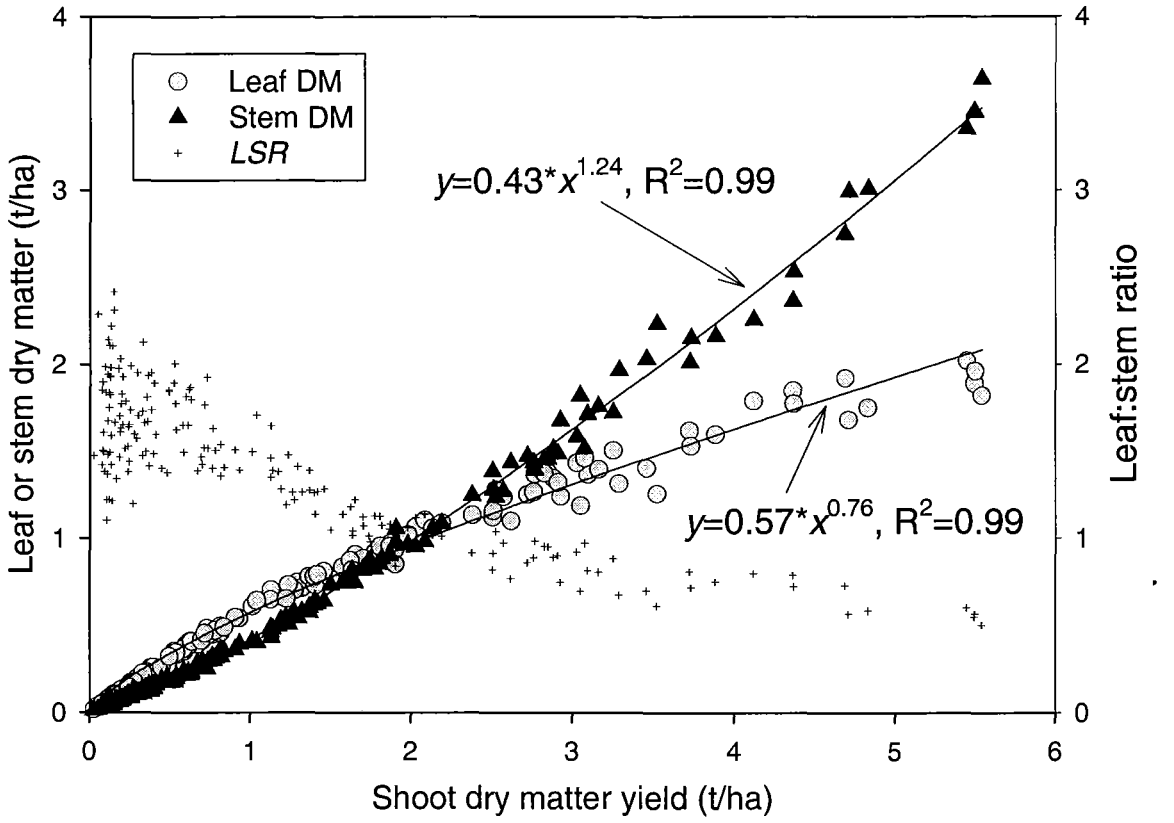

Figure 5.10 Relationship between leaf dry matter (○), stem dry matter (▲) and leaf:stem ratio (+) with shoot dry matter of lucerne crops subjected to four contrasting defoliation regimes in the 2002/03 and 2003/04 growth seasons at Lincoln University, Canterbury, New Zealand.

Note: Treatments/season are plotted combined. Leaf:stem ratio (*LSR*) was plotted for reference and is displayed in detail in Figure 5.9.

5.3.4 Yield components

In the following sections the effect of defoliation treatments on yield components (plant population, shoots/plant and yield/shoot) of lucerne crops were investigated individually.

5.3.4.1 Plant population

Plant population decreased ($P<0.01$) from 120 plants/ha on October 2002 to ~60 plants/ha in September 2004 (Figure 5.11). An exponential decay model ($R^2=0.75$) described the

decrease in population and this was unaffected (P<0.43) by defoliation treatments (Figure 5.11).

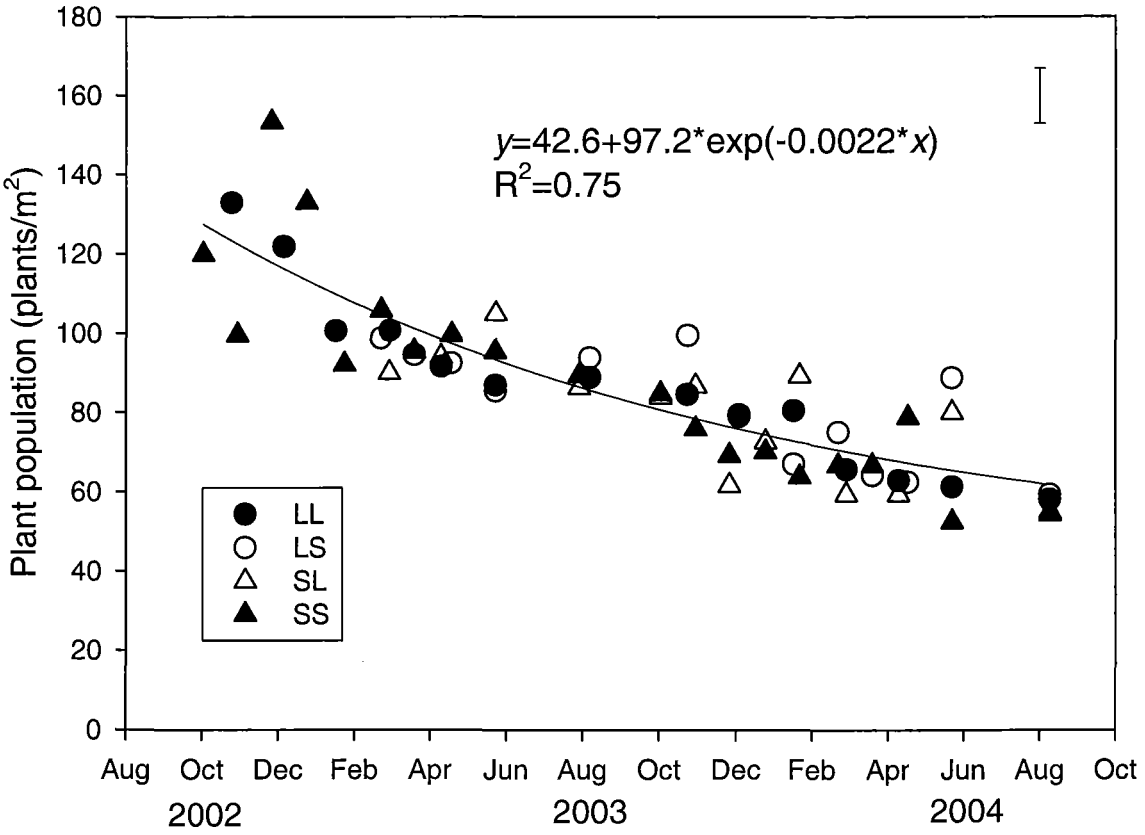

Figure 5.11 Plant population (plants/m^2) of lucerne crops subjected to four contrasting defoliation regimes in the 2002/03 and 2003/04 growth seasons at Lincoln University, Canterbury, New Zealand.

Note: Bar represents one pooled SEM. Data points represent the average plant population of each regrowth cycle (3-5 sampling dates).

5.3.4.2 Shoot population

Shoot population increased (P<0.01) similarly in all crops as leaf area developed within a regrowth cycle. Shoot population reached its maximum at a *LAI* of 2.1 as indicated by a peak function (R^2=0.64, P<0.01) fitted between shoot population and *LAI* including data from all regrowth cycles. From negligible values at grazing day, shoot population increased to a maximum of ~780 stems/m^2 at *LAI* of 2.1 and then declined (Figure 5.12).

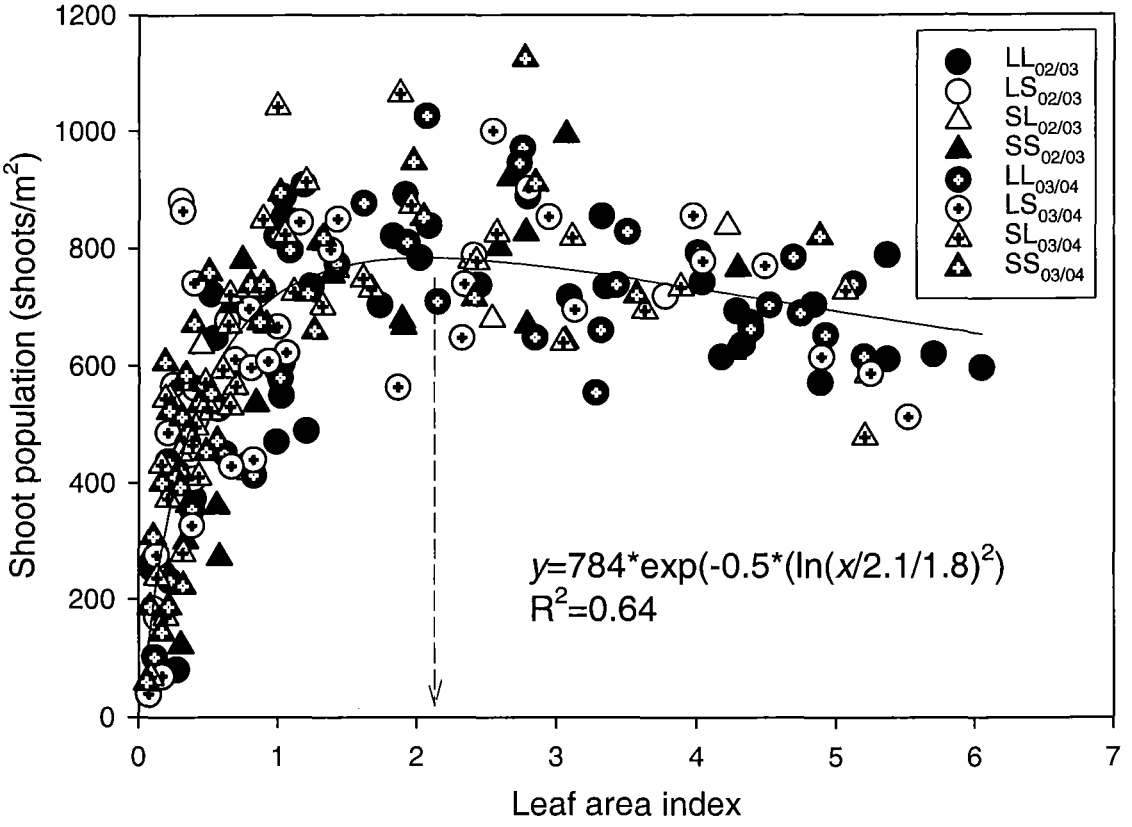

Figure 5.12 Shoot population (shoots/m^2) within a regrowth cycle as a function of leaf area index of lucerne crops subjected to four contrasting defoliation regimes in the 2002/03 and 2003/04 growth seasons at Lincoln University, Canterbury, New Zealand.

The effect of defoliation treatments on the rate of shoot initiation (*i.e.* bud appearance in crowns and axils) was tested during the initial phases of regrowth. To do this, linear regressions were fitted to shoot population and *Tt* accumulation <150°C ($\sum Tt_{<150}$) after grazing. Shoot population increased ($P<0.01$) at similar ($P<0.40$) rates (~6 shoots/m^2/°Cd), starting from an intercept not different ($P<0.44$) from zero (Figure 5.13).

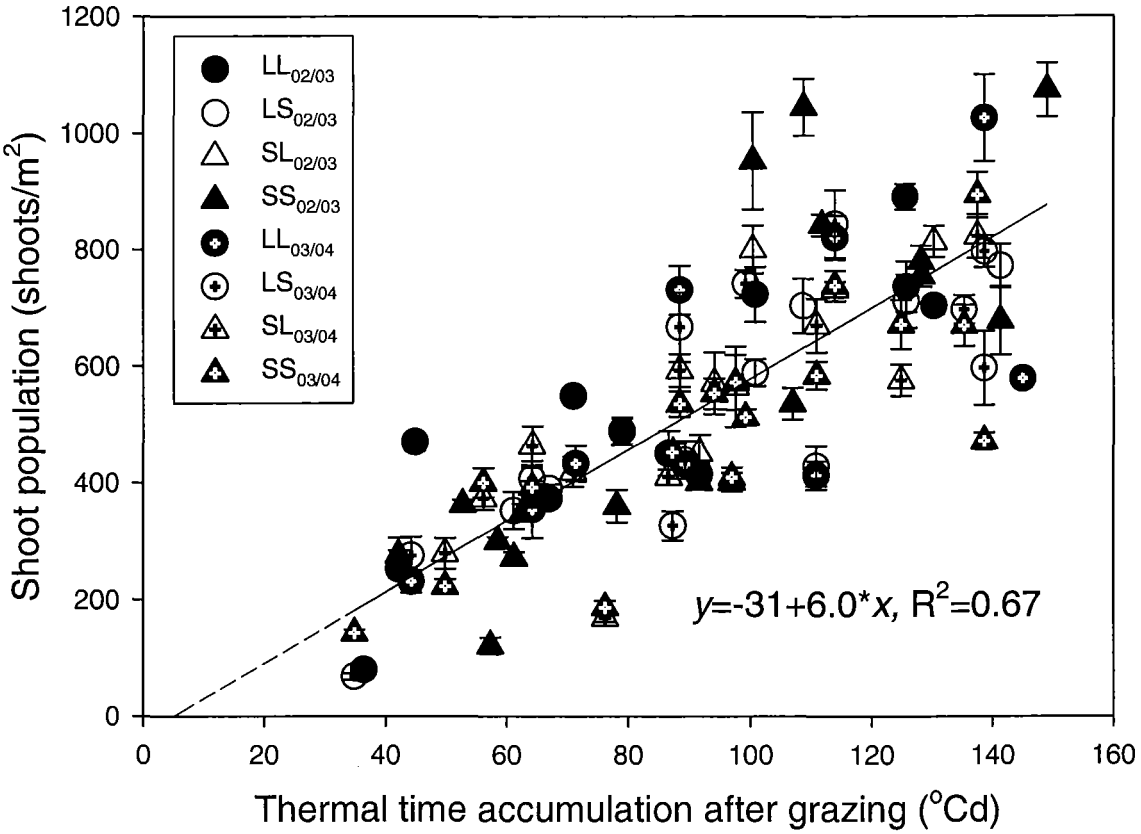

Figure 5.13 Relationship between shoot population and thermal-time accumulation ($\sum Tt_{b5}$; for Tt_{b5}<150°Cd) of lucerne crops subjected to four contrasting defoliation regimes in the 2002/03 and 2003/04 growth seasons at Lincoln University, Canterbury, New Zealand.

Note: Dashed line indicates the projection of the model to y=0.

5.3.4.3 Shoot categories

Shoots were classified into three categories of dominant (D_{shoot}), intermediate (I_{shoot}) and suppressed shoots (S_{shoot}) based on height relative to the tallest shoot in the canopy (Section 5.2.1). The fraction of DM_{shoot} in each category was plotted against *LAI* to demonstrate the dynamics of shoot recruitment for the LL crop (Figure 5.14 *a*). The fraction of D_{shoots} in DM_{shoot} increased (P<0.02) curvilinearly with *LAI* (R^2=0.86) from ~24% at low *LAI* values to ~90% of total DM_{shoot} at a *LAI* of 5.0 (Figure 5.14 *a*). At *LAI* values greater than 2.0, D_{shoots} made up more than half of DM_{shoot} while I_{shoots} and S_{shoots} represented ~30% and 15%, respectively. These empirical relationships developed for LL crops also explained the shoot dynamics of LS, SL and SS crops (Figure 5.14 *b*). The root mean squared deviation

(*RMSD*) between predicted and observed values for the other crops using the models developed for LL crop was 0.07.

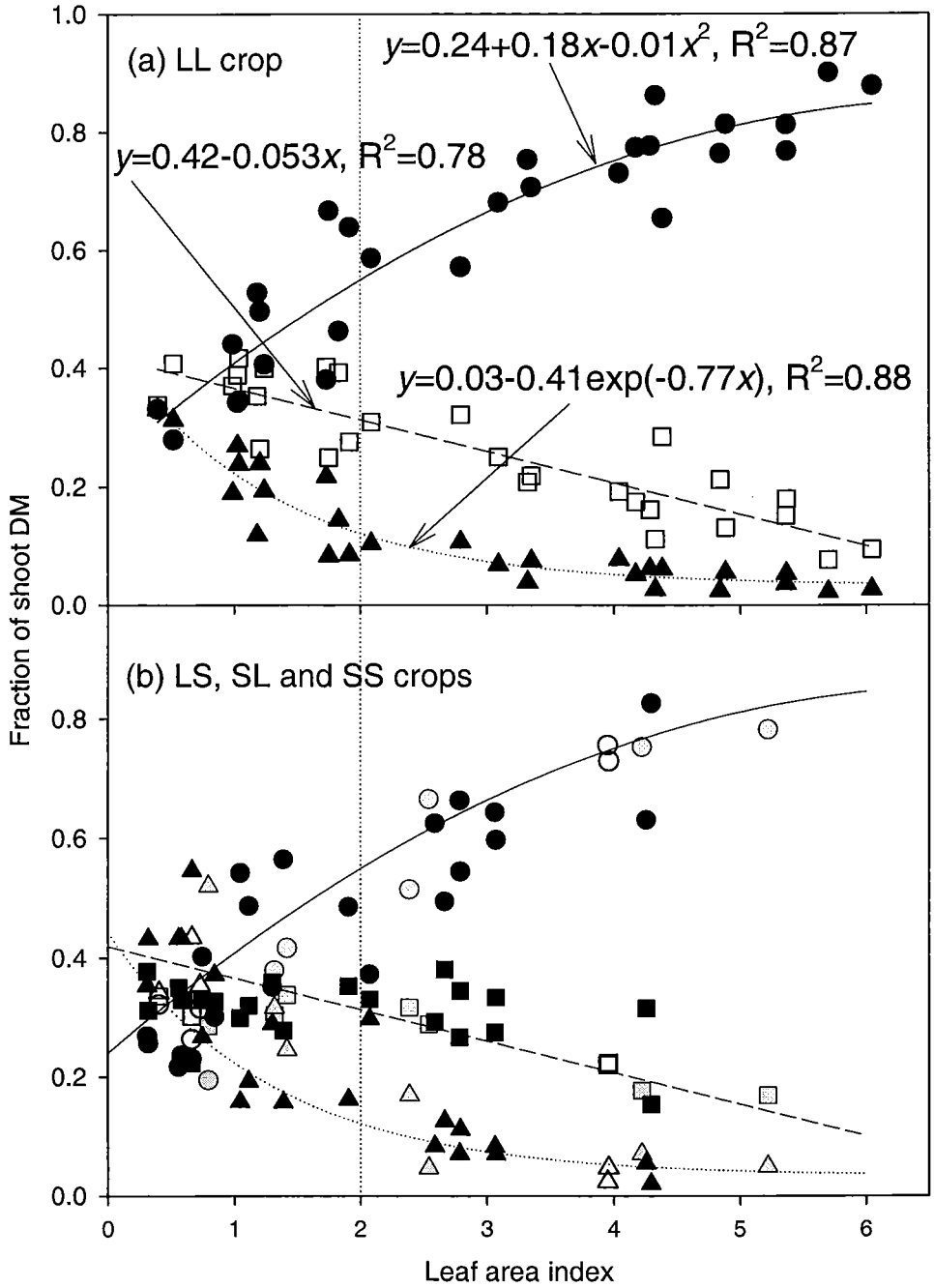

Figure 5.14 Relationship between leaf area index (*LAI*) and the fraction of shoot dry matter on dominant (●), intermediate (□) and suppressed (▲) shoots in (a) LL crops and (b) LS (●,■,▲),SL (●,■,▲), and SS crops(○,□,△) with LL derived relationships plotted.

Note: Vertical dashed line indicates *LAI* of 2.0 for reference.

5.3.4.4 Shoots per plant

The number of shoots per plant at harvest increased ($P<0.05$) at similar rates ($P<0.51$) in all treatments. Shoots/plant increased from ~5.5 at 140 plants/m^2 (spring 2002/03) to ~15 shoots/plant at 50 plants/m^2 (autumn 2003/04) (Figure 5.15). This pattern maintained shoot population at harvest of ~780 shoots/m^2.

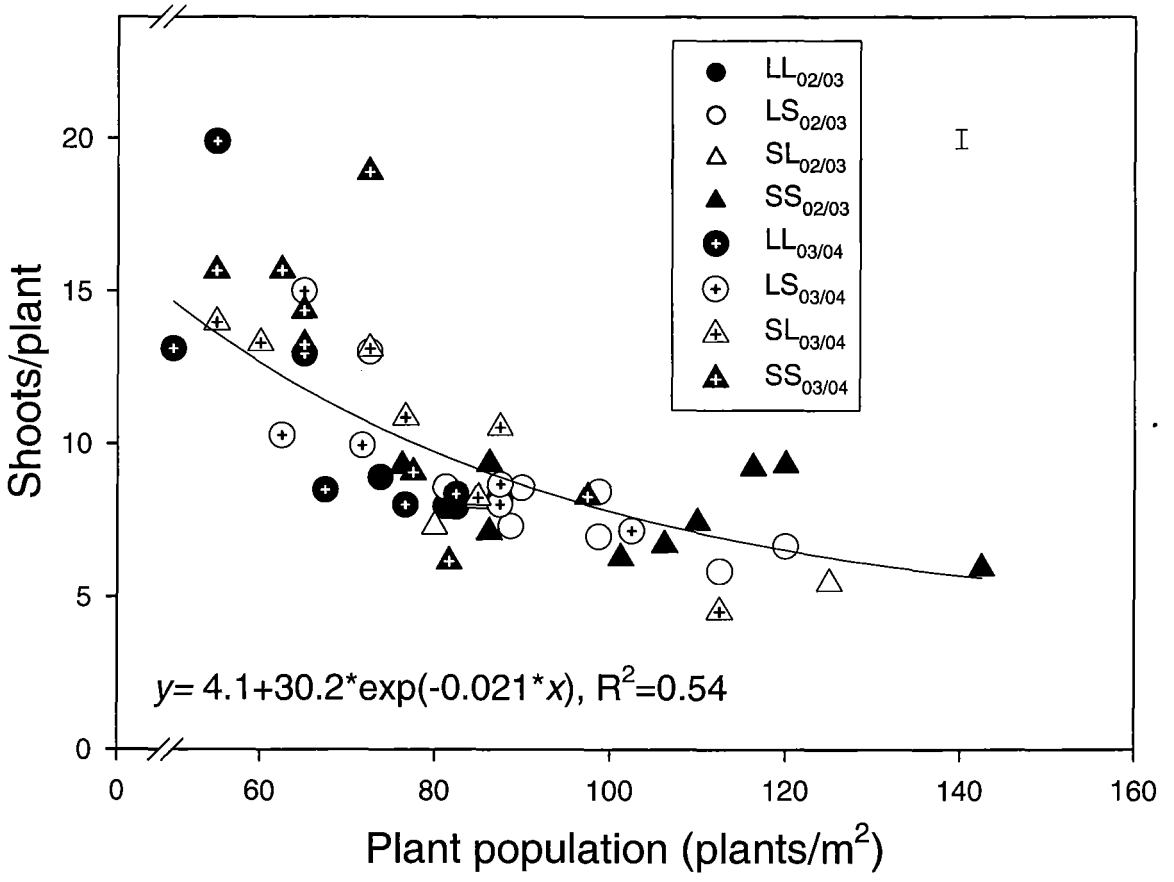

Figure 5.15 Relationship between shoots per plant and plant population at harvest of lucerne crops subjected to four contrasting defoliation regimes in the 2002/03 and 2003/04 growth seasons at Lincoln University, Canterbury, New Zealand.

Note: Bar represents one SEM.

5.3.4.5 Individual shoot mass

The individual shoot mass (*ISM*, g DM/shoot) explained 97% of the variation in DM_{shoot} yields (Figure 5.16). Shoot yield responded similarly in all treatments to increases in *ISM* from <0.1 g DM/shoot to ~1.0 g DM/shoot. A linear regression (DM_{shoot}=0.06+6.34 x *ISM)*

explained 95% of the variation. However, this model had an uneven distribution of residuals (predicted DM_{shoot}–observed DM_{shoot}), with a trend to overestimate DM_{shoot} at *ISM*>0.5. Therefore, a bi-linear (broken-stick) model (R^2=0.96) was used which reduced the *RMSD* from 0.28 t/ha to 0.23 t/ha. The broken-stick model indicated that, after shoots attained a weight of ~0.3 g DM, the slope of the relationship changed from 8 t DM_{shoot}/g *ISM* to ~5 t DM_{shoot}/g *ISM* (Figure 5.16). This change in slope was possibly caused by the self-thinning of shoot population that resumed when *LAI* > 2.1 (Figure 5.12).

In summary, the differences observed in seasonal shoot yield, caused by defoliation treatments and the level of perennial reserves, were mostly explained by the differential allocation of assimilates to each individual shoot, with minimal impact on the other yield components.

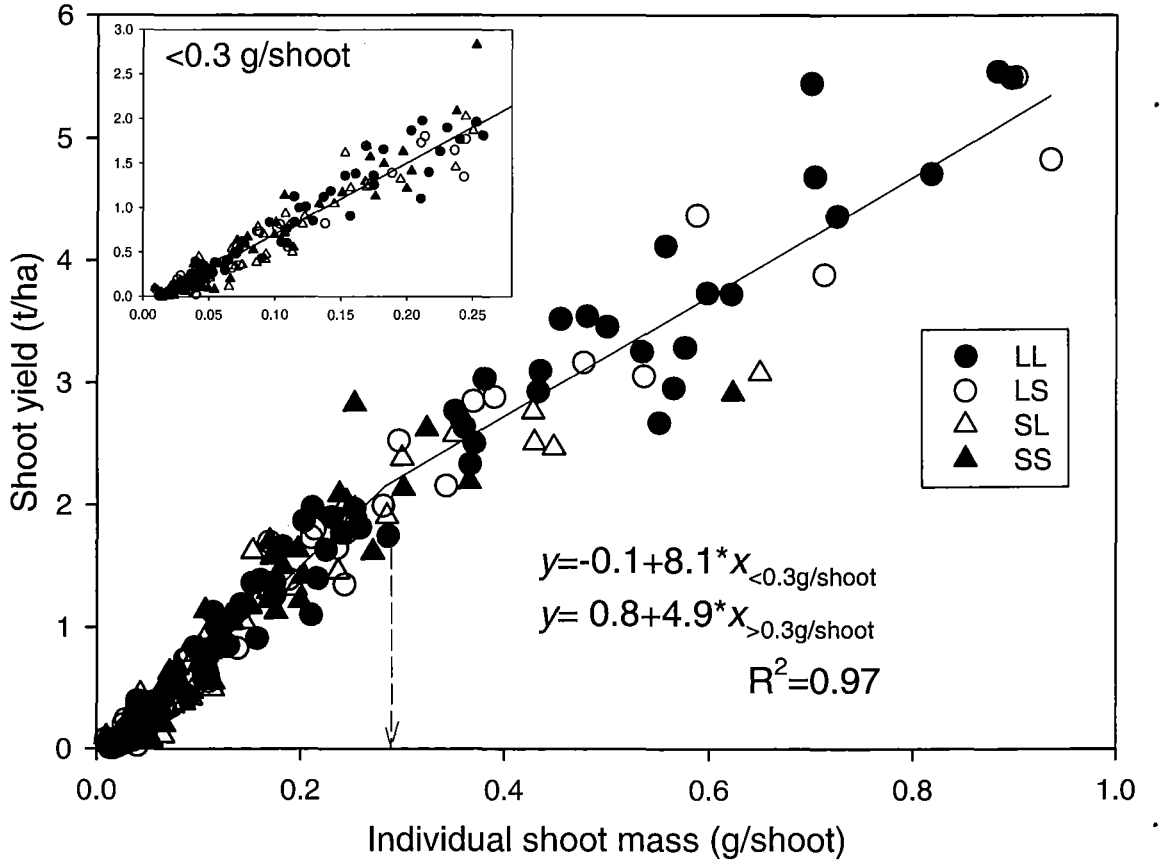

Figure 5.16 Relationship between individual shoot mass (g DM/shoot) and shoot yield (t DM/ha) of lucerne crops subjected to four contrasting defoliation regimes in the 2002/03 and 2003/04 growth seasons at Lincoln University, Canterbury, New Zealand.

Note: Vertical dashed line represents inflection point of broken-stick model (x=0.3). Insert shows in detail the distribution of data-points < 0.3 g/shoot in relation to the model.

5.4 Discussion

Defoliation treatments significantly affected the seasonal shoot yield of lucerne (Figure 5.1). The effect was mainly caused by a differential supply of assimilates to each individual shoot without a consistent change in the pattern of plant population decay or shoot population dynamics.

5.4.1 Shoot dry matter yield

The greatest annual DM_{shoot} yields of 24 t/ha in LL crops are comparable to previous experimental results for this location. Varella (2002) reported annual shoot yield of 17.5 t/ha of irrigated 'Kaituna' lucerne in Canterbury and Brown (2004) measured 25 t/ha in the 1997/98 season when working with lucerne in an adjacent field to I9.

The application of short defoliation cycles (28-day) at different times during the growing season reduced yield by 50-80% compared with LL crops. This decrease in DM_{shoot} is similar to the range observed by Gramshaw *et al.* (1993) in lucerne crops defoliated at intervals less than 35 days in Queensland, Australia. The short cycle applied during spring to mid-summer (*e.g.* SL crop) had a larger impact on the final annual yield than when it was applied in autumn, as SL crops yielded 30% less annual DM_{shoot} than LS crops (Figure 5.1). The difference occurred mainly because crops with longer rotations during early season (*e.g.* LL and LS crops) were able to grow for longer periods when linear growth rates (*LGR*) were the highest (Figure 5.3).

The *LGR* changed seasonally from less than 20 kg DM/ha/day in autumn to a maximum of ~170 kg DM/ha/day ($LS_{03/04}$ and $LL_{03/04}$) in summer. This agrees with Gosse *et al.*, (1988) who observed a decrease in *LGR* from 160 kg DM/ha/day in summer to 90 kg DM/ha/day in autumn at Lusignan, France (~46°N). The decrease in *LGR* during autumn is partially explained by the reduction in mean air temperature (T_{mean}) and available radiation (R_o, $MJ/m^2/day$) during this period (Section 2.1). A plethora of literature suggests that lower *LGR* during autumn are also due to a greater partitioning of photosynthates to perennial organs (Section 2.6). These issues will be further explored in Chapter 7.

The short defoliation cycle applied during the late season (LS crop) reduced shoot yield in the following early-spring growth. This can be seen by the reduction in the growth rate of $LS_{03/04}$ (~65% of $LL_{03/04}$) during early-spring 2003/04 (Figure 5.4). The reduction in DM_{shoot} highlights the impact of limited autumn perennial reserves (Section 4.3.6.4) on shoot yield during early-spring and is consistent with previous research (Belanger *et al.*, 1992; Haagenson *et al.*, 2003b).

5.4.2 Leaf:stem ratio

The search for predictors of leaf to stem ratio (*LSR*, g leaf/g stem), or alternatively leaf proportion (*LP*, g leaf/g shoot) are a major objective in lucerne simulation modelling (Fick *et al.*, 1994). The proportion of leaves in the dry matter is a major factor contributing to yield (*e.g.* photosynthesis and transpiration) (Lawlor, 1995) and quality (Buxton *et al.*, 1985) of lucerne crops. Thermal-time accumulation (T_b=5°C) explained 73% of the variation in *LP*, which decreased at a rate of $7x10^{-4}$ units/°Cd (Figure 5.8). Onstad and Fick (1983) also found Tt_{b5} adequate to predict leaf proportion (R^2>0.80) but Fick *et al.* (1994) indicated that the empiricism of the relationship limited its generalization to other sites and seasons from where models were developed. Interestingly, the only model published by Onstad and Fick (1983) that gave the closest fit to the whole data-set of 'Kaituna' was derived for the early-spring growth of several lucerne cultivars grown in central New York State (U.S.A.).

Alternatively, *LSR* was plotted against DM_{shoot} assuming an allometric increase of leaves and stems in total shoot DM (Lemaire *et al.*, 1992). Defoliation treatments and the level of perennial reserves had no apparent effect on the *LSR* pattern when crops where compared at similar DM_{shoot}, which explained 77% of the observed differences (Figure 5.9). For example, *LSR* decreased in all treatments from ~2.0 at the beginning of regrowth to 0.7 at 3 t/ha. Only LL and LS crops produced DM_{shoot} yields in excess of 3 t/ha, therefore the *LSR* of those treatments were usually lower than for SL and SS at the end of a regrowth cycle (Figure 5.7). Similarly, Lemaire *et al.* (1992) showed that *LSR* was conservative when compared at similar shoot yields regardless of growth cycles and mineral nitrogen supply. The allometric model for DM_{shoot} >1t/ha proposed by these authors, which was developed

for cultivar 'Europe' in France, was an accurate predictor of *LSR* in the experiment reported (Figure 5.9).

The greater variation in *LSR* at low DM_{shoot} (Figure 5.9) seemed to be an artefact of the imprecision of measurements at low yields because strong allometric relationships (R^2=0.99) explained the differences of leaf and stem DM based on DM_{shoot}. The implication is that at any given DM_{shoot}, the partitioning of dry matter to leaves (p_{leaf}) can be estimated by the rate of change in the allocation of leaf DM (DM_{leaf}) to shoots (Equation 5.2). This is analogous to the first derivative of the increase of DM_{leaf} with DM_{shoot} (Figure 5.10).

Equation 5.2

$$p_{leaf} = 0.26 \times \exp(0.68/(DM_{shoot} + 0.43))$$

Equation 5.2 demonstrates that the partitioning of dry matter to leaves is near 100% at negligible values of DM_{shoot} but it declines to a lower asymptote of ~26% as DM_{shoot} tends to the infinity.

5.4.3 The effects of perennial reserves on shoot yield

The effect of perennial reserves on shoot yield could be isolated during the first early-spring regrowth and in the cycles following the shift of defoliation treatments (post 4th February). The DM_{shoot} yield of LS crops successively decreased to be 160, 137 and 100% of SS crop values in the three regrowth cycles (Cycles 4, 5 and 6) following the switch of defoliation cycle. The higher level of perennial reserves in LS crops (Section 4.3.6.3) contributed to the increased yield in LS crops relative to SS in Cycles 4 and 5, but the impact was minimized by Cycle 6, when shoot yields were minimal. A similar but opposite residual effect was observed in SL crops where DM_{shoot} yield increased to be 70, 83, and 93% relative to LL values after 4th February.

The crops defoliated frequently in autumn (LS and SS crops) had lower winter levels of perennial reserves than LL crops (Section 4.3.6.4) and this limited shoot growth rates during the following spring regrowth (Figure 5.4). Dhont *et al.* (2004) observed that an additional defoliation in mid-autumn reduced shoot yield in the following spring by 0.3 to

2.0 t/ha. Similarly, Trimble *et al.* (1987) observed that an extra autumn defoliation reduced yield in the following spring to ~80% of controls, possibly due to a reduction in the level of storage nitrogen in roots and crowns. The impact of autumn defoliation on the level of perennial organs, and consequently the regrowth potential in spring, has important implications for lucerne management in Canterbury. In New Zealand farms where lucerne comprises more than 30% of the area of forage production it is necessary to graze lucerne as early as possible in spring, when crops are near 0.2 m tall or yield is ~1.5 t/ha (Moot *et al.*, 2003). The time to reach this yield was delayed by 60°Cd (~15 days in spring) in crops with limited amounts of perennial reserves (Figure 5.4).

The winter amounts and concentrations of taproot reserves were tested as predictors of spring shoot linear growth rates (Figure 5.5). Carbohydrate concentrations were not related to differences in *LGR* ($0.23<P<0.35$). The relationship between taproot carbohydrate amounts and *LGR* was also not significant ($0.07<P<0.12$) although there was a trend of increasing *LGR* as the amounts of carbohydrates increased (Figure 5.5 *e, f*). Fankhauser *et al.* (1989) also observed no difference in shoot growth rates among lucerne crops with root carbohydrate levels differing by 3 fold. These findings agree with an abundance of literature that shows that levels of carbohydrates in perennial organs have little influence on growth potential of lucerne, as they are mostly consumed in root respiration (Avice *et al.*, 2001).

In contrast, winter nitrogen concentrations and mainly absolute 'nitrogen amounts' in taproots were strongly related to spring shoot growth rates (Figure 5.5 *a, d*). Linear growth rates increased from 50 kg DM/ha/day at 1.2% N or 20 kg N/ha to ~90 kg DM/ha/day at 1.8% N or 60 kg N/ha. Similarly, Ourry *et al.* (1994) observed a strong linear relationship between the amounts of N in lucerne perennial organs at the day of harvest and shoot yield. This because, after defoliation, root nitrogen is largely mobilized from roots (Barber *et al.*, 1996) to new growing shoots, making up more than 50% of shoot nitrogen after 30 days of regrowth (Avice *et al.*, 1996). The weaker relationship of N concentration and *LGR* ($R^2=0.58$) is in agreement with Avice *et al.* (1997b) who observed no relationship between taproot N concentration and final shoot yield. These results indicate that the amounts of nitrogen were a more reliable indicator of shoot potential growth rates than nitrogen concentrations. This is because the $N\%_{root}$ is counterbalanced by changes in total taproot biomass and therefore only partially reflects the differences in the availability of nitrogen for mobilization to shoots (Section 4.4).

5.4.4 Yield components

5.4.4.1 Plant population

The exponential decline in plant population over time (Figure 5.11) agreed with previous reports in the literature (Belanger *et al.*, 1992; Dhont *et al.*, 2004; Gosse *et al.*, 1984). By the end of the 2003/04 season, plant population had declined to ~40% of the 120 plants/m^2 observed at the beginning of the experiment (June 2002). Inter-plant competition for light was probably the major cause of this decline (Gosse *et al.*, 1988). This process is usually characterized by an exponential increase in shoot mass/plant as plant population declines. When plotted on a logarithmic scale, this relationship has a slope of ~1.0 to 1.7 which characterizes the self-thinning of plants (Berg *et al.*, 2005; Matthew *et al.*, 1995). In the current experiment the decline in plant population had no effect on shoot yield. Similarly, Volenec *et al.* (1987) showed that lucerne crops at varying plant populations (11 to 172 plants/m^2) yielded similarly because increases in the individual shoot mass (*ISM*) and shoots/plant compensated for changes in plant population.

Of note was the fact that defoliation frequency and the level of perennial reserves had no apparent effect on the rate of decline in plant population (Figure 12). This agrees with the observation of Purves and Wynn-Williams (1994) who recorded similar rates of plant population decay in lucerne crops grazed each 28 or 56 days in a four year trial using eight different lucerne cultivars. Belanger *et al.* (1992) observed a similar and conservative reduction in the stand from 100 to 60 plants/m^2 among lucerne crops subjected to eight contrasting cutting regimes. In contrast, literature often suggests that defoliation frequency increases the death of lucerne plants due to the reduction in the level of perennial reserves (Davies and Peoples, 2003). This is possibly because other stresses (*e.g.* weed competition, pests, diseases, water logging, drought) increase the rate of plant mortality (Lodge, 1991; Purves and Wynn-Williams, 1994), exacerbating the effect of frequent defoliations. In the current experiment, weed invasion would be expected to enhance competition for light in frequently defoliated crops (*e.g.* SS crops) but this was avoided through chemical weed control (Section 3.3.4.3).

5.4.4.2 Shoot population

In general, shoot population on the day of harvest was conservative at ~780 shoots/m^2 throughout different treatments/season combinations. This was due to a compensatory increase in the number of shoots/plant as plant population declined (Figure 5.15). This also agrees with Gosse *et al.* (1988) who observed a conservative final number of shoots in several regrowth cycles of cultivars 'Du Puits' and 'Europe'. The range in plant populations observed during the current experiment (50-140 plants/m^2) was therefore above the threshold where the number of shoots/plant was unable to compensate for plant population decline. This lower threshold may define the moment when the crop potential productivity declines. The upper threshold of plant population, where shoots/plant is unchanged, would appear to be above 140 plants/m^2 for 'Kaituna' lucerne. In Figure 5.15, the exponential decline of shoots/plant indicated a lower asymptote of 3.7 shoots/plant at high plant populations. This is close to the conservative 2.0 to 2.7 shoots/plant observed at 220 plants/m^2 in lucerne crops under contrasting K and P fertilization rates (Berg *et al.*, 2005).

After defoliation, shoot population increased at a rate of ~6 shoots/m^2/°Cd (Figure 5.13) in all treatments (Figure 5.12). Therefore basal and axillary shoot initiation, and consequently shoot appearance rate, were not limited by the levels of perennial reserves in this experiment. Most probably, morphogenetic responses to environmental factors defined shoot appearance rates (Davies and Thomas, 1983). Air temperature was possibly an important driver of shoot appearance rates but other factors should be involved as the relationship between shoot population and $\sum Tt_{b5}$ had an R^2 of 0.62. The light environment was managed by mowing to avoid any influence on shoot appearance rates. In contrast, at more advanced stages of regrowth, the light environment limited shoot appearance rates and self-thinning of shoots resumed. At *LAI* of 2.0, only ~20% of the available light reached the basal buds (assuming k=0.81, Section 6.3.2) and this would be expected to reduce the red-far red light ratio that stimulates bud initiation (Casal *et al.*, 1985). This value of transmittance is close to the light-compensation point of 0.15 observed by Lemaire *et al.* (1991) for lucerne. These authors demonstrated that nitrogen content of lucerne leaves declines at faster rates at transmittances below 0.15, ultimately leading shoots to a negative carbon balance, senescence and shoot death. As shoot population declined, there was a clear segregation of shoot height categories after a *LAI* of ~2.0

(Figure 5.14). For example, dominant shoots (D_{shoot}) represented ~80% of DM_{shoot} at a *LAI* of 4.0, but only 50% at *LAI* of 2.0.

5.4.4.3 Individual shoot mass

Individual shoot mass (*ISM*, g DM/shoot) was the yield component that explained most of the variation (R^2=0.96) in DM_{shoot} throughout seasons and among treatments (Figure 5.16). DM_{shoot} increased bi-linearly with *ISM* at 8.1 t/g *ISM* when *ISM* was <0.3 g/shoot but at 4.9 t/g *ISM* after that. The point of inflection of the relationship (*ISM*=0.3 g/shoot) can be empirically associated (R^2=0.87) with an *LAI* of 2.7 (PAR transmittance of 0.11), and a DM_{shoot} of 2.2 t/ha (R^2=0.99) in the present experiment. Again, it seems that the competition for light modified the shoot population dynamics from ~700-800 shoots/m^2 when the canopy was open (PAR transmittance>0.15) to nearly 500 shoots/m^2 at more advanced stages of regrowth. The inflection point, where self-thinning resumed, was near a *LAI* of 2.0 but the decline in the response of DM_{shoot} to *ISM* became evident at *LAI*>2.7. At this point, gains in *ISM* were partially offset by the death of intermediate and suppressed shoots (Figure 5.14). The *ISM* was also shown to explain most of the yield differences among lucerne crops under contrasting P and K fertilization rates (Berg *et al.*, 2005). The present experiment indicated that lucerne shoot yield reflected changes in the weight of each individual shoot, regardless of (*i*) defoliation regimes, (*ii*) the level of perennial reserves or (*iii*) seasonal environmental factors. The implication is that, for modelling purposes, the crop can be treated as a group of homogenous shoots, as long as plant population is above a threshold where it does not limit shoot appearance rates and *LAI* development.

The differences in the allocation of assimilates to individual shoots and consequently shoot yield may be explained by changes in resource capture (*e.g.* light interception), efficiency of conversion of resources in biomass (*e.g. RUE*) and/or by different partitioning patterns of DM between shoots and roots. These issues will be addressed in the following chapters.

5.5 Conclusions

The results displayed in this chapter permit the following conclusions:

- The defoliation frequency applied in spring-summer largely determined total annual yield that differed from 13 to 24 t DM/ha.
- The proportion of leaves in the shoot differed from ~40 to 70% of DM but could be predicted by an allometric relationship with shoot yield for all treatments and seasons.
- Autumn management affected shoot growth rates in the following early-spring regrowth due to reduced availability of perennial reserves.
- The nitrogen component of taproot reserves had the strongest relationship ($0.6<R^2<0.8$) with shoot growth rate.
- Treatments and seasons affected lucerne shoot yield by changes in individual shoot weight. Plant population and shoots/plant had compensatory dynamics which maintained optimum shoot populations for the duration of the experiment.

The effects of contrasting defoliation frequencies and environmental factors on shoot yield were mainly expressed on the weight of individual shoots. Therefore mechanisms able to limit the allocation of DM to each individual shoot will be explored in the following chapters. More specifically C allocation to shoots differed among treatments and seasons and this could be caused by changes in (*i*) the amount of available resources for growth (*e.g.* light interception), (*ii*) the efficiency of conversion of resources to DM_{shoot} (*e.g RUE*) or (*iii*) the allocation of DM to different organs. These possibilities will be analysed individually in Chapters 6 and 7.

6 PAR interception and canopy development

6.1 Introduction

Shoot yield of lucerne is strongly related to the amount of photosynthetic active radiation (PAR) intercepted by the crop (Gosse *et al.*, 1982a). The interception of PAR is a function of canopy expansion rates, canopy structure and the optical properties of leaves (Section 2.3).

The reduction in shoot yield observed in frequently grazed lucerne crops (Chapter 5) could be caused by reduced PAR interception compared with LL crops. Alternatively, a decrease in the *RUE* (Section 2.5) or an increase in the partitioning of DM to perennial organs could reduce shoot yield.

The objective of this chapter is to quantify seasonal differences and the effect of defoliation treatments on PAR interception. Differences are analysed in terms of (*i*) canopy architecture through the extinction coefficient for diffuse light (k_d) and (*ii*) canopy expansion through the leaf area index (*LAI*). The development of *LAI* is segmented into its components (leaf appearance rates and branching) and growth components (shoot population, individual leaf area and leaf senescence).

Differences in these variables are analysed and discussed in relation to environmental seasonal signals and the level of perennial reserves of crops.

6.2 Materials and methods

6.2.1 Accumulated PAR interception

Accumulated intercepted PAR was calculated by summing daily estimates of intercepted PAR (PAR_i) from each regrowth period. Daily PAR_i was obtained by multiplying the available above canopy PAR of each day (PAR_o) by the fractional PAR interception (PAR_i/PAR_o) of the same day for each treatment plot.

Fractional PAR interception was estimated from measurements of fractional diffuse non-interceptance (DIFN) taken with a canopy analyser LAI-2000 (LI-COR Inc., Lincoln, Nebraska, USA). Readings of DIFN were taken in predominantly diffuse light conditions at 7 day intervals, starting 10 days after the last grazing day of each regrowth cycle. The equipment was set to take one reading above and five readings below canopy in each plot. The canopy analyser measures the fractional transmission of diffuse PAR (*i.e.* DIFN) through the canopy at wave lengths lower than 490 nm from readings at 5 different zenith angles (7, 23, 38, 53 and 68°). Therefore, DIFN represents the fraction of sky that is not blocked by foliage (Jonckheere *et al.*, 2004) and represents $1-(PAR_i/PAR_o)$.

To evaluate the accuracy of 1-DIFN as a measure of PAR_i/PAR_o, the relationship between 1–DIFN (diffuse PAR interception) and fractional total solar radiation interception (R_i/R_o) was tested. This was done by plotting readings of 1–DIFN from 27 dates with independent measurements of R_i/R_o taken from tube solarimeters during the same days (Figure 6.1). Measurements of R_i/R_o were calculated by dividing daily intercepted solar radiation (R_i) by the above canopy solar radiation (R_o) averaged through 3 tube solarimeters located in plots 14 and 15 (LL crop). There was a strong linear relationship (R^2=0.96) between 1–DIFN and R_i/R_o with a slope (P<0.0001) of 1.03 ± 0.09 (95% confidence interval) and an intercept (P<0.01) of 0.08 (±0.06). This implies that the canopy analyser consistently measured 0.08 more fractional interception than the tube solarimeters regardless of the amount of canopy cover. This positive intercept would be expected because the canopy analyser measures wavelengths in the blue region of the solar spectrum (<490 nm) while the tube solarimeters are sensitive to a larger band of the entire solar spectrum (400-2200

nm). Based on these observations, fractional PAR interception (PAR_i/PAR_o) throughout this thesis was assumed to be equal to diffuse interceptance (1–DIFN) measured with the canopy analyser. Daily values of PAR_i/PAR_o were estimated by linearly interpolating weekly measurements of 1–DIFN.

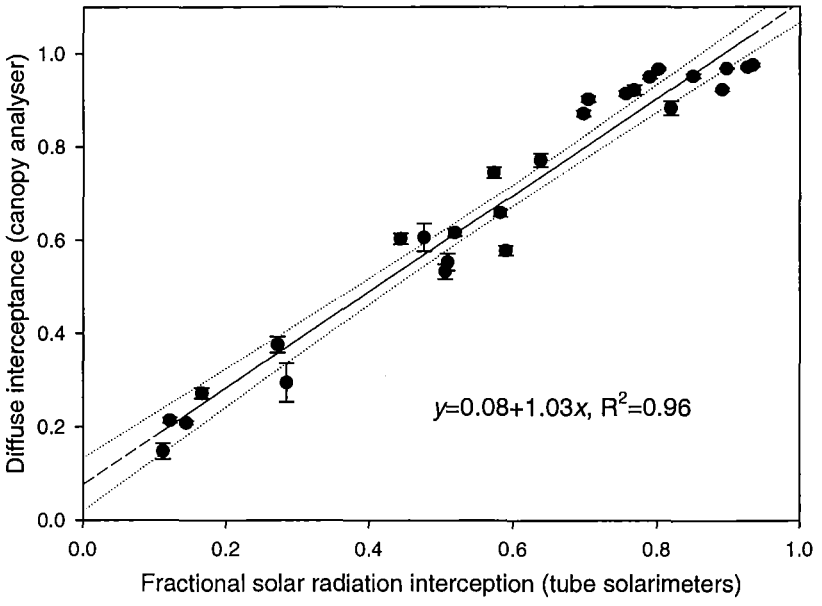

Figure 6.1 Relationship between fractional solar radiation interception from tube solarimeters measurements and diffuse interceptance (1–DIFN) from canopy analyser (LAI-2000) for a lucerne crop during the 2003/04 season at Lincoln University, Canterbury, New Zealand.

Note: Dashed line represents the extrapolation of the model to x=0. Dotted lines delimit 95% confidence intervals of the estimate.

6.2.2 Leaf area index

Leaf area index (*LAI*) was estimated from calibrated computations of plant area index ($PAI_{LAI\text{-}2000}$) taken with the canopy analyser on the same dates when DIFN readings were performed (Section 6.2.1). All readings at $PAI_{LAI\text{-}2000}<1.5$ were taken with the sensor lens at ground level. This was done by placing the canopy analyser sensor inside channels (30 mm depth x 300 mm length) that were dug before the first measurement of each regrowth cycle. This procedure guaranteed that the transmittance of light by short canopies was measured by the sensors. When $PAI_{LAI\text{-}2000}>1.5$ the readings were taken at sensor height (~30 mm above ground level).

$PAI_{LAI\text{-}2000}$ computations were calibrated with 110 destructive measurements of *LAI* taken from 2 June 2003 to 16 March 2004 (Section 6.2.2.1). *LAI* increased linearly ($P<0.0001$) with $PAI_{LAI\text{-}2000}$ with a slope of 0.93 (±0.05) and an intercept not different ($P<0.32$) from zero. Therefore $PAI_{LAI\text{-}2000}$ overestimated actual *LAI* by ~7% and this was corrected by adjusting $PAI_{LAI\text{-}2000}$ as in Equation 6.1.

Equation 6.1.

$$LAI = 0.93 \times PAI_{LAI-2000}$$

6.2.2.1 Destructive LAI measurements

During the first half of the 2003/04 growth season, sub-samples of 5-10 'dominant' shoots were separated from the DM_{shoot} sample (Section 5.2.1). All the leaves of the selected shoots were removed, opened onto a flat A4 white paper background and photographed with a Nikon digital camera model CoolPix 950 (Nikon Co., Japan). Pictures were analysed with the image software 'QUANT' v.1.0.1 (Vale et al., 2003) and individually calibrated to the number of pixels contained in a 200 mm reference scale. Leaf samples were then dried in a forced air oven for at least 48 hours at 65°C to a constant weight and the average canopy specific leaf weight (*SLW*, g/m^2) was calculated as leaf mass (g DM) per unit area of green leaf (m^2). Destructive leaf area index (LAI_{dest}) was then calculated as:

Equation 6.2

$$LAI_{dest} = DM_{leaf}/SLW$$

Where DM_{leaf} is the total amount of leaf DM (g/m^2) estimated for a given plot (Section 5.2.1) and *SLW* is the specific leaf weight.

6.2.3 Extinction coefficient for diffuse radiation

The extinction coefficient for diffuse radiation (k_d) was calculated as the linear slope between the natural log of PAR transmission [1–(PAR_i/PAR_o)] during overcast conditions and *LAI* (Hay and Walker, 1989b). The value of k_d was estimated by plotting 110 measurements of 1–(PAR_i/PAR_o) taken with the canopy analyser with independent destructive measurements of *LAI* from 2 June 2003 to 16 March 2004 (Section 6.2.2.1).

6.2.4 Thermal-time calculation and temperature threshold

Daily thermal-time (*Tt*, °Cd) was calculated using a broken stick threshold where *Tt* is assumed zero for mean air temperatures (T_{mean}) below the base temperatures (T_b) (Section 2.4.1.1). In this framework *Tt* is accumulated linearly from T_b to an optimum temperature (T_{opt}) of 30°C. Above T_{opt} values of *Tt* decline linearly to zero at a maximum (T_m) of 40°C. Thermal-time accumulation ($\sum Tt$) was then calculated as the sum of daily *Tt* throughout each regrowth cycle.

6.2.4.1 Validation of base temperature

The most suitable base temperature for the thermal-time calculation was estimated through three different methods: (*i*) *x*-intercept; (*ii*) least variable; and (*iii*) regression coefficient (Sharratt *et al.*, 1989).

Method (*i*), the *x-intercept* method (Arnold, 1959), consisted of plotting the main-stem leaf appearance rate (leaves/day) against the mean air temperature of the respective regrowth cycle. Firstly, primary leaf appearance rate (*LAR*, days/leaf) was calculated as the linear slope between the number of primary leaves and the number of days after grazing for each regrowth cycle. Secondly, *LAR* was plotted as a function of T_{mean}, and the extrapolation of the linear relation to y=0 gave the x-intercept.

Method (*ii*), the *least variable* method (Sharratt *et al.*, 1989), consisted of determining the value of T_b which resulted in the lowest coefficient of variation (CV%) of *Tt* for a particular developmental stage over different periods. In this thesis the mean phyllochron (°Cd/main-stem leaf) was calculated for each regrowth cycle and the CV% among cycles was calculated for 10 different T_b values (from T_b=1 to T_b=10°C at intervals of 1°C). The T_b that produced the lowest CV% was assumed to be the correct base temperature.

Method (*iii*), the *regression coefficient* method, consisted of finding a T_b that makes the variation in *Tt* requirement for a given developmental stage null in respect to different T_{mean} (Hoover (1955) cited by Sharratt *et al.* (1989)). Specifically, the phyllochron for each regrowth cycle was calculated using 10 different T_b (from T_b=1 to T_b=10°C) at intervals of 1°C. Phyllochrons were then plotted against average T_{mean} for the respective regrowth

cycle. The selected T_b was the one that produced a slope with the highest probability (*P* value) of not being different from zero.

6.2.5 Leaf area expansion rate

Leaf area expansion rate (*LAER*, $m^2/m^2/°Cd$) was calculated as the slope of the linear regression between *LAI* against $\sum Tt$ for each treatment-regrowth cycle combination. The *LAER* was then plotted against the mean date of each regrowth cycle to test the seasonal pattern of the relationship.

6.2.6 Shoot population

Shoot population was measured weekly by counting the number of shoots in a 0.2 m^2 quadrat randomly placed in each plot. Detailed methods are described in Section 5.2.

6.2.7 Primary leaf appearance and senescence

Fully expanded primary leaves were counted from 80 marked shoots (5 per plot) on 255 dates from 22 August 2003 to 8 June 2004. At the beginning of each regrowth cycle a group of five dominant shoots (Section 5.2.1) per treatment plot (from different plants) were marked with numbered labels. Starting from 7-10 days after grazing, these marked shoots were assessed every 7 days for (*i*) the number of fully expanded primary leaves, (*ii*) stem height (from ground to the apical bud) and (*iii*) the number of senesced leaves (2003/04 growth season only). A leaf was considered senesced when more than half of its area was pale-yellow or when the leaf was not attached to the node. Measured shoots that exhibited an early senescence or death were discarded and replaced with new shoots. This bias was intentionally used to ensure that only dominant shoots were assessed as they contributed to the majority of the yield (Section 5.3.4.3).

6.2.8 Phyllochron calculation

The number of primary leaves per shoot (Section 6.2.7) was plotted against thermal-time accumulation (Section 6.2.4) of each rotation. The slope of the linear regression represents the phyllochron or the average accumulated thermal-time required for the appearance of one primary leaf during each regrowth cycle (°Cd/leaf).

The average photoperiod (*Pp*) of each regrowth cycle was tested as a predictor of phyllochron. This was done by plotting phyllochron as a function of increasing and decreasing *Pp* and testing the relationship with linear and non-linear regressions.

6.2.9 Number of axillary leaves (branching)

The number of axillary leaves at each main-stem node was counted during the summer-autumn period of the 2003/04 growth season (19 February 2004 to 5 May 2004). This was done on the same marked shoots used for the leaf appearance measurements (Section 6.2.7). Measurements were taken in LL (cycles 4 and 5), LS (cycles 5, 6 and 7), SL (cycle 7) and SS crops (cycles 6, 7 and 8) on the same dates that leaf appearance was measured.

6.2.10 Individual area of primary and axillary leaves

Leaf area of individual primary and axillary leaves was measured on 3 occasions from 1 October 2003 to 16 March 2004. For each sampling date 20 dominant shoots (5 per plot) of treatments LL and SS were harvested. Leaves of each main-stem node position were detached and photographed. Images were analysed using the software 'QUANT' (Vale *et al.*, 2003) and the area of each leaf was calculated as detailed in Section 6.2.2.1.

Leaf area was plotted against main-stem node position from the base of the shoot. A bell-shaped function (Dwyer and Stewart, 1986) commonly used to model leaf area in cereals (Elings, 2000) was tested to describe the variation in leaf area with node position:

Equation 6.3.

$$Y = Y_0 \times \exp[a \times (X - X_0)^2 + b \times (X - X_0)^3]$$

Where Y is the individual leaf area (mm^2) at node position X, Y_0 is the mature leaf area of the largest leaf (mm^2), X is the leaf number counted from the base of the main-stem, X_0 is the position of the largest leaf in the main-stem (inflection point of the curve), and a and b are empirical constants. Parameter a quantifies the kurtosis or "breadth" of the curve whereby low values of a result in a sharp increase or decrease of the curve. Parameter b quantifies the degree of "skewness" of the curve with positive values resulting in curves skewed to the right (towards leaf positions greater than X_0).

To test the similarity of parameters among crops and regrowth cycles the values of X were normalized by the final number of leaves (X_{max}). Similarly, the values of Y were normalized by area of the largest leaf (Y_0). This was done by dividing Y/Y_0 and X/X_{max} and plotting the resulting normalized variables (Elings, 2000).

6.3 Results

6.3.1 Annual accumulated PAR interception

The accumulated amount of intercepted PAR (PAR_i, MJ/m^2) throughout 2002/03 and 2003/04 growing seasons is shown in Figure 6.2. As expected, intercepted PAR mimicked annual DM_{shoot} accumulation (Section 5.3.1) and increased in a sigmoidal pattern.

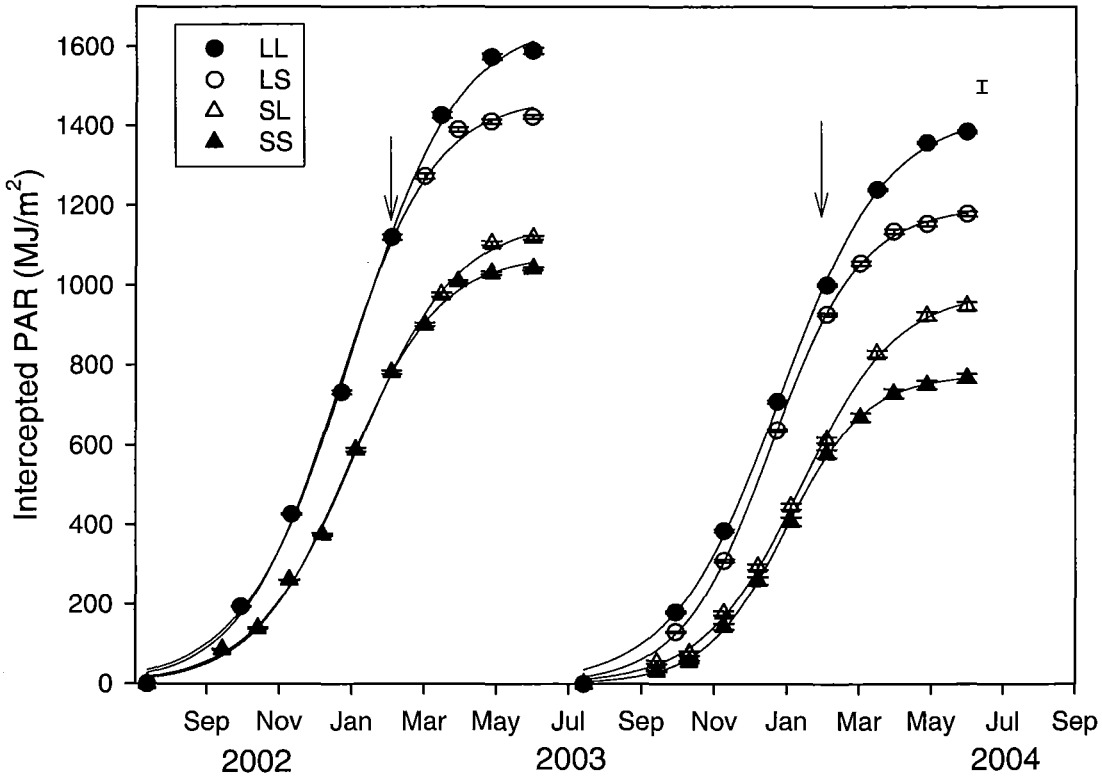

Figure 6.2 Seasonal accumulated PAR interception (MJ/m^2) of lucerne crops subjected to four contrasting defoliation regimes in the 2002/03 and 2003/04 growth seasons at Lincoln University, Canterbury, New Zealand.

Note: Arrows indicate the date when defoliation treatments were shifted (4th February). Solid lines are sigmoid functions; parameters are displayed in Appendix 2. Bar represents one SEM for final annual PAR interception.

The LL crops intercepted the greatest (P<0.01) amount of PAR in both growing seasons. During 2002/03, LL intercepted 1,600 MJ/m^2 followed by LS (1,400 MJ/m^2), SL (1,100

MJ/m^2) and SS (~1,000 MJ/m^2). The ranking of the treatments was similar in 2003/04 but the difference between LL and the other crops increased.

Interestingly, $LL_{03/04}$ crops intercepted ~200 MJ/m^2 less PAR than $LL_{02/03}$ but yielded similar amounts of DM (24 t/ha, Section 5.3.1). This implies a possible difference in the efficiency of conversion of PAR to DM (*i.e. RUE*) or partitioning of assimilated carbon to shoots. These processes are discussed in Chapter 7.

The lower interception of PAR in LS, SL and SS crops when compared with the LL crops suggested that the area of green leaves (*i.e. LAI*) or the efficiency of interception per unit of leaf (*e.g.* different canopy architecture) was reduced in these more frequently grazed crops.

6.3.2 Extinction coefficient as an indication of canopy architecture

Canopy architecture (*i.e.* leaf angles and leaf distribution) was described by the extinction coefficient for diffuse PAR (k_d, Section 6.2.3). There was no difference ($P<0.95$) in the pattern of light interception per unit of *LAI* among the four defoliation treatments. A conservative k_d of 0.81 indicated that all crops had a similar critical *LAI* (LAI_{crit}) of 3.6, when 95% of available PAR (PAR_o) was intercepted (Figure 6.3).

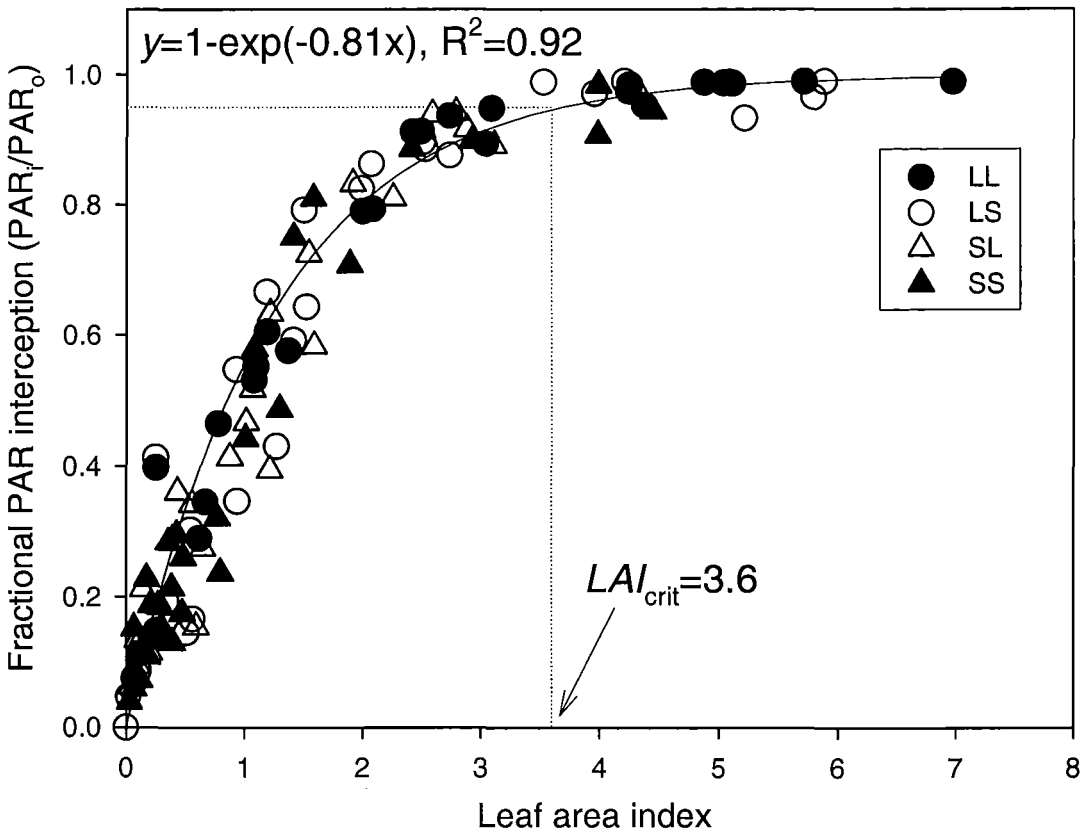

Figure 6.3 Relationship between *LAI* and the fractional PAR interception of lucerne crops subjected to four contrasting defoliation regimes in the 2003/04 growth season at Lincoln University, Canterbury, New Zealand.

Note: *LAI* readings were taken from shoot destructive samples and fractional light interception (PAR_i/PAR_o) from canopy analyser diffuse interceptance (1–DIFN).

6.3.3 Seasonal leaf area index development

The pattern of *LAI* development differed among seasons (Figure 6.4). The maximum value observed for *LAI* was ~6 in LL and LS crops during the summer regrowth cycles (Figure 6.4 *a, b*). Treatments with short defoliation intervals had a lower ($P<0.05$) *LAI* than LL crops in both growth seasons. LL crops reached LAI_{crit} during most regrowth cycles, the exception being the last autumn cycle (cycle 6) in both growth seasons and Cycles 0 and 5 in 2003/04 (Figure 6.4 *a*). In contrast, SS crops only reached LAI_{crit} in 3 of their 18 regrowth cycles (Cycle 4 in 2002/03 and Cycle 5 during both growth seasons) (Figure 6.4 *d*). LS crops reached LAI_{crit} in most of the spring-summer regrowth cycles (apart from Cycle 0 – 2003/04). SL crops only reached LAI_{crit} in Cycles 5 and 6 (both growth seasons) and Cycle 4 in 2002/03 (Figure 6.4 *c*).

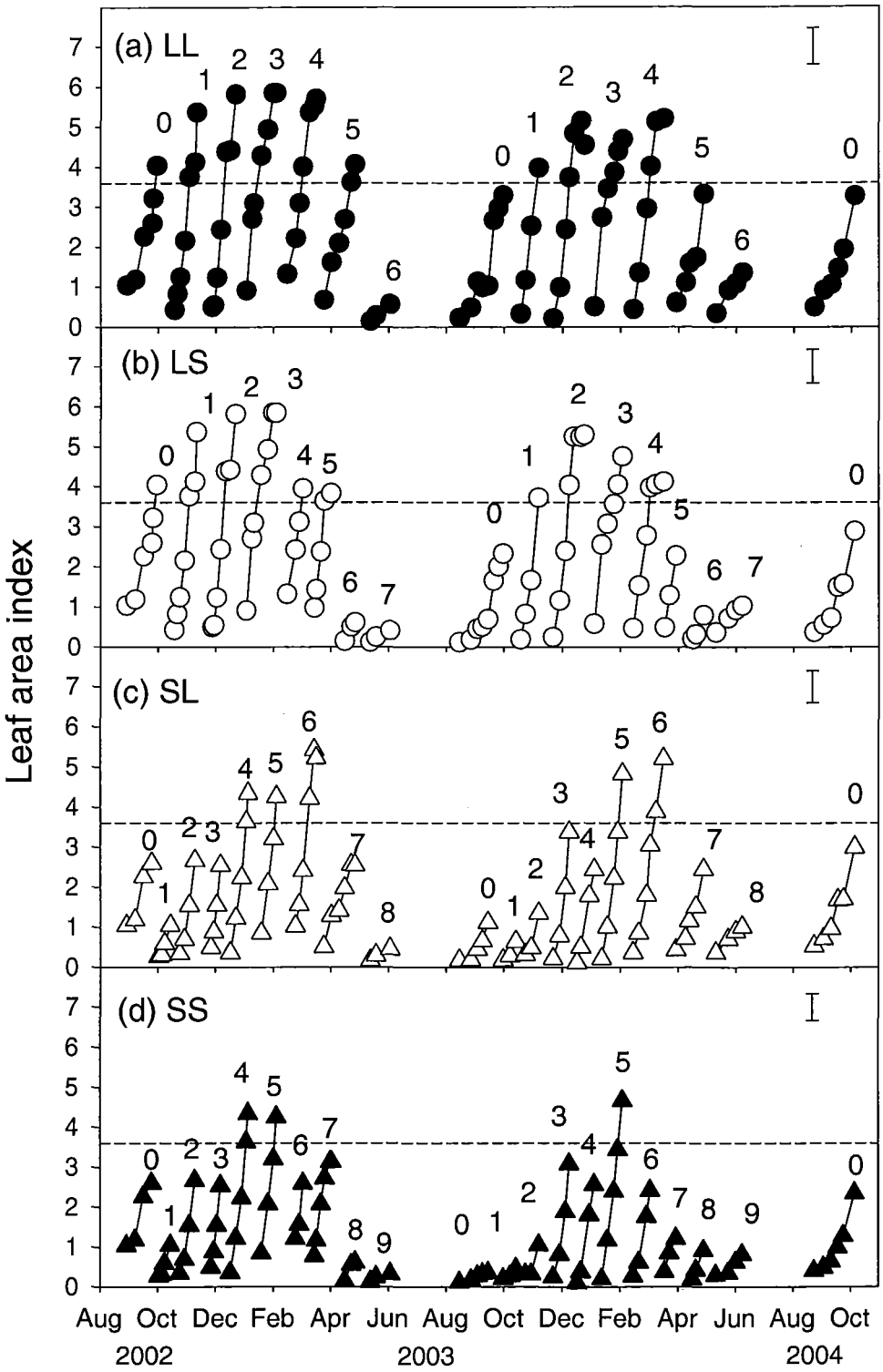

Figure 6.4 Seasonal leaf area index of lucerne crops subjected to four contrasting defoliation regimes in the 2002/03 and 2003/04 growth seasons at Lincoln University, Canterbury, New Zealand.

Note: Bars represents one standard error of the mean (SEM) pooled among regrowth cycles within each treatment. Numbers indicate the order of regrowth cycles of each growing season. Horizontal dotted line represents the critical *LAI* of 3.6 for reference.

With the objective of explaining the seasonal differences observed in *LAI* between regrowth cycles, *LAI* development was calculated on a thermal-time (*Tt*) basis ($m^2/m^2/°Cd$). This required the validation of a base temperature (T_b) that minimizes variation in *Tt* requirements for a given developmental stage (Section 6.2.4.1). In the case of the current experiment, leaf appearance rate was used as the variable to estimate T_b and calculate *Tt* requirements.

6.3.4 Estimation of base temperature for thermal-time calculation

Initially the value of the base temperature (T_b) for main-stem leaf appearance was calculated for the control crop (LL) using the '*x*-intercept' method (method *i*, Section 6.2.4.1). There was a strong relationship (R^2=0.96) between primary leaf appearance rates and the mean daily air temperature. The extrapolation of the model to *y*=0 (null development) gave an estimate of T_b of 5.2°C ± 95% confidence interval of 0.8°C (Figure 6.5). Estimates of T_b using 'least-variable' (method *ii*) and 'regression coefficient' (method *iii*) methods confirmed the statistical validity of T_b=5°C (Table 6.1), and gave estimates of T_b of 5.5°C (±2.1) and 5.5°C (±1.3), respectively.

Table 6.1 Base temperature for thermal-time calculation of 'Kaituna' lucerne grown at Lincoln University, Canterbury, New Zealand.

Method	Mean T_b	SEM	95% Confidence interval
(*i*) *x*-intercept	5.2	0.31	4.8-5.6
(*ii*) Least variable	5.5	0.74	3.4-7.6
(*iii*) Regression coefficient	5.5	0.42	4.2-6.8

Note: Details about methods are given in Section 6.2.4.1

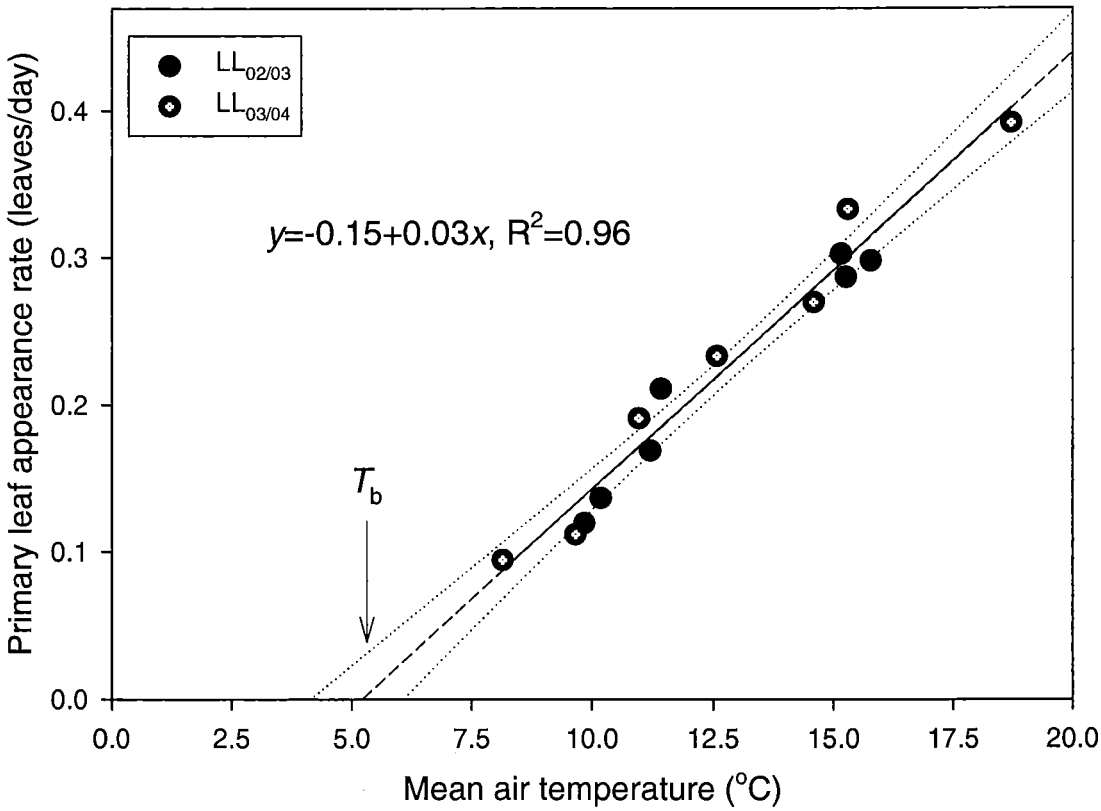

Figure 6.5 Relationship between leaf appearance rate (*LAR*) of primary leaves and mean air temperature for the lucerne control crop (LL) in the 2002/03 and 2003/04 growth seasons at Lincoln University, Canterbury, New Zealand.

Note: Dotted lines represent 95% confidence interval for slope. Dashed line represent projection of model to y=0 where x=T_b.

In addition to the validation of Tt_{b5}, a test of the broken-stick model using $Tt_{b1/5}$ (Moot *et al.*, 2001) was performed by the least-variable and the regression coefficient methods (Table 6.2). The coefficient of variation of phyllochron among regrowth cycles decreased from 21% for $Tt_{b1/5}$ to 15% for Tt_{b5}. Additionally, when Tt_{b5} was used in the calculations, T_{mean} had no systematic influence (slope=-0.27, P<0.63) on phyllochron calculation. In contrast, the phyllochron calculated using $Tt_{b1/5}$ decreased with T_{mean} (P<0.02) at a rate of 1.83°Cd/leaf/°C (Table 6.2).

Table 6.2 Test values for comparison of two temperature thresholds used to calculate thermal-time for lucerne crops subjected to a 42-day grazing rotation in the 2002/03 and 2003/04 growth seasons at Lincoln University, Canterbury, New Zealand.

Method	CV (%)	*b*	*P* value
Tt_{b5}	15	-0.27	0.63
$Tt_{b1/5}$	21	-1.83	0.02

Note: CV (%) is the coefficient of variation of phyllochron values calculated using a different T_b throughout the 2002/03 and 2003/04 growing seasons. Value of *b* represents the slope (°Cd/leaf/°C) of the linear model between mean air temperature and phyllochron calculated by the regression coefficient method. *P* is the probability that *b* is not different to zero.

6.3.5 Seasonal leaf area expansion rate

The reliability of thermal-time accumulation (Tt_{b5}) as a predictor of leaf area index (*LAI*) expansion was tested by regression analysis (Figure 6.6). The linear slope of the relationship was defined as leaf area expansion rate (*LAER*, $m^2/m^2/°Cd$). The *LAER* was not constant among regrowth cycles ($P<0.001$) and declined ($P<0.02$) from spring to autumn. For example in the LL crop, *LAER* decreased from a maximum of $25x10^{-3}$ $m^2/m^2/°Cd$ in spring-summer to less than $5x10^{-3}$ $m^2/m^2/°Cd$ in the last autumn regrowth cycle (Figure 6.6). Interestingly, during both growth seasons *LAER* of LL and LS crops had a peak in Cycle 1 (October-November) at $25x10^{-3}$ $m^2/m^2/°Cd$. Empirical broken-stick models ($0.76<R^2<0.99$) were fitted to all treatments in 2002/03 season and to LL crops in 2003/04 to determine the date when *LAER* declined at faster rates. For both seasons, the point of breakage of the bi-linear model was close to the autumn solstice (21 March) ± 6 days. After this date the decline in *LAER* was $0.2x10^{-3}$ $m^2/m^2/°Cd$ per day.

Short intervals of defoliation, mainly in spring-summer (SL and SS crops) reduced *LAER* notably in the 2003/04 growing season (Figure 6.6). In addition, the defoliation treatment imposed in the previous growth season carried an effect in *LAER* for the following early-spring regrowth. For example, *LAER* of SL crops was 34% and 20% greater than SS crops in the early spring regrowth periods of 2003/04 and 2004/05 respectively (Figure 6.6).

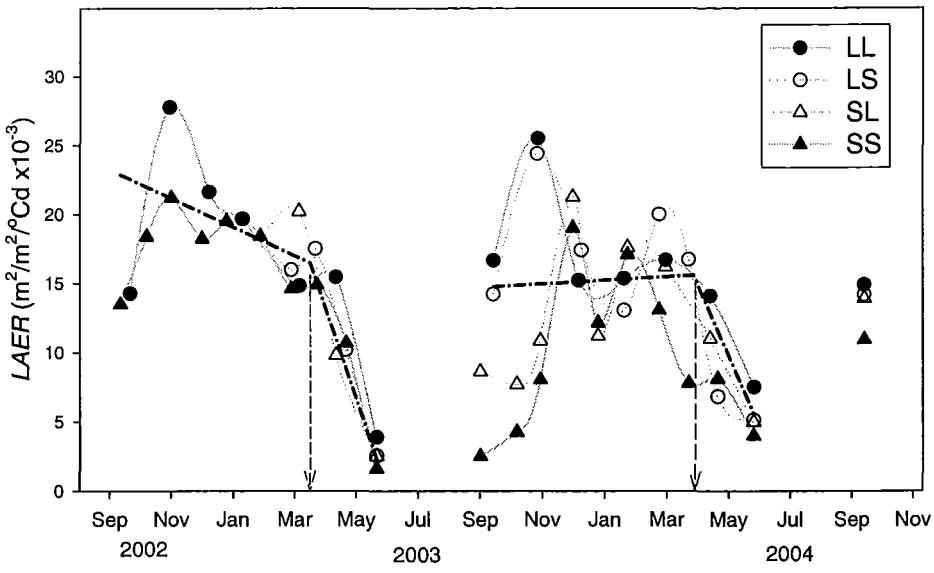

Figure 6.6 Seasonal variation of leaf area expansion rate (*LAER*) of lucerne crops subjected to four contrasting defoliation regimes in the 2002/03 and 2003/04 growth seasons at Lincoln University, Canterbury, New Zealand.

Note: Dark dashed-lines (—·—·—) represent a broken-stick model where x is days after 1 September 2002. Arrows indicate point of breakage of bi-linear models for all treatments in 2002/03 (x=200=19 Mar 03, R^2=0.78) and in 2003/04 for LL crops (x=574=27 Mar 04), excluding data-point from cycle 1. Linear model (y=a+bx) coefficients (intercept and slope respectively) in 2002/03 are: 23.2, -0.034 for y<200; 59.3,-0.22 for y>200. In 2003/04 coefficients are 14.72, -0.004 for y<574; 50.99,-0.16 for y>574.

6.3.5.1 LAER and photoperiod

The *LAER* was plotted against the mean photoperiod (*Pp*) of each respective regrowth cycle and the point of model breakage on 22 March (Figure 6.6) was positioned in the *Pp* of ~12.5 h (Figure 6.7). Empirical quadratic functions ($0.55<R^2<0.67$) were fitted to the data-set to quantify the consistent trend of decline in *LAER* at *Pp* <12.5 h. This trend of saturation at *Pp*>12.5 h was more evident in LL and LS crops although during the spring regrowth (Cycle 1) *LAER* was consistently higher at $25x10^{-3}$ $m^2/m^2/°Cd$ when *Pp* was ~15.5 h in both 2002/03 and 2003/04. In LL crops *LAER* declined from $16x10^{-3}$ $m^2/m^2/°Cd$ at *Pp* of 12.5 h to $5x10^{-3}$ $m^2/m^2/°Cd$ at *Pp* of 10.5 h (Figure 6.7*a*). The reduction in *LAER* of SL and SS crops (Figure 6.6) showed that the relationship of *LAER* and *Pp* was influenced by the low level of perennial reserves of these crops, particularly at *Pp* >13 h (Figure 6.7 *c, d*).

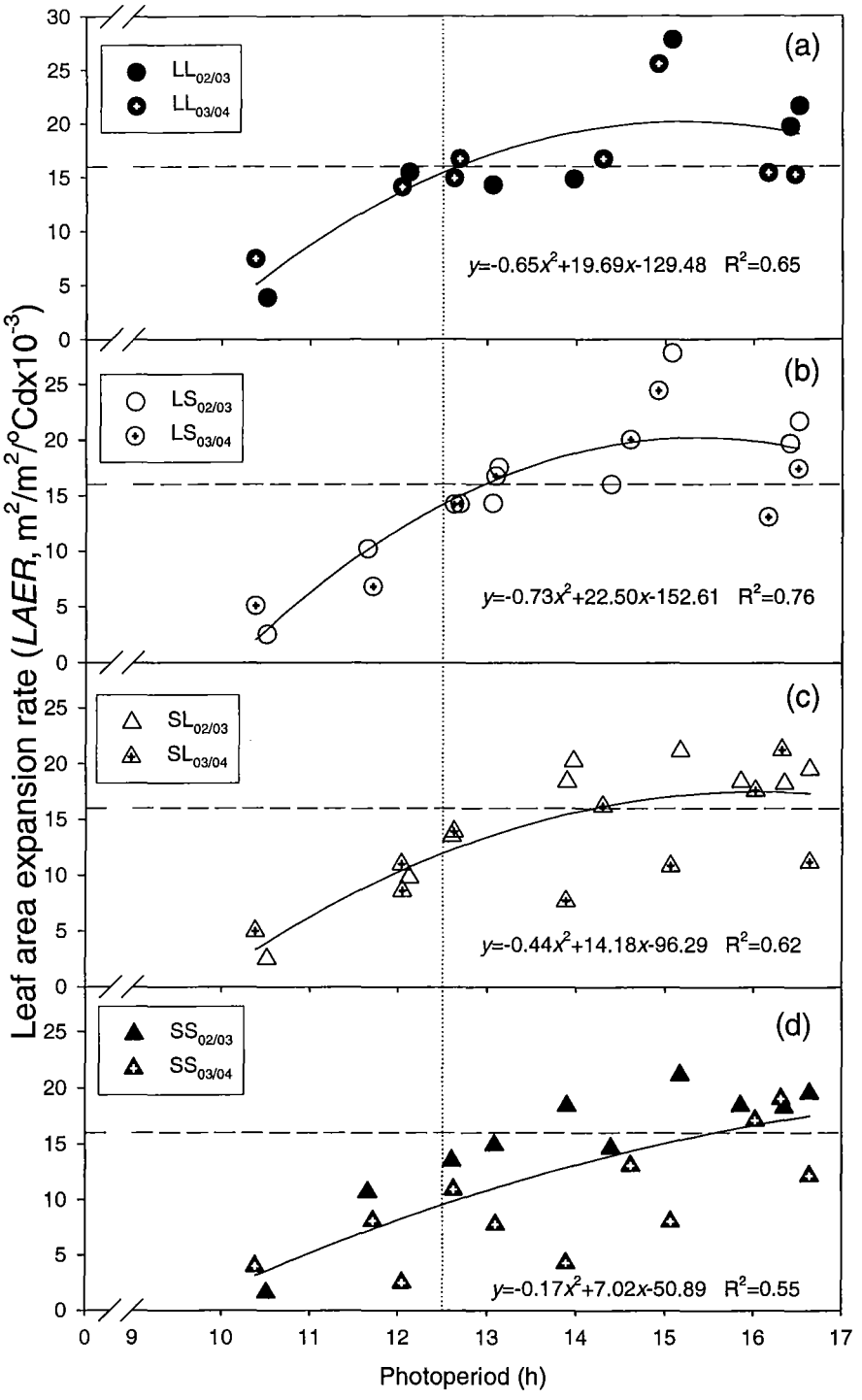

Figure 6.7 Relationship between leaf area expansion rate (*LAER*) and the mean photoperiod of the respective regrowth cycles of lucerne crops subjected to four contrasting defoliation regimes in the 2002/03 and 2003/04 growth seasons at Lincoln University, Canterbury, New Zealand.

Note: Horizontal dashed line represents the summer average of *LAER* (16×10^{-3} $m^2/m^2/°Cd$) for LL crops as reference. Vertical dotted line indicates a *Pp* of 12.5 h which refers to the approximate timing when the rate of increase in *LAER* of LL crops began to decline (Figure 6.6).

6.3.5.2 *The influence of winter taproot reserves on spring LAER*

Early-spring *LAER* increased (R^2=0.80, P<0.01) as the amount of taproot dry matter in the previous winter period increased (Figure 6.8). The *LAER* during spring was ~11x10^{-3} $m^2/m^2/°Cd$ when winter taproot dry matter was ~1.5 t/ha but increased to 17x10^{-3} $m^2/m^2/°Cd$ at taproot DM of 3.3 t/ha.

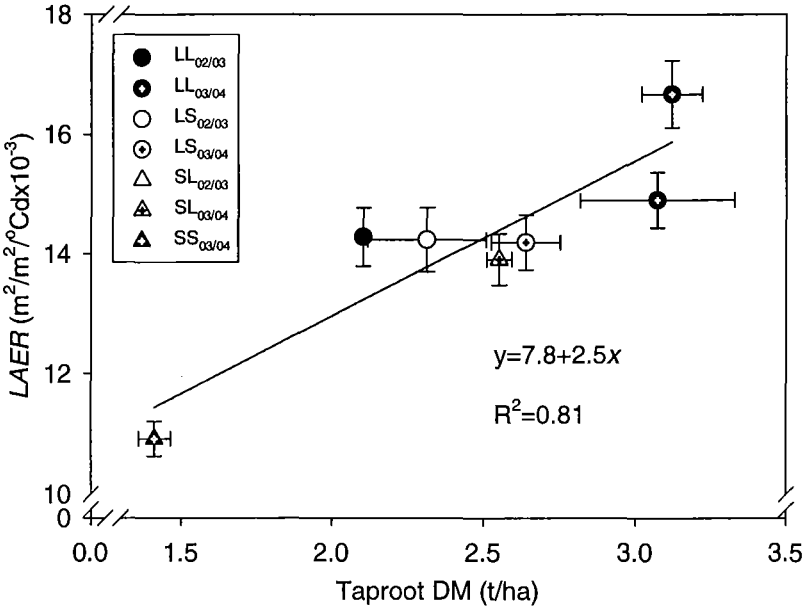

Figure 6.8 Relationship between leaf area expansion rate (*LAER*) during the early-spring regrowth and taproot DM (t/ha) harvested in the previous winter period of lucerne crops subjected to four contrasting defoliation regimes in the 2002/03 and 2003/04 growth seasons at Lincoln University, Canterbury, New Zealand.

Note: Bars represent one SEM for n=2 for DM_{root} and n=4 for *LAER*.

The relationship between early-spring *LAER* and concentrations (% of taproot DM) or amounts (kg/ha) of taproot winter reserves was tested by linear regression analysis (Figure 6.9). The concentration of carbohydrates or nitrogen in taproots was weakly related (0.14>P>0.99) to differences in *LAER* (Figure 6.9 *a*, *b* and *c*). In contrast, the amount of taproot nitrogen explained 67% of the variation (P<0.02) in *LAER* (Figure 6.9 *d*). Also, the amount of sugars was positively (R^2=0.60, P<0.04) related to *LAER* (Figure 6.9 *f*). In contrast, the amount of starch was poorly related (R^2=0.12) to *LAER* (Figure 6.9 *e*).

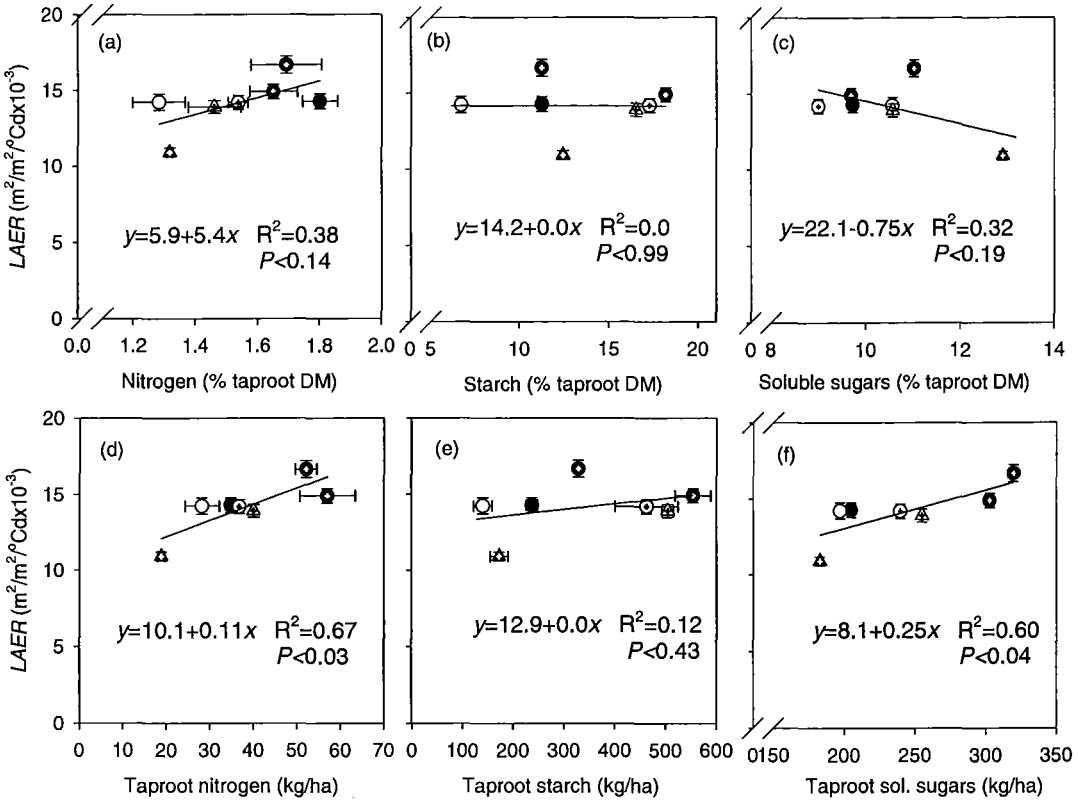

Figure 6.9 Relationship between leaf area expansion rate (*LAER*) during the first spring regrowth and the percentage (*a*, *b* and *c*) and total amounts (*d*, *e* and *f*) of taproots reserves from samples harvested in the previous winter period from lucerne crops subjected to four contrasting defoliation regimes in the 2002/03 and 2003/04 growth seasons at Lincoln University, Canterbury, New Zealand.

Note: Bars represent one SEM for n=2. Symbols are displayed in Figure 6.8.

6.3.6 Shoot population as a component of *LAI* expansion

Shoot population dynamics were unaffected by defoliation treatments (Section 5.3.4). After grazing the shoot population increased at a rate of ~6 shoots/m^2/°Cd (Figure 5.13) to a maximum of ~780 shoots/m^2 when *LAI* was 2.0 and then decreased (Figure 5.14).

6.3.7 Primary leaf appearance rate

Leaf appearance rate (*LAR*, leaves/day) of primary leaves increased from <0.10 leaves/day in autumn/winter to >0.40 during summer (Figure 6.10). During mid-spring and summer, *LAR* was similar (P<0.92) among all treatments. The differences in *LAR* among treatments

and seasons were then assessed in relation to thermal-time accumulation by the analysis of the phyllochron (Section 6.3.8).

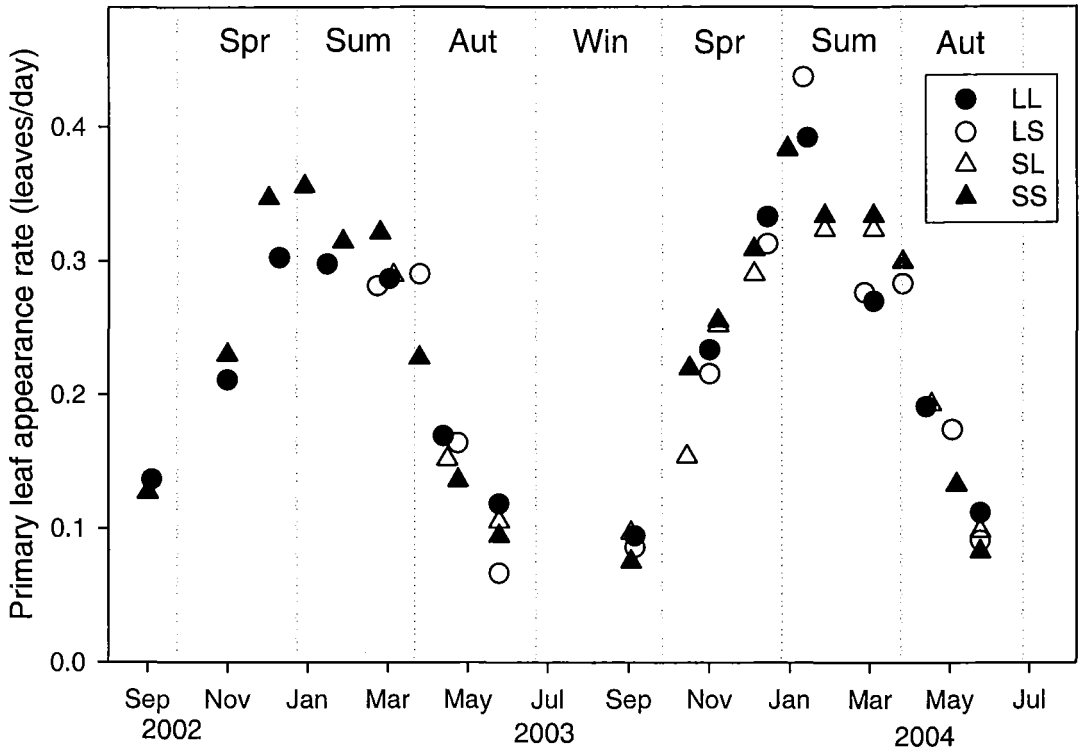

Figure 6.10 Primary leaf appearance rate (leaves/day) of lucerne crops subjected to four contrasting defoliation regimes in the 2002/03 and 2003/04 growth seasons at Lincoln University, Canterbury, New Zealand.

Note: Vertical dotted lines delimit seasons of the year: spring (Spr), summer (Sum), autumn (Aut) and winter (Win).

6.3.8 Phyllochron in primary leaves

During the spring-summer period, the phyllochron (°Cd/primary leaf) was similar (P<0.88) for all crops at ~34°Cd/leaf (Figure 6.11). In contrast, it increased to 40-65°Cd during autumn-winter. During this period, LL crops had a lower (P<0.02) phyllochron (~40°Cd/leaf) than LS (63°Cd/leaf) and SS (56°Cd/leaf) but similar to SL crops (47°Cd/leaf).

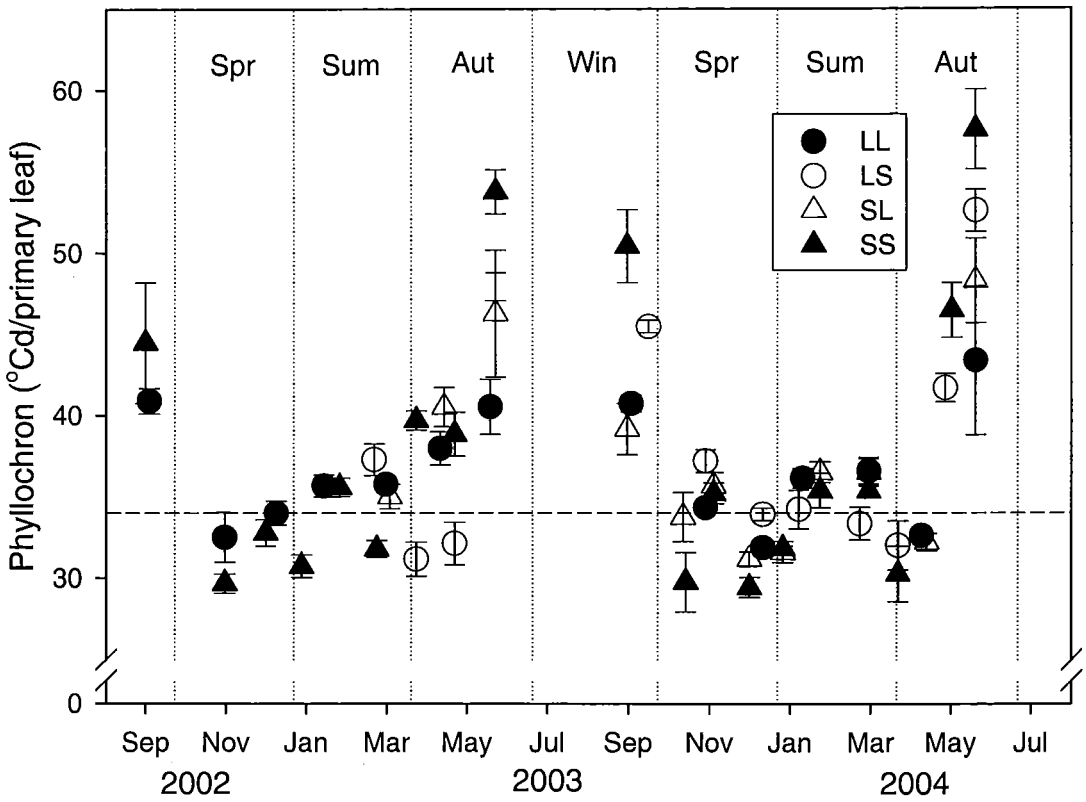

Figure 6.11 Phyllochron of lucerne crops subjected to four contrasting defoliation regimes in the 2002/03 and 2003/04 growth seasons at Lincoln University, Canterbury, New Zealand.

Note: Dashed line represents an average phyllochron of 34°Cd/main-stem leaf. Bars represent one SEM for the mean phyllochron of each regrowth cycle.

6.3.8.1 Phyllochron in relation to photoperiod

Phyllochron decreased exponentially (R^2=0.76) from 42°Cd/leaf at a photoperiod of 10.5 h to ~34°Cd/leaf at 16.5 h in the LL crop (Figure 6.12). The critical *Pp* (Pp_{crit}), defined as the *Pp* when phyllochron was 5% greater than the asymptote (34°Cd), was 12.5 h for LL crop (Figure 6.12). Phyllochron was similar among treatments at $Pp>Pp_{crit}$. In contrast, for photoperiods less than Pp_{crit}, treatments defoliated at short intervals after 4th February (LS and SS) had an 18% higher (P<0.02) phyllochron (51°Cd/leaf) than LL and SL crops (43°Cd/leaf). Assuming a linear increase in phyllochron at $Pp<Pp_{crit}$, phyllochron increased at a rate of 3.5°Cd/h for each 1 h decrease in *Pp* in LL and SL crops and 9.2°Cd/h in LS and SS crops.

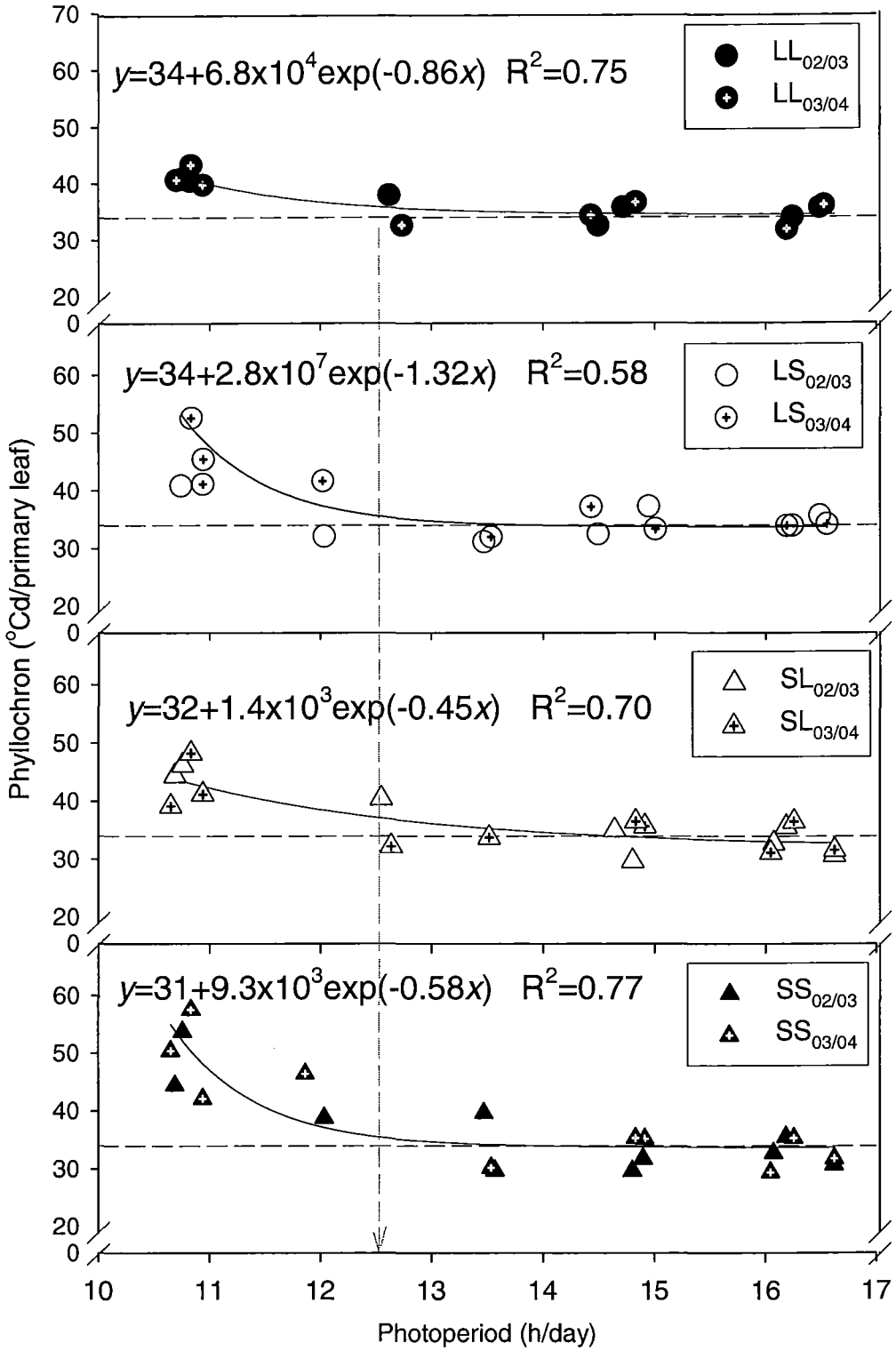

Figure 6.12 Relationship between phyllochron and mean photoperiod of lucerne crops subjected to four contrasting defoliation regimes in the 2002/03 and 2003/04 growth seasons at Lincoln University, Canterbury, New Zealand.

Note: Arrow indicates *Pp* of 12.5 h, when phyllochron is 5% greater than asymptote (34°Cd) for LL crops.

6.3.9 Axillary leaf appearance (branching)

Branching, quantified as the total number of leaves in relation to the number of primary leaves, was similar ($P<0.57$) for all treatments (Figure 6.13). The appearance of axillary leaves started approximately after the 4th primary leaf was fully expanded and progressed through a bi-linear relationship ($R^2=0.98$) with primary leaf appearance. Axillary leaves appeared at a similar rate ($P<0.31$) of 3.1 leaves/primary leaf until the expansion of the 9th primary leaf. After that, branching increased to 6.8 leaves/primary leaf until the expansion of the 11th primary leaf (the maximum number of primary leaves measured at that period).

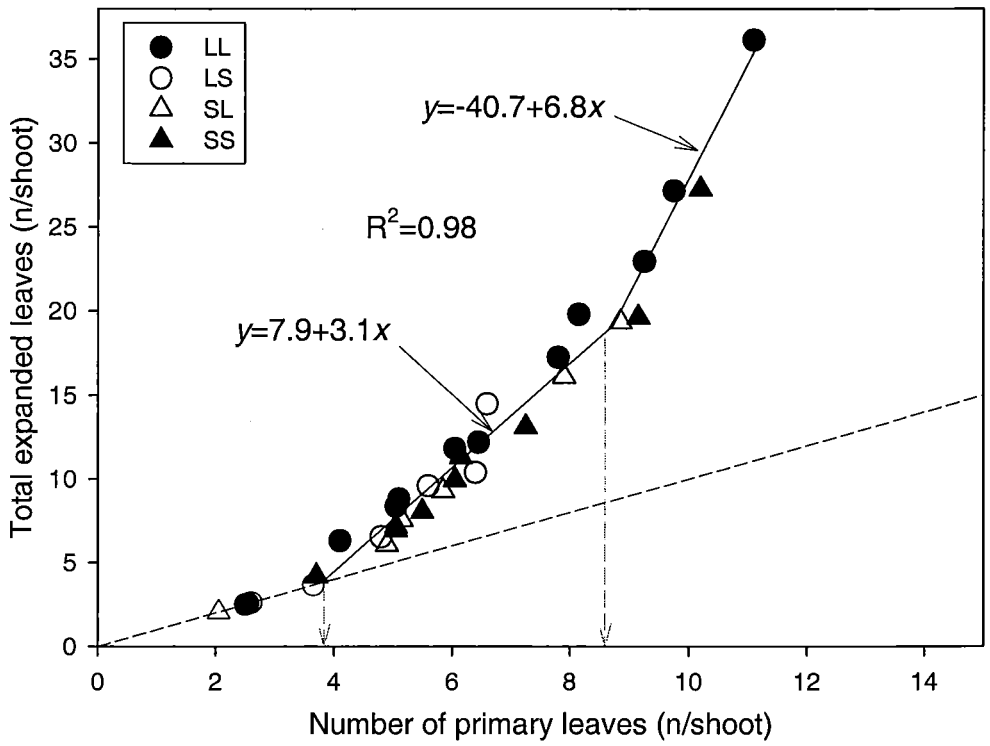

Figure 6.13 Total number of expanded leaves (primary and axillary) in relation to main-stem leaves (primary) of lucerne crops subjected to four contrasting defoliation regimes at Lincoln University, Canterbury, New Zealand.

Note: Dashed line represents $x=y$. Arrows indicate points of inflection for the start of branching ($x=4.0$) and acceleration of branching rate ($x=8.7$). R^2 is pooled for both equations.

6.3.10 Individual area of primary leaves

The area of each individual primary leaf (mm^2/leaf) increased from the smallest leaf at node position 1 (~120 mm^2) to a maximum at node position 8 (1000 to 2000 mm^2) in all crops (Figure 6.14). At higher node positions leaf area decreased to 800-1000 mm^2 at node position 11 in LL crops, which was the highest node position on which leaf area was measured.

From node position 1 to 6 there was no effect of defoliation treatments on primary leaf area. In contrast, from node positions 7 to 10, primary leaves in the SS crop were 60-85% smaller ($P<0.05$) than in LL crops. On average, these leaves represented 40 to 70% of the total primary leaf area of each individual shoot.

Primary leaves of each node position were largest ($P<0.05$) in the regrowth of 16 March 2004 (mean of 1,110 mm^2) followed by 24 December 2003 (755 mm^2) and 1 October 2003 (455 mm^2) in both treatments (Figure 6.14).

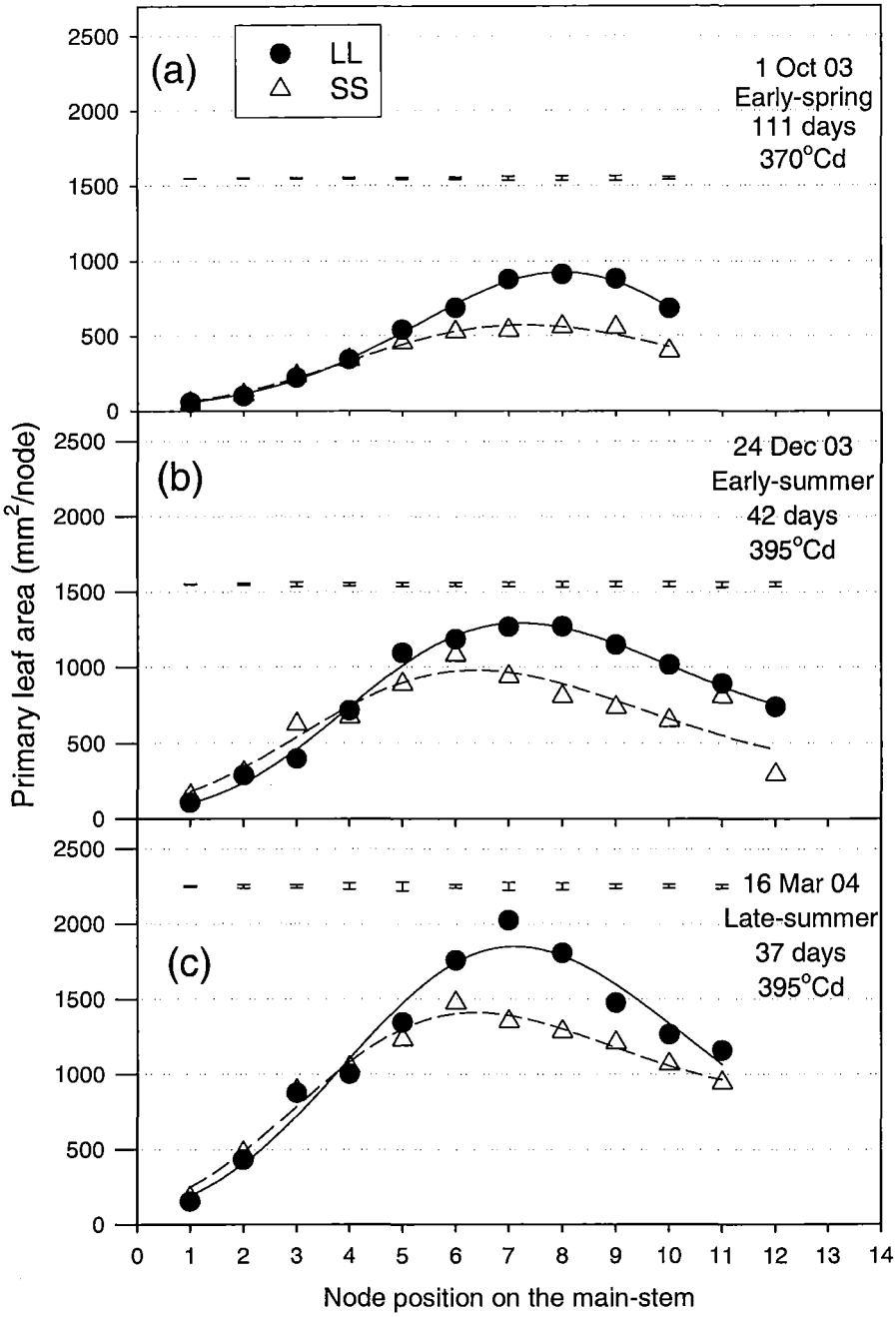

Figure 6.14 Area of primary leaves (mm^2/leaf) at each node position from the base of the main-stem of lucerne crops subjected to a long (42 days, LL) or a short (28 days, SS) defoliation interval in the 2002/03 and 2003/04 growth seasons at Lincoln University, Canterbury, New Zealand.

Note: Bars indicate one pooled SEM for each node position. Bell-shaped curves are:
(a) LL: $y=927*\exp(0.07(x-8.0)^2+0.0019(x-8.0)^3)$; SS: $y=575*\exp(0.04(x-7.3)^2-0.0016(x-7.3)^3)$;
(b) LL: $y=1293*\exp(0.04(x-7.2)^2+0.0039(x-7.2)^3)$; SS: $y=983*\exp(0.04(x-6.4)^2-0.0031(x-6.4)^3)$;
(c) LL: $y=1850*\exp(0.05(x-7.1)^2+0.0020(x-7.1)^3)$; SS: $y=1411*\exp(0.04(x-6.4)^2-0.004(x-6.4)^3)$.
All equations $R^2>0.95$ apart from (b) SS where $R^2=0.85$. Harvest dates are displayed in each graph.

6.3.10.1 Describing the size of primary leaves with a bell-shaped function

A bell-shaped function (Dwyer and Stewart, 1986) explained most of the variation ($0.85<R^2<0.95$) in leaf area in relation to node position from the base of the shoot (Figure 6.14). Functions for all treatments and regrowth cycles had similar kurtosis (a = 0.0554, $P<0.25$) and skewness ($b=3.06\text{x}10^{-3}$, $P<0.71$). The position of the largest primary leaf (X_{0p}) at the 7th main-stem was also similar ($P<0.16$) in all treatments. During early-spring (1 October 03) the value of X_{0p} was 0.6 units higher ($P<0.04$) than the two other sampling dates (7.4 vs. 6.8 respectively). The area of the largest primary leaf (Y_{0p}) was sensitive to defoliation treatments and was on average 30% greater ($P<0.007$) in LL (1,300 mm^2) than SS crops (1,000 mm^2). Also, the average Y_{0p} was smaller ($P<0.001$) during early-spring regrowth (1 October 03, ~580 mm^2) than by early-summer (24 December 2003, 1,000 mm^2) or late-summer (16 March 2004, 1,430 mm^2).

On the basis that only Y_{0p} was affected by treatments, results were normalized for Y_{0p} (*i.e.* Y_p/Y_{0p}) to test if a single model could explain leaf area for all defoliation treatments and seasonal cycles (Figure 6.15). This single bell-shaped function showed that most of the variation (R^2=0.90) in the normalized primary leaf area (Y'_p) was explained by main-stem node position (X).

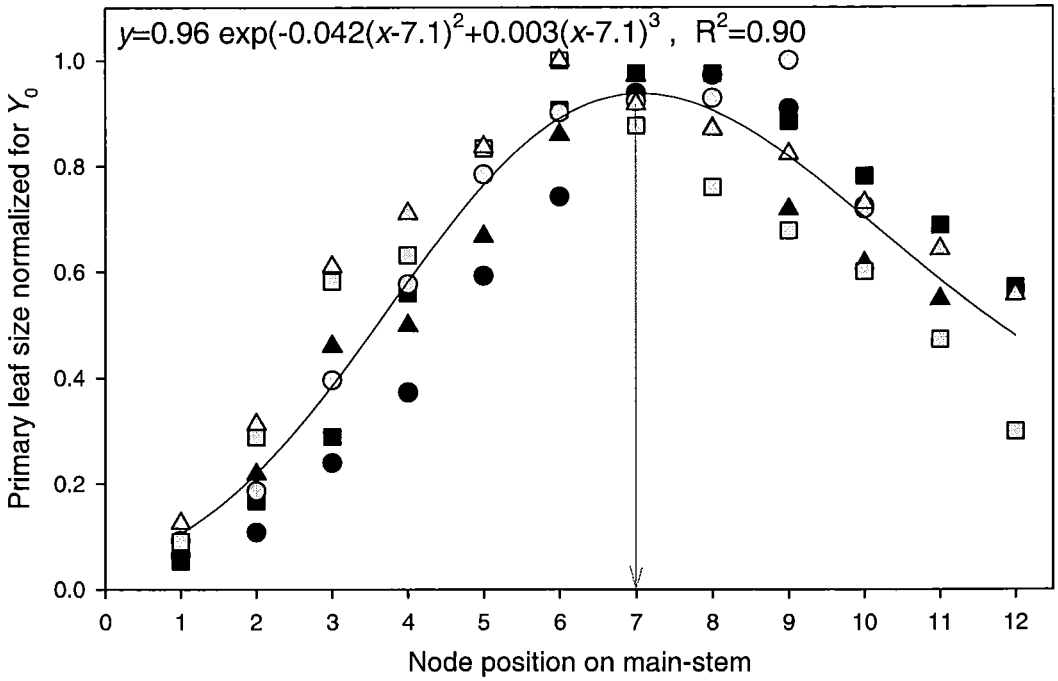

Figure 6.15 Normalized area of individual primary leaves as a function of node position from the base of the main-stem of lucerne crops subjected to four contrasting defoliation regimes at Lincoln University, Canterbury, New Zealand.

Note: Arrow indicates the position of the largest primary leaf (X_{0p}). Treatments are: LL (black symbols); SS (grey symbols). Dates of harvest were 1 October 2003 (circles); 24 December 03 (triangles) and 16 March 04 (squares).

6.3.11 Axillary leaf area per node position

The total area of axillary leaves for each node position was affected by defoliation treatments and differed among seasons (Figure 6.16).

Axillary leaves were larger ($P<0.05$) in LL crops than SS crops from the 3rd to the 7th node position with no difference at higher or lower nodes. The greatest difference ($P<0.03$) was in the area of the largest axillary leaf (Y_{0ax}) that was on average 1,530 mm^2 for LL crops but 726 mm^2 on SS crops.

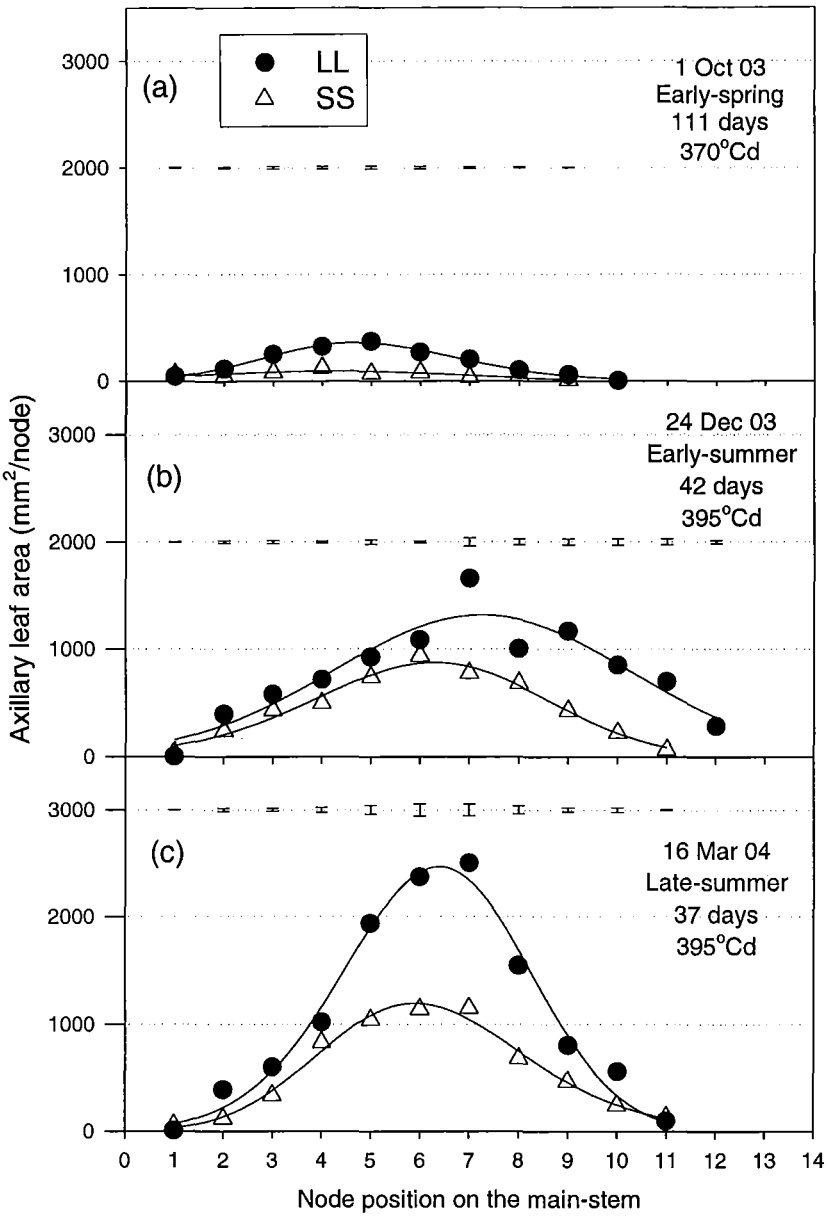

Figure 6.16 Area of axillary leaves (mm^2/node) at each node position from the base of the main-stem of lucerne crops subjected to a long (42 days, LL) or short (28 days, SS) defoliation interval in the 2002/03 and 2003/04 growth seasons at Lincoln University, Canterbury, New Zealand.

Note: Bars indicate one pooled SEM for each node position. Fitted models are:

(a) LL: $y=361*\exp(0.13(x-4.7)^2+0.0019(x-4.7)^3)$; SS: $y=94*\exp(0.07(x-4.2)^2-0.0016(x-4.2)^3)$;

(b) LL: $y=1320*\exp(0.06(x-7.3)^2+0.0039(x-7.3)^3)$; SS: $y=877*\exp(0.09(x-6.3)^2-0.0031(x-6.3)^3)$;

(c) LL: $y=2468*\exp(0.14(x-6.4)^2+0.0020(x-6.4)^3)$; SS: $y=1197*\exp(0.12(x-5.9)^2-0.004(x-5.9)^3)$.

All equations $R^2>0.97$ apart from (a) SS $R^2=0.62$ and (b) LL $R^2=0.87$. Harvest dates are displayed in each graph.

There was also a seasonal effect on axillary leaf area in both treatments. In early-spring (1 October 2003) the area of individual axillary leaves from nodes 4 to 8 was smaller ($P<0.05$) than in early-summer (24 December 2003) or late-summer (16 March 2004).

6.3.11.1 Describing axillary leaf area with a bell-shaped function

A bell-shaped function (Section 6.2.10) explained the variation in axillary leaf area for the final harvest of cycles ending on 1 October 2003, 24 December 2003, and 16 March 2004 (Figure 6.16). Parameters a and b were conservative ($P<0.30$) among all treatment-regrowth cycle combinations at 0.16 and 0.02, respectively. The value of X_{0ax} (the node position of the largest area of axillary leaves) was also similar among treatments ($P<0.71$) and regrowth cycles ($P<0.51$) and occurred at the 6th main-stem node. This was influenced by the timing of harvest because crops always had a final node count of 10 to 12 during these harvests. In reality, the position of the largest axillary leaf area (X_{0ax}) advances as new main-stem nodes are produced (Brown *et al.*, 2005b).

The size of the largest axillary leaf (Y_{0ax}) was the parameter that differed the most between treatments and regrowth cycles. On average, SS crops had a Y_{0ax} 47% lower ($P<0.02$) than LL crops. Similarly, averaged between treatments, Y_{0ax} was the lowest ($P<0.01$) during early-spring at 180 mm^2 but increased to 1,200 mm^2 in early-summer and 1,900 mm^2 in late-summer.

Knowing that Y_{0ax} differed with treatments and that the position of X_{0ax} progresses with X_{max}, a double-normalization of the variables (Elings, 2000) was performed to identify similarities in the pattern of leaf size in axillary leaves (Figure 6.17). When all three datasets were plotted together the normalized bell-shaped function for branches had an R^2 of 0.82. There was symmetry in leaf area from X_{0ax} because b was not different from zero ($P<0.77$). The largest axillary leaf area occurred at around half ($X'_{0ax}=0.54$) of the distance between the first and last node where branching was expressed.

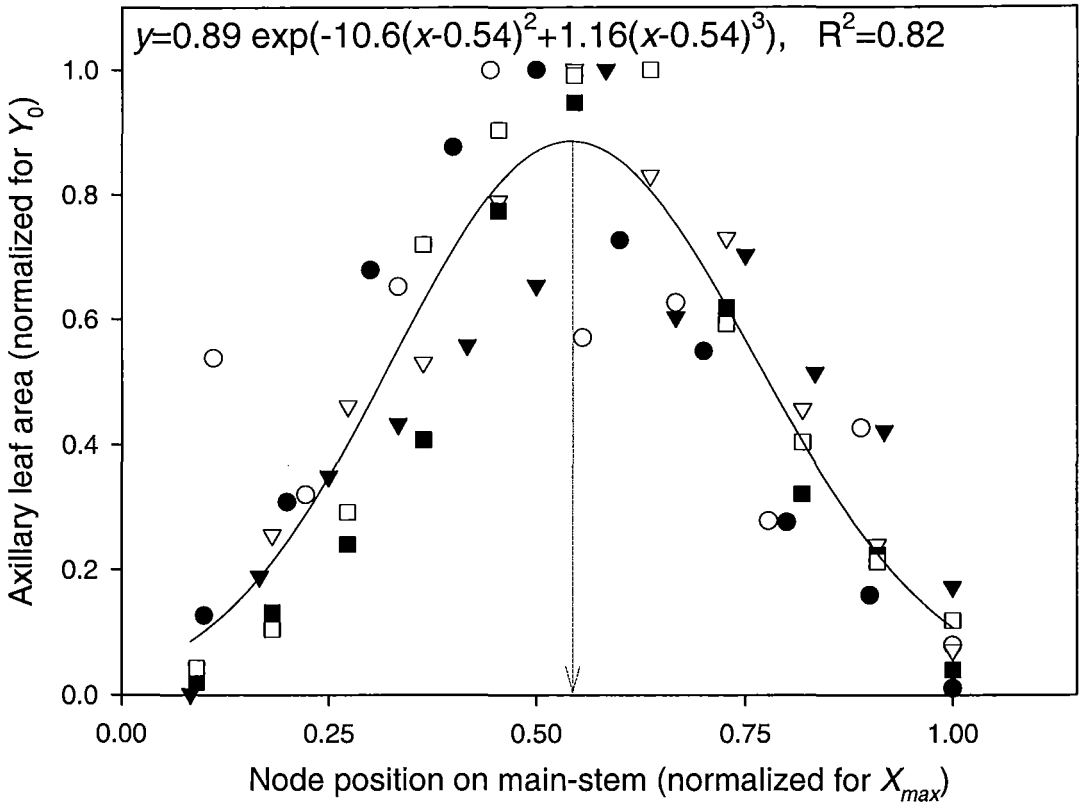

Figure 6.17 Double-normalized bell-shape function of axillary leaf area per node position on the main-stem of lucerne crops subjected to long (42 days, dark symbols) and short (28 days, empty symbols) contrasting defoliation regimes at Lincoln University, Canterbury, New Zealand.

Note: Arrow indicates the position of the normalized largest primary leaf (X'_0). Dates of harvest are: 1 October 2003 (circles); 24 December 2003 (triangles) and 16 March 2004 (squares).

6.3.12 Senescence of primary leaves

During the entire 2003/04 season leaf senescence of primary leaves was recorded on the marked shoots (Section 6.2.7). Leaf senescence occurred at a similar (P<0.17) rate for all defoliation treatments. A broken-stick model explained 89% of the variation of the relationship between the accumulated number of senesced primary leaves and the number of main-stem nodes (Figure 6.18). The model indicated that senescence of the first primary leaf started at the time of appearance of the 3rd main stem-node. In this first stage, senescence proceeded at a rate of 0.2 primary leaves/main-stem node until the appearance of the 6th main-stem node. After the appearance of node 6, senescence rate increased to 0.48 leaves/main-stem node.

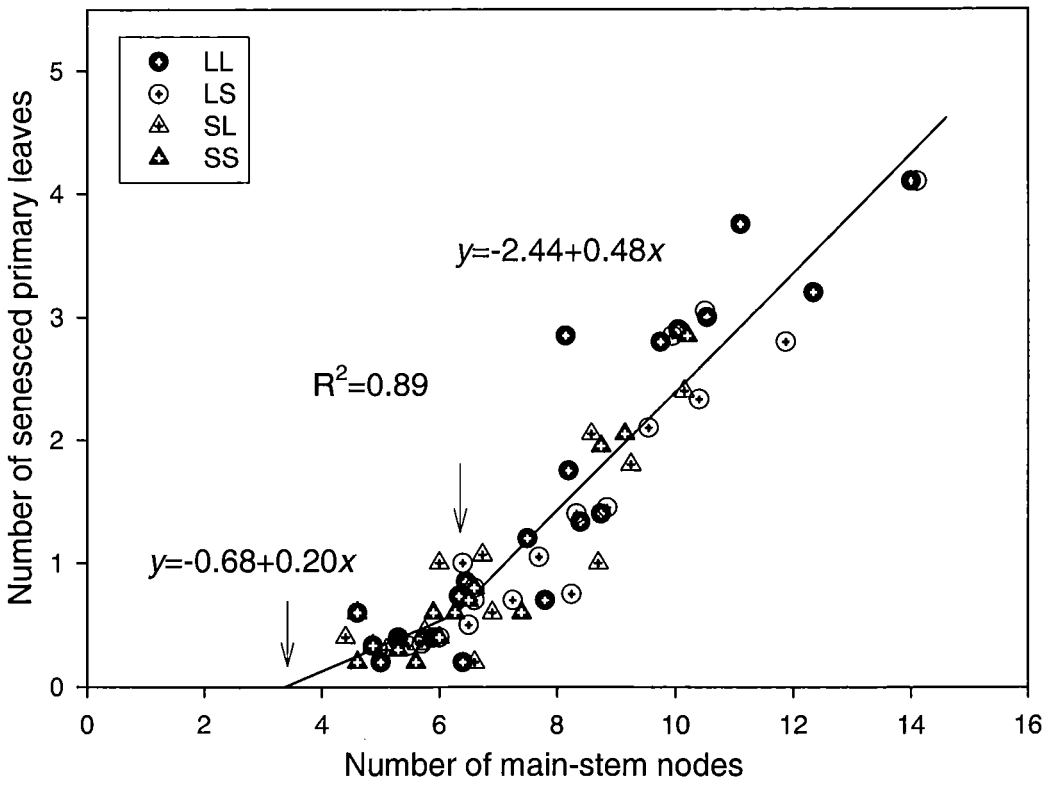

Figure 6.18 Number of primary senesced leaves per main-stem node position of lucerne crops subjected to four contrasting defoliation regimes in the 2003/04 growth seasons at Lincoln University, Canterbury, New Zealand.

Note: Arrows indicate estimated point of senescence initiation (x=3.6) and bi-linear model breakage (x=6.3) when senescence rate accelerates.

6.3.13 Annual shoot yield as a function of accumulated PAR_i

Accumulated intercepted PAR ($\sum PAR_i$) explained ~84% of the annual shoot yield of lucerne crops (Figure 6.19). The relationship departed from an intercept not significantly different (P<0.73) from zero. The slope of the linear equation gives an idea of a "general" efficiency of conversion of PAR_i to DM_{shoot} (annual RUE_{shoot}). This pooled annual RUE_{shoot} was 1.6 g DM/MJ PAR_i but the model in Figure 6.19 showed that individual treatment and growing seasons were not randomly scattered around the line. This suggests that there may be differences in the RUE_{shoot} for treatments and seasons and this will be explored in Chapter 7.

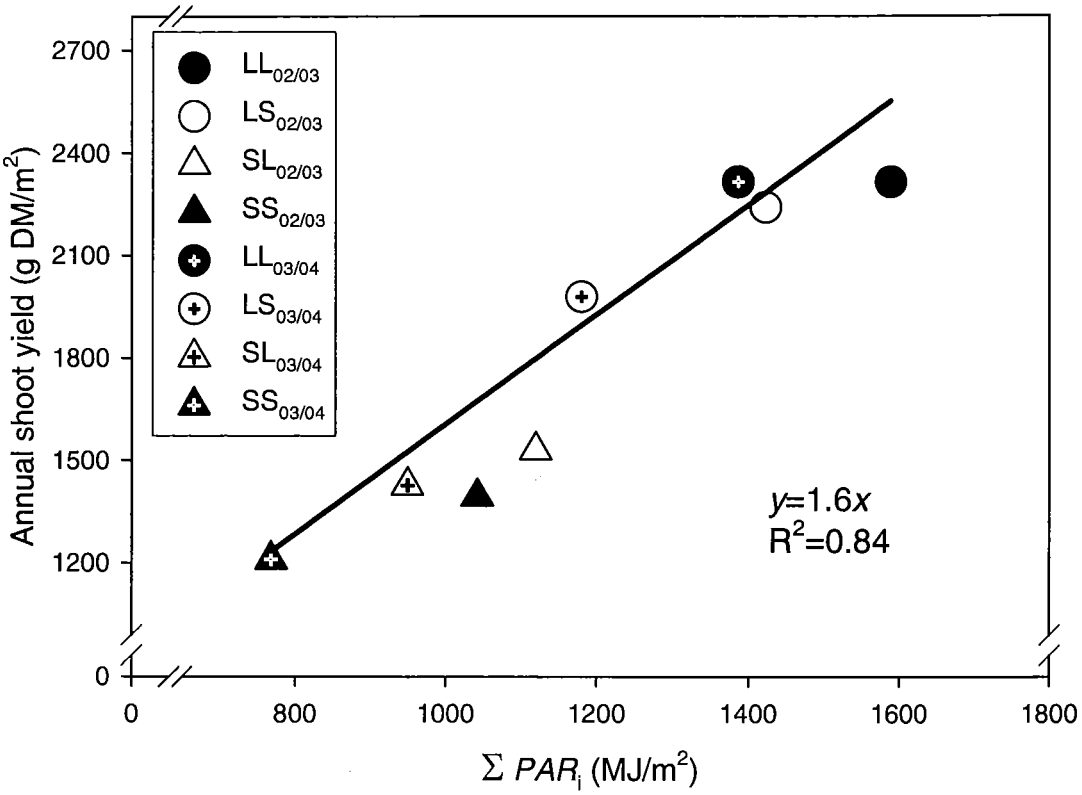

Figure 6.19 Annual accumulated shoot yield as a function of accumulated intercepted PAR ($\sum PAR_i$) of lucerne crops subjected to four contrasting defoliation regimes in the 2002/03 and 2003/04 growth seasons at Lincoln University, Canterbury, New Zealand.

6.4 Discussion

Accumulated PAR interception ($\sum PAR_i$) explained ~84% of the differences in annual shoot yield among crops (Figure 6.19). Therefore, frequent defoliations and low levels of perennial reserves reduced DM assimilation mainly by limiting the amount of energy captured and used for photosynthesis. The causes of differences in $\sum PAR_i$ were then explored by studying canopy architecture and canopy expansion.

6.4.1 Canopy architecture

The extinction coefficient for diffuse PAR (k_d) was used as an indicator of morphological changes in canopy architecture. All crops had a similar k_d of 0.81 which demonstrates that canopy architecture (*i.e.* mean canopy leaf angle and optical properties) was unaffected by seasons, defoliation treatments and the level of perennial reserves (Figure 6.3). This lack of morphological changes in canopy architecture in response to stresses was also observed in lucerne by Varella (2002) who showed that k_d was unchanged in crops grown in full sun or severe shade. This could be justified by the fact that lucerne already has an efficient canopy architecture (Duncan, 1971) with erect leaves in the top and flatter leaves at the bottom of the canopy, which are able to track solar radiation efficiently (Travis and Reed, 1983).

The implication of a single and conservative k_d value is that, for any given *LAI*, it is possible to predict the PAR interception for crops subjected to different environments and managements. This becomes a sound framework to estimate carbon assimilation in lucerne simulation models (Gosse *et al.*, 1984).

6.4.2 Canopy expansion

The lower interception of PAR observed in frequently defoliated crops (Figure 6.19) was mostly explained by differences in canopy expansion. Canopy expansion, quantified as *LAI*, was affected by defoliation treatments and also by the levels of perennial reserves (Figure 6.4). Crops that were frequently defoliated during spring-summer (SL and SS

crops) reached LAI_{crit} only in 20% of the regrowth cycles (Figure 6.4 *c, d*). In contrast, LL and LS crops had full canopy closure in 65% of the regrowth cycles and remained above LAI_{crit} for longer periods (Figure 6.4 *a, b*). In this sense, the regrowth length *per se* limited PAR interception in frequently defoliated crops during spring-summer (SL and SS crops).

Leaf area expansion rates (*LAER*, $m^2/m^2/°Cd$) were also reduced by low levels of perennial reserves (Figure 6.6). Slow canopy expansion caused a delay in the time to reach complete PAR interception (*i.e.* LAI_{crit}, Figure 6.4 *d*) which limited photosynthesis per unit of area and consequently linear growth rates. For example, final *LAI* was ~30% lower in SS than LL crops during the last early spring regrowth of 2004/05 (Cycle 0, Figure 6.4 *a, d*) and it was highly related (R^2=0.81) to the winter amount of taproot dry matter (Figure 6.8). The *LAER* increased from ~0.011 $m^2/m^2/°Cd$ at 1.4 t/ha to 0.017 $m^2/m^2/°Cd$ at 3.2 t/ha. Although this strong relationship is in accordance with Justes *et al.* (2002), the authors observed a faster response of *LAER* to DM_{root} which increased from ~0.014 to 0.028 $m^2/m^2/°Cd$ as lucerne DM_{root} (200 mm depth) increased from ~0.5 to 2.0 t/ha respectively.

The amount of taproot nitrogen (kg N/ha) was the strongest predictor (P<0.04, R^2<0.64) of early-spring *LAER*. (Figure 6.9 *d*). The measurement of the "amount" of reserves (*e.g.* kg N/ha) incorporates the differences in both concentration (*e.g.* $N\%_{root}$) and size of the storage organs (*e.g.* DM_{root}). This makes the amount of reserves a more reliable indicator of the real availability of assimilates for mobilization. Meuriot *et al.* (2005) also showed that limited supply of taproot nitrogen to shoots, during early regrowth, reduced *LAI* development by delaying recovery of photosynthetic capability and nitrogen uptake of lucerne plants. There was a weak relationship between *LAER* and starch (amounts and concentrations) which agrees with previous reports (Louahlia *et al.*, 1998). This is explained by the fact that carbohydrates are mostly used for respiration of perennial organs and only slightly mobilized to shoots in the early stages of regrowth (Section 2.6.1). Nevertheless, the amount of soluble sugars in taproots measured in the previous winter was significantly (P<0.04, R^2=0.60) related to spring *LAER* (Figure 6.9 *f*). This was possibly an artefact of the strong relationship between *LAER* and DM_{root} (that decreased in frequently defoliated crops) and the stability of sugar concentrations (Section 4.3).

6.4.3 Seasonality of leaf area expansion rate

The expansion of leaf area per unit of Tt_{b5} (*i.e. LAER*) was inconsistent throughout the year and decreased sharply during autumn (Figure 6.6). Therefore, thermal-time accumulation ($\sum Tt_{b5}$) alone was not a stable predictor of *LAI* expansion throughout an entire growth season. This agrees with Gosse *et al.* (1984) who found temperature sum a reliable predictor of lucerne *LAI* during spring-summer, but the relationship did not hold in autumn. Interestingly, the decline in *LAER* in both growth seasons occurred near the autumn equinox (21st March) which implies a strong environmental control of canopy morphogenesis. Other environmental factors influence the rate of *LAI* development, notably photoperiod (Hodges, 1991). The *LAER* increased with photoperiod ($0.55<P<0.76$) in all crops (Figure 6.7). In LL crops *LAER* increased from ~0.005 $m^2/m^2/°Cd$ at a *Pp* of 10.5 h to a summer average of 0.016 $m^2/m^2/°Cd$ (Figure 6.7 *a*). The *LAER* was particularly high (0.020-0.025 $m^2/m^2/°Cd$) during Cycle 1 in LL and LS crops (Figure 6.6). This cycle occurred from 6 October and 12 November, a period when partitioning of DM to perennial organs is minimal (Section 4.3.2) and the average maximum temperatures are near the optimum for lucerne photosynthesis. These processes were possibly the cause of differences in canopy specific leaf weight (SLW_{can}, g DM/m^2 leaf) which is reflected in leaf thickness (Appendix 3). During early-spring (~21st September) the average canopy SLW_{can} of LL crops achieved the highest ($P<0.03$) values of ~50 g/m^2 compared with a season average of 30 g/m^2. This was possibly the result of an increase in the flux of assimilates to leaves at rates more than proportional to increases in *LAER* during early-spring. This dynamic highlights the independence of *LAER* from carbon assimilation and the plasticity of *SLW* in response to seasonal changes in carbon balance and leaf expansion (Tardieu *et al.*, 1999). Therefore, these seasonal differences in *LAER* indicate that other factors limit *LAER* in winter/early-spring (*e.g.* leaves formed under sub-optimal conditions) and autumn (*e.g.* preferential partitioning of DM to perennial organs).

6.4.4 Area of individual leaves

Differences in *LAI* were mostly explained by changes in the area of individual leaves on primary and axillary nodes (Section 0 and 6.3.11). The area of leaves was the most sensitive component of *LAI* to seasonal signals and to the levels of perennial reserves. The area of the largest primary leaf (Y_{0p}, Section 0) was on average ~30% greater in LL crops

than SS crops (Figure 6.14). This is consistent with the lower availability of perennial reserves in SS crops, particularly taproot nitrogen. Leaf expansion rates are strongly limited by low availability of nitrogen (Simon *et al.*, 2004; Thornton and Millard, 1997) but are less sensitive to the supply of carbohydrates (Tardieu *et al.*, 1999). The decline in the individual area of primary leaves was particularly evident after the 5th primary leaf (Figure 6.14). This indicates that crops may be still dependent on the supply of matter from perennial organs after the 5th expanded leaf. Alternatively, the exogenous supply of C (photosynthesis) or N (mineral uptake) may be compromised at more advanced stages of regrowth due to the effect of low levels of perennial reserves on physiological processes (*e.g.* photosynthesis) early in regrowth (Meuriot *et al.*, 2005). The conservative area of leaves at lower node positions may be because the demand of assimilates to expand these leaves was lower than the supply from perennial organs, even at the minimum levels observed in SS crops. Alternatively, leaf thickness could be compromised to maintain leaf area expansion rates. These issues will be explored in Chapter 7.

The area of axillary leaves was also significantly reduced in crops with limited amount of reserves (Figure 6.16). The area of the largest axillary leaves (Y_{0ax}) was again the most sensitive parameter of the bell-shaped function (R^2=0.78) that related axillary leaf area and node position. The Y_{0ax} in SS crop was approximately half of LL crops (Figure 6.16). Therefore the expansion of axillary leaves was relatively more sensitive to the level of perennial reserves than the area of primary leaves. Axillary leaves were extremely important for canopy formation as they comprised 25 to 60% of the final *LAI* (Figure 6.16) mainly during periods of fast growth (*e.g.* summer) and in crops with high levels of perennial reserves (*e.g.* LL crop).

There were also seasonal differences in the area of individual leaves, regardless of treatment. The largest area of leaves per node position (Y_0) was smaller in spring than summer. The Y_0 was 60% lower in primary leaves and 90% lower in axillary leaves in spring than summer. Smaller leaves during spring were previously observed in 'Kaituna' and are possibly caused by sub-optimal temperatures for growth or development processes during leaf formation in winter (Brown *et al.*, 2005b). The extensibility of cell walls to turgor pressure declines at low temperatures and this limits cell expansion (Pollock, 1990; Tardieu *et al.*, 1999). Alternatively, a lack of carbon or nitrogen to form new leaves reduces potential leaf expansion mainly in the early phases of cell division, when the leaf is heterotrophic (Tardieu *et al.*, 1999). There was probably no C or N limitation for

expansion in spring because during the onset of spring regrowth (early September) there was a significant increase in canopy specific leaf weight (Appendix 3). This increase in leaf thickness signals that the flux of assimilates to leaves was greater than the demand for the expansion of leaves formed in winter.

Seasonal differences were also evident in axillary leaf area which was smaller in early-spring compared with late-summer (Figure 6.16). These results highlight the importance of understanding branching patterns when developing mechanistic lucerne simulation models which is not currently the case (Robertson *et al.*, 2002).

6.4.5 Development component of leaf area index

Developmental processes of *LAI* formation (*e.g.* leaf appearance, branching and shoot initiation) were less sensitive than on growth processes (*e.g.* leaf expansion) to defoliation treatments and the level of perennial reserves.

The phyllochron in spring-summer was conservative among defoliation treatments at ~34°Cd/leaf (Figure 6.11) which indicates that temperature was the main driver of primary leaf appearance during this period. Robertson *et al.* (2002) also derived a mean phyllochron of 34°Cd (T_b=5°C) for lucerne which was included as a parameter in the APSIM-lucerne model. The insensitivity of phyllochron to defoliation treatments and the level of perennial reserves during spring-summer agrees with other reports where a conservative phyllochron of ~34-37°Cd was observed under moisture stress and light limiting conditions (Brown, 2004; Varella, 2002). Nevertheless, during autumn-winter, phyllochron increased to 40°Cd in LL and SL crops and ~55°Cd in LS and SS crops. In accordance with Brown *et al.* (2005b), photoperiod (*Pp*) was tested as a predictor of phyllochron. The phyllochron deviated from 34°Cd only when Pp<12.5 h (Figure 6.12) and this was assumed to be the critical photoperiod (Pp_c) for leaf appearance (Hodges, 1991). The mechanism for such increase in phyllochron may be triggered by the activity of genes that is enhanced below Pp_c, as assumed in the model proposed for long-day plants by Yan and Wallace (1998). Alternatively, high values of phyllochron in autumn may be due to a limited availability of assimilates to shoots (Brown *et al.*, 2005b) because the DM partitioning to crowns and roots is high at this period (Section 2.6). This hypothesis is reinforced by the fact that crops with low levels of reserves in autumn (*i.e.* LS and SS

crops) had higher phyllochrons than LL and SL only at *Pp*<12.5 h (Figure 6.12). Developmental processes are expected to be affected by assimilate supply only at extreme levels of stress (Grant and Barthram, 1991). This was possibly the case for LS and SS crops at *Pp*<12.5 h. These crops had the lowest levels of perennial reserves in autumn (Section 4.3.6.4) when the sink strength of shoots is expected to be low (Noquet *et al.*, 2004).

The rate of branching was unaffected by defoliation treatments and could be predicted as a function of primary leaf appearance, as previously observed by Brown *et al.* (2005b). Branching started after the expansion of the 4th leaf and progressed at a rate of ~2 axillary leaves/node, until main-stem node number 9. From this point, the rate of branching increased to ~6 axillary leaves/node which resembles the exponential increase in the number of axillary buds of other legumes (Ranganathan *et al.*, 2001). The observed rate of branching is possibly lower than the genetic potential of 'Kaituna' because there was strong competition for light among shoots (Section 5.3.4.3) and this could limit the expression of potential branching rates (Ranganathan *et al.*, 2001). Nevertheless, competition for light was similar among all treatments (Section 5.3.4.3) which validates their comparison in terms of branching patterns.

Shoot appearance dynamics were similar in all crops (Section 5.3.4.2) and had no apparent influence on the differences observed in *LAI* development. Therefore the extent by which defoliation treatments reduced the level of perennial reserves was insufficient to limit basal bud initiation.

6.4.6 Thermal-time calculations

The validity of the commonly used T_b=5°C (Section 6.3.4) was tested due to its importance for proper estimation of *Tt* accumulation. Using the three methods detailed in Section 6.2.4.1, T_b was not different from 5°C and a further test with a broken-stick threshold (Moot *et al.*, 2001) showed no improvement in *Tt* calculations. This was contrary to previous observations for lucerne grown in Canterbury which had a more stable phyllochron when *Tt* was calculated using a faster *Tt* accumulation at T_{mean}<15°C (Brown *et al.*, 2005b; Moot *et al.*, 2001). This contrast may be because the curvilinear response of development processes to temperature (Bonhomme, 2000) was not totally captured in the

range of T_{mean} (7.5°C<T_{mean}<15°C) where phyllochron was measured. Nevertheless, this indicates that the use of a single T_b of 5°C allowed estimation of leaf appearance rates in lucerne grown in most seasons of the temperate climate of Canterbury.

6.4.7 Senescence of primary leaves

The rate of senescence of primary leaves was unaffected by defoliation treatments (Figure 6.18). Hence low levels of perennial reserves (*e.g.* SS crops) did not accelerate the remobilization of assimilates from older leaves to expanding ones. Senescence started after the 3rd primary leaf and proceeded from the bottom to the top of the canopy at a rate of 0.2 leaves/main-stem node until main-node position 6. This agrees with previous reports in 'Kaituna' (Brown *et al.*, 2005b). After the expansion of the 6th primary leaf, senescence was faster at 0.48 leaves/main-stem node. Assuming an average phyllochron of 34°Cd (Section 6.3.8) the longevity of each primary leaf was estimated according to main-node appearance and varied from 165°Cd until node 6 to ~70°Cd/leaf after that. At the onset of the expansion of the 6th primary leaf, *LAI* was around 2.0, which gives an interception of 80% of the available PAR (Figure 6.3). This was the stage where the decay of shoot population resumed (self-thinning) (Section 5.3.4.2) demonstrating that competition for light probably triggered senescence of leaves and shoot death, simultaneously. These rates of senescence differ slightly from Brown *et al.* (2005b) who observed 1.08 senesced leaves/main-stem node occurring after the 9th main-stem node, when canopy was near LAI_{crit}. In practical terms, this difference is minor because the area of senesced leaves in the first 42 days of regrowth is minimal.

6.4.8 The $\sum PAR_i$ as a predictor of annual shoot yield

On average for each 1 MJ PAR_i there was a production of 1.6 g of shoot DM (Figure 6.19). This "annual" conversion efficiency (annual *RUE*) is close to the figure of 1.72 g DM/MJ of "absorbed" PAR reported in Durand *et al.* (1989) if absorption is assumed to be 90% of intercepted PAR (Gosse *et al.*, 1984). Nevertheless, the unevenness of distribution of the data-points around the model suggested that the seasonal pattern of *RUE* deserves further investigation. The seasonal pattern of shoot *RUE* for each regrowth cycle/treatment combination will be assessed in Chapter 7.

6.5 Conclusions

The results presented in this Chapter allowed the following conclusions:

- Accumulated PAR_i explained most (R^2=0.84) of the differences observed in annual shoot yield.

- The differences in radiation interception were mainly due to differences in individual primary and axillary leaf area, always smaller in crops defoliated frequently and consequently with less available perennial reserves.

- Canopy architecture was unaffected by defoliation treatments or the level of perennial reserves and a conservative k of 0.81 was found for 'Kaituna'.

- Leaf appearance rate was conservative on a Tt_{b5} basis at a phyllochron of 34°Cd/leaf in spring-summer. In autumn-winter (Pp<12.5 h) phyllochron increased to ~40°Cd in LL and SL crops and to ~55°Cd in LS and SS crops.

- Senescence and shoot appearance rates were unaffected by defoliation treatments or the level of perennial reserves.

The results presented in this chapter indicate that the greater yield observed in crops defoliated at longer intervals (Chapter 4) could be explained by the greater amount of PAR intercepted (PAR_i) by these crops. This was due to (*i*) longer spelling periods that allowed crops with long rotations to reach full canopy closure ($LAI>LAI_{crit}$) and (*ii*) faster *LAI* development in early stages of regrowth possibly due to greater availability of perennial reserves. There was a minor effect of defoliation treatments on leaf appearance rate, and no change in canopy architecture, branching pattern and senescence rate. The faster *LAI* development in LL crops, when compared with SS, was due to a faster leaf expansion rate in primary and axillary leaves which lead to larger leaf sizes. In the following chapters the efficiency of conversion of PAR in terms of shoot DM (RUE_{shoot}) and total DM (RUE_{total}) will be examined in detail.

7 Radiation use efficiency, DM partitioning and shoot N dynamics

7.1 Introduction

In Chapter 6 the differences in shoot yield of lucerne crops with contrasting levels of perennial reserves were mostly (R^2=0.84) explained by an "annual" *RUE* for shoot dry matter of 1.6 g DM/MJ PAR_i. The radiation use efficiency for the production of aerial biomass has been successfully used to study the responses of annual crops to environmental factors (Monteith, 1977). The strength of the relationship between radiation receipts and aerial DM yield allowed the use of *RUE* as a major parameter to derive DM assimilation in crop simulation models (Sinclair and Seligman, 1996). The stability of *RUE* as a parameter relies on the assumptions that (*i*) the relationship between photosynthesis and respiration is constant and (*ii*) that the partitioning of DM to unharvested organs is constant within the crop cycle (Sinclair and Muchow, 1999).

These assumptions fit the reality of annual crops but are severely broken when applied to perennial crops. In lucerne, the *RUE* for the production of shoot biomass (RUE_{shoot}) was shown to vary seasonally (Gosse *et al.*, 1984) due to changes in the differential partitioning of DM to perennial organs (Khaiti and Lemaire, 1992). These authors proposed the concept of *RUE* for the total lucerne biomass (RUE_{total}), this being constant at 2.3 g DM/MJ PAR regardless of time of the year. Avice *et al.* (1997a) showed that low levels of root reserves, particularly endogenous nitrogen, reduced RUE_{shoot} in lucerne crops. But it was not clear if these effects were due to changes in RUE_{total} or in the partitioning of DM to perennial organs (p_{per}).

In this chapter the seasonal pattern of RUE_{shoot} is examined and the null hypothesis that RUE_{total} and p_{per} were stable among seasons and unaffected by the level of perennial reserves is tested. Analyses of leaf photosynthesis and the nitrogen nutrition status of the crops are used to interpret the results.

7.2 Materials and methods

7.2.1 Radiation use efficiency for shoot DM

Shoot radiation use efficiency (RUE_{shoot}, g DM/MJ PAR_i) was calculated from linear regression (y=a+bx) of DM_{shoot} against PAR_i for each regrowth cycle where the coefficient (b) represents *RUE*. The intercept (a) of regressions was not forced through the origin because, unlike annual crops, there may be an allocation of DM from perennial organs to shoots during the early stages of lucerne regrowth (Section 2.6).

7.2.2 Radiation use efficiency for total DM

Radiation use efficiency for total DM (RUE_{total}) represented the conversion of PAR_i to total crop DM. Total crop DM was calculated as the sum of DM_{shoot} and 1.25 x DM_{per}. The adjustment was because DM_{per} (crown + taproots at 300 mm depth) was assumed to be 80% of the total perennial biomass (Section 4.2.1). This was done using data-points taken after ~14 days of regrowth, when DM_{per} was expected to increase (phases II and III of regrowth, Section 2.5.2). When DM_{per} was stable or declined (net loss of DM_{per}), RUE_{total} was omitted for that regrowth cycle (Figure 7.1 *b*). This resulted in 24 estimates of RUE_{total} from 72 available regrowth cycles.

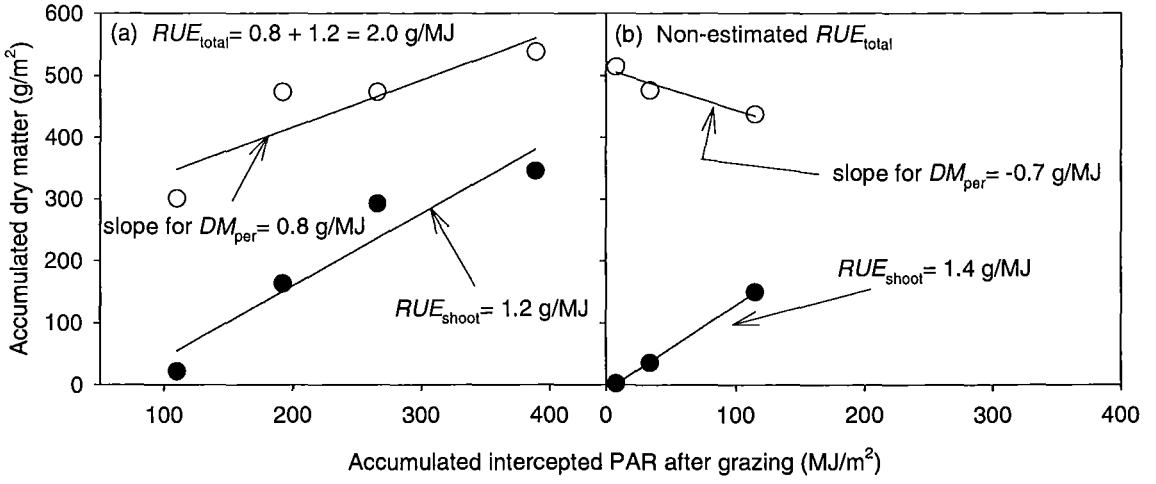

Figure 7.1 Representation of shoot (●) and perennial dry matter (○) against accumulated PAR_i as an example of the methodology used to estimate RUE_{total} in each regrowth cycle.

Note: In the example of graph *a* (cycle 3, $LL_{02/03}$ crop) there was a measurable increase in DM_{per} that made possible the estimation of RUE_{total}. In graph *b* (cycle 8, $SS_{02/03}$ crop) DM_{per} declined and therefore RUE_{total} was not estimated for this cycle. Note that crops grazed with short cycles (*e.g.* graph *b*) had only 3 data-points available for curve fitting compared with 4 data-points in long cycle (42-days) crops.

Due to the effects of temperature on lucerne *RUE* (Section 2.5.1.4), the estimated values of RUE_{total} were reported as a function of mean air temperature (T_{mean}) using the framework proposed by Brown (2004) ± a 95% confidence limit of 10%. In this temperature framework, RUE_{total} is nil at 0°C but increases linearly to an optimum (RUE_{opt}) of 3.2 g DM/MJ PAR_i at a T_{mean} of 18°C (Figure 2.1).

7.2.3 Dry matter partitioning to perennial organs

Fractional dry matter partitioning to perennial organs (p_{per}) was estimated as the reciprocal of the relationship between RUE_{shoot} and RUE_{total} (Equation 7.1).

Equation 7.1

$$p_{per} = 1 - \frac{RUE_{shoot}}{RUE_{total}}$$

Fractional partitioning was plotted against the mean photoperiod (*Pp*) experienced by crops during each regrowth cycle. This analysis was segmented in periods of increasing *Pp*

(*IPp*) and decreasing *Pp* (*DPp*) because lucerne response to environmental factors may differ with the direction of *Pp* (Brown *et al.*, 2005b; Holt *et al.*, 1975).

Alternatively, p_{per} was also related to the ratio between soil (100 mm profile) and air temperature (T_{soil}/T_{air}) as suggested by Hargreaves (2003). This was based on the simplified rationale that the metabolic activity of shoots and perennial organs respond solely and similarly to temperature with a common base temperature of 0°C. The ratio T_{soil}/T_{air} then defines the sink strength of the organ at any given time (Section 2.6). In both approaches, p_{per} was assumed to be nil when $RUE_{shoot} \geq RUE_{total}$.

7.2.4 Leaf net photosynthesis rate

7.2.4.1 Spot readings at 1000 µmols photons/m²/s (Pn_{1000})

Leaf net photosynthesis (Pn_{1000}, µmol $CO_2/m^2/s$) was measured each 15-30 days (as weather permitted) in LL and SS crops. Pn_{1000} measurements were taken between 1100 and 1400 h in clear sky conditions. Readings were taken on 3-4 of the youngest fully expanded leaves per plot, at artificial light fluxes (PPFD) of 1000 µmol photons/m^2/s using a portable photosynthesis system LI-6400 (LI-COR Inc, Lincoln, Nebraska, USA). The temperature in the leaf chamber was set to 21°C and the CO_2 concentration at 400 ppm. Readings were taken after a coefficient of variation (CV) $\leq 3\%$ was obtained for the Pn_{1000} logs. Readings were adjusted according to the actual area of the leaf contained in the equipment chamber. Individual leaf area was quantified after *Pn* measurements by removing the leaf and photographing it to calculate leaf surface by image analysis (Section 6.2.2.1).

Pn_{1000} data are reported in two forms. Firstly, when data from similar periods of regrowth were compared, Pn_{1000} is reported as measured. Alternatively, when data from different dates were compared in relation to a single variable (*e.g.* chlorophyll concentration, Section 7.2.5), Pn_{1000} was normalized by the highest average daily Pn_{1000} ($Pn_{1000max}$) and multiplied by the assumed optimum Pn_{1000} from all sampling dates (Equation 7.2).

Equation 7.2

$$Pn'_{1000} = Pn_{1000opt} \times \frac{Pn_{1000}}{Pn_{1000\max}}$$

The optimum Pn_{1000} ($Pn_{1000opt}$) was assumed to be 31.5 μmol $CO_2/m^2/s$ because it was the average maximum Pn observed in LL crops at T_{mean}>25°C on 24 January 2004. This value agrees with previous reports of Pn_{1000} in Canterbury in summer (Varella, 2002).

7.2.4.2 Light response curves

In addition to the Pn_{1000} readings, full photosynthetic light response curves were measured with the photosynthesis system. Measurements were taken on 3 or 4 of the youngest fully expanded leaves of each plot from LL and SS crops. Readings were taken at seven PPFD levels: 0, 100, 250, 500, 750, 1000, 2000 μmol photons/m^2/s. The criteria for taking measurements were a minimum waiting time of 60 seconds and a CV ≤ 3% for each PPFD level. The photosynthesis system configurations and criteria used to perform the light response curves were the same as the Pn_{1000} readings (Section 7.2.4.1).

A non-rectangular hyperbola (Equation 7.3) was fitted to the data to obtain the main parameters from the light-response curves (Thornley and Johnson, 2000):

Equation 7.3

$$Pn = \frac{(P_{\max} + \alpha \times PPFD) - [(P_{\max} + \alpha \times PPFD]^2 - [4 \times \theta \times \alpha \times PPFD \times P_{\max}])}{2 \times \theta} - R_d$$

Where Pn is the leaf net photosynthesis rate (μmol $CO_2/m^2/s$), R_d is the rate of dark respiration (μmol $CO_2/m^2/s$), $PPFD$ is the photosynthetic photon flux density (μmol photons/m^2/s). The parameters α, θ and P_{max} represent the initial slope (μmol CO_2/μmol photons), the convexity (dimensionless) and the upper asymptote (μmol $CO_2/m^2/s$) of the light-response curve. Curves were fitted with Sigmaplot v.8 (SPSS, Inc.) using the following constraints: α>0; 0.3<θ<1.0; 2.0< P_{max}<70.0; R_d <5.0.

Based on the observation that the effects of the defoliation treatment on crop yield (Section 5.3.2) and perennial biomass (Section 4.3.2) occurred mainly after the first spring of 2002/03, the parameters of light-response curves were pooled within spring and summer-

autumn periods. Parameters from light response curves of LL and SS crops were then compared using ANOVA between each of these two periods.

7.2.5 Chlorophyll readings

Leaf chlorophyll concentration was estimated using a chlorophyll meter (SPAD-502, Minolta Camera Co, Japan). The SPAD readings were taken on 627 leaves where photosynthesis was also measured from January 2003 to May 2004. Readings were taken at noon ± 2 h on sunny days. The SPAD reader measures the transmittance of blue light (430 nm) in relation to the near infra-red (750 nm) through a leaf (Markwell *et al.*, 1995). Thus, SPAD readings were used primarily as an indication of the level of chlorophyll and consequently N nutrition of the youngest fully expanded leaves. SPAD readings were calibrated against actual chlorophyll concentration measured by wet chemistry (Section 7.2.5.1).

7.2.5.1 Chlorophyll extraction and SPAD calibration

Readings of SPAD of 33 youngest fully expanded leaves were calibrated against actual chlorophyll *a+b* concentration per unit area (Chl_{a+b}, mg/m^2 leaf) obtained by the dimethyl sulphoxide (DMSO) method (Hiscox and Israelstam, 1979; Tait and Hik, 2003). For the calibration, leaves were collected on a sunny day (14 March 2003) within ±2 h from noon to avoid variations in specific leaf weight (Hoel and Solhaug, 1998). The youngest fully expanded leaves were subjectively selected according to their greenness to generate a wide range of SPAD readings. The average weight of one individual leaf was ~0.017 g DM, so the whole leaf was used for the determination. After measuring individual leaf area (Section 6.2.2.1) each leaf was incubated for 2 hours in a water bath at 65°C with 7 ml of DMSO. After extraction, the volume of the decanted supernatant was adjusted with fresh DMSO to 10 ml to standardize the dilution. The absorbance at wavelengths (λ) of 645 and 663 nm was measured using a Shimadzu UV-160 spectrophotometer (Shimadzu Corporation, Kyoto, Japan). The calculation of chlorophyll content (mg/l) was based on Equation 7.4 (Arnon, 1949; Hiscox and Israelstam, 1979).

Equation 7.4

$$Chl_{a+b} = (20.2 \times \lambda 645) + (8 \times \lambda 663)$$

For the calibration curve, chlorophyll concentrations were expressed on a leaf area basis (mg/m^2 leaf) and regressed against SPAD readings (Figure 7.2).

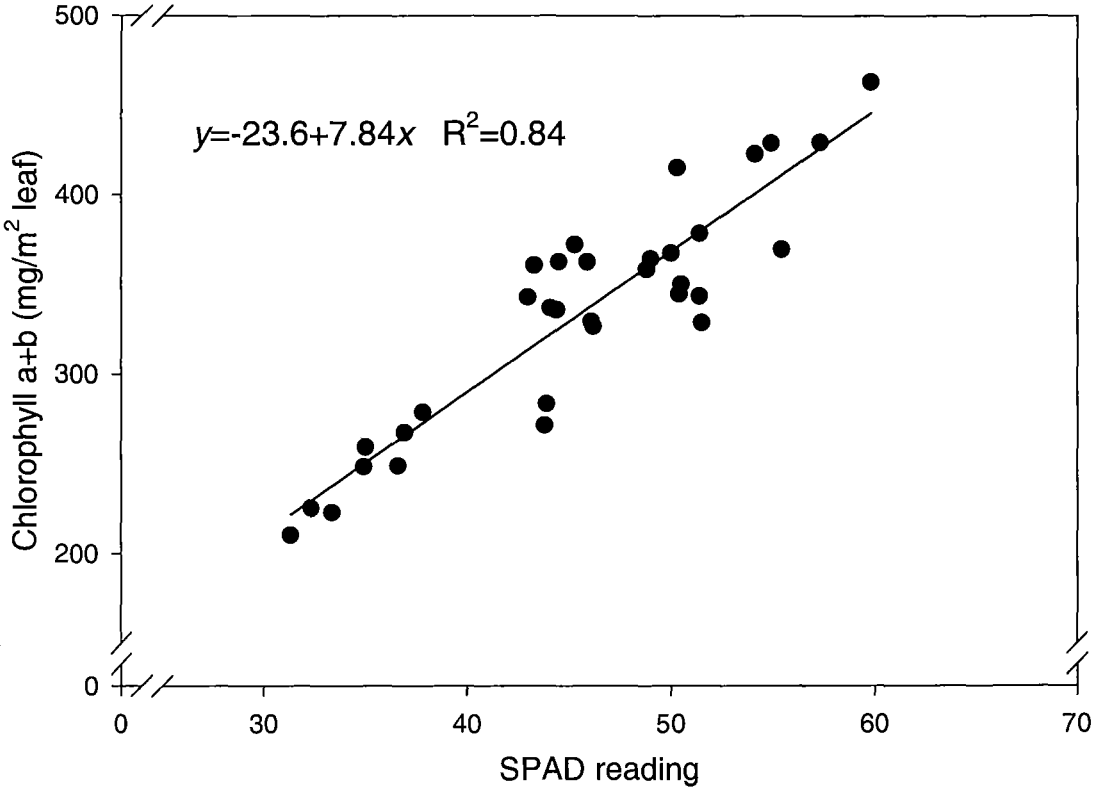

Figure 7.2 Calibration curve between chlorophyll concentration per unit leaf area (mg/m^2) and SPAD reading of lucerne leaves at Lincoln University, Canterbury, New Zealand.

Note: Leaves were randomly collected on 14 March 2003 from all crops by subjectively selecting youngest fully expanded leaves with contrasting levels of greenness.

To test the SPAD calibration equation an independent set of 20 leaves randomly sampled from all treatments on 20 April 2005 was analysed for Chl_{a+b}. The relationship between predicted and observed values was similar to 1.0 (P<0.05) and the intercept was not different from zero (P<0.38); with an *RMSD* of the model of 11.5 mg/m^2 (3.5% of the mean value).

From 18 March to 28 April 2003, 54 leaves (3 to 4 per plot) of LL and SS crops which had Pn_{1000} previously measured, were also analysed for total chlorophyll content (Chl_{a+b}, mg/m^2) by wet chemistry. These leaves were used to test the relationship between leaf photosynthesis and Chl_{a+b}.

7.2.6 Specific leaf weight

Specific leaf weight (*SLW*, g/m^2) of individual leaves, where photosynthesis was recorded (Section 7.2.4), was measured on dates when LL and SS crops were at a similar number of days post grazing. *SLW* was calculated by dividing leaf weight (g) by the area of each leaf (m^2) as estimated by digital image analysis (Section 6.2.2.1).

7.2.7 Leaf nitrogen concentration and specific leaf nitrogen

Leaf nitrogen concentration (% of DM) was measured by Kjeldahl extraction from shoot samples (Section 4.2.2). After sampling, shoots were kept in a cold chamber (4°C) before being processed into leaves (leaflets), stems (stem and petioles) and senesced tissues. Samples were then dried in a forced air oven at 60°C for 48 h.

Specific leaf nitrogen (*SLN*, g N/m^2 leaf) was obtained by multiplying N concentration by the specific leaf weight (*SLW*, g/m^2) of fully expanded leaves from where photosynthesis measurements were previously taken. *SLN* was estimated from pooled samples (3-4 leaflets) per plot on 18 March 2003, 9 April 2003, 29 November 2003, 26 December 2003, 15 January 2004 and 23 January 2004.

7.2.8 Nitrogen nutrition index calculation

The nitrogen nutrition index (*NNI*) was calculated as the relationship between the actual nitrogen concentration ($N\%_{act}$) and the critical nitrogen concentration ($N\%_{crit}$) of shoots (Lemaire and Gastal, 1997) as shown in Equation 7.5:

Equation 7.5

$$NNI = \frac{N\%_{act}}{N\%_{crit}}$$

The value of $N\%_{crit}$ was calculated as the minimum nitrogen concentration in shoots able to promote the maximum rates of growth (Lemaire and Gastal, 1997). For lucerne crops with DM_{shoot} (t/ha) greater than 1 t/ha the value of $N\%_{crit}$ was calculated according to Equation 7.6 (Lemaire *et al.*, 1985).

Equation 7.6

$$N\%_{crit} = 4.8 \times (DM_{shoot})^{-0.34}$$

For DM_{shoot} less than 1 t/ha, an exponential curve with three parameters (R^2=0.92, P<0.01) described the decline of $N\%_{act}$ and DM_{shoot} in the LL crop (Appendix 6).

This model (Equation 7.7) assumed that LL crops were not N limited or had luxury N consumption at DM_{shoot}<1t/ha and $N\%_{crit}$ was 5.8% at a hypothetical null DM_{shoot}.

Equation 7.7

$$N\%_{crit} = 1.96 + 3.79 \times \exp(-0.24 \times DM_{shoot})$$

The *NNI* was compared between LL and SS crops throughout both growing seasons. Furthermore, *NNI* was plotted against the number of primary leaves at specific dates when crops had a similar development stage (5 Jun to 14 Sep 03; 16 Feb to 2 Mar 04 and 11 May to 9 Jun 04) or when the number of primary leaves was > 7.

7.3 Results

7.3.1 Seasonal shoot *RUE* (RUE_{shoot})

The values of seasonal RUE_{shoot} ranged from 1.0 to ~2.5 g DM/MJ PAR_i (Figure 7.3). RUE_{shoot} changed ($P<0.01$) throughout the year, the lowest values of each growth season usually occurred in autumn for all treatments. In general RUE_{shoot} was >1.5 g DM/MJ PAR_i from August to February (winter/mid-summer) but declined to <1.2 g DM/MJ PAR_i by April (autumn). The exceptions for this pattern were the last autumn cycles of $LL_{02/03}$ and $SL_{02/03}$ which had RUE_{shoot} of ~2.5 g DM/MJ PAR_i (Figure 7.3 *a, c*). However, the final shoot yield in this last cycle was less than 400 kg DM/ha in both treatments. During the early-spring regrowth of 2004/05, when all crops were harvested on 5 October 2004, RUE_{shoot} was similar in all treatments at 1.2 g DM/MJ PAR_i.

The effect of treatments on RUE_{shoot} was characterized by a strong interaction ($P<0.01$) with annual season. During spring, there was no difference in RUE_{shoot} among treatments with an overall average of 1.5 g DM/MJ PAR_i (Figure 7.3). In summer LL and LS crops had 20% greater RUE_{shoot} than SL and SS crops (1.6 and 1.4 g DM/MJ PAR_i respectively). In autumn, SS crops had the lowest average RUE_{shoot} (1.0 g DM/MJ PAR_i). During the winter period, SL and SS crops showed the highest ($P<0.05$) values of RUE_{shoot} at ~2.0 g DM/MJ PAR_i (Figure 7.3 *b, c*). This was possibly an artefact of the time of the first grazing of the growth season (*i.e.* winter/early-spring grazing), that was 15 days earlier for SL and SS crops than for the other two crops (Section 3.3).

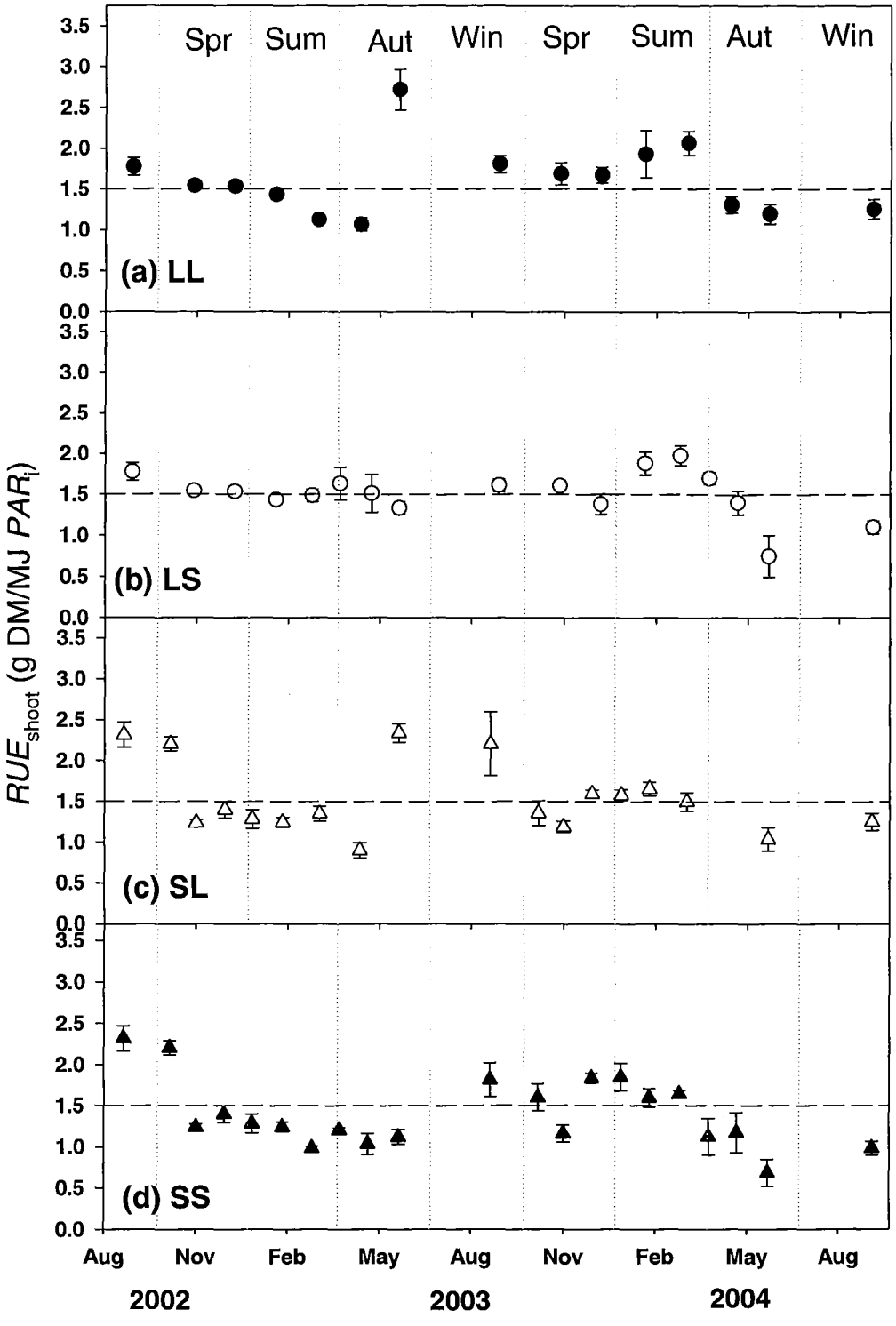

Figure 7.3 Seasonal radiation use efficiency for shoot yield (RUE_{shoot}) of lucerne crops subjected to four contrasting defoliation regimes in the 2002/03 and 2003/04 growth seasons at Lincoln University, Canterbury, New Zealand.

Note: Vertical dotted lines represent first day of annual seasons. Horizontal dashed line represents pooled averaged RUE_{shoot} of 1.5 g DM/MJ PAR_i for reference. Bars represent one SEM of each regrowth cycle/treatment combination (n=4).

7.3.2 Radiation use efficiency for total dry matter (RUE_{total})

The pooled average of RUE_{total} among treatments was 2.2±0.4 g DM/MJ PAR_i, with individual values ranging from 1.3 to 3.6 g DM/MJ PAR_i. To account for temperature effects, estimated values of RUE_{total} were plotted on the temperature framework (Figure 7.4) proposed by (Brown, 2004). RUE_{total} of LL crops tended to increase with T_{mean} (P<0.11) at a rate of 0.10 g DM/MJ PAR_i/°C. In contrast, no systematic differences (0.43<P<0.88) were observed in the other treatments.

The root mean squared deviation (*RMSD*) in relation to the *RUE*-T_{mean} framework was lower in LL and LS crops (*RMSD* of 0.4 to 0.7 g/MJ or ~20% of the mean) than in SL and SS crops (*RMSD* of ~0.9 g/MJ or 48% of the mean). The high *RMSD* in SL and SS crops was due to a group of four cycles of SS crops, two of which were also shown in $SL_{02/03}$ (Figure 7.4 *d*), that were segregated at 0.7-1.0 g/MJ below the confidence interval lines. The other four available data-points from SS crops were close to the proposed framework. In SL crops the other three cycles for 2003/04 also showed the predicted response to temperature (Figure 7.4 *c*).

Due to the practical difficulties involved to obtain accurate estimates of RUE_{total} in field conditions (Section 2.5.2), measured RUE_{total} was mainly used to validate the temperature framework. To continue the calculation of fractional partitioning to perennial organs (p_{per}), which depends on estimates of RUE_{total} for each regrowth cycle, the temperature framework was assumed as a correct basis for deriving values of RUE_{total} for each regrowth cycle.

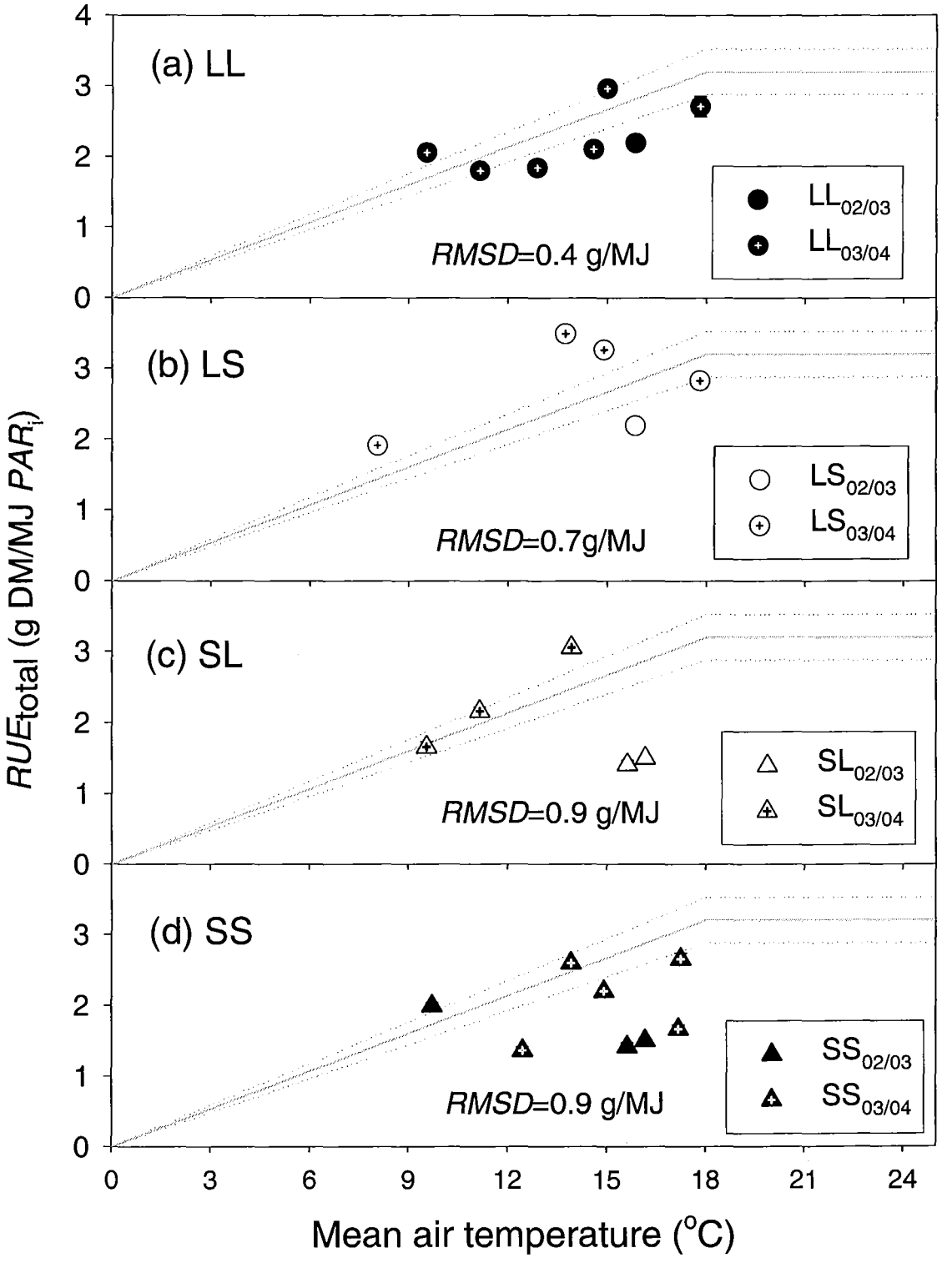

Figure 7.4 Estimated values of RUE_{total} plotted against mean air temperature of each respective regrowth cycle of lucerne crops subjected to four contrasting defoliation regimes in the 2002/03 and 2003/04 growth seasons at Lincoln University, Canterbury, New Zealand.

Note: Solid line represents an assumed linear increase in RUE_{total} with temperature and dotted lines delimit ± 10% of the model (Section 7.2.2).

7.3.3 Partitioning of DM to perennial organs

Seasonal changes in the partitioning of dry matter to perennial organs were analysed by comparing "measured RUE_{shoot}" and "calculated RUE_{total}" throughout the growth season (Figure 7.5). RUE_{total} was calculated assuming an optimum RUE_{total} of 3.2 g DM/MJ PAR_i adjusted for the temperature limitation at T_{mean}<18°C (Brown, 2004). Measured values of RUE_{shoot} were as displayed in Figure 7.1. In this sense, the reciprocal of the relationship between RUE_{shoot} and RUE_{total} represents the fractional partitioning of DM to perennial organs (p_{per}). In SS crops, estimates of RUE_{total} were also displayed with a hypothetical 30% decrease in relation to the potential seasonal RUE_{total}. The objective was to demonstrate a possible decline in RUE_{total} with a similar magnitude as observed in the four data-points that were positioned below the RUE-T_{mean} framework (Figure 7.4 *d*).

During the early-spring regrowth cycles, RUE_{total} in LL and LS crops was similar to RUE_{shoot} at 1.8 g DM/MJ PAR_i (Figure 7.5 *a, b*). This indicates that the partitioning of dry matter to perennial organs was negligible during early-spring. For SL and SS crops, which had the first harvest of each season 15 days before LL and LS crops, measured RUE_{shoot} was ~0.7 to 1.0 g DM/MJ PAR_i higher than the estimated RUE_{total} in both years. This implies a flow of dry matter from perennial organs to shoots during these early stages of regrowth. For all crops, the difference between RUE_{shoot} and RUE_{total} increased to a maximum in mid-summer that was maintained throughout autumn.

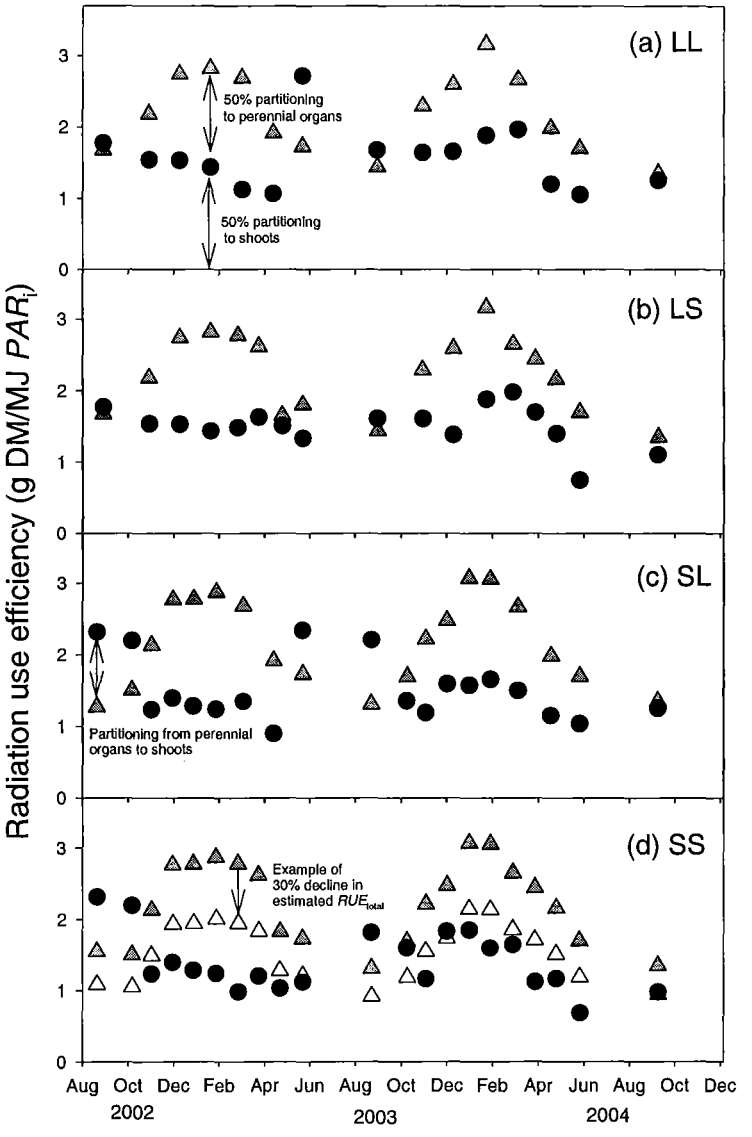

Figure 7.5 Seasonal estimated total radiation use efficiency (▲) and measured shoot radiation use efficiency (●) of lucerne crops subjected to four contrasting defoliation regimes in the 2002/03 and 2003/04 growth seasons at Lincoln University, Canterbury, New Zealand.

Note: Potential estimated RUE_{total} was calculated using an optimal RUE_{total} of 3.2 g/MJ and temperature adjustment (Section 7.2.2). In SS crops an example of estimated RUE_{total} with an assumed 30% decline in estimated RUE_{total} (△) during spring-summer regrowth cycles (Section 7.3.2). Arrows indicate that the difference between RUE_{shoot} and RUE_{total}. This difference defines the extent of DM partitioning to perennial organs.

7.3.3.1 *Fractional partitioning of DM to perennial organs in relation to photoperiod and temperature*

The estimated fractional partitioning of DM to perennial organs (p_{per}) was calculated for each regrowth cycle (Section 7.2.3) and plotted against the average photoperiod (*Pp*) (Figure 7.6). A hysteresis model was needed to describe changes in p_{per} at increasing (*IPp*) or decreasing (*DPp*) photoperiods.

In LL crops at *IPp*, p_{per} increased ($P<0.01$) from <0.10 at a *Pp* of 10.5 h to ~0.50 at a *Pp* of 16.5 h (Figure 7.6 *a*). This implies that for each increment of one hour of *IPp* there was an increase of 0.07 in the partitioning of DM to perennial organs. As *Pp* decreased (late-summer and autumn) p_{per} was maintained at ~0.40-0.50 with no systematic influence ($P<0.66$) of *DPp*.

Fractional partitioning to perennial organs in LS and SL crops followed a similar pattern of increase ($0.76<R^2<0.89$) with *IPp*, as in LL crops (Figure 7.6 *b, c*). Values of p_{per} increased ($P<0.01$) with *IPp* at 0.07/h for LS and 0.08/h in SL, rates which were similar to LL crops. As photoperiod declined, LS crops maintained a p_{per} of ~0.35 while SL crops were between 0.40-0.60, both showing a greater variability than LL crops but still with no significant influence ($0.10<P<0.49$) of *DPp*.

In SS crops, assuming a 30% decline in RUE_{total} (Section 7.3.3), p_{per} increased ($P<0.02$) at 0.05/h. This rate of increase of p_{per} with *IPp* was lower ($P<0.05$) than the other crops. At *DPp* there was no significant effect of *Pp* on p_{per} with an average of ~0.25 (Figure 7.6 *d*).

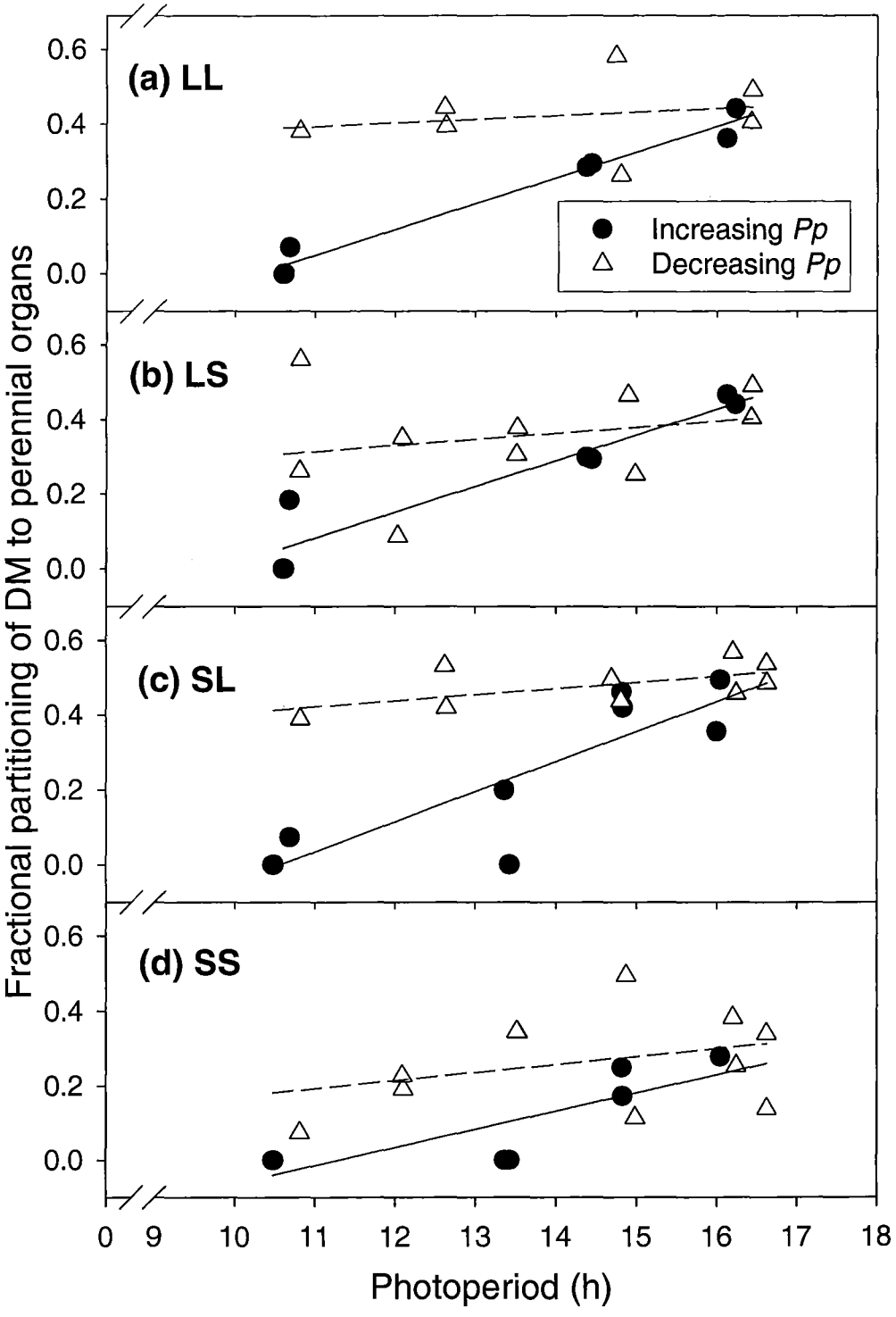

Figure 7.6 Estimated fractional partitioning of dry matter to roots of lucerne crops subjected to four contrasting defoliation regimes in the 2002/03 and 2003/04 growth seasons at Lincoln University, Canterbury, New Zealand.

Note: Lines represent linear regressions of p_{per} with *IPp* (—) and *DPp* (----). For *IPp*, slopes were significantly ($P<0.05$) different from zero for all crops at 0.07/h for LL, LS and SL and 0.05/h for SS crops. For *DPp* all slopes were not different from zero ($0.20<P<0.97$).

Because the estimated value of p_{per} is dependent on the calculated RUE_{total}, p_{per} was also calculated for SS crop without considering any decrease in RUE_{total} (Appendix 4). With this assumption p_{per} for SS crop would have an increase with *IPp* at 0.097/h similar to the other crops and be unaffected by *Pp* (P<0.81) at 0.44 at *DPp*.

The ratio between soil (100 mm depth) and air temperature (T_{soil}/T_{air}, Section 7.2.3) was tested as an alternative predictor of seasonal differences in p_{per} (Figure 7.7). The p_{per} increased (P<0.05) in all treatments as T_{soil}/T_{air} increased from 0.9 to 1.3. There was a trend for faster rates of increase of p_{per} with T_{soil}/T_{air} in LL and SL (~1.0) than SS and SL (~0.7). Nevertheless, the large standard error of the slope (0.27) implied no significant difference among defoliation treatments (Figure 7.7).

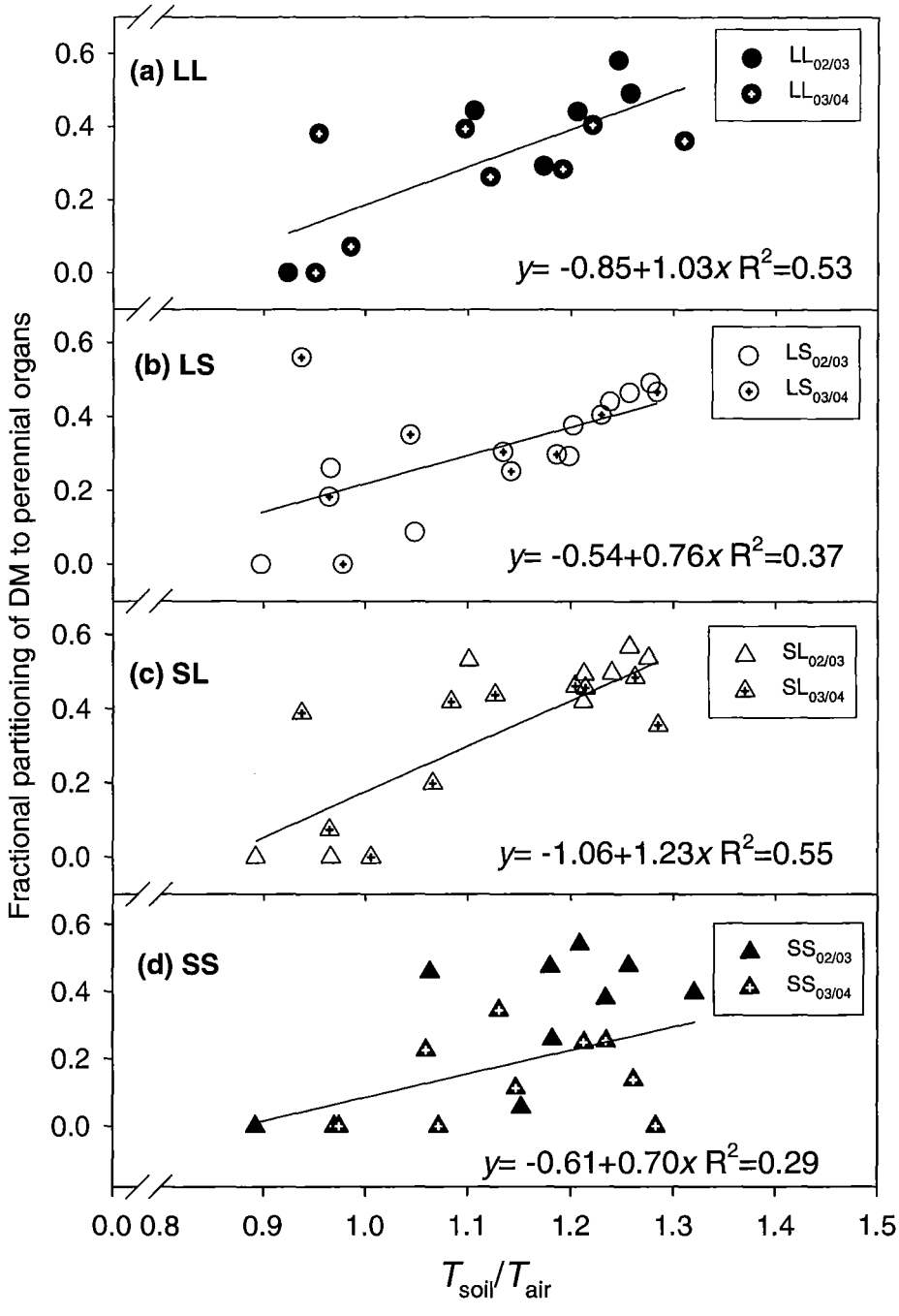

Figure 7.7 Relationship between fractional partitioning of DM to perennial organs (p_{per}) and the ratio between soil and air temperatures (T_{soil}/T_{air}) of lucerne crops subjected to four contrasting defoliation regimes in the 2002/03 and 2003/04 growth seasons at Lincoln University, Canterbury, New Zealand.

Note: Estimates of p_{per} for SS crop without a -30% in RUE_{total} are displayed in Appendix 4

Nevertheless, the strong relationship (R^2=0.90) between *Pp* and T_{soil}/T_{air} (Figure 7.8 *b*) indicates that, in field conditions, it was not possible to isolate their individual effects on p_{per}.

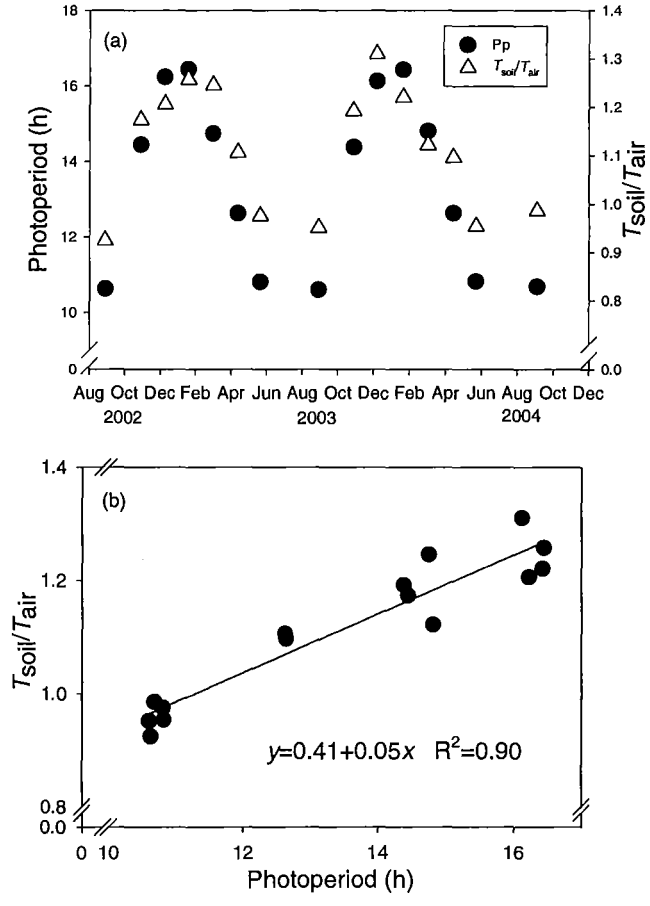

Figure 7.8 Seasonal variation in the average photoperiod and average T_{soil}/T_{air} of each regrowth cycle (*a*), and linear relationship between the average T_{soil}/T_{air} and photoperiod (*b*) of regrowth cycles of lucerne crops grazed each 42-day at Lincoln University, Canterbury, New Zealand.

Based on the fact that there was some evidence of a decline in RUE_{total} of SS crops (Figure 7.4 *d*) a further investigation of photosynthetic capacity and nitrogen nutritional status of LL and SS crops was undertaken.

7.3.4 Leaf photosynthesis rates

Light-response curves of LL and SS crops were measured in the 2002/03 growth season and spot readings of *Pn* at 1000 μmol $CO_2/m^2/s$ (Pn_{1000}) in both 2002/03 and 2003/04 growth seasons (Section 7.2.4).

7.3.4.1 Light response curves and seasonal photosynthesis

The analysis of the light response curve parameters was segmented into an early (spring) and a late (summer-autumn) period of the first growth season (2002/03). During the spring of 2002, all four parameters of the light response curves were unaffected by short or long regrowth cycles (Table 7.1). On average, P_{max} was 36 μmol $CO_2/m^2/s$; alpha (α) was 0.07 μmol CO_2/μmol photons, theta (θ) was 0.61 and dark respiration (R_d) was 1.82 μmol $CO_2/m^2/s$. In contrast, during summer-autumn, LL crops had 20% greater ($P<0.01$) P_{max} than SS crops, the other three parameters being similar between treatments (Table 7.1).

Table 7.1 Parameters of light response curves of lucerne crops subjected to 28-day (SS) and 42-day (LL) regrowth cycles in the spring and summer-autumn of the 2002/03 growth season at Lincoln University, Canterbury, New Zealand.

	P_{max} (μmol $CO_2/m^2/s$)	α (μmol CO_2/μmol photons)	θ (dimensionless)	R_d (μmol $CO_2/m^2/s$)
Spring				
LL	34.9_a	0.065_a	0.54_a	1.78_a
SS	36.2_a	0.068_a	0.67_a	1.87_a
SEM	*1.99*	*0.0034*	*0.055*	*0.095*
Summer-Autumn				
LL	39.6_a	0.065_a	0.47_a	1.92_a
SS	32.5_b	0.055_a	0.62_a	2.04_a
SEM	*0.66*	*0.0045*	*0.054*	*0.33*

Note: Within columns, values with the same letter are not significantly different (α=0.05) when comparing data of each seasonal period. SEM is the standard error of means for n=4. Spring was assumed as the period from 23 Sep 02 to 22 Dec 02 and summer-autumn from 23 Dec 02 to 21 Mar 03.

7.3.4.2 *Leaf photosynthesis at 1000 μmol photons/m²/s within cycles*

Leaf net photosynthesis at 1000 μmol photons/m²/s (Pn_{1000}) was used to test the hypothesis that photosynthetic capacity was similar between treatments throughout an entire regrowth cycle. To test this hypothesis, linear regressions were plotted between Pn_{1000} and thermal-time accumulation ($\sum Tt_{b5}$) for LL and SS crops. Leaf Pn_{1000} was on average 24 μmol $CO_2/m^2/s$ for LL crops (b=0, P<0.89) with no systematic effect of $\sum Tt_{b5}$ on photosynthesis. In contrast, Pn_{1000} of SS crops increased (P<0.03, R^2=0.28) by 0.03 μmol $CO_2/m^2/s$ for each 1°Cd of Tt_{b5} accumulation (Appendix 5). This suggested that Pn_{1000} in SS crops was lower than LL crops mainly during the first half (~150°Cd) of an average regrowth cycle. Following this rationale, Pn_{1000} values were grouped in early (<150°Cd), or late (>151°Cd) stages of each regrowth cycle. Pooled Pn_{1000} values were then compared by ANOVA. Pn_{1000} readings taken prior to 150°Cd were ~20% greater (P<0.03) in LL crops (24.9 μmol $CO_2/m^2/s$) than SS crops (20.4 μmol $CO_2/m^2/s$) (Table 7.2). In contrast, after 150°Cd, both crops had a similar (P<0.34) Pn_{1000} of 23.8 μmol $CO_2/m^2/s$.

Table 7.2 Leaf photosynthesis at 1000 μmol photon/m²/s of lucerne crops subjected to 28-day (SS) or 42-day (LL) grazing regrowth cycles.

Thermal-time sum (°Cd, T_b=5°C)	LL	SS
	μmol $CO_2/m^2/s$	
0-150	24.9_a	20.4_b
151-350	23.5_a	24.2_a

Note: Values with the same letter within rows are not significantly different (α=0.05). SEM is 0.702.

7.3.4.3 *Chlorophyll concentration and photosynthesis rates*

There was a strong linear relationship (R^2=0.70; P<0.01) between Pn_{1000} and *in vitro* chlorophyll (Chl_{a+b}) concentration (Figure 7.9 *a*). Pn_{1000} increased at a rate of 0.04 μmol $CO_2/m^2/s$ for each milligram increase in leaf Chl_{a+b}/m^2.

The same relationship was tested using leaf Chl_{a+b} estimated by SPAD readings under a wide range of climatic conditions in the field (Section 7.2.5.1). From the spring of 2002/03 to the autumn of 2003/04, the relationship between leaf Pn'_{1000} (Pn_{1000} normalized as a

fraction of the optimum daily Pn_{1000}, Section 7.2.4.1) was plotted as a function of SPAD readings (Figure 7.9 *b*). Pn'_{1000} had a weak (R^2=0.38) but significant (P<0.01) increase of 0.03 of Pn'_{1000} for each one mg Chl_{a+b}/m^2. This rate of increase had a SEM of 0.006 and therefore was similar to the slope observed in laboratory conditions (Figure 7.9 *a*).

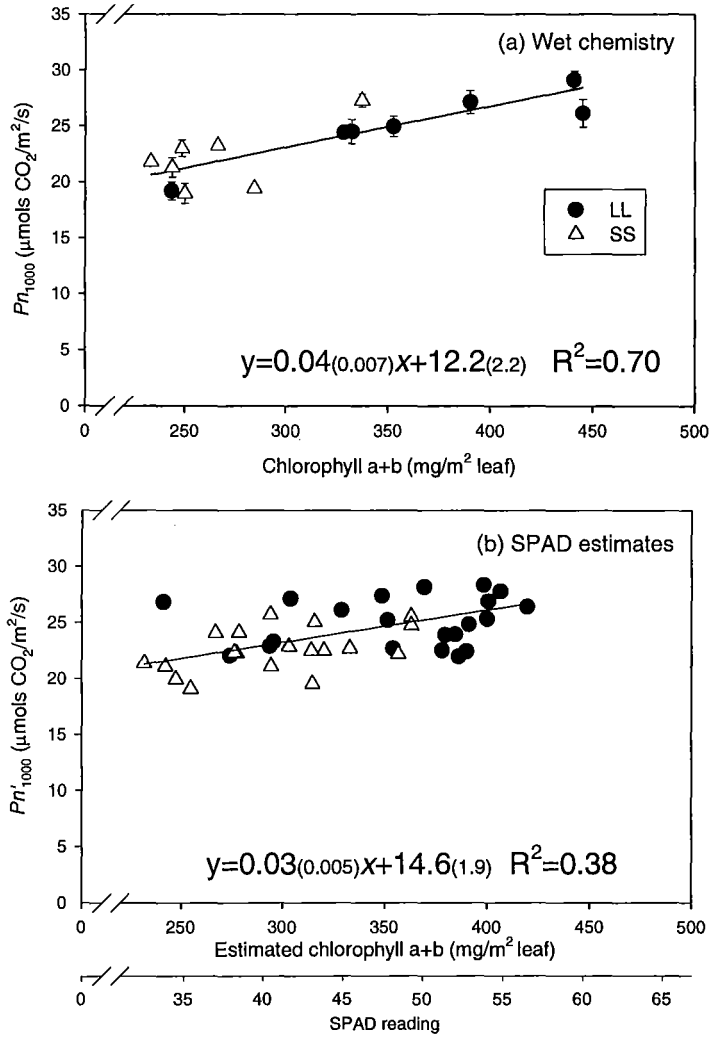

Figure 7.9 Relationship between leaf net photosynthesis and chlorophyll content of the youngest fully expanded leaf of lucerne crops subjected to 28-day (SS) or 42-day (LL) regrowth cycles in the 2002/03 and 2003/04 growth seasons at Lincoln University, Canterbury, New Zealand.

Note: In graph *a* values of chlorophyll (pooled per plot) were measured *in vitro* using DMSO extraction with leaves collected on 18 Mar 2003, 9 Apr 2003 and 28 April 2003. In graph *b* chlorophyll values (pooled per day) were estimated from SPAD readings collected in the field at various dates in 2002/03 and 2003/04 season, normalized by the maximum Pn_{1000} of each day and multiplied by an assumed optimum Pn_{1000} of 31.5 µmol $CO_2/m^2/s$ (Section 7.2.4). Values in parenthesis are one SEM of coefficients. Bar is one SEM

In both *in vitro* measurements and SPAD readings, the leaf Chl_{a+b} values ranged from 250 to 450 mg/m^2. In both data sets, Chl_{a+b} of leaves from SS crops ranged from 250 to 350 mg/m^2. In contrast in LL crops leaf Chl_{a+b} values covered the entire observed range with a greater concentration of data-points from 350 to 450 mg/m^2 (Figure 7.9).

7.3.5 Leaf photosynthesis rates and leaf nitrogen concentration

The relationship between leaf Pn'_{1000} and specific leaf nitrogen (*SLN*, g N/m^2), was tested by using a three parameter equation (Sinclair and Horie, 1989). This relationship (Equation 7.8) explained 68% of the variation in Pn'_{1000} that increased ($P<0.01$) from 15 μmol CO_2/m^2/s at a *SLN* of 1.5 g/m^2 to ~30 μmol CO_2/m^2/s at a *SLN* of 3.4 g/m^2.

Equation 7.8

$$Pn'_{1000} = 31.4 \times \left(\frac{2}{1 + \exp(-1.58 \times (SLN - 0.92))} - 1 \right)$$

Equation 7.8 indicates that Pn'_{1000} reached an asymptote at 31.4 μmol CO_2/m^2/s, this being an artefact of the assumed optimum Pn'_{1000} of 31.5 μmol CO_2/m^2/s (Section 7.2.4). Maximum values of Pn'_{1000} were observed from a *SLN*> 2.0 g/m^2 mostly in LL crops. A projected nil Pn_{1000} at *SLN* of 0.92 g/m^2 could also be extrapolated from the relationship.

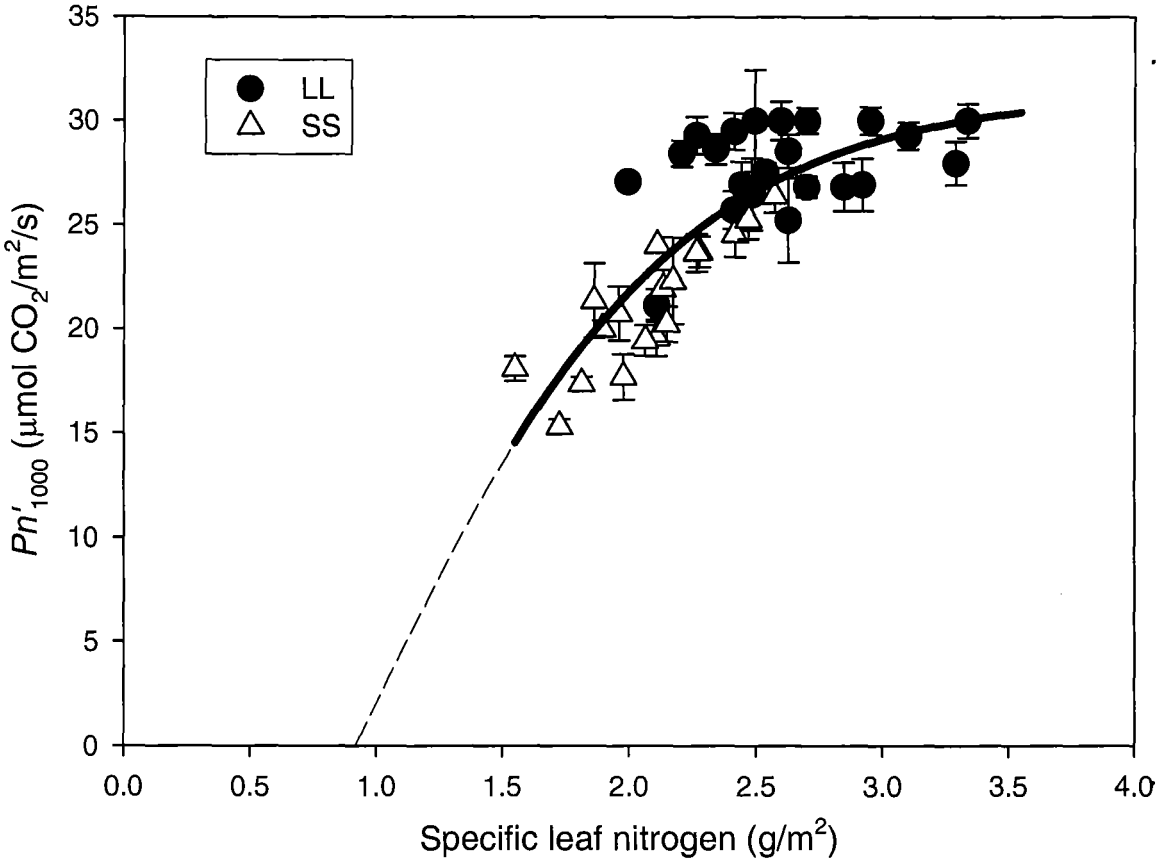

Figure 7.10 Relationship between normalized leaf photosynthesis rates at 1000 µmol photons/m^2/s (Pn'_{1000}) and specific leaf nitrogen (*SLN*, g/m^2) of lucerne crops subjected to 28-day (SS) and 42-day (LL) regrowth cycles in the 2002/03 and 2003/04 growth seasons at Lincoln University, Canterbury, New Zealand.

Note: Bars represent one SEM of each replicate (n=4). Solid line represents Equation 7.8 and dashed lines represent its projection to y=0.

7.3.5.1 Leaf nitrogen concentration ($N\%_{leaf}$) and specific leaf weight (SLW)

The two components of *SLN* (*SLW* and $N\%_{leaf}$) of the youngest fully expanded leaves were tested as independent predictors of Pn'_{1000} (Figure 7.11).

The same equation used for *SLN* (Section 7.3.5) was tested to explain differences in Pn'_{1000} with *SLW*. This relationship explained ~80% of the variation in Pn'_{1000} (Figure 7.11 *a*). In contrast $N\%_{leaf}$ was not related to Pn'_{1000} ($0.29<P<0.70$) being on average 4.9% DM ±0.08.

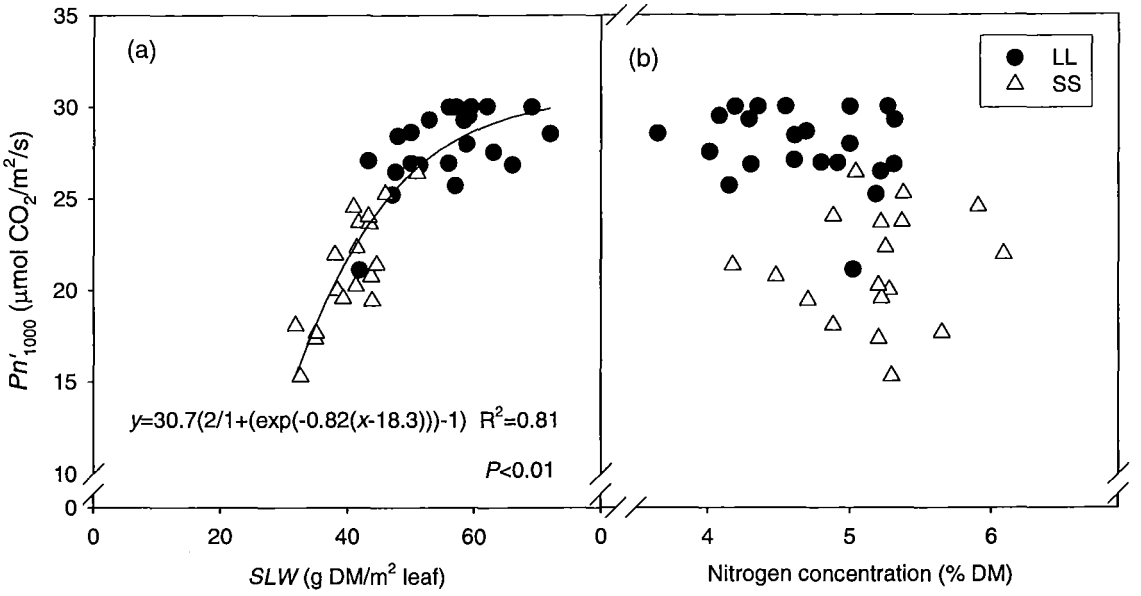

Figure 7.11 Relationship between normalized leaf photosynthesis at 1000 µmol photons/m^2/s (Pn'_{1000}) and (*a*) specific leaf weight (*SLW*) and (*b*) leaf nitrogen concentration (% of DM).

Note: Data-points represent average of 3-4 leaves per replicate.

The Pn'_{1000} values in LL crops were on average higher than in SS crops at similar levels of $N\%_{leaf}$ (Figure 7.11 *b*). For example, at $N\%_{leaf}$ of 5.0% DM, LL crops had an average Pn'_{1000} of 27 µmol photons/m^2/s in comparison with 21 µmol photons/m^2/s for SS crops. This was probably an effect of higher *SLW* of LL crops at any $N\%_{leaf}$ in comparison with SS crops.

7.3.6 Nitrogen status of LL and SS crops

Nitrogen concentration of shoots ($N\%_{shoot}$) and its components (leaf and stem) differed throughout the year (Appendix 6) but differences were mostly explained by DM_{shoot} (Figure 7.12 *a*). $N\%_{shoot}$ declined ($P<0.01$) from ~5.0-6.0% at minimal shoot yields to ~3% at DM_{shoot}>6 t/ha. This pattern of decline was compared with a model of critical nitrogen level ($N\%_{crit}$) for lucerne shoots (Section 7.2.8). All data-points of LL crops were close or above the $N\%_{crit}$ model. This indicated that these crops were non N-stressed as demonstrated by the nitrogen nutrition index ($N\%_{act}$ /$N\%_{crit}$, *NNI*) > 1.0 in LL crops at any given shoot yield (Figure 7.12 *b*). In contrast at DM_{shoot}<1t/ha, SS crops displayed a group

of data-points below the $N\%_{crit}$ line (Figure 7.12 *a*) which consequently led to a $NNI < 1.0$ that indicates N deficiency (Figure 7.12 *b*).

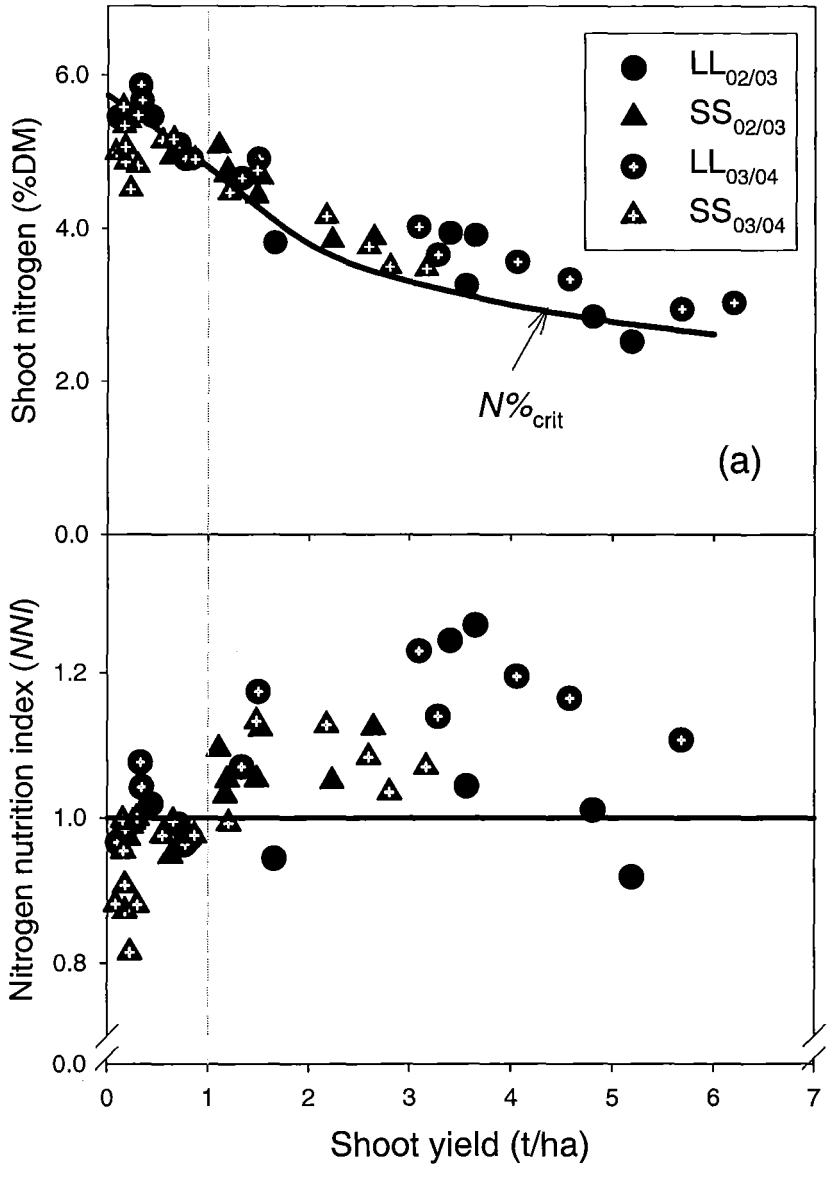

Figure 7.12 Relationship between (*a*) nitrogen content of shoots ($N\%_{act}$) and (*b*) nitrogen nutrition index (*NNI*, $N\%_{act}/N\%_{crit}$) with shoot yield of lucerne crops subjected to four contrasting defoliation regimes in the 2002/03 and 2003/04 growth seasons at Lincoln University, Canterbury, New Zealand.

Note: Critical nitrogen ($N\%_{crit}$) of shoots was calculated after Lemaire *et al.*(1985) for $DM_{shoot} > 1$ t/ha and derived from LL data for $DM_{shoot} < 1$ t/ha (Section 7.2.8).

Throughout the vegetative development, characterized by the number of expanded primary leaves, *NNI* in LL crops was similar ($P<0.13$) and above 1.0 regardless of the number of expanded leaves (Figure 7.13). LL crops displayed a greater occurrence of $NNI \geq 1.0$

throughout the whole range of development stages (2 to 13 expanded primary leaves) than SS crops. In contrast, *NNI* of SS crops tended to increase (R^2=0.32, P<0.01) at later developmental stages. This was characterized by *NNI* values <1.0 (sub-optimal N nutrition) mainly before the expansion of the 7th primary leaf. From the 7th to the 10th leaf *NNI* in SS crops was always greater than 1.0 but did not reach the same levels of LL crops (~1.2).

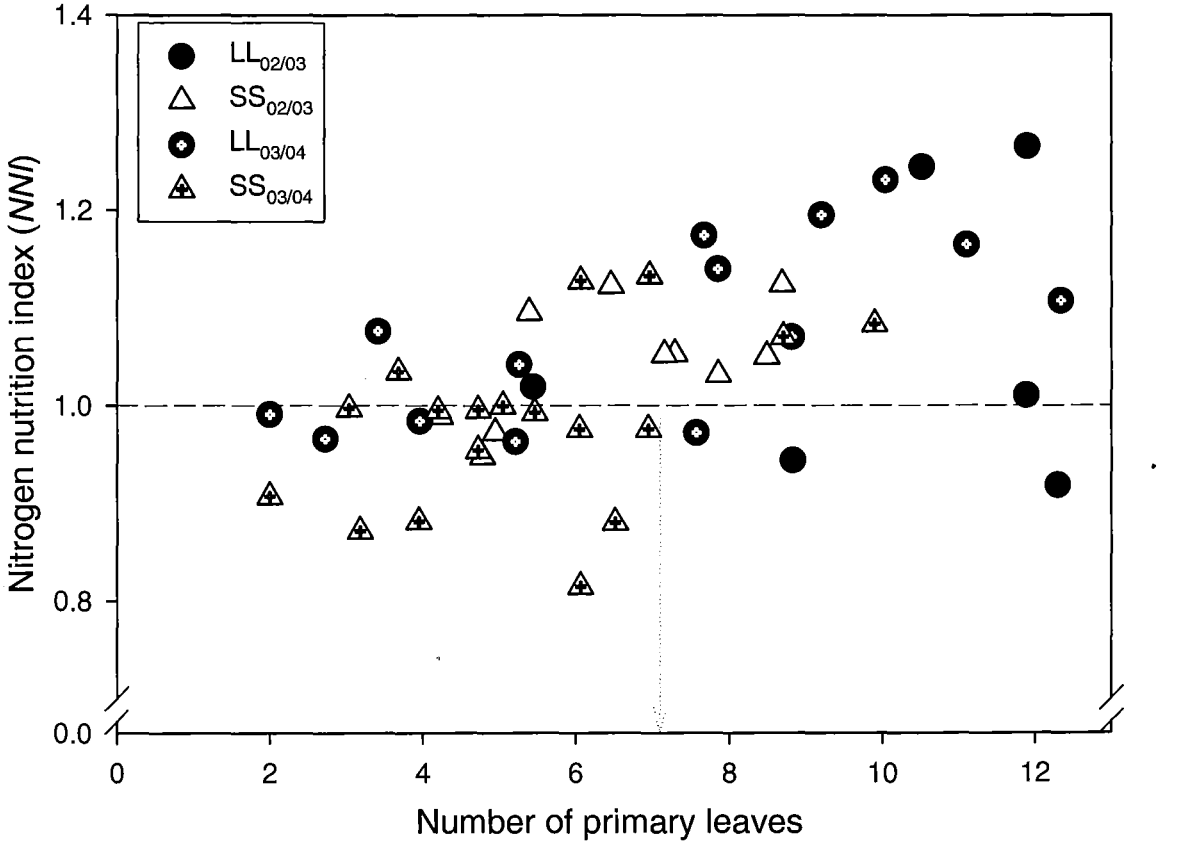

Figure 7.13 Relationship between nitrogen nutrition index (*NNI*) or the number of primary leaves of lucerne crops subjected to four contrasting defoliation regimes on the 2002/03 and 2003/04 growth seasons at Lincoln University, Canterbury, New Zealand.

Note: Data from cycles when LL and SS crops grew simultaneously and number of primary leaves was > 7.0 (Section 7.2.8). Dotted arrow indicates leaf position 7.

7.4 Discussion

7.4.1 *RUE* for shoot dry matter

Spring-summer RUE_{shoot} of LL crops was within the range of 1.5 to 1.8 g DM/MJ PAR_i (Figure 7.3). In autumn RUE_{shoot} declined in all treatments to ~1.0-1.2 g DM/MJ PAR_i. This seasonal decline in RUE_{shoot} has been previously shown for the temperate climates of France (Khaiti and Lemaire, 1992) and Canterbury, New Zealand (Brown, 2004). The reduction in RUE_{shoot} in autumn was previously attributed to an increasing allocation of photoassimilates to lucerne roots in response to environmental signals (Gosse *et al.*, 1983; Khaiti and Lemaire, 1992). The "seasonal pattern" of autumn decline in RUE_{shoot} was similar among defoliation treatments although crops had very contrasting levels of perennial reserves (Section 4.3.2) and consequently different source-sink balances. A similar partitioning regardless of the level of reserves apparently goes against the Münch hypothesis (Bancal and Soltani, 2002) which assumes that the osmotic potential, created by the concentration of C and N substrate in sources and sinks, is the main driving force for partitioning. However the concentration of soluble sugars was conservative in lucerne taproots regardless of defoliation management (Section 4.3.3). Sucrose concentrations are particularly important in defining the osmotic potential of plant cells (Farrar and Jones, 2000). This plasticity of lucerne crops in maintaining sucrose concentration in taproots may have buffered the potential for large changes in the C flow between shoots and roots, consequently maintaining the seasonal pattern of RUE_{shoot} in all treatments.

The most important differences in RUE_{shoot} among treatments occurred during summer, when RUE_{shoot} of LL and LS crops were ~13% higher than in SL and SS crops. This may be caused by the lower amounts of perennial reserves in SL and SS crops, particularly nitrogen reserves (Section 4.3.5). Avice *et al.* (1997a) showed that low levels of nitrogen in lucerne roots were associated with a decline of 22% in RUE_{shoot} of 'Europe' lucerne. The authors inferred that an initial period of nitrogen deficiency in 'Europe' was the cause of reduced RUE_{shoot} due to changes in DM partitioning between roots and shoots, with no mention about possible changes in the crop photosynthetic capacity. RUE_{shoot} is sensitive to any factor that affects the shoot carbon balance such as photosynthesis, respiration and DM partitioning (Section 2.5). In this sense, a lower summer RUE_{shoot} in SS crops could have

been caused either by a decrease in C fixation (*i.e.* lower leaf *Pn*) or in the sink capacity (*i.e.* increased partitioning of DM to perennial organs).

7.4.2 *RUE* for total dry matter

In LL crops RUE_{total} was on average 2.2 g DM/MJ PAR_i (Figure 7.4) which is consistent with the 2.3 g DM/MJ PAR_i observed in France (Durand *et al.*, 1989; Khaiti and Lemaire, 1992). These authors however have not assumed or observed changes in *RUE* with temperature. In contrast Brown (2004), working with 'Kaituna' lucerne in Canterbury, observed a maximum RUE_{total} of 3.2 g DM/MJ PAR_i in summer (~18°C) and a decline in RUE_{total} with temperature at a rate of 0.18 g DM/MJ PAR_i/°C. This temperature framework was compared with estimates of RUE_{total} (Figure 7.4). In the LL crop, the positive slope ($P<0.11$, $R^2=0.30$) and the low *RMSD* (0.4 g DM/MJ PAR_i) suggested a temperature effect on RUE_{total} (Figure 7.4 *a*). The justification for the use of a temperature response for RUE_{total} in temperate climates relies on the fact that lucerne net photosynthesis responds to temperature in a bell-shaped pattern (Murata and Honma, 1968) and that *RUE* and photosynthesis are strongly related (Sinclair and Horie, 1989). Therefore the temperature framework was further used to estimate RUE_{total} for each regrowth cycle in the p_{per} calculations. The values of *RMSD* for RUE_{total} increased to 0.7 g DM/MJ PAR_i in LS and ~0.9 g DM/MJ PAR_i in SL and SS crops (Figure 7.4 *c, d*). This increase in the *RMSD* showed that the relationship between RUE_{total} and T_{mean} was altered in treatments with lower perennial reserves than LL crops. Specifically, four regrowth cycles of SS crops had RUE_{total} values at ~50% of those predicted. As discussed for RUE_{shoot} (Section 7.4.1), a limited supply of nitrogen from perennial reserves to shoots could explain the reduction in RUE_{total} through a reduction in photosynthetic capacity.

7.4.3 Leaf photosynthesis rate

The photosynthetic capacity during the summer-autumn period, measured as leaf P_{max}, was 39 μmol $CO_2/m^2/s$ in LL crops but only 33 μmol $CO_2/m^2/s$ in SS crops (Table 7.1). This difference was consistent with the trends in RUE_{total} (Figure 7.4). When leaf Pn_{1000} was analysed within regrowth cycles, the Pn_{1000} was also ~20% lower in SS crops but only in the earlier stages of regrowth ($\sum Tt_{b5}<150$°Cd). This recovery of photosynthetic capacity could be explained by the diminishing dependency of shoots on nitrogen reserves as crop

growth progresses (Louahlia *et al.*, 1998). In the early stages of regrowth, the proportion of nitrogen from endogenous sources, recovered in shoots, is nearly 100% (Kim *et al.*, 1991). This figure has been shown to decrease to less than 30% after four weeks of regrowth, when mineral uptake accounts for the remaining 70% (Kim *et al.*, 1991). Therefore a limited supply of endogenous nitrogen to growing shoots could explain this low photosynthetic capacity in the early periods of regrowth. Nitrogen is preferably allocated to the synthesis of structural protein and thus affects cell division and development (Lawlor *et al.*, 2001). At the plant level, the mechanisms responsible for the trade off between leaf expansion (leaf area) and leaf composition (*e.g. SLN*) seemed to prioritize leaf expansion in the first 150°Cd. Assuming that carbon is the most limiting resource after complete defoliation, maximizing photosynthetic area at the expense of photosynthetic efficiency (*i.e.* leaf *Pn*) seems a logical adaptative strategy of lucerne. This rationale would be in accordance with the idea of a functional equilibrium between shoot and roots (Lemaire and Millard, 1999).

This initial period of low leaf photosynthetic capacity represented proportionally more of a short cycle crop (*e.g.* SS crop) than a long cycle one (*e.g.* LL crop). Assuming an average phyllochron of 34°Cd (Section 6.3.8), a $\sum Tt_{b5}$ of 150°Cd corresponds to the expansion of ~5 primary leaves. These first 5 primary leaves were those that appeared incapable of changing their individual area despite the contrasting defoliation treatments (Section 6.4.4). Thus, it seems that for both LL and SS crops these first 5 leaves were expanded to their potential leaf area, maximizing light capture. However in SS crops these leaves had a lower photosynthetic potential, which would consequently lead to a lower RUE_{total} during this period. Additionally, as the crop grows, a larger proportion of the nitrogen is directed to the upper part of the canopy (Lemaire and Gastal, 1997) at the expense of lower shaded leaves, creating an exponential gradient of nitrogen concentration though the canopy profile (Lemaire *et al.*, 1991). This, together with an increasing N uptake, would guarantee a recovery of photosynthetic capacity of leaves expanded later in the regrowth cycle (*i.e.* above the 5th main-stem node).

The nitrogen status of LL and SS crops was assessed by the nitrogen nutrition index (*NNI*). SS crops had a higher frequency of data-points at $NNI<1.0$ (N limited), mainly concentrated in the early stages of regrowth ($DM_{shoot}<1$t/ha or ~6th leaf stage). These results reinforce the idea of sub-optimal supply of nitrogen to shoots in the early stage of regrowth. This limited supply of N is also consistent with the 20% lower chlorophyll

content (Chl_{a+b}) found in leaves of SS crops in comparison with LL crops (Figure 7.9). Okubo *et al.*(1975) has shown a highly significant correlation between lucerne of saturated leaf *Pn* and the levels of Chl_a under field conditions. Chlorophyll-protein complexes account for about 20% of the total nitrogen of C_3 plants and influence light absorption, energy transfer and electron transfer in the photosynthesis process (Lawlor, 2001). This is consistent with the linear increase of Pn_{1000} to the observed range of leaf Chl_{a+b} at 0.04 μmol photons/m^2/s for each additional 1.0 mg/m^2 Chl_{a+b} (Figure 7.9). The maximum concentrations of Chl_{a+b} measured in this experiment (~450 mg/m^2) were in agreement with values found by Evans (1993) in the top leaves of lucerne canopies.

The effect of limited N supply in reducing photosynthesis rates can be caused by changes in the chemical and anatomical traits of lucerne leaves (Section 2.5.1.3). Specific leaf nitrogen (*SLN*) explained 68% of the differences in normalized Pn_{1000} (Figure 7.10). The response of *Pn* to *SLN* followed a typical saturation curve as proposed by Sinclair and Horie (1989) with a projected null Pn'_{1000} at 0.77 g/m^2. In fact, if the values of *SLN* for LL crops are analysed alone, there seems to be no systematic change in photosynthesis until a *SLN* of ~2.2 g/m^2 when Pn'_{1000} was ~25 to 30 μmol CO_2/m^2/s. The *SLN* is the product of changes in the metabolic (*i.e.* leaf nitrogen content, $N\%_{leaf}$) and structural (*i.e.* specific leaf weight, *SLW*) components of leaves (Reich *et al.*, 1998). While $N\%_{leaf}$ ranged from 4 to 6% DM, without any systematic effect on leaf Pn'_{1000}, *SLW* ranged from 35 to 70 g/m^2 and explained 81% of the variation of leaf Pn'_{1000} (Figure 7.11). The strong positive relationship between lucerne photosynthetic capacity and *SLW* was also observed by Pearse *et al.* (1969a) who found an increase of 2.5 fold in P_{max} as *SLW* increased from 19 to 53 g/m^2. Similarly, Okubo *et al.* (1975) measured an increase in saturated leaf *Pn* from ~6 μmol CO_2/m^2/s at an *SLW* of 20 g/m^2 to 25 μmol CO_2/m^2/s at an *SLW* of 55 g/m^2. The structural components of lucerne leaves have a marked plasticity to adjust *SLW* (Hodgkinson, 1974). Evans (1993) showed that more than 40% of the decline observed in *SLW* within the canopy profile can be attributed to anatomical changes in lucerne leaves, such as the reduction of palisade mesophyll cell layers.

The low photosynthetic rates observed in the leaves of SS crops could therefore be mainly attributed to a reduction in the thickness of these leaves (*i.e.* lower *SLW*). Although photosynthesis was shown to respond positively to $N\%_{leaf}$ in several crops (Evans, 1989; Lawlor *et al.*, 2001) there was no clear effect from the observed range $N\%_{leaf}$. This lack of response of *Pn* to $N\%_{leaf}$ was possibly because the reduction in leaf area and thickness in

SS crops maintained $N\%_{leaf}$ within an optimum range for photosynthesis. The occurrence of nitrogen deficiency during the very early stages of regrowth, when cell division in the shoot meristematic tissues was taking place, would limit the number of cells in the shoot primordia leading to low *SLW* later in growth. A sufficient flux of N substrate is needed in the very early stages of cell division in leaves due to DNA replication and protein synthesis (Lemaire and Millard, 1999). Leaves formed in a N limiting environment would be expected then to have fewer cell layers and consequently have lower demand for nitrogen to achieve similar levels of $N\%_{leaf}$ in relation to unstressed leaves.

7.4.4 Partitioning of DM from shoots to perennial organs

Fractional partitioning of DM to perennial organs (p_{per}) was calculated using the relationship between measured RUE_{shoot} and calculated RUE_{total} using the temperature framework (Section 2.5.1.4). The largest differences between RUE_{shoot} and RUE_{total} occurred during mid-summer (Figure 7.5). This was consistent with the observation that perennial DM (DM_{per}) accumulation resumed in late-December (Section 4.3.2). During this period of the year the flux of C substrate to perennial organs was sufficient to promote growth and offset the increasing costs of root maintenance respiration. Assuming a Q_{10} of 2.0 for root R_m at 20°C for a vegetative crop (Hay and Walker, 1989a; Lawlor *et al.*, 2001) and an index value of 1.0 for R_m during winter (T_{mean}=7.5°C in Canterbury); R_m would be expected to increase to 1.2 in autumn (T_{mean}=10°C), 1.4 in spring (T_{mean}=12°C), and 1.8 in summer (T_{mean}=16°C). Therefore the largest absolute fluxes of dry matter to roots probably occurred in mid-summer instead of autumn as commonly suggested in current literature (Section 2.6).

Literature also often suggests p_{per} as changing from about 0.20 in spring-summer to an autumn value of ~0.50 (Section 2.6). In the present experiment the observed change in p_{per} was not abrupt, but occurred gradually (Figure 7.6) which indicates a systematic response to seasonal environmental stimuli. In fact, a major proportion of DM was allocated to roots from late December on, when absolute carbon assimilation was high due to fast canopy expansion, high photosynthetic rates and PPFD levels above 1000 μmol photons/m^2/s. This pattern agrees with the "shared control" hypothesis of C transport to roots (Farrar and Jones, 2000) where the C flux is "pushed" by substrate availability (*e.g.* high photosynthesis rates) and simultaneously "pulled" by sink demand (*e.g.* low level of

soluble sugars in roots in summer). Obviously, more complex underling mechanisms may be involved in these processes such as gene activation by substrate concentration or environmental signals, and phloem transport resistances. These processes are however poorly quantified to become part of mechanistic models able to explain partitioning of dry matter to roots (Farrar and Jones, 2000). In autumn, although p_{per} remained high at ~0.40 (Figure 7.6), lower absolute quantities of DM were allocated to perennial organs as total DM accumulation rates declined. This shows that in this experiment, the mid-summer period (February-March) was a key period for accumulation of DM in perennial organs.

Temperature and photoperiod were previously suggested to be the triggers for nitrogen and carbon partitioning patterns in lucerne (Section 2.6). In early-spring p_{per} was less than 0.15 but it increased to a maximum of 0.50 in mid-summer being strongly related to increasing photoperiod (Figure 7.6). Similarly, Morot Gaudry *et al.* (1987) measured marked carbon (^{14}C) allocation to lucerne roots to be 20% in spring but increase to 50% in autumn. From mid-summer to autumn, when *Pp* decreases, p_{per} showed a non significant decline with *Pp* to be ~0.35-0.40 in late autumn.

Lucerne plants grown at longer photoperiods, as in summer, were shown to develop greater shoot/root ratios than at short photoperiod (Noquet *et al.*, 2003). These authors measured an increase in shoot/root ratio from 1.8 at *Pp* of 8 h to 3.8 at *Pp* of 16 h in controlled conditions. The hypothesis behind *Pp* controlling p_{per} is that genes that control shoot and root morphogenesis respond to photoperiod. Organ initiation, differentiation and expansion then imposes a demand (sink strength) for assimilates which balances with C and N supply and defines the direction and rate of flow of assimilates in the plant (Lemaire and Millard, 1999; Woolley *et al.*, 2001). Low photoperiods have been shown to increase the partitioning of N to lucerne taproots, with accumulation of specific N pools (Noquet *et al.*, 2001; Noquet *et al.*, 2003). Other authors however observed no systematic effect of *Pp* on the partitioning of DM between shoots and roots of lucerne (Philippot *et al.*, 1991; Singh, 1974). In asparagus low photoperiods only partially explained the seasonal DM partitioning between shoots and roots and an interaction with low temperatures was suggested as a possible explanation (Woolley *et al.*, 2001).

The use of T_{soil}/T_{air} as an alternative predictor of p_{per} eliminated the hysteresis that was evident in the relationship between *Pp* and p_{per}, but demonstrated that other factors were involved because the maximum R^2 obtained was only 0.55 (Figure 7.7). The use of T_{soil}/T_{air}

assumes that the flow of DM from shoots to roots is in direct proportion to the temperature of each organ and consequently to their metabolic activity. Possibly a single ratio T_{soil}/T_{air} with a base temperature of 0°C is a rather simplified way of deriving the relationship with p_{per}. Indeed, shoot activity (*e.g.* photosynthesis) and root activity (*e.g.* nitrogen uptake and fixation) are known to respond differently to temperature (Lemaire and Millard, 1999). Nevertheless, a direct effect of temperature of meristematic tissues was shown to control partitioning of DM between shoots and roots in wheat and maize (Engels, 1994). Hargreaves (2003), after reanalyzing data from Khaiti and Lemaire (1992), suggested that temperature of shoots and roots could explain most of the partitioning patterns of lucerne. Singh (1974) measured an increase in the flow of ^{14}C to lucerne roots as day/night temperatures decreased from 30/25°C to 20/15°C in a controlled environment. Similarly, Noquet *et al.*(2001) observed an increase in the partitioning of nitrogen to roots as day/night temperatures decreased from 20/18°C to 5/5°C. Both authors however have not tested the differential temperature between shoots and roots as a driving variable for partitioning.

The high correlation between Pp and T_{soil}/T_{air} in temperate climates (Figure 7.8) makes it difficult to isolate the effects on p_{per} in field experiments. The potential for an interaction between temperature and Pp suggests the need for experiments in controlled environments.

Defoliation treatments apparently affected p_{per} only in SS crops which had lower p_{per} than the other treatments (Figure 7.6 and Figure 7.7). This level of response was not accurately quantified as it depends on the assumption about the extent of decline in RUE_{total} for SS crops (Appendix 4). Even assuming that calculated p_{per} for SS crops was lower than LL crops could be misleading because p_{per} may be always low in early stages of regrowth. In short cycled crops, this period can be overweighed in partitioning calculations. This problem brings the issue of the pattern of DM partitioning to roots "within cycles". It is intuitive to expect that the relative flux of DM to perennial organs increases throughout each regrowth cycle, regardless of seasonal patterns of partitioning. This would decrease the cycle averaged values of p_{per} in SS crops compared with crops with 42-day regrowth cycles, as an artefact of the regrowth lengths. Despite this, SS crops also had an apparent "seasonal pattern" of p_{per}, suggesting that the crop was still sensitive to the same seasonal signals that control partitioning, regardless of the level of reserves in perennial organs. This would agree with Engels (1994) who observed that temperature controlled

partitioning between shoots and roots despite the concentration of nitrogen or carbohydrates in roots of wheat and maize.

7.5 Conclusions

- In general, RUE_{shoot} displayed a seasonal pattern with the highest values in spring-summer (1.5-2.0 g DM/MJ PAR_i) and the lowest in autumn (1.0-1.2 g DM/MJ PAR_i).

- Treatments with higher levels of perennial reserves in mid-summer (LL and LS crops) had 20% greater RUE_{shoot} than SL and SS crops during this period.

- An apparent decline of 30% in RUE_{total} in SS crops in relation to LL crops was observed in four regrowth cycles.

- A decline of ~20% in the photosynthetic capacity (P_{max}) of the first 5 primary leaves (<150°Cd) of SS crops in relation to LL crops was consistent with low RUE_{total}.

- Differences in leaf photosynthesis rates were largely explained by the N status of crops. These were consistent with declines in chlorophyll content and *SLN*. Differences in *SLN* were mostly explained by changes in *SLW* with a non significant effect on leaf *N%*.

- The effect of defoliation treatments on DM partitioning to perennial organs (p_{per}) was unclear due to the difficulties in estimating perennial DM patterns within regrowth cycles. Nevertheless, all treatments were sensitive to seasonal signals and p_{per} increased from <10% in early-spring to a maximum of ~50% in mid-summer/autumn. These changes could be empirically related to *Pp* and the ratio of T_{soil}/T_{air}.

8 Simulation of lucerne growth and development

8.1 Introduction

The response of 'Kaituna' lucerne to environmental factors, derived from the previous results chapters (Chapters 4 to 7), can be integrated into a simple computer simulation model. This procedure allows the evaluation of the consistency of such relationships, by measuring the ability of the model to simulate crop growth, development and the underlying physiological processes.

One of the major challenges in constructing simulation models for perennial crops is to capture the seasonal changes of physiological processes in response to the environment (Section 2.7). Specifically, during the spring and autumn regrowth of lucerne, there are changes in the rate of canopy expansion (Section 6.3.5) and DM partitioning to roots (Section 7.3.3). These have not been sufficiently quantified to be included in the structure of previous models.

The model construction used in this chapter was based on empirical summary relationships (*e.g.* *RUE* and allometric partitioning coefficients) derived in the main from previous results chapters. The initial objective is to simulate seasonal crop growth and development of a 'Kaituna' lucerne crop in Canterbury, under non-limiting environmental (water and nutrients) and endogenous (root reserves) conditions (*e.g.* LL crop). Therefore the main drivers of crop growth and development are temperature, intercepted radiation and photoperiod. Secondly, for the parameters that were not assessed in the field experiment (*e.g.* root respiration rates), the model is used as a hypothesis testing tool to derive the most suitable coefficients from the literature to fit measured data. Finally, the model simulations are compared with measured data from crops with limited levels of reserves (LS, SL and SS) to quantify the effect of perennial reserves *per se* on yield.

8.2 Materials and Methods

The lucerne model was used to accomplish four specific objectives. Initially, the model was used to define the most suitable methods to (*i*) calculate daily thermal-time, (*ii*) define the predictor of the fractional partitioning of DM to roots and (*iii*) establish the moment of application of maintenance respiration on *DM_root*. The data used for this purpose were the original set from the field experiment; the same used to derive the proposed relationships (Section 8.2.1). Secondly, the model simulations were tested against observed data from the original and also from independent data-sets (Brown, 2004) to check the consistency of the assumptions. Thirdly, the model was used to test new hypotheses with regard to parameters or variables that were not assessed in the field experiment (*e.g.* root maintenance respiration rates). Finally, the model simulations of shoot yield were compared with those measured from crops at suboptimal levels of perennial reserves. The difference between predicted and observed values was assumed to quantify the effect of the level of reserves *per se* on shoot yield.

8.2.1 Model description

The model was constructed using the software ModelMaker version 4.0 (Cherwell Scientific Publishing, Ltd, UK) and runs in daily time-steps by assessing weather data from a text file. Weather data were obtained from Broadfields Meteorological Station (Section 3.4.1). Data are organized in the text file columns as: *t* (time, independent); *Rain* (mm/day); *Tmax*, *Tmin* and *Tmean* (°C, maximum, minimum and mean daily temperatures respectively), *Radn* (daily total solar radiation, MJ/m^2), *Ph* (photoperiod, h), *Ph_dir* (photoperiod direction of change) and *Tsoil* (°C, soil temperature at 100 mm depth). Photoperiod was calculated for the Iversen 9 site (43°38'S and 172°28'E) and added to the weather file as a daily input. At this stage the model assumes water is a non-limiting resource, therefore the variable *Rain* is not computed in the model calculations.

8.2.2 Model structure as in ModelMaker

Figure 8.1 shows the graphic representation of the lucerne model as displayed in the "Main view" of ModelMaker. Some of the variables were duplicated to test different frameworks. For example, node accumulation is calculated by a simple daily *Tt* sum (*Node_acc_simple_Tt*) and alternatively by the use of the methodology proposed by Jones *et al.* (1986) for the calculation of daily *Tt* (*Node_acc*, Section 8.2.3.2).

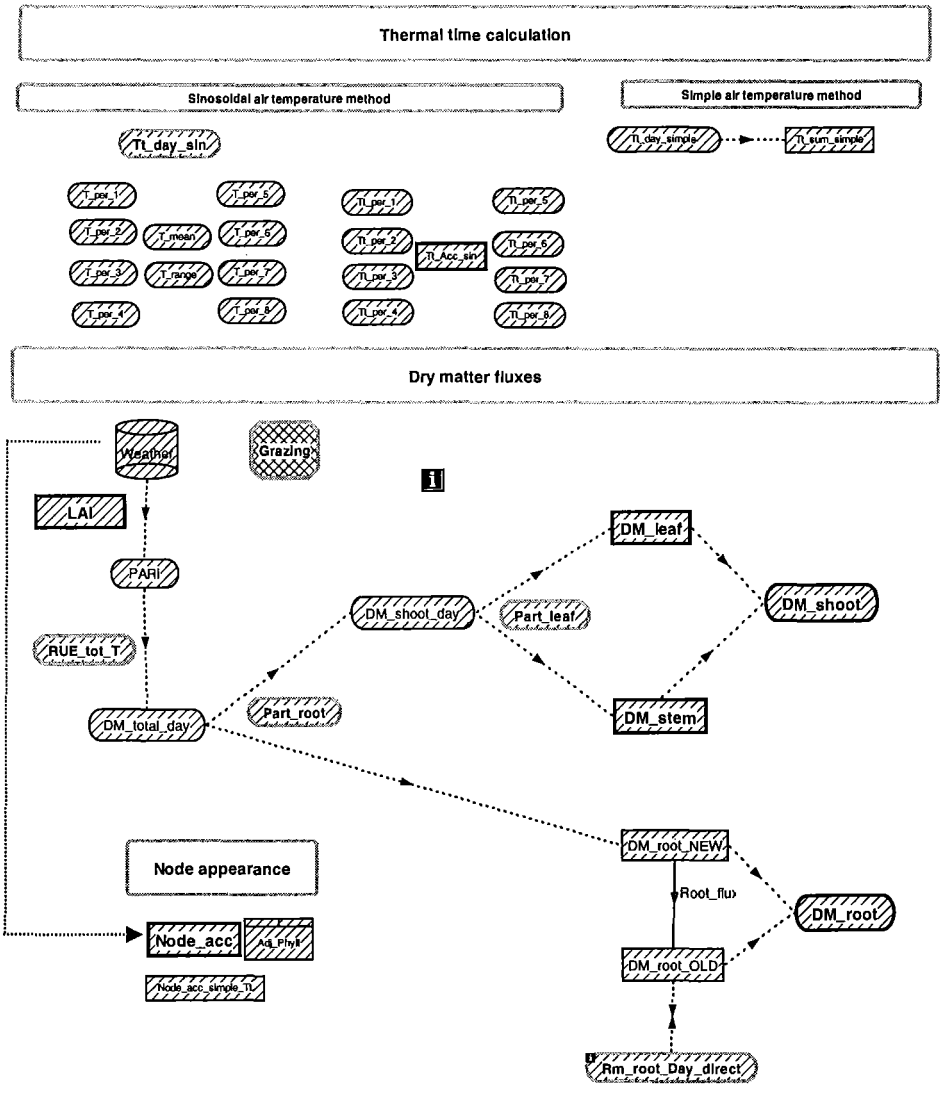

Figure 8.1 Basic structure of the lucerne model as displayed in the "Main view" of ModelMaker.

Note: Symbols and acronyms are refereed to in the text (Section 8.2.2).

The crop DM was divided in three components (*i.e.* model state variables): leaves (*DM_leaf*), stems (*DM_stem*) and roots (*DM_root*), all expressed in g DM/m^2 soil. *DM_root* was assumed to include all perennial dry matter (*i.e.* taproots and crowns, Section 4.2.1). Shoot dry matter is calculated by the sum of *DM_leaf* and *DM_stem*. *DM_root* is calculated as the sum of "new" assimilated dry matter which was partitioned to roots during each current regrowth cycle (*DM_root_new*) and the "old" root dry matter from the previous cycles (*DM_root_old*).

Each day, dry matter assimilation is calculated as the intercepted amount of PAR (*PARi*, MJ PAR/m^2) multiplied by the total *RUE* adjusted for temperature (*RUE_tot_T*, g DM/MJ PAR_i) as described in Section 8.2.4.1. This new daily assimilated dry matter (*DM_total_day*, g/m^2/day) is partitioned to shoots (*DM_shoot_day*, g DM/m^2/day) or integrated in the new root dry matter (*DM_root_new*, g/m^2). The partitioning of *DM_total_day* between shoots and roots is controlled by the fractional coefficient of partitioning to roots (*Part_root*, dimentionless) that ranges from 0 to 1. Two methodologies were tested to derive *Part_root*: (*i*) firstly as a function of photoperiod and (*ii*) alternatively as a function of the relationship between soil and air temperature (Section 8.2.5.1). *DM_shoot_day* is integrated in *DM_leaf* or *DM_stem*, according to the partitioning coefficient to leaves (*Part_leaf*, dimmentionless). *Part_leaf* declines exponentially with *DM_shoot* as a function of the allometric growth of these organs (Section 8.2.5.2).

Two methods were tested to discount the maintenance respiration from *DM_root*. In the first the new daily dry matter partitioned to perennial organs (*DM_root_new*) is not subjected to respiration. In this case root respiratory losses (*Rm_root*, g DM/m^2/day) are only subtracted from the root dry matter from previous regrowth cycles (*DM_root_old*) (Section 8.2.5.1). This approach assumes that, within a regrowth cycle, *RUE_tot_T* already accounts for the maintenance respiration of the DM partitioned to roots. At the start of each regrowth cycle (*i.e.* t=0) the *DM_root_new* from the previous regrowth cycle is added to *DM_root_old* and therefore at t=0, *DM_root_new* = 0. In the second method, *DM_root_new* is subjected to maintenance respiration from the time it is assimilated, simultaneously to *DM_root_old*.

8.2.2.1 Model parameters and variables

Weather (Table 8.1) and management data (*e.g.* grazing dates) are organized on a daily basis as a function of the independent variable "time" (*t*).

Table 8.1 Weather data inputs for the simulation model for lucerne crops defoliated at regrowth cycles of 42 days at Lincoln University, Canterbury, New Zealand.

Acronym	Definition	Units
Radn	Total solar radiation	$MJ/m^2/day$
Tmax	Daily maximum air temperature	°C
Tmin	Daily minimum air temperature	°C
Tmean	Daily mean air temperature	°C
Tsoil	Daily mean soil temperature at 100 mm depth	°C
Pp	Photoperiod	Hours
Pp_dir	Photoperiod direction (>0 for *IPp*, and <0 for *DPp*)	dimensionless

Note: *IPp* and *DPp* are the increasing and decreasing photoperiods respectively.

The lucerne model variables are displayed in Table 8.2.

Table 8.2 Variables for the simulation model for lucerne crops defoliated at regrowth cycles of 42 days at Lincoln University, Canterbury, New Zealand.

Acronym	Definition	Units
State variables		
DM_leaf	Accumulated leaf dry matter	$g\ DM/m^2$
DM_stem	Accumulated stem dry matter	$g\ DM/m^2$
DM_shoot	Accumulated shoot dry matter	$g\ DM/m^2$
DM_root	Accumulated root dry matter	$g\ DM/m^2$
LAI	Leaf area index	$m^2\ leaf/m^2\ ground$
Node_acc[(1)]	Accumulated number of main-stem nodes	nodes/main-stem
Other variables		
Rm_root	Daily maintenance respiration of roots	$g\ DM/m^2/day$
Part_leaf	Fractional partitioning of DM to leaves	dimensionless
Part_root[(1)]	Fractional partitioning of DM to roots	dimensionless

Note: [(1)] Different methods were tested to derive these variables.

The parameters of the lucerne model are displayed in Table 8.3.

Table 8.3 Parameters for the simulation model for lucerne crops defoliated at regrowth cycles of 42 days at Lincoln University, Canterbury, New Zealand.

Acronym	Definition	Value	Source
RUE_tot_opt	Total radiation use efficiency	3.2 g DM/MJ PAR	Brown (2004)
k_PAR	Extinction coefficient for PAR	0.81	Section 6.3.2
LAER_opt	Optimum leaf area expansion rate	0.016 $m^2/m^2/°Cd$	Section 6.3.5.1
PAR/R_o	Fraction of PAR in total solar radiation	0.50	(Szeicz, 1974)
Rm_root_rate	Maintenance respiration coefficient for root DM	0.015 DM/day[1]	Durand *et al.*(1991) Atkin *et al.*(2000)
Q_{10}*_Rm*	Q_{10} for maintenance respiration of root DM	1.8	Atkin *et al.*(2000)
Tref_Rm	Reference temperature for maintenance respiration rate of root DM	20°C	Atkin *et al.*(2000)
T^n_{mean}	Cardinal temperatures for *Tt* calculation	0, 5, 30, 40°C	Fick *et al.*(1988) ; Section 2.4.1.1
Tt_n	Tt_n accumulation for cardinal T^n_{mean}	0, 0, 25, 0°Cd	Fick *et al.*(1988); Section 2.4.1.1

Note: [1] *Rm_root_rate* was further calibrated to the best fit with original data-set of *DM_root*.

Conceptually, the model structure can be segmented into three major physiological processes: (*i*) PAR interception (*LAI* expansion), (*ii*) total DM accumulation (*RUE* and root respiration) and (*iii*) DM partitioning among leaves, stems and roots. Each of these processes is described in detail in the following sections.

8.2.3 Simulation of PAR interception

The interception of PAR is calculated by assuming an exponential decay of transmitted PAR through the canopy with *LAI* increments in accordance with Beer's law (Section 2.3). A single extinction coefficient for diffuse PAR (*k_PAR*) of 0.81 was used for 'Kaituna' lucerne (Section 6.3.2), which was assumed to integrate the changes of *k* within each day (Equation 8.1).

Equation 8.1

$$PAR_i / PAR_o = 1 - \exp(-0.81 \times LAI)$$

8.2.3.1 Simulation of LAI expansion

The *LAI* was calculated by assuming an optimum leaf area expansion rate (*LAEROpt*) of 0.016 $m^2/m^2/°Cd$ as a simplification of the relationships shown in Figure 6.7. This parameter is adjusted as a function of photoperiod by a linear decline of 0.0064 $m^2/m^2/°Cd/h$ for *Pp* below 12.5 h (Section 6.3.5.1), until zero at *Pp* of 10 h (Figure 8.2).

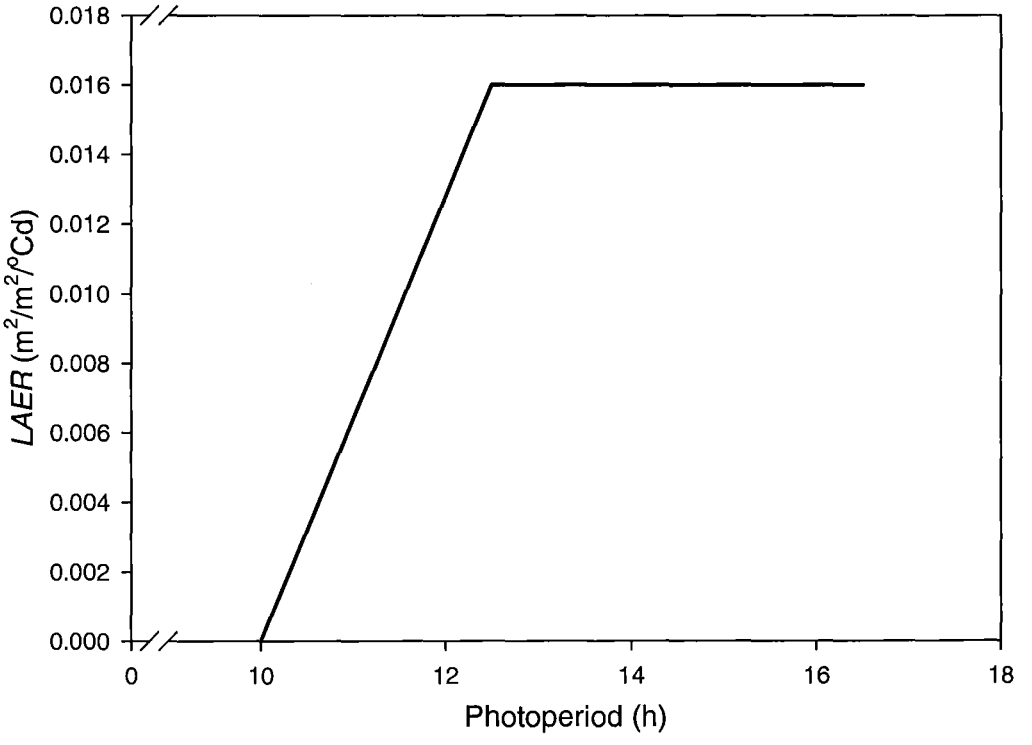

Figure 8.2 Leaf area expansion rate (*LAER*, $m^2/m^2/°Cd$) function in relation to photoperiod for the calculation of *LAI* expansion for 'Kaituna' lucerne at Lincoln University, Canterbury, New Zealand.

Leaf senescence was not included in the model because the crops from where relationships were derived never reached significant senescence in the maximum cycle of 42 days (Section 5.3.3). To account for a ceiling canopy cover, *LAI* expansion was held constant at a maximum value of 6.0.

8.2.3.2 Thermal-time calculation

Thermal-time is calculated as a function of mean air temperature (*Tmean*) using the framework suggested by Fick *et al.* (1988) (Figure 8.3) in which the base temperature (T_b) of 5°C was validated for 'Kaituna' (Section 6.2.4.1).

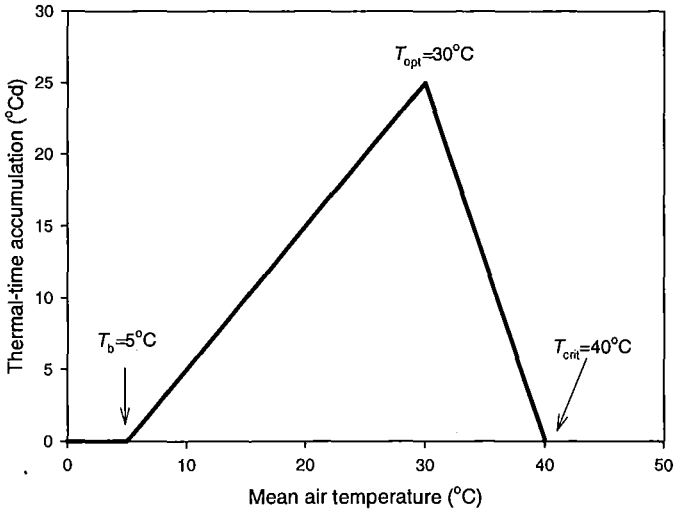

Figure 8.3 Temperature thresholds used for calculation of thermal-time of 'Kaituna' lucerne crops at Lincoln University, Canterbury, New Zealand.

Two approaches were tested to compute daily thermal-time: (*i*) using a simple daily *Tmean* directly from the weather file; or (*ii*) using calculated temperature for each of eight 3-hour intervals daily. The latter framework accounts for the sinusoidal diurnal fluctuation of temperature and was calculated by the method suggested by Jones *et al.* (1986). This is done through the use of a dummy variable, calculated by a 3rd order polynomial equation (first component of Equation 8.2), which segments the 24 h of the day in 8 periods of 3 h (Figure 8.4). An estimated value of temperature ($T^n_{diurnal}$) was then calculated for each period "*n*" using Equation 8.2.

Equation 8.2

$$T^n_{diurnal} = [(0.931 + 0.114 \times n - 0.0703 \times n^2 + 0.0053 \times n^3) \times (T_{max} - T_{min})] + T_{min}$$

Where n represents the n^{th} 3 h period of a day (1 to 8), $T^{n}_{diurnal}$ is the mean temperature for the period n of the day, and *Tmax* and *Tmin* are the maximum and minimum temperature of the day. In the model structure (Figure 8.1) these variables are denominated *T_per_1, T_per_2,...,* and *T_per_8.*

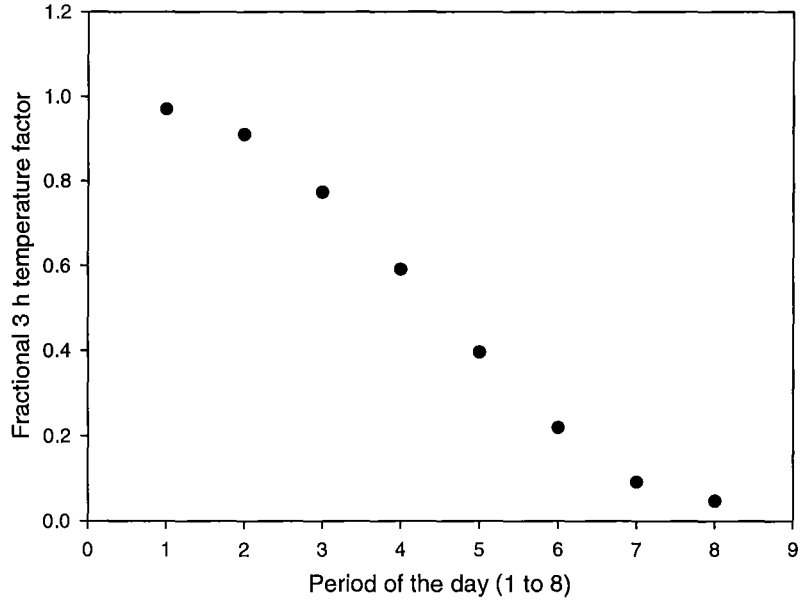

Figure 8.4 Sinusoidal pattern of daily air temperature used to calculate mean temperature fluctuation for thermal-time calculation.

Note: The relationship was based on Equation 8.2 after Jones *et al.* (1986).

The daily thermal-time accumulation is then calculated by averaging *Tt* estimates for each one of the 8 periods using the relationship between *Tt* and $T^{n}_{diurnal}$ (Figure 8.3). This procedure aimed to improve the accuracy of *Tt* calculation by compensating for the diurnal fluctuation of temperature and consequently avoiding underestimation of *Tt* during cold periods of the year by setting $Tt=0$ for intervals where $T^{n}_{diurnal}<T_b$.

8.2.3.3 Node appearance

Node appearance rate is calculated based on a phyllochron (*Phyl*) value of 34°Cd/node (*Tb*=5°C) at photoperiod (*Pp*)≥12.5 h, adjusted for an increase of 4°Cd/h from *Pp*<12.5 h until a maximum of 40°Cd at *Pp* of 10.5 h (Equation 8.3).

Equation 8.3

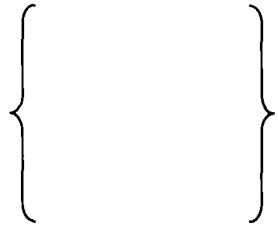

Node accumulation (Equation 8.4) is calculated as the sum of daily node appearance. Daily accumulated thermal-time using sinusoidal *Tmean* calculation (*Tt_day_sin*) is divided by the phyllochron adjusted for photoperiod (*Phyl*).

Equation 8.4

$$Node\_acc = \sum (Tt\_day\_\sin / Phyl)$$

Alternatively, node accumulation using a simple *Tt* calculation (*Node_acc_simple_Tt*) was used for comparison to define the most appropriate *Tt* calculation method.

8.2.4 Simulation of total dry matter accumulation

8.2.4.1 Daily total dry matter accumulation

Daily total dry matter accumulation is calculated as the product of *PARi* and *RUE_tot_T*. Daily *RUE_tot_T* is calculated by assuming an optimum RUE_{total} of 3.2 g DM/MJ PAR_i at T_{mean}>18°C (Section 2.5.1.4) which declines by 0.18 g/MJ/°C from 18°C to 0°C (Equation 8.5).

Equation 8.5

$$RUE\_tot\_T = RUE\_tot\_opt \times (Tmean / 18^{\circ}C)$$

8.2.4.2 Root respiration

The growth component of respiration of shoots and roots was assumed to be integrally accounted for in the value of total *RUE* (*RUE_total_T*). In this sense, only maintenance respiration of root dry matter (*Rm_root*) was considered further.

Root maintenance respiration (*Rm_root_day*, g DM/m^2/day) is applied exclusively onto *DM_root* at a rate of 1.5% DM/day (*i.e. Rm_root_rate* = 0.015) at a reference soil temperature (*Tref_soil_Rm*, 100 mm depth) of 20°C (Equation 8.6). The values of these two parameters were assumed based on suggested values in the literature (Durand *et al.*, 1991; Ziska and Bunce, 1994) and further adjusted to a best fit with measured data using ModelMaker sensitivity analysis run (Figure 8.15). As soil temperature fluctuates, *Rm_root_rate* is adjusted by a Q_{10} of 2.0 (Atkin *et al.*, 2000; Tjoelker *et al.*, 2001).

Equation 8.6

$$Rm\_root\_day = [Rm\_root\_rate \times Q_{10}^{(\frac{T_{soil}-T_{ref}}{10})}] \times DM_{root}$$

Two methods were tested in relation to the timing of application of maintenance respiration on *DM_root*. In method (*i*) *Rm_root_day* was discounted only from the *DM_root_old* and therefore *DM_root_new* was without respiration. This rationale assumes that for the time course of one regrowth cycle *RUE_tot_T* accounts for the respiration losses of the "recently" accumulated DM. In method (*ii*) *Rm_root_day* is applied on *DM_root* immediately after DM assimilation, consequently assuming the maintenance respiration of perennial organs is not implicit in the value of *RUE_tot_T*. Both approaches were compared and the one with the lowest *RMSD* (Section 8.2.7) incorporated in the final model structure.

8.2.5 Simulation of dry matter partitioning

8.2.5.1 Partitioning between shoots and roots

Two hypothetical approaches were tested to drive DM partitioning to perennial organs (*i.e.* "roots" in the model nomenclature). In method (*i*) dry matter partitioning between shoots and roots is described as a function photoperiod and its direction (Equation 8.7 *a* and *b*) based on Section 7.3.3.

Equation 8.7

(a) For increasing photoperiod:

$$\left\{ \qquad \right\}$$

(b) For decreasing photoperiod:

$$\left\{ \qquad \right\}$$

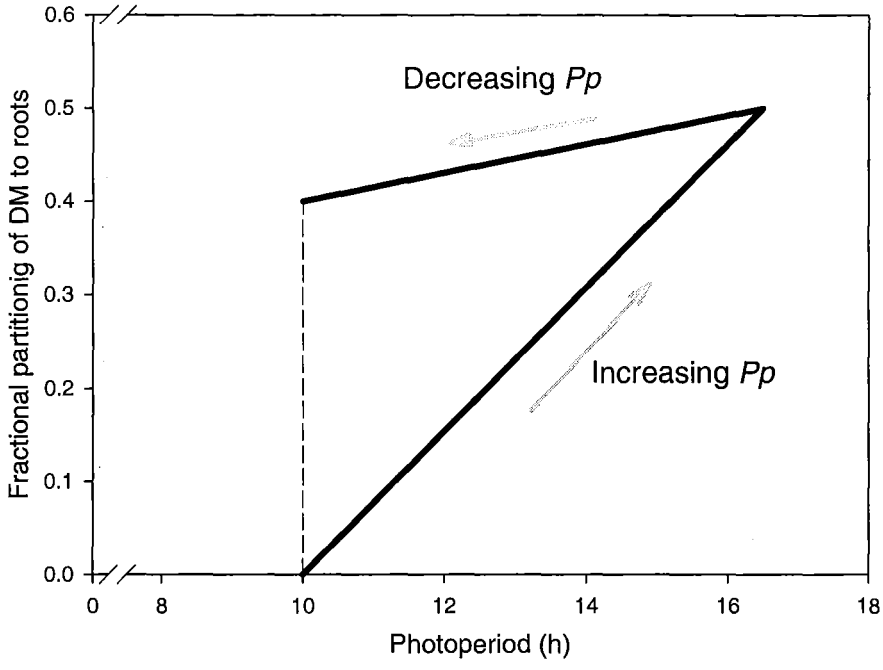

Figure 8.5 Relationship between the fraction of dry matter partitioned to roots and *Pp* incorporated in the simulation model for 'Kaituna' lucerne grown at Lincoln University, Canterbury, New Zealand.

Alternatively, in method (*ii*) dry matter partitioning between shoots and roots was described as a function of the ratio between soil and air temperatures (Figure 8.6, Equation 8.8) based on the relationships found for the LL crops (Figure 7.7).

Equation 8.8

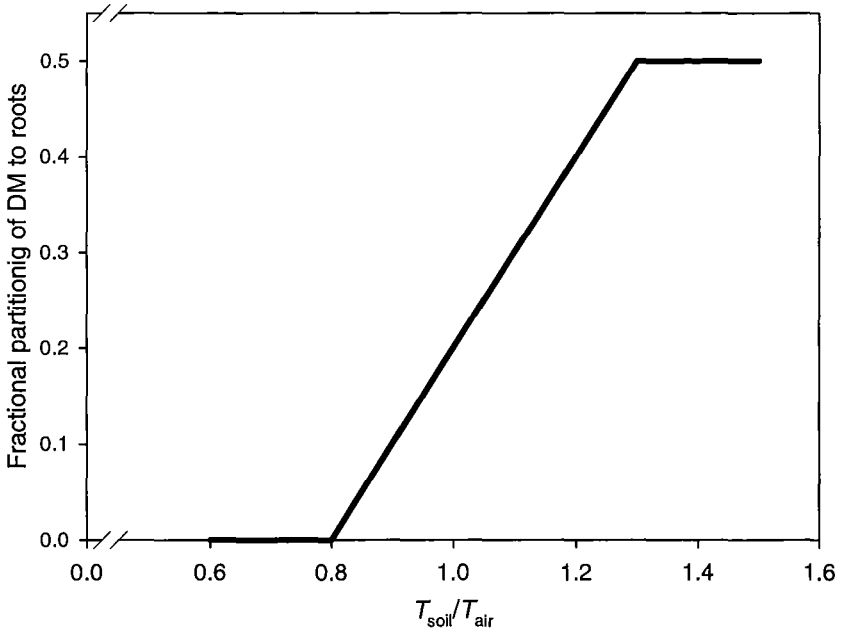

Figure 8.6 Relationship between the fraction of dry matter partitioned to roots and T_{soil}/T_{air} incorporated in the simulation model for 'Kaituna' lucerne grown at Lincoln University, Canterbury, New Zealand.

8.2.5.2 Partitioning of shoot DM between leaves and stems

The fraction of daily assimilated DM (*DM_total_day*) directed to shoots (*DM_shoot_day*) was then partitioned to leaves or stems according to an allometric relationship based on shoot yield (*DM_shoot*) as in Equation 8.9.

Equation 8.9

$$p\_leaf = 0.26 \times \exp(0.67/(DM\_shoot/100) + 0.43)$$

Equation 8.9 assumes an exponential decline in the partitioning of DM as *DM_shoot* increases based on the derived relationships from the field experiment observations (Equation 5.2).

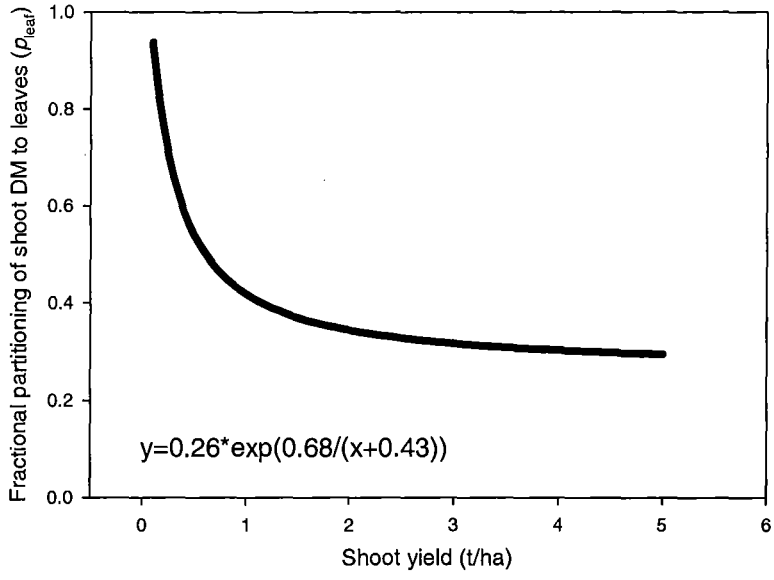

Figure 8.7 Relationship between the fractional partitioning of dry matter to leaves (*p_leaf*) and shoot yield incorporated in the simulation model for 'Kaituna' lucerne grown at Lincoln University, Canterbury, New Zealand.

8.2.6 Resetting of variables at harvest

To simulate sequential harvests the model requires the input of the respective values of the independent variable t when the events occurred. For example, for LL crops the model assumes 1 January 02 as day 1 (t=1) and the first grazing date on 5 October 2002 (t=262). At the start of each cycle, a group of state variables is reset to initial values. The initial value of *DM_leaf* was assumed 0.0030 g/m^2 (*i.e.* 0.03 kg DM/ha) and *DM_stem* as 0.0015 g/m^2. The definition of a negligible initial *DM_shoot*, with a leaf to stem ratio (*LSR*) of 2.0 (the maximum observed *LSR*, Section 5.3.3.1), was necessary to allow the recommencement of the model computations without divisions by zero. Similarly, the *LAI* was set to 0.0001 m^2/m^2 at every new cycle by assuming an average canopy *SLW* of 30 g DM/m^2 leaf (Appendix 3). The number of main-stem nodes (*Node_acc*) was set to 1.0 as this was the y intercept for the measurements on LL crops (Appendix 8). Additionally at each cycle thermal-time accumulation (*Tt_acc_sin*) was set to 0°Cd.

8.2.7 Model evaluation

The simulated and measured values were compared using the root mean squared deviation (*RMSD*) as in Equation 8.10 (Kobayashi and Salam, 2000).

Equation 8.10

$$RMSD = \sqrt{\frac{1}{n}\sum_{i=1}^{n}(m_i - s_i)^2}$$

Where n is the number of measurements, m_i is the measured value for observation i and s_i is the simulated value for observation i.

The *MSD* (*i.e.* $RMSD^2$) values were further segmented in their components (Equation 8.11) to quantify the causes of deviation of the model (Dolling *et al.*, 2005; Gauch *et al.*, 2003).

Equation 8.11

$$MSD = SB + NU + LC$$

Where *SB* is the standard bias or the squared difference between the means of simulated and measured values (Equation 8.12), *NU* is the non-unit slope (Equation 8.13) and *LC* is the lack of correlation (Equation 8.14).

Equation 8.12

$$SB = (\bar{m} - \bar{s})^2$$

Where $\bar{m}$ and $\bar{s}$ are the average of all measured (m) and simulated (s) values respectively.

Equation 8.13

$$NU = (1-b)^2 \times (\sum (s - \bar{s})^2 / n)$$

Where b is the slope of the least-squared regression between measured (y axes) and simulated values (x axes).

Equation 8.14

$$LC = (1 - R^2) \times (\sum (m - \bar{m})^2 / n)$$

Where R^2 is the coefficient of determination calculated from the linear relationship between measured and simulated values.

Measured and simulated values were plotted and the significance of the intercept (a) and linear slope (b) were assessed by testing the null hypothesis H_0 that a=0 and b=1.

8.3 Results

8.3.1 Simulation of crop development

8.3.1.1 Model improvement for Tt calculation

The accuracy of primary leaf appearance simulations was used as the criteria to define the most suitable calculation for daily thermal-time (Tt_{b5}). The use of Jones *et al.* (1986) method (Section 8.2.3.2) improved the accuracy of the model, predominantly during winter/early-spring (Figure 8.8). At that period, the residual mean squared deviation (*RMSD*) was up to three fold lower using the Jones *et al.* (1986) method than for the simple T_{mean} calculation. For example, in the spring 2003, the *RMSD* was 0.55 primary leaves/shoot when the segmented framework was used, compared with 1.9 primary leaves/shoot for the simple T_{mean} calculation (Figure 8.8). During mid-spring/summer, when temperatures were higher, both methods predicted leaf appearance with similar *RMSD* (Figure 8.8).

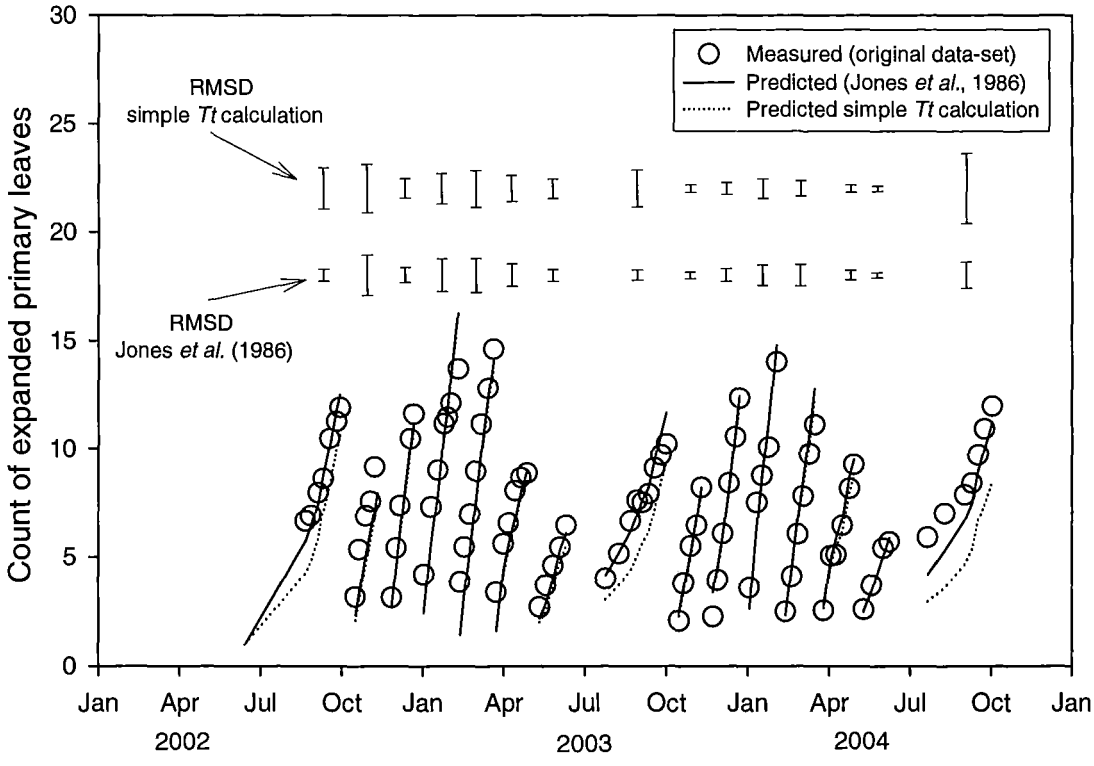

Figure 8.8 Simulation of primary leaf appearance using a simple *Tt* calculation (·····) or the Jones *et al.* (1986) method (——) in comparison with measured data (○) from lucerne crops subjected to a 42-day regrowth cycle in the 2002/03 and 2003/04 growth seasons at Lincoln University, Canterbury, New Zealand.

Note: Bars indicate one residual mean square deviation (*RMSD*) for each regrowth cycle. Details about *Tt* calculation methodologies are given in Section 8.2.2.2.

8.3.1.2 Model testing for the number of primary leaves/shoot

Leaf appearance was simulated with a *RMSD* of 0.9 leaves/shoot (13% mean) for the original data-set and 1.7 leaves/shoot (19% mean) for the independent data-set (Table 8.4). In both data-sets there was a slight rotation of the fit between simulated and measured data (20%<*NU*<46% *MSD*) with consequent significant slope and intercept (Table 8.4).

Table 8.4 Statistics for the comparison of simulated and measured count of primary leaves of lucerne crops grown at Lincoln University, Canterbury, New Zealand.

	Original data-set	Brown (2004) data-set
RMSD	0.9	1.7
RMSD (% mean)	13	19
SB (% *MSD*)	2	3
NU (% *MSD*)	20	46
LC (% *MSD*)	77	50
Intercept	1.1*	2.7*
Slope	0.9*	0.7*
R^2	0.92	0.86

Note: (ns) Non-significant; (*) Indicates intercept different from zero or slope different from unit at a level of significance (α) of 0.05.

In mid-spring/summer (Oct-Mar) there was agreement between simulated and measured data (Figure 8.9). The higher *RMSD* for the independent data-set (Table 8.4) was mainly caused by underestimations in the autumn of 2002 (Apr-Jul) cycles (Figure 8.9) when there was a high number of main-stem nodes at the beginning of the regrowth period.

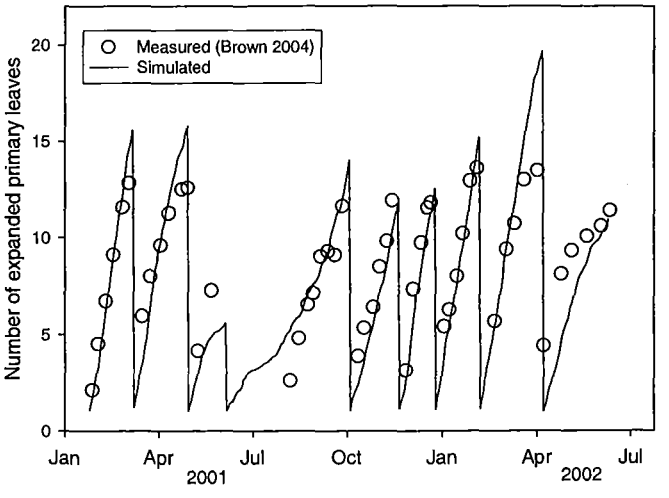

Figure 8.9 Comparison of measured and simulated number of expanded primary leaves (independent data-set) of lucerne crops grown at Lincoln University, Canterbury, New Zealand.

8.3.2 Simulation of leaf area expansion

Leaf area index was simulated with a *RMSD* of 0.6 m^2/m^2 (24% of mean) for the original data-set and 0.8 m^2/m^2 (25% of mean) for the independent data-set (Table 8.5). In both data-sets the slope and intercept of the fit between simulated and measured values were not different from unit and zero respectively (Table 8.5). This was reflected in the high lack of correlation (84%<*LC*<95% *MSD*) indicating a random distribution of bias.

Table 8.5 Statistics for the comparison of simulated and measured leaf area index of lucerne crops grown at Lincoln University, Canterbury, New Zealand.

	Original data-set	Brown (2004) data-set
RMSD	0.6	0.8
RMSD (% mean)	24	25
SB (% *MSD*)	5	15
NU (% *MSD*)	0	1
LC (% *MSD*)	95	84
Intercept	-0.09_{ns}	0.96_{ns}
Slope	0.99_{ns}	-0.19_{ns}
R^2	0.88	0.81

Note: (ns) Non-significant; (*) Indicates intercept different from unit or slope different from zero at a level of significance (α) of 0.05.

For the independent data-set, most of the simulations of *LAI* less than 3.6 (LAI_{crit}) were close to measured data (Figure 8.10). At later stages of canopy development there were underestimations in the October 2001 cycle and overestimations in the March 2002 cycle when senescence was not captured by the model.

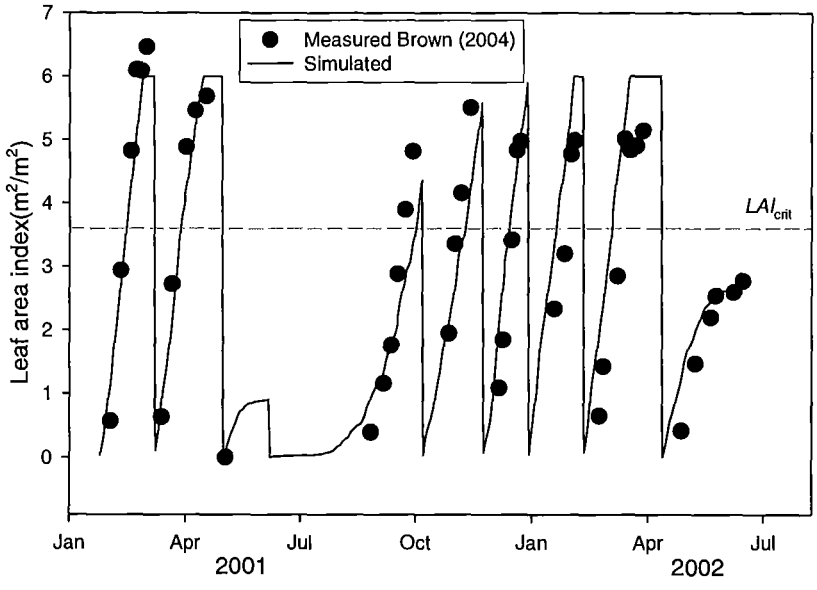

Figure 8.10 Comparison of simulated and measured leaf area index (independent data-set) of lucerne crops grown at Lincoln University, Canterbury, New Zealand.

8.3.3 Simulation of shoot growth

8.3.3.1 Model improvement for the predictor of Part_root

The criteria to define the most suitable method to derive partitioning of DM to roots (*Part_root*) was the minimization of the *RMSD* for shoot yield predictions. Simulations of *DM_shoot* using photoperiod as a driver of partitioning (Figure 8.11, *a*) had a *RMSD* of 0.4 t/ha (25% of mean *DM_shoot*). Simulations were improved by the use of T_{soil}/T_{air} (Figure 8.11, *b*) which decreased the *RSMD* to 0.3 t/ha (20% of mean *DM_shoot*). Additionally, the use of T_{soil}/T_{air} improved the ability of the model to simulate the mean *DM_shoot* as the *SB* component of *MSD* decreased from 24% with the *Pp* method to only 2% of the *MSD* when T_{soil}/T_{air} was used. With the use of T_{soil}/T_{air} the greatest component of *MSD* was the *LC* (96% *MSD*) which indicates that the bias was not systematic (Figure 8.11 *b*). In contrast there was a ~10% underestimation (b=1.1, P<0.01) when *Pp* was used to derive partitioning (Figure 8.11 *a*).

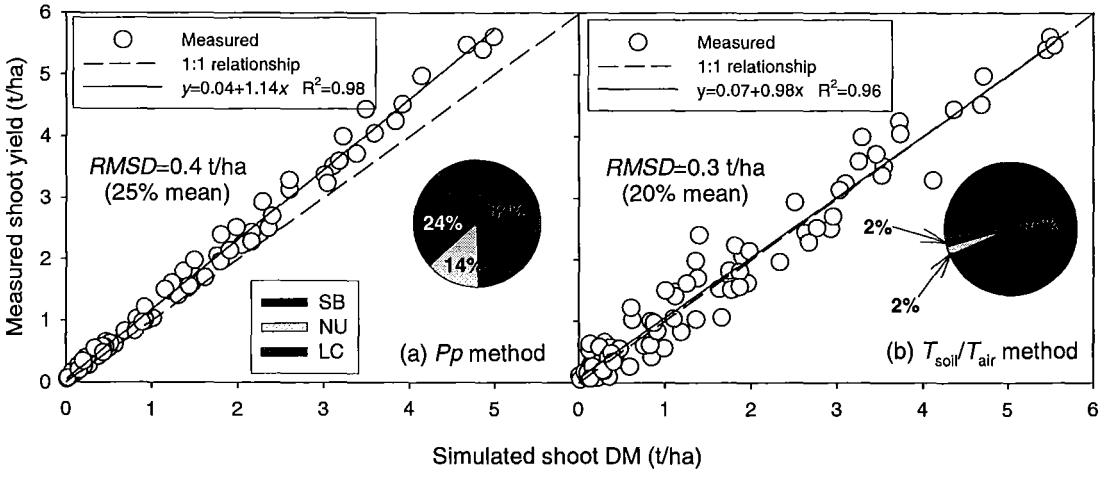

Figure 8.11 Simulated and measured values of shoot dry matter for lucerne crops subjected to a 42-day cycle defoliation regime in the 2002/03 and 2003/04 growth seasons at Lincoln University, Canterbury, New Zealand. Simulations were performed with a partitioning coefficient of DM to roots driven by (*a*) photoperiod (*Pp*) or (*b*) the relationship between soil and air temperature (T_{soil}/T_{air}).

Note: Details about methodologies to derive partitioning are described in Section 8.2.5.1. *SB*, *NU* and *LC* are the components of the mean squared deviation (*MSD*, Section 8.2.7). *RMSD* is the root mean squared deviation.

8.3.3.2 Model testing for shoot yield

There was a close agreement between simulations and measured data for shoot yield in the original data-set (Figure 8.12). Shoot yield was simulated with a *RMSD* of 0.3 t/ha (20% of mean) with the original data-set (Figure 8.11 *b*) and 0.6 t DM/ha (31% of the mean) in relation to independent data (Figure 8.13 *b*). Shoot yield was only underestimated for the original data-set during the April 2003 cycle (autumn). Three data-points collected after the onset of canopy senescence (pointing arrows in Figure 8.13 *a*) were not included in the calculations of *RMSD*, as senescence was out of the scope of the model. The test with independent data gave a slight rotation of the fitted regression (*NU*=20% *MSD* and *b*=0.80) but the mean shoot yield was accurately estimated (*SB*=1% *MSD*).

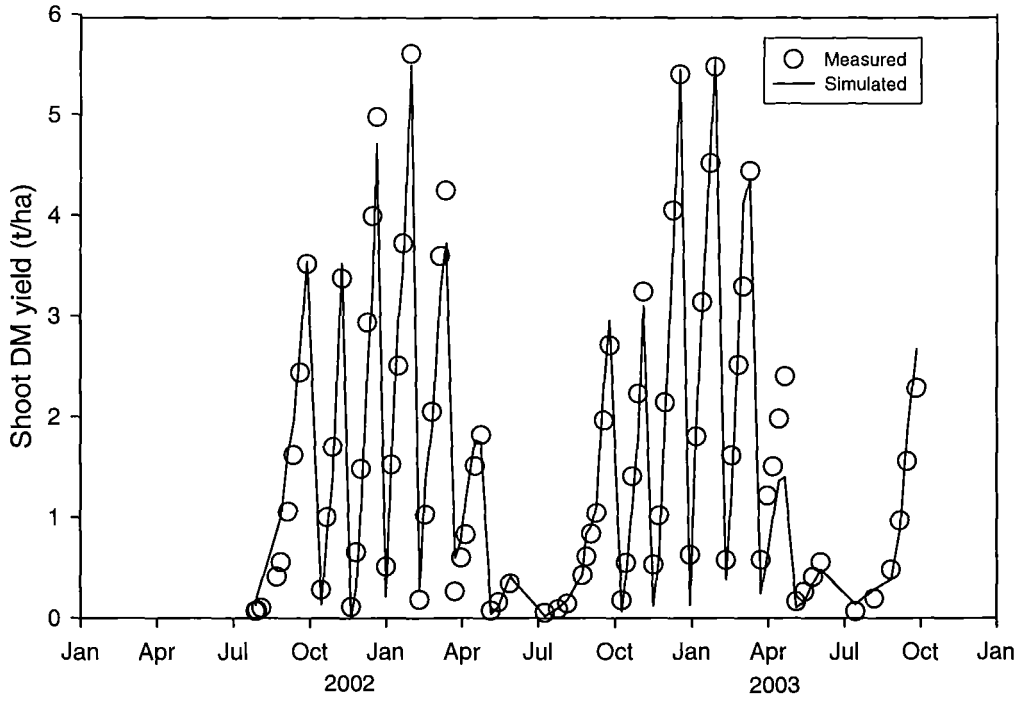

Figure 8.12 Comparison of simulated and measured shoot yield for lucerne crops subjected to a 42-day cycle defoliation regime in the 2002/03 and 2003/04 growth seasons at Lincoln University, Canterbury, New Zealand.

Note: Statistics for the fit are given in Figure 8.11 *b*.

The increase in the *RMSD* for shoot yield when the simulations were compared with the independent data-set were mainly caused by a large underestimation in the April to early-September (autumn/winter) period of 2001 (Figure 8.13 *a*). For the original data-set, the autumn/winter period was usually accurately simulated, with the exception of the April 2003 cycle (Figure 8.12). From October to March (spring/summer) simulations of shoot yield were accurate in both data-sets (Figure 8.12 and Figure 8.13).

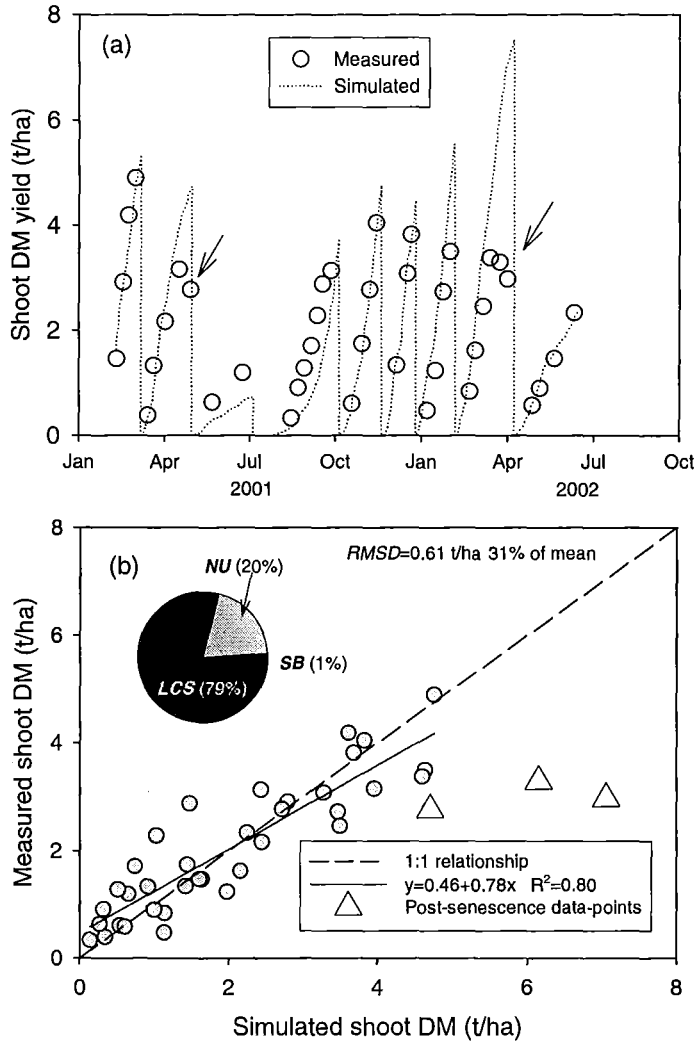

Figure 8.13 Comparison of simulated and measured shoot yield (independent data-set) of lucerne crops grown at Lincoln University, Canterbury, New Zealand.

Note: In Figure 8.13 *a* simulated and measured values are compared. Arrows indicate data-points post-senescence that were not included in the calculation of the *RMSD* value shown in Figure 8.13 *b*. Pie chart represents the percent composition of the mean squared deviation (*MSD*) as detailed in Section 8.2.7.

8.3.4 Simulation of root DM

8.3.4.1 Model improvement for the timing of application of Rm on root DM.

Either the (*i*) application of maintenance respiration (*Rm*) on *DM_root_new* immediately after assimilation (Rm_{direct} method) or (*ii*) after one regrowth cycle (Rm_{delay} method) were tested as the best method to estimate *DM_root*. Both approaches poorly simulated measured values of *DM_root* with a *RMSD* of 1.8 t/ha for Rm_{direct} method (33% mean) and

1.9 t/ha Rm_{delay} method (35% mean). The *NU* was the most significant component of *MSD* in both simulations (52-73% *MSD*) which indicated a large systematic bias in the simulations.

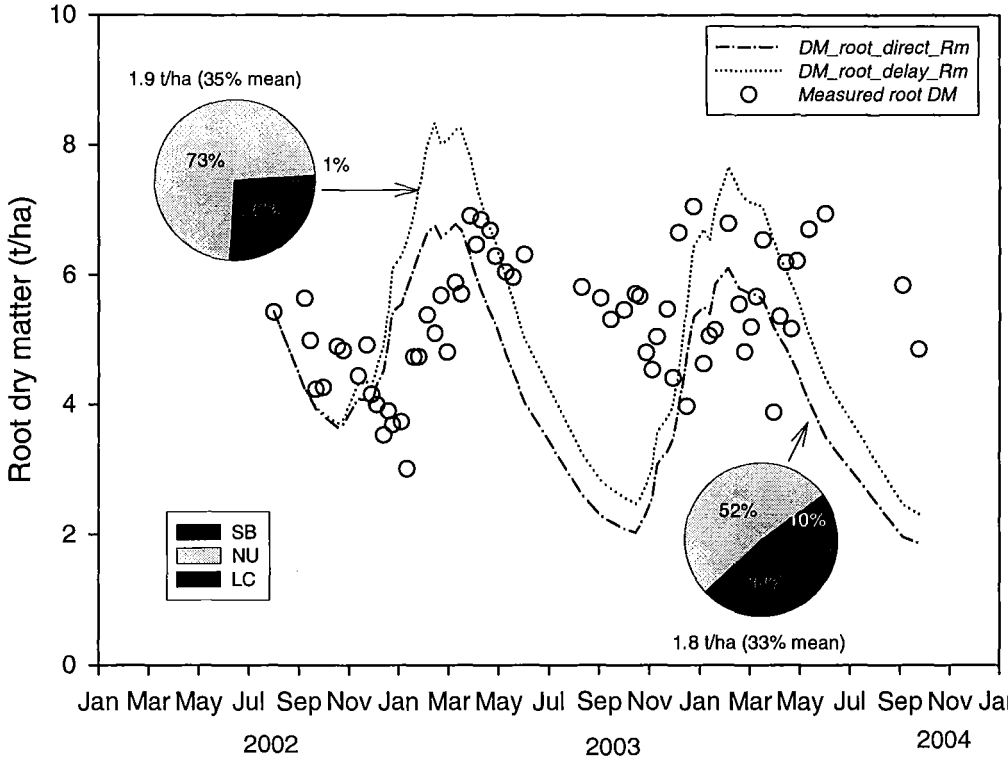

Figure 8.14 Simulated and measured values of root dry matter for lucerne crops subjected to a 42-day cycle defoliation regime in the 2002/03 and 2003/04 growth seasons at Lincoln University, Canterbury, New Zealand.

Note: The model variable root dry matter (*DM_root*) was assumed to represent the measurements of perennial dry matter (Section 4.2.1); estimated as 1.25 x (crown DM plus taproot DM to a 300 mm depth). *SB*, *NU* and *LC* are the three independent additive components of the mean squared deviation (*MSD*) which are shown in the pie charts (Section 8.2.7). *RMSD* is the root mean squared deviation.

A possible cause of large *NU* values was the use of an incorrect maintenance respiration rate. Therefore other maintenance respiration rates were tested using the sensitivity analysis function of ModelMaker v.4.0. There was no improvement in the fit between simulated and measured data with any fixed *Rm_root* ranging from 0.005 to 0.03 DM/day (Figure 8.15).

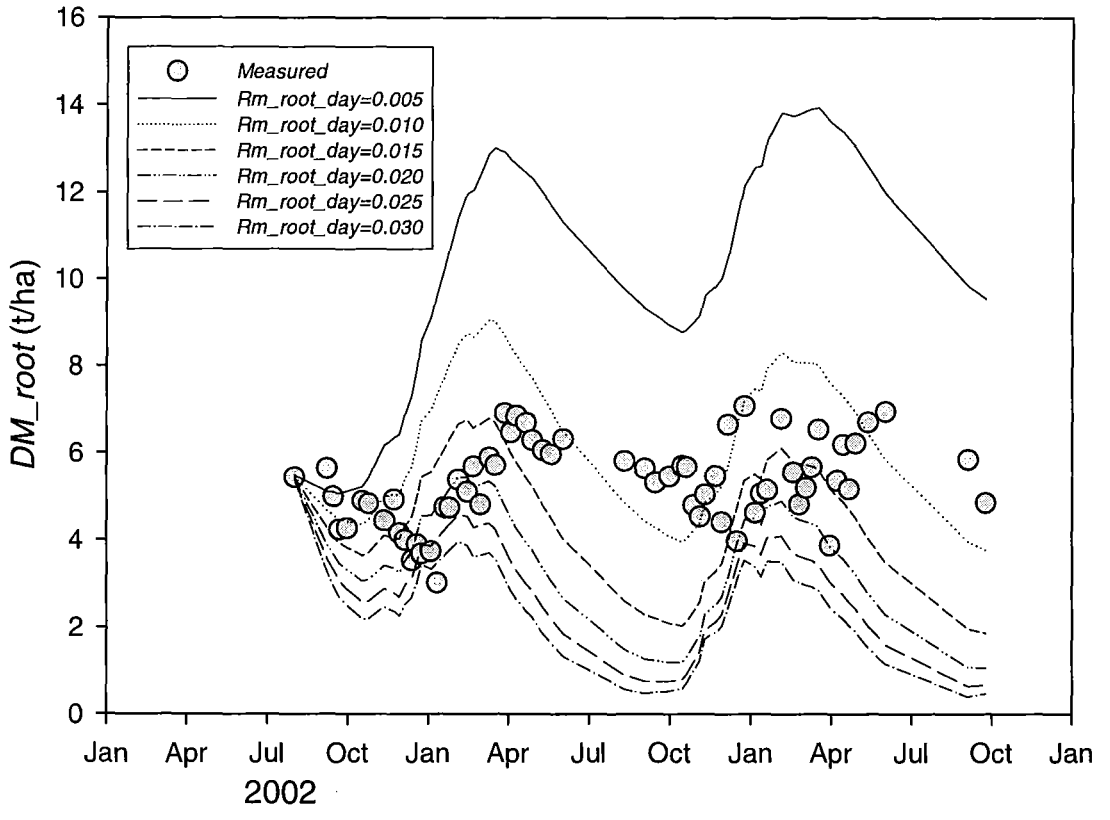

Figure 8.15 Testing of six values of maintenance respiration rates of root DM (0.005-0.030 DM/day) for lucerne crops subjected to a 42-day cycle defoliation regime in the 2002/03 and 2003/04 growth seasons at Lincoln University, Canterbury, New Zealand.

Note: *Rm_root_day* is the fractional daily maintenance respiration rate of root DM. The model variable root dry matter (*DM_root*) was assumed to represent the measurements of perennial dry matter (Section 4.2.1); estimated as 1.25 x (crown DM plus taproot DM to a 300 mm depth).

The overall seasonal pattern of accumulation and depletion of *DM_root* was mimicked by the simulation (Figure 8.14). However in general, the pattern of accumulation and depletion was anticipated by ~90 days. For example, an accumulation of *DM_root* was measured in December but the model simulated this increase from September. There was also an anticipation of the decline in *DM_root* which resumed in late-April but was simulated from late-February.

8.3.4.2 Improving the simulation of root dry matter

To improve the simulation of root dry matter, an alternative hypothesis with regard to root respiration was tested. This assumed that (*i*) root respiration rates fluctuated seasonally in response to differences in the metabolic activity of roots; (*ii*) the Q_{10} for any rate is

constant at 1.8 and; (*iii*) during solstices and equinoxes there was a shift in respiration rates to adjust for a best fit as a broken-stick model (Figure 8.16). These assumptions allowed adjusting of *Rm_root* to the "most probable" respiration rate at the beginning of each season by trial and error, until a close fit was achieved (Figure 8.17).

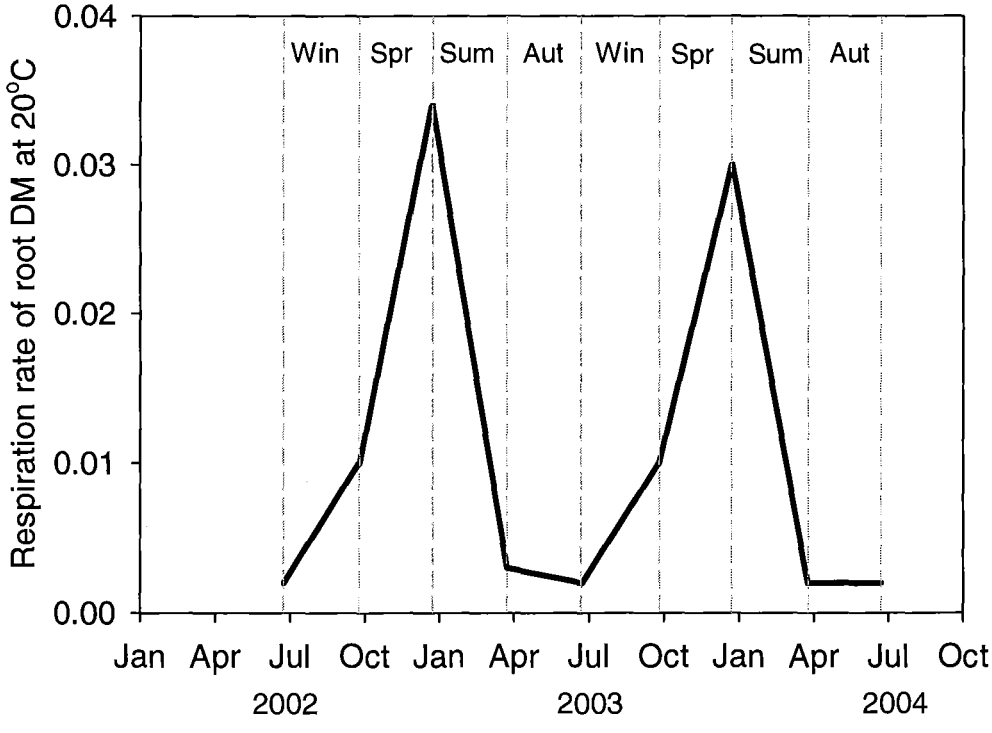

Figure 8.16 Assumed seasonal pattern of respiration rates to adjust root dry matter simulations to create a best fit with measured data of lucerne crops grazed at 42-days regrowth cycles at Lincoln University, Canterbury, New Zealand.

The adjustment of respiration rates with seasons (Figure 8.16) allowed an improvement in the *RMSD* for *DM_root* to 0.7 t/ha (14% mean) and a reduction in the systematic bias of the simulation as *LC* increased from 38% to 85% of the *MSD*.

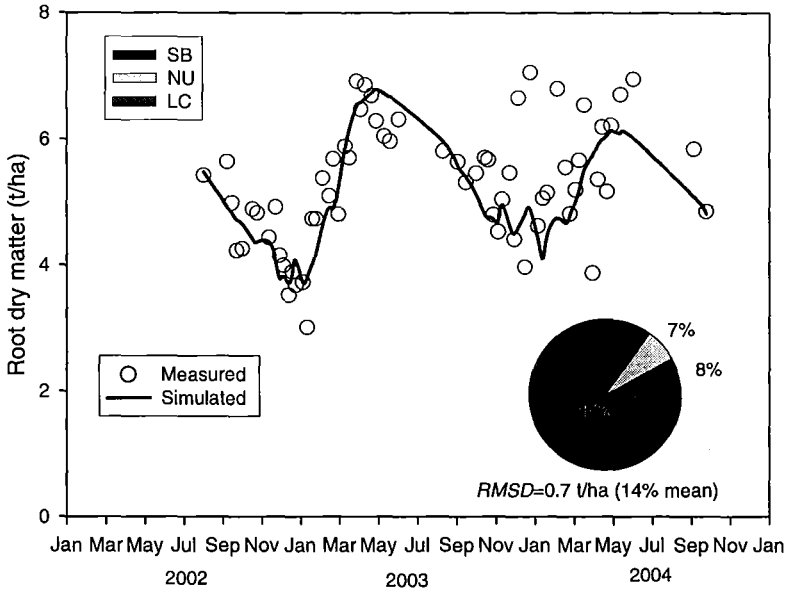

Figure 8.17 Adjusted fit of root dry matter simulation for lucerne crops grazed at 42-days regrowth cycles at Lincoln University, Canterbury, New Zealand.

Note: *SB*, *NU* and *LC* are the three independent additive components of the mean squared deviation (*MSD*) which percent is shown in the pie graphs (Section 8.2.7). *RMSD* is the root mean squared deviation.

8.3.5 Comparing simulations of shoot yield among defoliation treatments

The simulated annual shoot yield for LL crops was 23.4 t DM/ha, similar to the 23.1 t/ha actually measured in the field. The model accurately predicted the yield of a crop with non-limiting levels of perennial reserves (*e.g.* LL crops) and therefore any difference between simulated and measured yield for the other crops (LS, SL and SS) can be assumed as caused by a lack of reserves for growth processes. The remainder of the difference in relation to LL yield can be then assumed as the effect of defoliation *per se* on shoot yield. For example, SS crops yielded 11.1 t/ha less shoot DM than LL crops from which 6.8 t/ha were caused by low levels of perennial reserves and 4.2 t/ha were due to the short regrowth length (*i.e.* harvests before LAI_{crit}). The reduction in shoot yield caused by low levels of reserves was 1.1 t/ha for LS but increased to 5.6 t/ha for SL (Figure 8.18).

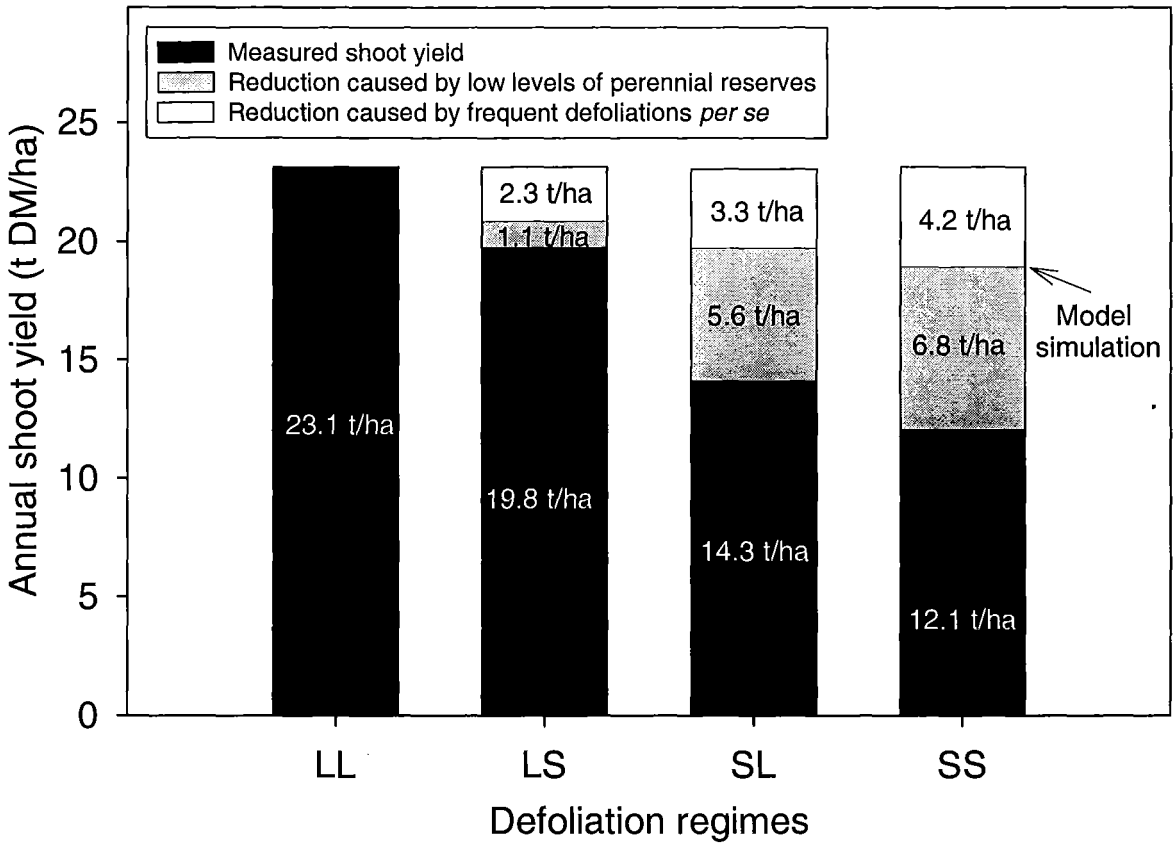

Figure 8.18 Measured and simulated annual shoot yield for lucerne crops subjected to four contrasting defoliation regimes in the 2002/03 and 2003/04 growth seasons at Lincoln University, Canterbury, New Zealand.

Note: Arrow indicates the shoot yield simulated for SS crops (18.9 t/ha) by the lucerne model as a reference.

8.4 Discussion

The objective of this chapter was to describe the construction and test the accuracy of a lucerne simulation model. The relationships derived in the result chapters were successfully integrated in the model which simulated seasonal growth and development of lucerne crops.

8.4.1 Overview

The model structure was adapted from the original framework proposed by Monteith (Monteith, 1977) and applied for lucerne crops by Gosse (Gosse *et al.*, 1984) in which shoot yield is a product of PAR_i and RUE_{shoot} (Section 2.1). The main limitation for the use of this framework in lucerne is the inconsistency of physiological responses (*e.g. LAI* expansion and *RUE*) to the seasonal environment (Section 2.7). To overcome such limitations and predict seasonal yield accurately, the model structure was improved in four main aspects by assuming (*i*) a seasonal rate of leaf expansion based on thermal-time with a T_b of 5°C (Section 8.2.3), (*ii*) *RUE* for total biomass instead of RUE_{shoot} (Section 8.2.4.1), (*iii*) the use of a temperature correction for RUE_{total} (Section 2.5.1.4), and (*iv*) a seasonal partitioning coefficient of DM to roots (Section 8.2.5). The simulations with the adapted model were then used to find the most suitable method (*i*) for thermal-time calculation (Figure 8.8), (*ii*) to derive partitioning of DM to roots (Figure 8.11) and (*iii*) to apply maintenance respiration on root DM (Figure 8.14).

The improved model simulated leaf appearance (Figure 8.9), leaf area index (Figure 8.10) and shoot yield (Figure 8.13) with acceptable accuracy (polled *RMSD* of 22±2% mean; *LC* of 80±7% *MSD*). However, the simulations of root DM were initially poor (*RMSD* of 31% mean, *LC* of only 38% *MSD*; Figure 8.14). To improve the simulations of root DM, the hypothesis of a seasonally variable root maintenance respiration rate was tested (Figure 8.16). This adjustment improved simulations of root DM and reduced the *RMSD* to 14% mean (Figure 8.17). The model was then used to quantify the exclusive impact of perennial reserves on the annual shoot yield of each one of the four defoliation regimes (Figure

8.18). Simulations showed that low levels of perennial reserves caused a decline in yield from 1.1 t/ha for LS crops to 6.8 t/ha for SS crops.

8.4.2 Simulation of shoot DM

The simulation of shoot DM for the original data-set was accurate with a *RMSD* of 0.3 t/ha or 20% of the mean (Figure 8.13). This compares with a *RMSD* of 0.8 t/ha (33% mean) of APSIM-lucerne (Dolling *et al.*, 2005; Robertson *et al.*, 2002). During mid-spring/summer there was a strong agreement between simulated and measured data in both data-sets. However, for the independent data-set, the *RMSD* increased to 30% of the mean (0.6 t/ha), this being caused by underestimations of shoot yield from June-September 2001 (Figure 8.13). This was consistent with the underestimation of *LAI* at the same period (Figure 8.10), indicating that PAR explained part of these differences. For the independent data-set, the model also largely overestimated shoot yield during the autumn cycles of 2001 and 2002 (Figure 8.13). The overestimation was caused by the occurrence of significant senescence during these autumn cycles (Brown *et al.*, 2005b) with decline in the accumulated shoot yield (Figure 8.13). These results highlight the need to include a senescence function in the model and to define the drivers of such process (*e.g.* reproductive stage, shoot C balance, leaf life span).

The use of T_{soil}/T_{air} to drive p_{per}, instead of *Pp* improved the simulations of shoot DM making the *RMSD* decline from 0.4 to 0.3 t/ha and reducing the *SB* from 24 to 2% of *MSD* (Figure 8.11). This improvement was because the bias involved in the hysteresis model based on *Pp* (Figure 7.6) was greater than for the overall unifying relationship for T_{soil}/T_{air} (Figure 7.7), mainly at decreasing photoperiod. A unifying relationship between T_{soil}/T_{air} and p_{per} was possible because there is a lag between the increase in soil and air temperature, which slightly uncouples the fluctuation of T_{soil}/T_{air} from the seasonal *Pp* pattern in autumn (Figure 7.8).

The use of T_{soil}/T_{air} as the predictor of p_{per} for lucerne modelling is a simplification of the hypothesis proposed by Hargreaves (2003) in which the flux of DM from shoots to roots is in direct response to the ratio of temperature of these organs. Although the empirical relationship between p_{per} and T_{soil}/T_{air} does not imply a direct causal mechanism; it is based on the hypothesis that the metabolic rate of each organ responds to temperature (Engels,

1994) and this defines the direction and intensity of DM flow. Of note, the inclusion of any variable to drive p_{per} in lucerne models possibly demands the use of cultivar specific parameters because partitioning patterns may be different according to the level of winter-dormancy (Dolling *et al.*, 2005; Lemaire and Millard, 1999; Volenec *et al.*, 2002; Volenec *et al.*, 1996).

8.4.3 Simulations of leaf area expansion

There was a close agreement between simulated and measured *LAI* during spring/summer (Figure 8.10). Therefore, a single *LAER* (0.016 $m^2/m^2/°Cd$, T_b=5°C) was successfully used as the main driver of lucerne *LAI* expansion during the warmer months. Gosse *et al.* (1984) also showed that *LAI* was linearly related to thermal-time sum (T_b=0°C) for 'du Puits' lucerne in France, but the relationship was different for the spring/summer and winter/autumn periods. Two changes were made to the Gosse *et al.* (1984) model to improve winter/autumn simulations: (*i*) an empirical adjustment of *LAER* based on photoperiod and (*ii*) the use of T_b of 5°C to calculate *Tt*. Using this new structure, the *RMSD* for *LAI* was ~25% of the measured mean for both original (0.6 m^2/m^2) and independent (0.8 m^2/m^2) data-sets (Table 8.5). For the independent data-set, there was a trend to (*i*) underestimate *LAI* in September 2001 (early-spring cycle) and (*ii*) overestimate *LAI* in the early stages of regrowth in half of the analysed cycles (Figure 8.10). The dynamics of early regrowth in lucerne is a challenging process to model because several factors, apart from temperature, influence *LAI* expansion immediately after harvest. For example, early rates of canopy expansion may be affected by (*i*) the level of perennial reserves (Section 6.3.5.2), (*ii*) the initial number of growing points and (*iii*) the residual leaf area at the start of regrowth (Meuriot *et al.*, 2005).

To simulate *LAI* expansion by a more mechanistic approach would be to model leaf appearance rate and the area of individual leaves as in APSIM-lucerne (Robertson *et al.*, 2002). However, using such an approach, APSIM-lucerne gave a poor estimation of *LAI* with a *RMSD* of 56% of the mean (1.4 m^2/m^2) (Robertson *et al.*, 2002). This reinforces the need for gaining quantitative understanding of canopy forming processes. This thesis bring initial insights about some of these issues such as the seasonality of phyllochron (Section 6.2.8), branching patterns (Section 6.3.9) and the effect of perennial reserves on individual leaf area (Section 6.3.10) that can be incorporated in future lucerne models. Therefore at

this stage the use of a empirical approach for *LAI* simulation, such as *LAER* adjusted for *Pp*, can be justified for predictive purposes (Sinclair and Seligman, 1996).

8.4.4 Simulations of primary leaf appearance

Simulations of primary leaf appearance (Figure 8.8) were improved by the calculation of thermal-time using the Jones *et al.* (1986) method instead of a using T_{mean} from the weather file (Section 8.2.3.2). This was characterized by a decline in the overall *RMSD* from 1.4 leaves/shoot to 0.9 leaves/shoot. The use of Jones *et al.* (1986) method improved the simulations because the T_{mean} during the winter/early-spring period is often lower than the T_b of 5°C which causes the underestimation of Tt_{b5} (Figure 8.8). Therefore, in cool temperate climates such as Canterbury, it was necessary to take into account the diurnal temperature fluctuation for the accurate calculation of $\sum Tt$.

With the improved *Tt* calculation, leaf appearance was accurately simulated with an *RMSD* of 0.9 leaves/shoot (13% mean) for the original data-set and 1.5 leaves/shoot (19% mean) for the independent data-set. The increase in the *RMSD* for leaf appearance in the independent data-set was mainly caused by (*i*) large overestimations in the end of autumn cycles (Mar-Apr) and (*ii*) the underestimation observed in the early stages of regrowth during the last measured autumn cycle (April 2002). The reason for these poor simulations was the occurrence of flowering and senescence in the autumn cycles (Brown *et al.*, 2005b). These processes were not accounted in the model framework. The occurrence of flowering significantly decreases the rate of leaf appearance in lucerne (Brown *et al.*, 2005b). Therefore it is necessary to include an adjustment of leaf appearance rates as a function of the reproductive stage of the crop. This seems to be a straightforward approach because the moment of flowering can be predicted from the thermal-time accumulation and photoperiod in lucerne (Moot *et al.*, 2001).

A function to account for senescence is also necessary to improve simulations for long regrowth cycles. During the early autumn cycles from the independent data-set crops regrew for 54-62 days (Brown, 2004) in comparison with 42 day cycles in LL crops. This long regrowth allowed the occurrence of senescence at a level that caused net loss of shoot DM (Figure 8.13). Most probably, senescence allowed light to penetrate through the open canopy increasing the red/far-red ratio at crown level and triggering the initiation of basal

shoots. These shoots were already developed (~4 main-stem nodes; Figure 8.9) in the beginning of the following cycle (last cycle of 2002) which explains the underestimation of the number of primary leaves at this time because the model assumed a single expanded leaf at the beginning of regrowth cycle.

In a model framework where canopy development and DM assimilation are simulated independently, as the one proposed in this chapter, senescence may be considered for leaves (*e.g. LAI* dynamics) and for shoots (*e.g.* DM loss) as result of self-thinning (Section 5.3.4.3). The senescence of *LAI* can be predicted from main-stem node appearance (Section 6.3.12) as previously proposed by other authors (Brown *et al.*, 2005b; Ranganathan *et al.*, 2001; Robertson *et al.*, 2002). Accurate simulations of leaf appearance are necessary to allow more mechanistic approaches of *LAI* modelling in the future as used in APSIM-lucerne (Robertson *et al.*, 2002).

8.4.5 Simulation of root DM

The simulations of root DM were extremely poor (Figure 8.14) when the initial assumptions about root dynamics were used (Section 8.2.4.2). In the original model structure, root DM is calculated as a function of (*i*) total DM assimilation; (*ii*) the fractional partitioning of DM to roots and; (*iii*) root maintenance respiration losses. The first two components were assumed to be correct as they also impacted on shoot yield simulations, which were accurate (Section 8.3.3). Therefore the poor simulation of root DM was assumed to be mainly caused by incorrect assumptions about the root maintenance respiration rate (*Rm_root_rate*).

The model was then used to test a range of fixed *Rm_root_rate* (0.005 to 0.03 DM/day) with no significant improvement in simulations (Figure 8.15). Therefore a new hypothesis assuming a seasonally variable *Rm_root_rate* was tested (Bouma *et al.*, 2000). This approach considerably improved the simulations and allowed the derivation of the most probable respiration rates for each season (Figure 8.16). The use of very low respiration rates (<0.005 DM/day) in autumn which increased slowly to ~0.01 DM/day at the end of the winter and reached a maximum of 0.035 DM/day in early-summer gave a low *RMSD* of 0.7 t/ha (14% of the mean) for the simulation (Figure 8.17). This seasonal pattern for *Rm_root_rate* is consistent with the expected changes in the metabolic activity of crowns

and taproots throughout the seasons. For example, from spring to summer there is a strong mobilization of reserves, notably nitrogen, from perennial organs to shoots (Volenec *et al.*, 2002). This process implies the degradation of soluble proteins and transport of amino acids to shoots, which may cause an increase in respiration to provide energy for such processes. During mid-summer to early-autumn maintenance respiration may progressively decrease as a function of a reduction in the total amount of assimilates being stored in perennial organs. Nevertheless, during this period the energy costs related to active transport of assimilates for storage should exist (Lambers *et al.*, 1996). During mid-autumn to mid-winter there may be a reduction in the metabolic activity of perennial organs, possibly in accordance to the dormancy level of the cultivar. From mid-winter to early-spring maintenance respiration would be expected to increase again as a function of the activation of shoot meristem and increasing demand for perennial reserves.

The importance of a correct understanding of root maintenance respiration relies on the fact it has a major impact on the total crop C budget, consuming up to 50% of the daily fixed carbon (Atkin *et al.*, 2000). However, due to the lack of quantitative understanding about root *Rm*, most crop simulation models assume a constant maintenance factor over root biomass (Marcelis *et al.*, 1998) or carbohydrate basis (Holt *et al.*, 1975). The alternative approach of a broken-stick model with a seasonally variable root *Rm* (Figure 8.16) offers an innovative mode to quantify lucerne roots dynamics. There is reasonable evidence for a variable root *Rm* in other perennial crops such as apple trees (Bouma *et al.*, 2000). These authors showed that root *Rm* changed more than 4 fold with the root ageing and with environmental conditions. There are several possible reasons to justify a variable root *Rm*. Root respiration differs depending on the chemical composition of organs (*e.g.* protein content) and the energetic costs of performing different metabolic activities such as N uptake, uptake of others ions, N fixation, phloem loading and protein turnover (Bouma *et al.*, 1996; Cannell and Thornley, 2000). Also, the sensitivity of root respiration to temperature, quantified as the Q_{10}, may vary with the chemical composition of roots (Atkin *et al.*, 2000) and temperature itself (Lemaire and Millard, 1999; Tjoelker *et al.*, 2001).

In this sense, a more accurate modelling of root dynamics would demand the compartmentalization of roots into structural (passive) and labile reserves (active) tissues (Bouma *et al.*, 2000). The definition of labile (*e.g.* starch, sugar, soluble proteins) and structural (*e.g.* cellulose, protein associated with cell walls) would give a more realistic representation of the pools that are prone to mobilization (Cannell and Thornley, 2000). In

addition, root exudation was not considered in the model although it can contribute with a significant loss of C from roots (Lemaire and Millard, 1999).

Other issue to be considered for the simulation of lucerne root DM is the respiration and reserves translocation pattern 'within' a regrowth cycle. Root respiration rates in lucerne increase shortly after defoliation (Singh, 1974). However the metabolic activity of roots in response to defoliations is expected also to vary seasonally because carbon storage is faster in autumn than spring (Morot Gaudry *et al.*, 1987). All these potential improvements in root *Rm* dynamics would involve the aggregation of relationships that are not properly quantified which would compromise the accuracy of the model. Therefore at this stage, a simple and easily traceable model structure, as proposed in this chapter, becomes a useful tool to quantify the general pattern of root dynamics regardless of the empiricism of the relationships.

8.4.6 Isolating the effect of perennial reserves on shoot yield

The model was used to quantify the exclusive effect of perennial reserves on shoot yield. The lower shoot yields observed in frequently defoliated crops (LS, SL and SS) were caused by (*i*) the effect of defoliation frequencies *per se* (*e.g.* harvesting before LAI_{crit}, Section 6.3.3) and (*ii*) the effect of low perennial reserves by reducing growth rates by their effect on *LAER* and *RUE* (Section 6.3.5.2).

The decline in yield caused by perennial reserves increased from 1.1 t/ha/year in LS crops to 6.8 t/ha/year in SS crops being 32% and 62% of the total difference respectively. This shows that physiological processes responsible for growth rates (*e.g.* canopy expansion and photosynthesis) were affected twice as much in SS crop than LS crop by the level of reserves. On the other hand, simulations showed that shorter period of regrowth were responsible for declines in 2.3 to 4.2 t/ha of annual shoot DM in relation to LL crop. This was caused by the greater occurrence of lag phases of growth in crops grazed frequently and also due to shorter periods of regrowth under near complete PAR interception (*i.e.* $LAI \geq LAI_{crit}$).

8.5 Conclusion

The specific conclusions for this chapter are:

- It was possible to integrate the mathematical relationships developed in the previous results chapters into a simple simulation model.

- The model simulated seasonal shoot yield and development with an acceptable level of accuracy. In general the *RMSD* was 13-24% of the measured mean for the original data-set and 19-31% mean for the independent data-set.

- The most accurate predictions of growth and development were obtained by using the following methodologies:
    - Segmentation of day in 8 periods of 3 h for Tt_{b5} calculation (Jones *et al.*, 1986)
    - The use of T_{soil}/T_{air} to derive fractional DM partitioning to roots

- Root DM was poorly simulated (*e.g. RMSD*=33% mean, *NU*=52% *MSD*) initially and required a change in the assumptions about maintenance respiration rates to improve simulations.

- Root DM simulations were greatly improved (*e.g. RMSD*=14% of mean, *NU*=7% *MSD*) by assuming a seasonal root maintenance respiration rate instead of a fixed one.

The modelling exercise performed in this chapter demonstrated that it was possible to simulate seasonal lucerne growth and development by the use of summary relationships such as *RUE* and *LAER*. The level of empiricism and specificity of such relationships deserve further testing before being extrapolated to other sites and cultivars.

9 General discussion

9.1 Overview

The aim of this thesis was to improve the understanding of lucerne physiological responses to environmental factors, as affected by the level of perennial reserves (Section 1.2). To accomplish this, four defoliation regimes were imposed on a 'Kaituna' lucerne crop to create contrasting levels of perennial reserves (Section 3.3). The four treatments involved a factorial combination of two regrowth lengths (28 or 42 day cycle) applied at two periods of the growth season (before and/or after 4th February).

The seasonal patterns of growth and development of the lucerne crops were then monitored through two growth seasons (2002-2004), based on the yield framework proposed by Monteith (1972). In this framework shoot yield is analysed as the product of intercepted PAR (PAR_i), the radiation use efficiency (*RUE*, g DM/MJ PAR_i), and the harvest index (Equation 2.1). These three components were used to segment the study of crop physiological processes into (*i*) canopy development, (*ii*) photosynthetic capacity and (*iii*) DM partitioning to perennial organs (p_{per}), respectively. The relationships derived from this study were then integrated into a simple computer simulation model. The lucerne model aimed to predict seasonal yield and development of 'Kaituna' lucerne with non-limiting perennial reserves in the cool temperate climate of Canterbury. The model testing enabled the evaluation of the consistency of the assumed relationships and highlighted areas for further research.

9.2 Agronomical implications

The use of the four defoliation regimes was effective in creating lucerne crops with contrasting amounts of perennial DM and different concentrations of carbohydrates and nitrogen in perennial organs (Section 4.3). For example, after the first 5 months, SS crops had 58% less nitrogen, 78% less starch, 30% less soluble sugars and 17% of the structural DM than LL crops. This demonstrated that a 13 day shorter regrowth period for SS crops

was sufficient to limit carbon assimilation (*i.e.* photosynthesis) and N assimilation (*i.e.* mineral uptake and N_2 fixation) which reduced assimilate storage.

Regardless of the defoliation treatment, all crops went through a similar seasonal pattern of accumulation and depletion of perennial reserves. For example, perennial DM in $LL_{02/03}$ crops was 3 t/ha in early-summer but increased to ~5 t/ha in late-autumn (Figure 4.3.2). In general, the amounts and concentrations of perennial reserves reached the highest levels in early-autumn (March-April). These reserves declined throughout the winter/spring period until the lowest levels in early-summer (December-January). From mid-summer to autumn reserves and structural DM again accumulated in perennial organs. This pattern agrees with previous reports for the seasonal concentrations of C and N in lucerne roots (Cunningham and Volenec, 1998). However the largest influxes of carbon to perennial organs occurred in mid-summer rather than autumn, as is commonly suggested in the literature (Section 2.6).

The differences in the concentration of N and carbohydrates in taproots had no apparent effect on the seasonal pattern of DM_{per}. The concentration of reserves in taproot cells defines the osmotic potential that, according to Münch theory, is the main force driving carbon partitioning in plants (Bancal and Soltani, 2002). The soluble fraction of carbohydrates, measured as *Sugar%*, is an important component to define the cellular osmotic potential in plants (Farrar and Jones, 2000). The effect of defoliation treatments on *Sugar%* was transient and minor when compared with the differences observed for $N\%_{root}$ and *Starch%*. Possibly the osmotic potential and consequently the sink strength of perennial organs was maintained at similar levels among treatments. The *Sugar%* tended to a seasonal homeostasis in all crops which may have caused the similar seasonality of DM_{per}. Nevertheless, the mechanisms and signals that control the seasonality of *Sugar%* deserve further investigation.

The seasonality of DM partitioning has practical implications for lucerne management. Farmers use defoliation frequency as a management tool to balance forage yield, quality and persistence (Keoghan, 1982). If the aim is to improve crop persistence and yield, by restoring the level of C and N in perennial organs, the best time to apply long regrowth lengths is from mid-summer to early-autumn because (*i*) the relative partitioning of DM to perennial organs (*i.e.* p_{per}) is the highest (Figure 4.3.2) and (*ii*) photosynthetic rates are highest (Table 7.1). Belanger *et al.* (1999) also observed that harvests 'early' in autumn are

more deleterious to the following spring growth than when an extra defoliation is applied late in the growth season. Consequently, long spells in late-autumn (May-Jun) are expected to have little impact on the level of perennial reserves because total carbon assimilation is limited by low radiation receipts and low temperatures. On the other hand, if crops are allowed to rest for longer periods during mid-summer/early-autumn (Feb-Apr), the absolute amount of C and N allocated to perennial organs is maximized. This was confirmed by the recovery of reserves in $SL_{03/04}$ crops by late-autumn (Figure 4.9). Within regrowth cycles, the recovery of nitrogen and carbohydrate reserves started at ~250°Cd after defoliation, which is close to when crops reached LAI_{crit} (assuming *LAER* of 0.016 $m^2/m^2/°Cd$, Section 8.2.3.1) and senescence and self-thinning of shoots resumed (Figure 5.14). This suggests a synchronicity of physiological events in shoots and taproots.

Frequent defoliations decreased annual shoot yields from 23 t/ha in LL crops to 14 t/ha in SS crops (Section 5.4.1). The differences in shoot yield were analysed through the study of each yield components of plants/m^2, shoots/plant and individual shoot mass (*ISM*). The individual shoot mass (*ISM*, g DM/shoot) was the yield component which explained most of the differences in shoot yield (Figure 5.16). This agrees with previous observations in lucerne at different populations and levels of fertility (Berg *et al.*, 2005; Volenec *et al.*, 1987). Therefore, a reduction in the availability of C and N for the growth of each individual shoot was the primal mechanism by which frequent defoliations or low level of reserves affected shoot yield. Defoliation treatments had no effect on plant population (Figure 5.11) and on the number of shoots/plant (Figure 5.12). Therefore, the observed range in the level of reserves was not sufficient to accelerate plant mortality or to limit shoot appearance. The main cause of plant population decay was possibly the inter-plant competition for light (Gosse *et al.*, 1988). Suppressed lucerne plants are progressively deprived of light which reduces root biomass and the levels of endogenous reserves, notably soluble proteins (Avice *et al.*, 1997a). Therefore, the low level reserves are not the cause of plant death, but rather indicative of a negative C balance, as a consequence of reduced capacity to compete for light with neighbouring plants. This mechanism of plant self-thinning occurred similarly in all crops, although the ranking in terms of absolute amounts of reserves was greater for LL than SS crops. Under farm conditions, weed invasion in paddocks of crops with low level of reserves may accelerate the decay of plant population. Crops grazed frequently will be prone to intense weed invasion because the canopy is open for longer periods and growth rates are limited by the low levels perennial reserves. In this case, competition for light among species would be expected to accelerate

death of lucerne plants. In the present experiment, weed invasion was avoided by intense chemical control of invading species, mainly in SS crops (Section 3.3.4.3). The rate of shoot initiation was also not affected by the level of perennial reserves. Immediately after defoliation the shoot primordia are the main sinks for assimilates, however the absolute demand for C and N was possibly lower than the supply, even for SS crops.

These observations suggest that predictive lucerne simulation models may successfully operate at the 'crop level' without the need to assess plant and shoot population dynamics. This would be untrue if plant population is lower than the threshold in which the compensatory increases in shoots/plant are unable to maintain optimum shoot populations (Figure 5.15). For 'Kaituna' there was no limitation in shoot yield until ~60 plants/m^2, the lowest observed plant population (Figure 5.11). Belanger *et al.* (1992) found that shoot yields declined only when plant population was lower than 46 plants/m^2 for cultivars 'Apica' and 'Oneida VR' grown in Atlantic Canada (~46° N).

Leaf to stem ratio was conservative when related to shoot yield (Figure 5.9). Interestingly, the allometric growth of leaf and stem for 'Kaituna' (Figure 5.9) was in close agreement the report for 'Europe' in France (Lemaire *et al.*, 1992). Shoot yield is an empirical but reliable predictor of DM partitioning between leaf and stem and can be used for such in predictive simulation models (Figure 8.7).

The dynamics of shoot self-thinning was also similar among crops (Figure 5.14). The segregation of shoot classes (Section 5.2.1) was evident after an *LAI* of 2.0, when a maximum shoot population of ~780 shoots/m^2 was reached and self-thinning resumed (Figure 5.12). This suggests that a common mechanism controlled shoot death, probably through competition for light (Gosse *et al.*, 1988; Lemaire *et al.*, 1992; Simon and Lemaire, 1987). Self-thinning of shoots in 'Kaituna' started when fractional transmitted PAR was ~0.20 (Figure 5.14). This can be incorporated as a mechanism to model shoot population in the future.

9.3 Physiological implications

After quantifying the effect of defoliation treatments on perennial DM and shoot DM, the focus of this thesis moved to the physiological explanation of these differences. This was

done by the analysis of the accumulated intercepted PAR ($\sum PAR_i$), the radiation use efficiency (*RUE*) and the partitioning of DM to perennial organs (p_{per}).

As expected, the $\sum PAR_i$ was reduced by the use of short regrowth cycles (Figure 6.2). The interception of PAR in short cycle crops was limited by (*i*) a direct effect of the 13 days shorter regrowth period, and (*ii*) indirectly by slower canopy expansion rates at the beginning of each cycle, caused by low levels of perennial reserves. In short cycle crops the canopy was often harvested before LAI_{crit} was achieved, impeding full PAR interception (Figure 6.4). In contrast when long regrowth cycles were used, the crops frequently reached LAI_{crit} and experienced longer periods under complete PAR interception (*i.e.* closed canopy).

The causes of differences in $\sum PAR_i$ were then analysed by studying (*i*) canopy architecture, (*ii*) shoot population, (*iii*) leaf appearance rates, and (*iv*) the individual leaf area. The main cause of differences in leaf area expansion rates (*LAER*, $m^2/m^2/°Cd$) was the reduction in the expansion of individual leaves at primary and axillary nodes in SS crops. In primary leaves these differences were only evident after the 5th main-stem node. These first 5 expanded leaves however had lower photosynthetic capacity (Pn_{1000}, Section 7.3.4.2) which was consistent with the low values of RUE_{total} observed in SS crops (Figure 7.4 *d*). Differences in leaf photosynthetic rates were explained by the specific leaf nitrogen (*SLN*, Section 7.3.5.1) that ranged from 1.5 to 3.5 g N/m^2 leaf. Low values of *SLN* were mainly a consequence of a reduction in leaf thickness (*i.e. SLW*, Figure 8.11 *a*) with no significant effect of the nitrogen concentration ($N\%_{leaf}$) that was relatively high (4-6% leaf DM, Figure 8.11 *b*). Leaf chlorophyll content was also lower in SS than LL crops, and linearly related to Pn_{1000} (Figure 7.9). These results imply that SS crops were N limited in the early stages of regrowth. This hypothesis was further reinforced by a lower nitrogen nutrition index (*NNI*) in SS crops at $DM_{shoot} < 1$ t/ha or 6 primary leaves when compared with LL crops (Figure 7.12 and Figure 7.13).

Canopy architecture was conservative in all the crops which had a common extinction coefficient for diffuse PAR (k_d) of 0.81 (Figure 6.3). Therefore k_d can be used as a fixed parameter to estimate PAR_i in lucerne simulation models, regardless of the levels of perennial reserves of these crops. Shoot population dynamics were also unaffected by defoliation treatments (Figure 5.12) and consequently was not the cause of differences in *LAER*.

Leaf appearance rates were characterized by the value of the phyllochron (°Cd/primary leaf) which was conservative at 34°Cd (T_b=5°C) during photoperiods >12.5 h (mid-spring to early-autumn) for all crops. Plant developmental processes are usually conservative among a wide range of environmental and management conditions (Grant and Barthram, 1991). In contrast, at *Pp* <12.5 h (late-autumn/winter) the phyllochron increased to ~44 to 60°Cd, being greater for crops with low levels of perennial reserves. The autumn increase in phyllochron may be caused by an increasing dependency of leaf appearance on perennial reserves at a period when conditions are limiting for photosynthesis (*e.g.* low temperatures and low PPFD receipts). This hypothesis is consistent with the fact that the highest values of phyllochron were observed in crops with the lowest levels of perennial reserves in autumn (Figure 6.12). Brown *et al.* (2005b) also observed an increase of 'Kaituna' phyllochron in autumn but proposed a hysterisis model in which the phyllochron changed abruptly in summer. This contrast was partially due to different base temperature used for $\sum Tt$ calculation ($T_{b1/5}$, Section 2.4.1.2) which indicates that the values and the seasonality of the phyllochron can be an artefact of the chosen T_b. A future assessment of node appearance rates in controlled conditions would be necessary to isolate the effects of temperature and photoperiod on lucerne development. The rate of appearance of axillary nodes (branching) was unaffected by defoliation treatments or the level of perennial reserves (Section 6.2.9) and was related to main-stem node position as previously (Brown *et al.*, 2005b).

The effect of limited perennial reserves on reducing leaf area expansion rates (*LAER*, $m^2/m^2/°Cd$) was most evident in the spring cycles of SS crops in 2003/04 (Figure 6.6 and Figure 6.7). The *LAER* was strongly related to the total amount of taproot dry matter (R^2=0.81), nitrogen (R^2=0.67) and soluble sugars (R^2=0.60) in taproots. Justes *et al.* (2002) also observed a rise in *LAER* with increasing root biomass and soluble protein content in lucerne. Possibly the relationship between *LAER* and soluble sugar amounts was an artefact of its strong relationship with total taproot biomass. This is because carbohydrate reserves are often not associated with canopy expansion (Section 2.6.1) and *Sugar%* was similar among treatments.

The interpretation of these results suggests that limited nitrogen reserves reduced shoot growth rates by different means according to the developmental stage of the crop (Figure 9.1). In the early stages of regrowth (<~5 primary leaves) N deficiency reduced specific

leaf nitrogen (*SLN*) compromising the photosynthetic capacity of these leaves and reducing the RUE_{total} of these crops. The continuous scarcity of N or C, after the appearance of the 6th primary leaf, reduced the expansion of these leaves and restricted PAR_i (Figure 9.1).

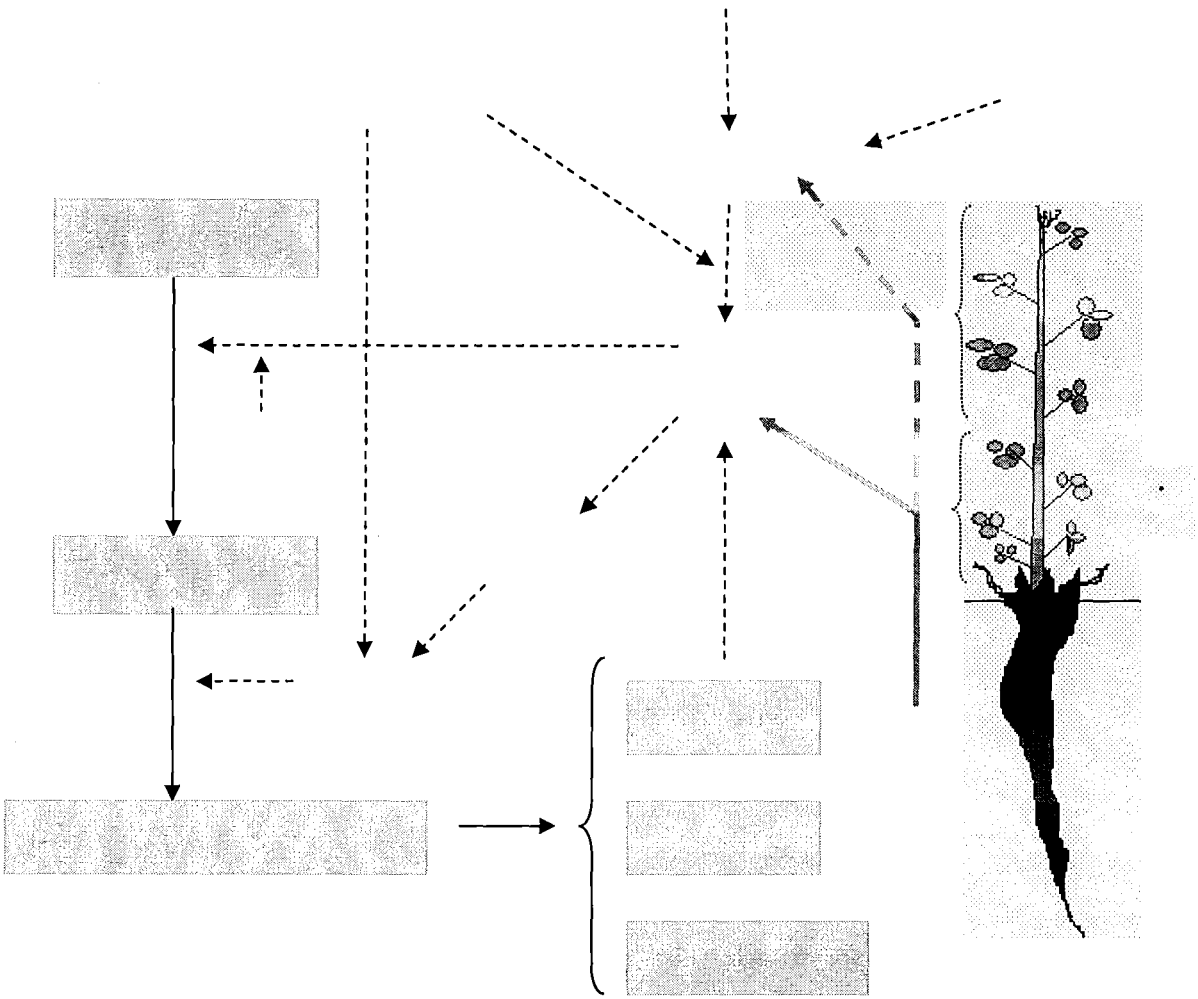

Figure 9.1 Schematic representation of the effect of limited N reserves in perennial organs on the growth of 'Kaituna' lucerne crops during early (≤5 leaves) and late (>5 leaves) stages of regrowth.

Note: Grey boxes represent physical components of the system connected by a flow of energy or matter (→). Dashed arrows indicate influence among processes. *LAER* is the leaf area expansion rate, *SLN* is the specific leaf nitrogen, *SLW* is the specific leaf weight, *LAI* is the leaf area index, $N\%_{leaf}$ is the nitrogen concentration of leaves, *RUE* is the radiation use efficiency, *k* is the extinction coefficient.

Immediately after defoliation carbon is the most limiting resource for growth and N mobilization, therefore lucerne plants maximize leaf expansion (*e.g. LAER*) and consequently PAR_i, at the expense of photosynthetic capacity (*e.g. RUE*). After the canopy is initially established, if resources are still limiting, there is a reduction in leaf expansion

which causes photosynthetic components to accumulate in young leaves and boost *RUE* (Figure 9.1). This trade off between leaf expansion and photosynthetic capacity is consistent with the hypothesis of a functional equilibrium occurring between shoots and roots (Lemaire and Millard, 1999). The reduction in individual leaf expansion at later stages of regrowth may be caused by a continuous dependence on N reserves for cell division and expansion when the crop prioritizes photosynthetic efficiency. Alternatively, leaf expansion may be limited due to the low carbon assimilation of previous leaves. This mechanism was previously proposed to explain reductions in leaf area for sweet corn (*Zea mays*) at contrasting phosphorous nutrition (Fletcher, 2004).

The fractional partitioning of DM to perennial organs (p_{per}) was estimated by dividing the RUE_{shoot} by RUE_{total}. The RUE_{total} was estimated for each regrowth cycle from the framework proposed by Brown (2004) that accounts for temperature effects on *RUE*. The framework was validated for the experimental conditions (Figure 7.4). A general pattern of increase in partitioning to perennial organs was evident from p_{per}<0.05 in winter/early-spring to a p_{per} of ~0.50 in summer (Figure 7.6). This was consistent with the fast accumulation of perennial DM observed from summer to autumn (Figure 4.2) and agrees with previous reports in the literature (Section 2.6). The transport of carbon to roots may be regulated by signals in sink (roots) and source (shoots) simultaneously, as in the 'shared control' hypothesis (Farrar and Jones, 2000). The uncertainties about the underlying mechanisms involved in these processes justify the use of empirical approaches for predicting p_{per} (Sinclair and Seligman, 1996). In this sense, temperature and photoperiod were tested as predictors of p_{per} (Section 2.6). The relationship of p_{per} with *Pp* was inconsistent and a hysteresis model was necessary to explain p_{per} in periods of increasing or decreasing *Pp* (Figure 7.6). For example in LL crops at *Pp* of 10.5 h, p_{per} was ~0.05 at winter/spring (increasing *Pp*) but 0.40 in autumn (decreasing *Pp*). This differential response of p_{per} to *Pp* was previously observed in field grown lucerne (Fick *et al.*, 1988) and suggests that (*i*) lucerne physiology responds to *Pp* direction of change or (*ii*) other factor(s) control p_{per}. Alternatively, the ratio of soil to air temperature (T_{soil}/T_{air}) was tested as a predictor for p_{per} (Hargreaves, 2003). The T_{soil}/T_{air} gave a relationship closer to an unifying linear increase (R^2=0.53) at ~0.10 units of p_{per} for each 0.10 units T_{soil}/T_{air} for LL crops. The p_{per} increased from 0.05 at T_{soil}/T_{air} of 0.8 to 0.50 at T_{soil}/T_{air} of 1.3 (Figure 7.7).

Nevertheless, the relationship of p_{per} with any environmental factor does not imply a direct causal mechanism. The partitioning of DM to perennial organs may also be affected by (*i*)

a different effect of temperature on the metabolic rates of shoots and roots (J. Hargreaves, pers. comm., 2005); (*ii*) different base temperature for the response in metabolic rates of roots and shoots (P. Jamieson, pers. comm., 2005); (*iii*) seasonality of chemical composition of perennial organs (Lemaire and Millard, 1999); (*iv*) physical limits for root growth; and (*v*) the interaction between temperature and photoperiod in controlling morphogenesis and growth (Durand *et al.*, 1991). Therefore the assumption that the flow of C is directed to the organ that experiences the highest temperatures, and consequently has the highest metabolic rates, is more of a functional than a mechanistic approach.

9.4 Considerations for mechanistic modelling of lucerne crops

The physiological relationships derived from result chapters were integrated in a lucerne simulation model (Chapter 8). The model was successfully used to test the consistency of these relationships in predicting lucerne growth and development. Additionally the model was used to test a new hypothesis to explain lucerne physiological responses to the environment.

Initially, the simulations demonstrated that lower *RMSDs* (*i.e.* better fits) were obtained when (*i*) *Tt* was calculated by the method suggested by Jones *et al.* (1986) instead of T_{mean} from the weather file; (*ii*) maintenance respiration was constantly applied to roots instead of assumed implicit in RUE_{total}; and (*iii*) p_{per} was derived from T_{soil}/T_{air} instead of *Pp*.

In general there was agreement between simulated and measured *LAI* data mainly during spring/summer (Figure 8.10). Therefore during the warmer months $LAER_{opt}$ (T_b=5°C) can be used as an accurate and single predictor of *LAI* as previously shown by Gosse *et al.* (1984). These authors also observed that *LAER* (T_b=0°C) was a poor predictor of *LAI* in autumn/winter. To improve *LAI* simulations during autumn/winter two changes were incorporated in the lucerne model (*i*) the use of a T_b of 5°C and; (*ii*) an empirical reduction in *LAER* at $Pp<12.5$ h. This adjustment accounts for the response of physiological mechanisms to seasonal signals, other than T_{mean}, that may limit plant morphogenesis (*e.g.* leaf appearance rates and branching, Section 6.2.8) and plant growth (*e.g.* low C assimilation and allocation to shoots, Section 7.3.1) during autumn/winter. The site specificity of such adjustment depends on the actual mechanisms that regulate canopy

expansion (*e.g.* gene activation, hormonal signals and/or phytochrome mediated responses). Also, the level of change in *LAER* during autumn may be different among lucerne cultivars with contrasting winter hardiness and levels of dormancy (Volenec *et al.*, 2002).

Shoot dry matter assimilation was simulated by assuming RUE_{shoot} as a "variable" derived from the product of RUE_{total} and p_{per} (Section 8.2.4). This approach differs from other published simulation models which use RUE_{shoot} as a "parameter" adjusted for temperature like CropSyst (Confalonieri and Bechini, 2004), or adjusted for seasonal changes in p_{per} like APSIM-lucerne (Robertson *et al.*, 2002). Therefore, the use of RUE_{total} and p_{per} as parameters gave an additional mechanistic level to the model by exposing the components responsible for the seasonality of RUE_{shoot}. To make the lucerne model more mechanistic requires an assumption that p_{per} is a variable controlled by the balance between the supply and demand for assimilates in shoots and roots (Durand *et al.*, 1991). The direction and intensity of the C flux in the plant would be then a function of the supply of C from photosynthesis and the demand of C from the product between (*i*) plant morphogenesis and (*ii*) the mass/volume ratio of plant organs. The hierarchy of DM allocation to leaves, stems and roots would then be the next level of empiricism of such an approach (Durand *et al.*, 1991).

The initial simulation of root DM was extremely poor (Figure 8.14). The initial structure of the model assumed a fixed root *Rm* of 0.015 DM/day (Section 8.2.4.2). To improve root DM simulations an alternative hypothesis of a "seasonally variable" root *Rm* was tested. The simulations were significantly improved when root *Rm* was assumed to increase from <0.005 DM/day in winter to ~0.035 DM/day in summer (Figure 8.17). By adjusting the values of R_m on a seasonal basis the *RMSD* declined from 33% to 14% of the measured mean. Obviously, the seasonal *Rm* is a simplification of several physiological changes that may occur in lucerne roots. For example, the known response of Q_{10} to temperature and substrate availability (Atkin *et al.*, 2000; Tjoelker *et al.*, 2001) were not incorporated in the model because they are not yet quantified in lucerne roots.

The simulations showed the potential of the lucerne model as a useful tool to identify gaps of knowledge on lucerne physiology and also to test alternative hypothesis that can be validated in the future.

9.5 Suggestions for future research

The result chapters and the modelling exercise indicated areas where further research is needed to complement the current knowledge of lucerne physiology. Some of the points that deserve future investigation follow.

a) The understanding of yield components dynamics for modelling genetically contrasting lucerne cultivars. Yield component (Section 5.2.2) can be monitored on lucerne cultivars with various levels of winter dormancy, sown at a range of plant populations (Volenec *et al.*, 1987). It is particularly important to quantify plant population by harvesting roots instead of counting crowns because the later method tends to underestimate plant populations.

b) The physiological mechanism that reduces individual leaf area after a certain node position (X_0, Section 6.2.10) needs clarification. It could be hypothesized that leaves are smaller because there are fewer cells in the leaf primordia or because cell expansion is reduced. This could be quantified by counting the number and measuring the area of mesophyll cells in transversal cuts of leaflets, taken from different main-stem node positions.

c) Low levels of perennial reserves limited individual leaf expansion. However the effect of C and N reserves and the mechanism by which leaf area is reduced are not clear. Again, transversal sections of lucerne leaflets can provide information about changes in cell division or cell expansion (Section 9.5 *b*). Perennial reserves could be manipulated in controlled environment. The critical demand for N to support leaf growth occurs before the demand for C (Lemaire and Millard, 1999) and therefore the study of cell growth and expansion can bring some light to these issues.

d) The actual mechanisms and the signals that control the seasonal partitioning of C to lucerne roots are unknown. Temperature or photoperiod may influence p_{per} through the control of plant morphogenesis and metabolism (Section 2.6). Therefore the first step would be to isolate the individual contribution of Pp and T_{mean} to the seasonality of p_{per}. One option would be to maintain Pp constant at the maximum for the site (*e.g.* ~16.5 h at Lincoln, Canterbury). The natural Pp could be complemented to 16.5 h by the use of LED panels with low level of PPFD output. The rationale would be to cancel phytochrome

mediated responses without changing the $\sum PAR_i$ of crops. Possible quantitative or obligatory responses to *Pp* would be tested by varying the time and level of *Pp* treatment during specific periods of the growth season. It would be interesting to set a field experiment with plants grown in PVC columns (Figure 9.2) making the access to roots less laborious and more accurate (Brown, 2004).

e) The proposed hypothesis about a seasonal change in the rate of root maintenance respiration (Section 8.3.4.2) deserves further testing. This would demand quantification of the carbon balance of lucerne plants in field conditions. One possibility would be to grow lucerne plants in PVC columns at ground level in the field (Brown, 2004) and access the CO_2 exchange, root biomass and chemical composition at different times of the growth season (Figure 9.2). The CO_2 exchange of leaves and roots from the known volume of soil inside the columns (root and soil respiration) could be measured with a portable photosynthesis system similar to the LI-6400 (Section 7.2.4). The advantages of such method would be the possibility of harvesting the entire plant immediately after photosynthesis and respiration rates are taken. Additionally, mass and concentrations of C and N could be measured in the plants. A further sophistication of this method would be the inclusion of photoperiod treatments (Section 9.5 *c*) or defoliation regimes (Section 3.3).

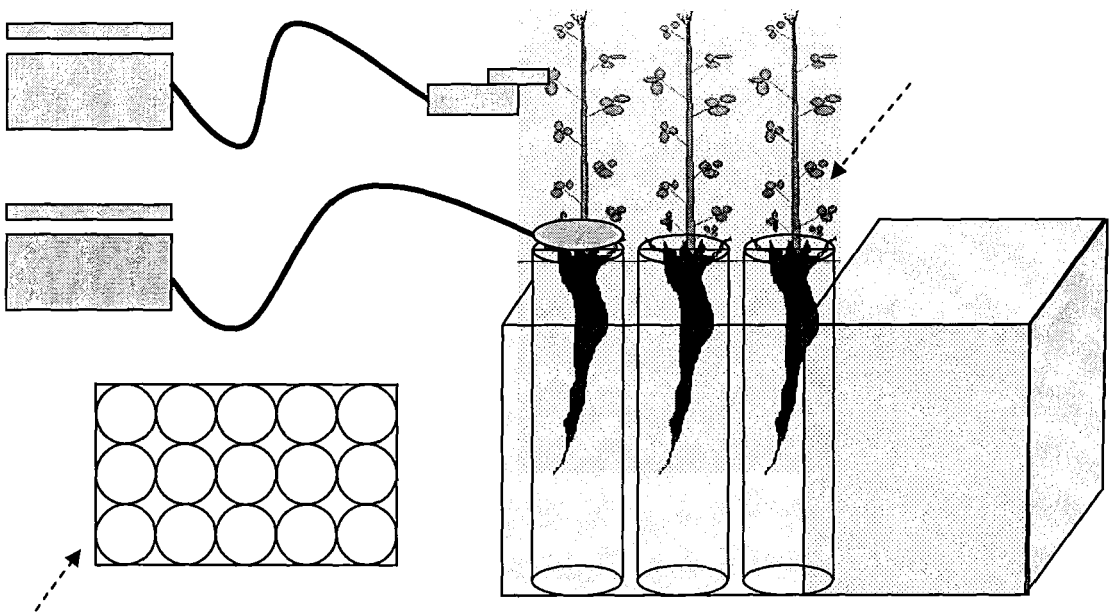

Figure 9.2 Schematic representation of an experimental method to quantify carbon balance of lucerne plants.

Note: Method adapted from Brown (2004). LI-6400 is the portable photosynthesis system (Section 7.2.4).

e) There is a clear need to integrate the large amount of knowledge currently available on lucerne physiology. Simulations models, such as the APSIM-lucerne model (Robertson *et al.*, 2002), are effective tools to amalgamate and test the coherence of hypothesis about physiological mechanisms (Hammer *et al.*, 2002). The results of this thesis showed that lucerne simulation models need to better address DM partitioning and root respiration for accurate predictions of total DM accumulation. This knowledge will be necessary to create the basis for further modelling of the effects of perennial reserves on shoot yield.

9.6 Conclusions

Frequent defoliations limited shoot yield and the accumulation of perennial DM in lucerne crops. Low levels of perennial reserves also limited shoot yield through a reduction in canopy expansion and possibly in photosynthetic capacity. The main findings in each chapter were:

Chapter 4. Frequent defoliations (28 day cycle) reduced perennial DM accumulation by up to 20% when compared with LL crops. There was a seasonal pattern of accumulation (mid-summer/autumn) and depletion (winter/early-summer) of reserves in all crops, regardless of defoliation regime.

Chapter 5. Frequent defoliations and low levels of perennial reserves limited shoot regrowth rates. This reduction in yield was caused by limited allocation of assimilates for the growth of each individual shoot. No significant differences in plant and shoot population dynamics were observed among crops.

Chapter 6. Differences in annual shoot yield were mostly (R^2=0.84) explained by a reduction in $\sum PAR_i$ in frequently defoliated crops. Low $\sum PAR_i$ was caused by limited canopy expansion through smaller individual leaf areas in primary and axillary leaves.

Chapter 7. There was evidence for a reduction in RUE_{total} of crops with the lowest level of perennial reserves (SS crops). This was consistent with lower leaf photosynthetic capacity of these crops at early stages of regrowth (<5 leaves or ~150°Cd after grazing). Reductions

in leaf chlorophyll content, *SLN* and *NNI* were in agreement with the lower photosynthesis rates of these leaves.

Chapter 8. The integration of the relationships from result chapters was relatively successful in simulating leaf appearance, *LAI* and shoot yield of lucerne crops. However to accurately simulate root DM, a seasonally variable root maintenance respiration had to be assumed.

This thesis provides new knowledge about the response of lucerne crops to environmental factors and also the influence of perennial reserves on these relationships. The modelling exercise demonstrated the current knowledge about environmental physiology of lucerne is robust enough to allow the testing of new hypothesis and refocus research efforts.

References

Abdul Jabbar, A. S., Sammis, T. W., and Lugg, D. G. (1982). Effect of moisture level on the root pattern of alfalfa. *Irrigation Science*, **3** (3): 197-207.

Al Hamdani, S., and Todd, G. (1990). Effect of temperature regimes on photosynthesis, respiration, and growth in alfalfa. *Proceedings of the Oklahoma Academy of Science*, **70**: 1-4.

Andrade, F. H., Uhart, S. A., and Cirilo, A. (1993). Temperature affects radiation use efficiency in maize. *Field Crops Research*, **32** (1-2): 17-25.

AOAC (1995). Official methods of analysis of AOAC International. Vol. 2 16, AOAC International, Arlington, U.S.A.

Arnold, C. Y. (1959). The determination and significance of the base temperature in a linear unit heat system. *Proceedings of the American Society for Horticultural Science*, **74**: 430-445.

Arnon, D. (1949). Cooper enzymes in isolated chloroplasts. Polyphenol oxidase in *Beta vulgaris*. *Plant Physiology*, **24** (11): 1-15.

Atkin, O. K., Edwards, E. J., Loveys, B. R., Norby, R., Fitter, A., and Jackson, R. (2000). Response of root respiration to changes in temperature and its relevance to global warming. *New Phytologist*, **147** (1): 141-154.

Avice, J. C., Ourry, A., Lemaire, G., and Boucaud, J. (1996). Nitrogen and carbon flows estimated by ^{15}N and ^{13}C pulse-chase labeling during regrowth of alfalfa. *Plant-Physiology*, **112** (1): 281-290.

Avice, J. C., Lemaire, G., Ourry, A., and Boucaud, J. (1997a). Effects of the previous shoot removal frequency on subsequent shoot regrowth in two *Medicago sativa* L. cultivars. *Plant and Soil*, **188** (2): 189-198.

Avice, J. C., Ourry, A., Lemaire, G., Volenec, J. J., and Boucaud, J. (1997b). Root protein and vegetative storage protein are key organic nutrients for alfalfa shoot regrowth. *Crop Science*, **37** (4): 1187-1193.

Avice, J. C., Louahlia, S., Kim, A., Morvan-Bertrand, A., Prudhomme, M. P., Ourry, A., and Simon, J. C. (2001). Influence des reserves azotees et caerbonees sur la repousse des especes prairiales. *Fourrages*, **165**: 3-22.

Azam Ali, S. N., Crout, N. M. J., and Bradley, R. G. (1994). Perspectives in modelling resource capture by crops. *In* " Resource capture by crops" (J. L. Monteith, R. K. Scott and M. H. Unsworth, eds.), pp. 125-148. University of Nottingham Press, Loughborough, Leicestershire.

Bancal, P., and Soltani, F. (2002). Source-sink partitioning. Do we need Münch? *Journal of Experimental Botany*, **53** (376): 1919-1928.

Bange, M., Hammer, G., and Rickert, K. (1997). Effect of specific leaf nitrogen on radiation use efficiency and growth of sunflower. *Crop Science*, **37** (4): 1201-1207.

Barber, L., Joern, B., Volenec, J., and Cunningham, S. (1996). Supplemental nitrogen effects on alfalfa regrowth and nitrogen mobilization from roots. *Crop Science*, **36** (5): 1217-1223.

Belanger, G., Richards, J. E., and McQueen, R. E. (1992). Effects of harvesting systems on yield, persistence and nutritive value of alfalfa. *Canadian Journal of Plant Science*, **72** (3): 793-799.

Belanger, G., Kunelius, T., McKenzie, D., Papadopoulos, Y., Thomas, B., McRae, K., Fillmore, S., and Christie, B. (1999). Fall cutting management affects yield and persistence of alfalfa in Atlantic Canada. *Canadian Journal of Plant Science*, **79** (1): 57-63.

Belesky, D. P., and Fedders, J. M. (1997). Residue height influences stand dynamics of alfalfa grown on a shallow soil. *Agronomy Journal*, **89** (6): 975-980.

Berg, W. K., Cunningham, S. M., Brouder, S. M., Joern, B. C., Johnson, K. D., Santini, J., and Volenec, J. J. (2005). Influence of phosphorus and potassium on alfalfa yield and yield components. *Crop Science*, **45** (1): 297-304.

Boller, B. C., and Heichel, G. H. (1983). Photosynthate partitioning in relation to N_2 fixation capability of alfalfa. *Crop Science*, **23** (4): 655-659.

Bonhomme, R. (2000). Bases and limits to using "degree-day" units. *European Journal of Agronomy*, **13** (1): 1-10.

Bouchart, V., Macduff, J., Ourry, A., Svenning, M., Gay, A., Simon, J., and Boucaud, J. (1998). Seasonal pattern of accumulation and effects of low temperatures on storage compounds in *Trifolium repens*. *Physiologia Plantarum*, **104** (1): 65-74.

Bouma, T. J., Broekhuysen, A. G. M., and Veen, B. W. (1996). Analysis of root respiration of *Solanum tuberosum* as related to growth, ion uptake and maintenace of biomass. *Plant Physiology and Biochemistry*, **34** (6): 795-806.

Bouma, T. J., Bryla, D. R., Yadong, L., and Eissenstat, D. M. (2000). Is maintenance respiration in roots constant? *In* "The supporting roots of trees and woody-plants: form, function and physiology." (A. Stokes, ed.), Vol. 87, pp. 391-396. Kluwer Academic Publishers, Dordrecht, The Netherlands.

Boyce, P., and Volenec, J. (1992). Taproot carbohydrate concentrations and stress tolerance of contrasting alfalfa genotypes. *Crop-Science*, **32** (3): 757-761.

Brown, H. E. (1998). Dry matter production and water use of red clover, chicory and lucerne in irrigate and dryland conditions. B.Ag.Sc. (Hons) Dissertation, 96 p. Lincoln University, Lincoln, New Zealand.

Brown, H. E., Moot, D. J., Pollock, K. M., and Inch, C. (2000). Dry matter production of irrigated chicory, lucerne and red clover in Canterbury. *Proceedings of the 13th Annual Conference, Agronomy Society of New Zealand, Palmerston North, New Zealand*, **30**: 129-137.

Brown, H. E. (2004). Understanding yield and water use of dryland forage crops in New Zealand. Ph.D. Thesis, 288 p. Lincoln University, Lincoln, New Zealand.

Brown, H. E., Moot, D. J., and Pollock, K. M. (2005a). Herbage production, persistence, nutritive charactersistics and water use of perennial forages over 6 years on a Wakanui sil loam. *New Zealand Journal of Agricultural Research*, **48**: 423-439.

Brown, H. E., Moot, D. J., and Teixeira, E. I. (2005b). The components of lucerne (*Medicago sativa*) leaf area index respond to temperature and photoperiod in a temperate climate. *European Journal of Agronomy*, **23** (4): 348-358.

Brown, R. H., Pearse, R. B., Wolf, D. D., and Blaser, R. E. (1972). Energy accumulation and utilization. *In* "Alfalfa Science and Technology" (A. A. Hanson, ed.), Vol. 15, pp. 143-166. American Society of Agronomy, Madison, USA.

Brown, R. H., and Radcliffe, D. E. (1986). A comparison of apparent photosynthesis in *Sericea lespedeza* and alfalfa. *Crop Science*, **26** (6): 1208-1211.

Buxton, D., Hornstein, J., Wedin, W., and Maten, J. (1985). Forage quality in stratified canopies of alfalfa, birdsfoot trefoil and, red clover. *Crop Science*, **25** (1): 273-279.

Campbell, G. S., and van Evert, F. K. (1994). Light interception by plant canopies: efficiency and architecture. *In* "Resource capture by crops" (J. L. Monteith, R. K. Scott and M. H. Unsworth, eds.), pp. 35-52. University of Nottingham Press, Loughborough, Leicestershire.

Cannell, M. G. R., and Thornley, J. H. M. (1998). Temperature and CO_2 responses of leaf and canopy photosynthesis: a clarification using the non-rectangular hyperbola model of photosynthesis. *Annals of Botany*, **82** (6): 883-892.

Cannell, M. G. R., and Thornley, J. H. M. (2000). Modelling the components of plant respiration: some guiding principles. *Annals of Botany*, **85** (1): 45-54.

Casal, J. J., Deregibus, V. A., and Sanchez, R. A. (1985). Variations in tiller dynamics and morphology in *Lolium multiflorum* Lam. vegetative and reproductive plants as affected by differences in red/far-red irradiation. *Annals of Botany*, **56** (4): 553-559.

Charles-Edwards, D. A., Doley, D., and Rimmington, G. M. (1986). Modelling plant growth and development. (D. A. Charles-Edwards, D. Doley and G. M. Rimmington, eds.), 235 p., Academic Press, Sydney, Australia.

Cheeroo-naymuth, B. F. (1999). Crop modelling/simulation: an overview. *Food and Agricultural Research Council, Reduit, Mauritius*: 11-26.

Chen, T. H. H., and Chen, F. S. C. (1988). Relations between photoperiod, temperature, abscisic acid, and fall dormancy in alfalfa (*Medicago sativa*). *Canadian Journal of Botany*, **66** (12): 2491-2498.

Christian, K. (1987). Modelling pasture growth. *In* "Managed Grasslands" (R. W. Snaydon, ed.), pp. 47-60. Elsevier Science, Amsterdan.

Collino, D. J., Dardanelli, J. L., De Luca, M. J., and Racca, R. W. (2005). Temperature and water availability effects on radiation and water use efficiencies in alfalfa (*Medicago sativa* L.). *Australian Journal of Experimental Agriculture*, **45** (4): 383-390.

Confalonieri, R., and Bechini, L. (2004). A preliminary evaluation of the simulation model CropSyst for alfalfa. *European Journal of Agronomy*, **21** (2): 223-227.

Cralle, H. T., and Heichel, G. H. (1988). Photosynthate partitioning in alfalfa before harvest and during regrowth. *Crop Science*, **28** (6): 948-953.

Cunningham, S. M., and Volenec, J. J. (1998). Seasonal carbohydrate and nitrogen metabolism in roots of contrasting alfalfa (*Medicago sativa* L.) cultivars. *Journal of Plant Physiology*, **153** (1-2): 220-225.

Davies, A., and Thomas, H. (1983). Rates of leaf and tiller production in young spaced perennial ryegrass plants in relation to soil temperature and solar radiation. *Annals of Botany*, **51** (5): 591-597.

Davies, S. L., and Peoples, M. B. (2003). Identifying potential approaches to improve the reliability of terminating a lucerne pasture before cropping: a review. *Australian Journal of Experimental Agriculture*, **43** (5): 429-447.

Dhont, C., Castonguay, Y., Nadeau, P., Belanger, G., and Chalifour, F. P. (2002). Alfalfa root carbohydrates and regrowth potential in response to fall harvests. *Crop Science*, **42** (3): 754-765.

Dhont, C., Castonguay, Y., Nadeau, P., Belanger, G., Drapeau, R., and Chalifour, F. P. (2004). Untimely fall harvest affects dry matter and root organic reserves in field-grown alfalfa. *Crop Science*, **44** (1): 144-157.

Dolling, P. J., Robertson, M. J., Asseng, S., Ward, P. R., and Latta, R. A. (2005). Simulating lucerne growth and water use on diverse soil types in a Mediterranean-type environmnent. *Australian Journal of Agricultural Research*, **56** (1): 503-515.

Douglas, J. (1986). The production and utilization of lucerne in New Zealand. *Grass and Forage Science*, **41** (2): 81-128.

Draper, N., and Smith, H. (1998). Applied regression analysis. *In* "Wiley series in probability and statistics" 3rd Ed, John Wiley & Sons Inc. ed., New York.

Duncan, W. G. (1971). Leaf angles, leaf area, and canopy photosynthesis. *Crop Science*, **11** (1): 482-485.

Durand, J. L., Lemaire, G., Gosse, G., and Chartier, M. (1989). An analysis of the conversion of solar energy to dry matter in a lucerne (*Medicago sativa*) population subjected to water deficit. *Agronomie*, **9** (6): 599-607.

Durand, J. L., Varlet Grancher, C., Lemaire, G., Gastal, F., and Moulia, B. (1991). Carbon partitioning in forage crops. *Acta Biotheoretica*, **39** (3-4): 213-224.

Duru, M., and Langlet, A. (1995). Croissance de repousses de luzerne et de dactyle en conditions seches et irriguess. II. - modelisation. *Agrochimia*, **39** (2-3): 111-121.

Dwyer, L. M., and Stewart, D. W. (1986). Leaf area development in field-grown maize. *Agronomy Journal*, **78** (2): 334-343.

Elings, A. (2000). Estimation of leaf area in tropical maize. *Agronomy Journal*, **92** (3): 436-444.

Engels, C. (1994). Effect of root and shoot meristem temperature on shoot to root dry matter partitioning and the internal concentrations of nitrogen and carbohydrates in maize and wheat. *Annals of Botany*, **73** (1): 211-219.

Evans, J. R. (1989). Photosynthesis and nitrogen relationships in leaves of C_3 plants. *Oecologia*, **78** (1): 9-19.

Evans, J. R. (1993). Photosynthetic acclimation and nitrogen partitioning within a lucerne canopy. I. Canopy characteristics. *Australian Journal of Plant Physiology*, **20** (1): 55-67.

Fankhauser, J. J., Volenec, J., and Brown, G. (1989). Composition and structure of starch from taproots of contrasting genotypes of *Medicago sativa* L. *Plant Physiology*, **90** (3): 1189-1194.

Fankhauser Jr, J. J., Volenec, J. J., and Brown, G. A. (1989). Composition and structure of starch from taproots of contrasting genotypes of *Medicago sativa* L. *Plant Physiology*, **90** (3): 1189-1194.

Farrar, J. F., and Jones, D. L. (2000). The control of carbon acquisition by roots. *New Phytologist*, **147** (1): 43-53.

Fick, G. W. (1977). The mechanism of alfalfa regrowth: a computer simulation approach. *Search Agriculture*, **7** (3): 1-28.

Fick, G. W., Holt, D. A., and Lugg, D. G. (1988). Environmental physiology and crop growth. *In* "Alfalfa and alfalfa improvement" (A. A. Hanson, D. K. Barnes and R. R. Hill Jr., eds.), Vol. 29, pp. 163-194. American Society of Agronomy, Madison, U.S.A.

Fick, G. W., and Onstad, D. W. (1988). Statistical models for predicting alfalfa herbage quality from morphological or weather data. *Journal of Production Agriculture*, **1** (2): 160-166.

Fick, G. W., Wilkens, P. W., Cherney, J. H., and Fahey Jr, G. C. (1994). Modeling forage quality changes in the growing crop. *In* "Forage quality, evaluation, and utilization" (G. C. Fahey Jr, M. Collins, D. R. Mertens and L. E. Moser, eds.), pp. 757-795. American Society of Agronomy, Madison.

Fletcher, A. L. (2004). Understanding 'Challenger' sweet corn yield, quality and phenology responses to phosphorus. Ph.D. Thesis, 244 p. Lincoln University, Lincoln, New Zealand.

Flexas, J., and Medrano, H. (2002). Drought-inhibition of photosynthesis in C_3 plants: stomatal and non-stomatal limitations revisited. *Annals of Botany*, **89** (2): 183-189.

Fornasier, F., Pecceti, L., and Piano, E. (2003). Variation in crown and root organic reserves among lucerne genotypes of different morphology and flower colour. *Journal of Agronomy and Crop Science*, **189** (2): 63-70.

Gana, J. A., Kelengamaliro, N. E., Cunningham, S. M., and Volenec, J. J. (1998). Expression of beta-amylase from alfalfa taproots. *Plant Physiology*, **118** (4): 1495-1505.

Gastal, F., and Durand, J. L. (2000). Effects of nitrogen and water supply on N and C fluxes and partitioning in defoliated swards. *In* "International symposium on grassland ecophysiology and grazing ecology, Grassland ecophysiology and grazing ecology. Curitiba, Brazil." (G. Lemaire, J. Hodgson, A. Moraes, C. Nabinger and P. C. F. Carvalho, eds.), pp. 15-39. CABI Publishing; Wallingford; UK.

Gastal, F., and Lemaire, G. (2002). N uptake and distribution in crops: an agronomical and ecophysiological perspective. *Journal of Experimental Botany.*, **53** (370): 789-799.

Gauch, H. G., Jr., Hwang, J. T. G., and Fick, G. W. (2003). Model evaluation by comparison of model-based predictions and measured values. *Agronomy Journal*, **95** (6): 1442-1446.

Gosse, G., Chartier, M., Lemaire, G., and Guy, P. (1982a). Effect of climatic factors on lucerne production. *Fourrages*, **90** (1): 113-133.

Gosse, G., Chartier, M., Varlet Grancher, C., and Bonhomme, R. (1982b). Interception of photosynthetically active radiation by lucerne: variations and modelling. *Agronomie*, **2** (6): 583-588.

Gosse, G., Chartier, M., Monget, C., Fiala, V., and Bethenod, O. (1983). CO_2 balance and production of dry matter in alfalfa crop. *In* "Photosynthesis and plant productivity Joint meeting of the OECD and Studiezentrum Werkersheim" (H. Metzner, ed.), pp. 93-96. Wissenschaftliche Verlagsgesellschaft mbH, Stuttgart, German Federal Republic.

Gosse, G., Chartier, M., and Lemaire, G. (1984). Predictive model for a lucerne crop. *Comptes Rendus de l'Academie des Sciences, III Sciences de la Vie*, **298** (18): 541-544.

Gosse, G., Lemaire, G., Chartier, M., and Balfourier, F. (1988). Structure of a lucerne population (*Medicago sativa* L.) and dynamics of stem competition for light during regrowth. *Journal of Applied Ecology*, **25** (2): 609-617.

Gramshaw, D., Lowe, K. F., and Lloyd, D. L. (1993). Effect of cutting interval and winter dormancy on yield, persistence, nitrogen concentration, and root reserves of irrigated lucerne in the Queensland subtropics. *Australian Journal of Experimental Agriculture*, **33** (7): 847-854.

Grant, S. A., and Barthram, G. T. (1991). The effects of contrasting cutting regimes on the components of clover and grass growth in microswards. *Grass and Forage Science*, **46** (1): 1-13.

Haagenson, D. M., Cunningham, S. M., Joern, B. C., and Volenec, J. J. (2003a). Root physiology of less fall dormant, winter hardy alfalfa selections. *Crop Science*, **43** (4): 1441-1447.

Haagenson, D. M., Cunningham, S. M., Joern, B. C., and Volenec, J. J. (2003b). Autumn defoliation effects on alfalfa winter survival, root physiology, and gene expression. *Crop Science*, **43** (4): 1340-1348.

Habben, J., and Volenec, J. (1990). Starch grain distribution in taproots of defoliated *Medicago sativa* L. *Plant Physiology*, **94** (3): 1056-1061.

Hall, M. H., Sheaffer, C. C., and Heichel, G. H. (1988). Partitioning and mobilization of photoassimilate in alfalfa subjected to water deficits. *Crop Science*, **28** (6): 964-969.

Hammer, G. L., and Wright, G. C. (1994). A theoretical analysis of nitrogen and radiation effects on radiation use efficiency in peanut. *Australian Journal of Agricultural Research*, **45** (3): 575-589.

Hammer, G. L. (1998). Crop Modelling: Current status and opportunities to advance. *In* "Crop Models in Protected Cultivation" (L. F. M. Marcellis, ed.), Vol. 456, pp. 27-35. Acta Horticulturale.

Hammer, G. L., Kropff, M. J., Sinclair, T. R., and Porter, J. R. (2002). Future contributions of crop modelling - from heuristics and supporting decision making to

understanding genetic regulation and aiding crop improvement. *European Journal of Agronomy*, **18** (1-2): 15-31.

Hargreaves, J. (2003). Simulating below-ground reserves: some ideas. *In* "APSIM-lucerne workshop *(unpublished)*." Power point presentation. Geelong, Australia.

Hay, R. K. M., and Walker, A. J. (1989a). Mathematical models and crop physiology. *In* "An introduction to the physiology of crop yield" (R. K. M. Hay and A. J. Walker, eds.), pp. 237-253. Longman Scientific & Technical, New York.

Hay, R. K. M., and Walker, A. J. (1989b). An introduction to the physiology of crop yield. (R. K. M. Hay and A. J. Walker, eds.), pp. 292. Longman Scientific & Technical, New York.

Heichel, G. H., Delaney, R. H., and Cralle, H. T. (1988). Carbon assimilation, partitioning and utilization. *In* "Alfalfa and alfalfa improvement" (A. A. Hanson, D. K. Barnes and R. R. Hill Jr., eds.), Vol. 29, pp. 195-228. American Society of Agronomy, Madison, U.S.A.

Hendershot, K. L., and Volenec, J. J. (1992). Taproot nitrogen accumulation and use in overwintering alfalfa (*Medicago sativa* L.). *Journal of Plant Physiology*, **141** (1): 68-74.

Hendershot, K. L., and Volenec, J. J. (1993). Nitrogen pools in taproots of *Medicago sativa* L. after defoliation. *Journal of Plant Physiology*, **141** (2): 129-135.

Hewitt, A. E. (1993). New Zealand soil classification. *In* "Landcare research science series, no. 1" (A. E. Hewitt, ed.), Manaaki Whenua - Landcare Research, Lincoln, New Zealand.

Hiscox, J. D., and Israelstam, G. F. (1979). A method for the extraction of chlorophyll from leaf tissue without maceration. *Canadian Journal of Botany*, **57** (12): 1332-1334.

Hodges, H. (1991). Predicting crop phenology. (H. Hodges, ed.), 233 p., CRC Press, Boston, U.S.A.

Hodgkinson, K. C. (1974). Influence of partial defoliation on photosynthesis, photorespiration and transpiration by lucerne leaves of different ages. *Australian Journal of Plant Physiology*, **1** (4): 561-578.

Hoel, B. O., and Solhaug, K. A. (1998). Effect of irradiance on chlorophyll estimation with the Minolta SPAD-502 leaf chlorophyll meter. *Annals of Botany*, **82** (3): 389-392.

Holt, D. A., Bula, R. J., Miles, G. E., Schreiber, M. M., and Peart, R. M. (1975). Environmental physiology, modeling and simulation of alfalfa growth. 1. Conceptual development of SIMED. *Research Bulletin, Purdue University Agricultural Experiment Station.*, **907**: 1-26.

Inch, C. (1998). Dry matter production and water use of lucerne, red clover and chicory in irrigated and dryland conditions. B.Ag.Sc. (Hons) Dissertation, Lincoln University, New Zealand.

Irwin, J. A. G., Lloyd, D. L., and Lowe, K. F. (2001). Lucerne biology and genetic improvement - an analysis of past activities and future goals in Australia. *Australian Journal of Agricultural Research*, **52** (7): 699-722.

Jamieson, P. D., Martin, R. J., and Francis, G. S. (1995). Drought influences on grain yield of barley, wheat and maize. *New Zealand Journal of Crop and Horticultural Science*, **23** (1): 55-66.

Jonckheere, I., Fleck, S., Nackaerts, K., Muys, B., Coppin, P., Weiss, M., and Baret, F. (2004). Review of methods for in situ leaf area index determination: Part I. Theories, sensors and hemispherical photography. *Agricultural and Forest Meteorology*, **121** (1-2): 19-35.

Jones, C. A., Ritchie, J. T., Kiniry, J. R., and Godwin, D. C. (1986). Subroutine structure. *In* "CERES-Maize: A simulation model of maize growth and development." (C. A. Jones and J. R. Kiniry, eds.), pp. 49-67, 194 p. Texas A&M University Press, Texas, U.S.A.

Justes, E., Denoroy, P., Gabrielle, B., and Gosse, G. (2000). Effect of crop nitrogen status and temperature on the radiation use efficiency of winter oilseed rape. *European Journal of Agronomy*, **13** (2-3): 165-177.

Justes, E., Thiebeau, P., Avice, J., Lemaire, G., Volenec, J., and Ourry, A. (2002). Influence of summer sowing dates, N fertilization and irrigation on autumn VSP accumulation and dynamics of spring regrowth in alfalfa (*Medicago sativa* L.). *Journal of Experimental Botany*, **53** (366): 111-121.

Keoghan, J. M. (1982). Effects of cutting frequency and height on top-growth of pure lucerne stands. *In* "The Lucerne Crop" (R. H. M. Langer, ed.), pp. 117-128, Wellington.

Khaiti, M., and Lemaire, G. (1992). Dynamics of shoot and root growth of lucerne after seeding and after cutting. *European Journal of Agronomy*, **1** (4): 241-247.

Kim, T., Ourry, A., Boucaud, J., and Lemaire, G. (1991). Changes in source-sink relationship for nitrogen during regrowth of lucerne (*Medicago sativa* L.) following removal of shoots. *Australian Journal of Plant Physiology*, **18** (6): 593-602.

Kim, T. H., Bigot, J., Ourry, A., and Boucaud, J. (1993a). Amino acid content in xylem sap of regrowing alfalfa (*Medicago sativa* L.). *Plant and Soil*, **149** (2): 167-174.

Kim, T. H., Ourry, A., Boucard, J., and Lemaire, G. (1993b). Partitioning of nitrogen derived from N_2 fixation and reserves in nodulated *Medicago sativa* L. *Journal of Experimental Botany*, **44** (260): 555-562.

Kobayashi, K., and Salam, M. (2000). Comparing simulated and measured values using mean squared deviation and its components. *Agronomy Journal*, **92** (2): 345-352.

Lambers, H., Atkin, O. K., and Millenaar, F. F. (1996). Respiratory patterns in roots in relation to their functioning. *In* "Plant Roots: the hidden half" (Y. Waisel, A. Eshel and U. Kafkafi, eds.). Marcel Dekker Inc., New York; USA.

Lawlor, D. W. (1995). Photosynthesis, productivity and environment. *Journal of Experimental Botany*, **46** (special issue): 1449-1461.

Lawlor, D. W. (2001). Photosynthesis. (D. W. Lawlor, ed.), 386 p. 3rd Ed, BIOS Scientific Publishers Limited, Oxford.

Lawlor, D. W., Lemaire, G., and Gastal, F. (2001). Nitrogen, plant growth and crop yield. *In* "Plant nitrogen" (P. Lea and P. J. Morot-Gaudry, eds.), pp. 407. New York: Springer, Berlin.

Lemaire, G., Cruz, P., Gosse, G., and Chartier, M. (1985). Study of the relationship between the dynamics of nitrogen uptake and dry matter accumulation of lucerne (*Medicago sativa* L.). *Agronomie*, **5** (8): 685-692.

Lemaire, G., Onillon, B., Gosse, G., Chartier, M., and Allirand, J. M. (1991). Nitrogen distribution within a lucerne canopy during regrowth: relation with light distribution. *Annals of Botany*, **68** (6): 483-488.

Lemaire, G., Khaiti, M., Onillon, B., Allirand, J. M., Chartier, M., and Gosse, G. (1992). Dynamics of accumulation and partitioning of N in leaves, stems and roots of lucerne (*Medicago sativa* L.) in a dense canopy. *Annals of Botany*, **70** (5): 429-435.

Lemaire, G., and Gastal, F. (1997). N uptake and distribution in plant canopies. *In* "Diagnosis of the nutritional status in crops" (G. Lemaire, ed.), pp. 3-34. Springer Berlin, Heidelberg, New York.

Lemaire, G., and Millard, P. (1999). An ecophysiological approach to modelling resource fluxes in competing plants. *Journal of Experimental Botany*, **50** (330): 15-28.

Li, R., Volenec, J. J., Joern, B. C., and Cunningham, S. M. (1996). Seasonal changes in nonstructural carbohydrates, protein, and macronutrients in roots of alfalfa, red clover, sweetclover, and birdsfoot trefoil. *Crop Science*, **36** (3): 617-623.

Lodge, G. M. (1991). Management practices and other factors contributing to the decline in persistence of grazed lucerne in temperate Australia: a review. *Australian Journal of Experimental Agriculture*, **31** (5): 713-724.

Louahlia, S., Avice, J. C., Dily, F. l., Kim, T. H., Corre, N., Simon, J. C., MacDuff, J. H., Ourry, A., Boucaud, J., le Dily, F., Maillard, P., and Bonhomme, R. (1998). Role of N and C reserves during spring regrowth or regrowth following cutting in forage species. *In* "Fonctionnement des peuplements vegetaux sous contraintes environnementales" (P. Maillard, ed.), Vol. 93, pp. 61-86, Paris, France.

Luo, Y., Meyerhoff, P. A., and Loomis, R. S. (1995). Seasonal patterns and vertical distributions of fine roots of alfalfa (*Medicago sativa* L.). *Field Crops Research*, **40** (2): 119-127.

Marcelis, L. F. M., Heuvelink, E., and Goudriaan, J. (1998). Modelling biomass production and yield of horticultural crops: a review. *Scientia Horticulturae*, **74** (1-2): 83-111.

Markwell, J., Osterman, J. C., and Mitchell, J. L. (1995). Calibration of the Minolta SPAD-502 leaf chlorophyll meter. *Photosynthesis Research*, **46** (3): 467-472.

Matthew, C., Lemaire, G., Sackville Hamilton, N. R., and Hernandez Garay, A. (1995). A modified self-thinning equation to describe size/density relationships for defoliated swards. *Annals of Botany*, **76** (6): 579-587.

McAdam, J. W., and Nelson, C. (2003). Physiology of forage plants. *In* "Forages: an introduction to grassland agriculture" (R. F. Barnes, C. J. Nelson, M. Collins and K. J. Moore, eds.), pp. 73-97. Iowa State Press, Ames.

McCree, K. J. (1974). Equations for the rate of dark respiration of white clover and grain sorghum, as function of dry weight, photosynthesis rate, and temperature. *Crop Science*, **14** (4): 509-514.

Meuriot, F., Decau, M. L., Bertrand, A. M., Homme, M. P., Gastal, F., Simon, J. C., Volenec, J. J., and Avice, J. C. (2005). Contribution of initial C and N reserves in *Medicago sativa* recovering from defoliation: impact of cutting height and residual leaf area. *Functional Plant Biology*, **32** (4): 321-334.

Michaud, R., Lehman, W. F., and Rumbaugh, M. D. (1988). World distribution and historical development. *In* "Alfalfa and Alfalfa Improvement" (A. A. Hanson, D. K. Barnes and R. R. Hill Jr, eds.), Vol. 29. American Society of Agronomy, Madison, U.S.A.

Molloy, L. (1988). Soil in the New Zealand Landscape: the living mantle. 253 p. 2nd Ed, Mallison Rendel in association with the New Zealand Society of Soil Science, Wellington, New Zealand.

Monsi, M., and Saeki, T. (2005). On the factor light in plant communities and its importance for matter production. *Annals of Botany*, **95** (1): 549-567.

Monteith, J. L. (1972). Solar radiation and productivity in tropical ecosystems. *Journal of Applied Ecology*, **9** (3): 747-766.

Monteith, J. L. (1977). Climate and the efficiency of crop production in Britain. *Philosophical Transactions of the Royal Society of London - B.*, **281**: 277-294.

Monteith, J. L. (1981). Climatic variation and the growth of crops. *Quarterly Journal of the Royal Meteorological Society*, **107**: 749-774.

Monteith, J. L., and Unsworth, M. H. (1990). Principles of environmental physics. 291 p. 2nd Ed, Chapman and Hall, London.

Monteith, J. L. (1994). Principles of resource capture by crop stands. *In* "Resource capture by crops" (J. L. Monteith, R. K. Scott and M. H. Unsworth, eds.), pp. 1-15. University of Nottingham Press, Loughborough, Leicestershire.

Monteith, J. L., Scott, R. K., and Unsworth, M. H. (1994). Resource capture by crops. (J. L. Monteith, R. K. Scott and M. H. Unsworth, eds.), 469 p., University of Nottingham Press, Loughborough, Leicestershire.

Monteith, J. L. (1996). The quest for balance in crop modeling. *Agronomy Journal*, **88** (5): 695-697.

Moot, D. J., Robertson, M. J., and Pollock, K. M. (2001). Validation of the APSIM-Lucerne model for phenological development in a cool-temperate climate. *In* "10th Australian Agronomy Conference," pp. 1-5, Hobart.

Moot, D. J., Brown, H. E., Teixeira, E. I., and Pollock, K. M. (2003). Crop growth and development affect seasonal priorities for lucerne management. *In* "Legumes for dryland pastures" (D. J. Moot, ed.), pp. 201-208. New Zealand Grassland Association, Lincoln, Canterbury, New Zealand.

Morot Gaudry, J. F., Monget, C., Fiala, V., Nicol, M. Z., Deroche, M. E., and Jolivet, E. (1987). Transport et mise en reserve des photo-assimilats dans les racines de lucerne au curs de la vegetation de printemps et d'automne. *In* "Nutrition azotee des legumminoeuses - Les colloques de l'INRA" (P. INRA, ed.), Vol. 37, pp. 165-173, Versailles.

Morton, J., and Roberts, A. (1999). Fertilizer use on New Zealand sheep and beef farms. 36 p. Revised Edition, New Zealand Fertiliser Manufacturer's Association, Auckland.

Moss, D. N. (1984). Photosynthesis, respiration and photorespiration in higher plants. *In* "Physiological basis of crop growth and development" (M. B. Tesar, ed.), pp. 131-152. American Society of Agronomy: Crop Science Society of America, Madison, Wisconsin.

Muchow, R. C., and Bellamy, J. A. (1991). Climatic risk in crop production: models and management for the semiarid tropics and subtropics. *In* "Proceedings of an international symposium" (R. C. Muchow and J. A. Bellamy, eds.). CAB International, Wallingford, U.K.

Muchow, R. C., and Sinclair, T. R. (1994). Nitrogen response of leaf photosynthesis and canopy radiation use efficiency in field-grown maize and sorghum. *Crop Science*, **34** (3): 721-727.

Murata, Y., and Honma, T. (1968). Studies on the photosynthesis of forage crops. IV. Influence of air temperature upon the photosynthesis and respiration of alfalfa and

several southern type forage crops. *The Crop Science Society of Japan*, **34**: 154-158.

Nelson, C. J., and Smith, D. (1968). Growth of birdsfoot and alfalfa. II. Morphological development and dry matter. *Crop Science*, **8** (1): 21-25.

Noquet, C., Avice, J., Ourry, A., Volenec, J., Cunningham, S., and Boucaud, J. (2001). Effects of environmental factors and endogenous signals on N uptake, N partitioning and taproot vegetative storage protein accumulation in *Medicago sativa*. *Australian Journal of Plant Physiology*, **28** (4): 279-287.

Noquet, C., Meuriot, F., Caillot, S., Avice, J. C., Ourry, A., Cunningham, S. M., and Volenec, J. J. (2003). Short-day photoperiod induces changes in N uptake, N partitioning and accumulation of vegetative storage proteins in two *Medicago sativa* cultivars. *Functional Plant Biology*, **30** (8): 853-863.

Noquet, C., Avice, J. C., Rossato, L., Beauclair, P., Henry, M. P., and Ourry, A. (2004). Effects of altered source-sink relationships on N allocation and vegetative storage protein accumulation in *Brassica napus* L. *Plant Science*, **166** (4): 1007-1018.

Okubo, T., Sukeo, K., and Hoshino, M. (1975). Chlorophyll amount for analysis of matter production in forage crops. II. Seasonal variations in maximum crop growth rate and leaf photosynthesis, and their correlations with chlorophyll content in alfalfa and ladino clover. *Journal of the Japanese Grassland Society*, **21** (2): 124-135.

Onstad, D. W., and Fick, G. W. (1983). Predicting crude protein, *in vitro* true digestibility, and leaf proportion in alfalfa herbage. *Crop Science*, **23** (5): 961-964.

Ourry, A., Kim, T., and Boucaud, J. (1994). Nitrogen reserve mobilization during regrowth of *Medicago sativa* L. Relationships between availability and regrowth yield. *Plant Physiology*, **105** (3): 831-837.

Passioura, J. B. (1996). Similation models: science, snake oil, education, or engineering? *Agronomy Journal*, **88** (5): 691-694.

Pearse, R. B., Carlson, G. E., Barnes, D. K., Hart, R. H., and Hanson, C. H. (1969a). Specific leaf weight and photosynthesis of alfalfa. *Crop Science*, **9**: 423-426.

Pearse, R. B., Fissel, G., and Carlson, G. E. (1969b). Carbon uptake and distribution before and after defoliation of alfalfa. *Crop Science*, **9**: 79-85.

Pearson, C. J., and Hunt, L. A. (1972). Effects of temperature on primary growth and regrowths of alfalfa. *Canadian Journal of Plant Science*, **52**: 1017-1027.

Peri, P. L., Moot, D. J., McNeill, D. L., Varella, A. C., and Lucas, R. J. (2003). A canopy photosynthesis model to predict the dry matter production of cocksfoot pasture under varying temperature, nitrogen and water regimes. *Grass and Forage Science*, **58** (4): 416-430.

Philippot, S., Allirand, J. M., Chartier, M., and Gosse, G. (1991). The role of different daily irradiations on shoot growth and root/shoot ratio in lucerne (*Medicago sativa* L.). *Annals of Botany*, **68** (4): 329-335.

Pollock, C. (1990). The response of plants to temperature change. *Journal of Agricultural Science*, **115** (1): 1-5.

Purves, R. G., and Wynn-Williams, R. B. (1989). Lucerne - a fresh look. *Agronomy Society of New Zealand*, **19**: 95-102.

Purves, R. G., and Wynn-Williams, R. B. (1994). Development of more productive and persistent lucerne by selection under frequent cutting. *Proceedings of the New Zealand Grassland Association*, **56**: 113-116.

Ranganathan, R., Chauhan, Y. S., Flower, D. J., Robertson, M. J., Sanetra, C., and Silim, S. N. (2001). Predicting growth and development of pigeonpea: leaf area development. *Field Crops Research*, **69** (2): 163-172.

Rapoport, H., and Travis, R. (1984). Alfalfa root growth, cambial activity, and carbohydrate dynamics during the regrowth cycle. *Crop Science*, **24** (5): 899-903.

Reich, P. B., Ellsworth, D. S., and Walters, M. B. (1998). Leaf structure (specific leaf area) modulates photosynthesis-nitrogen relations: evidence from within and across species and functional groups. *Functional Ecology*, **12** (6): 948-958.

Richards, J. H. (1993). Physiology of plants recovering from defoliation. *In* "Grasslands for our world: 17th International Grassland Congress" (M. J. Baker, ed.), pp. 85-94. SIR Publishing, Palmerston North, New Zealand.

Ritchie, J. T., Muchow, R. C., and Bellamy, J. A. (1991). Specifications of the ideal model for predicting crop yields. *In* "International symposium on climatic risk in crop production: models and management for the semiarid tropics and subtropics." (M. R.C. and J. A. Bellamy, eds.), pp. 97-122. CAB International, Wallingford, U.K.

Robertson, M. J., Carberry, P. S., Huth, N. I., Turpin, J. E., Probert, M. E., Poultron, P. L., Bell, M. J., Wright, G. C., Yeates, S. J., and Brinsmead, R. B. (2002). Simulation of growth and development of diverse legumes species in APSIM. *Australian Journal of Agricultural Research*, **53** (4): 429-446.

Sanderson, M. A., Karnezos, T. P., and Matches, A. G. (1994). Morphological development of alfalfa as a function of growing degree days. *Journal of Production Agriculture*, **7** (2): 239-242.

Sands, P. J. (1995). Modelling canopy production. II. From single-leaf photosynthesis parameters to daily canopy photosynthesis. *Australian Journal of Plant Physiology*, **22** (4): 603-614.

Sands, P. J. (1996). Modelling canopy production. III. Canopy light-utilisation efficiency and its sensitivity to physiological and environmental variables. *Australian Journal of Plant Physiology*, **23** (1): 103-114.

Schaufele, R., and Schnyder, H. (2001). Carbon and nitrogen deposition in expanding tissue elements of perenial ryegrass (*Lolium perenne*) leaves during non-steady growth after defoliation. *Plant, Cell and Environment*, **24** (4): 407-417.

Sharratt, B. S., Sheaffer, C. C., and Baker, D. G. (1989). Base temperature for the application of the growing-degree-day model to field-grown alfalfa. *Field Crops Research*, **21** (2): 95-102.

Simon, J. C., and Lemaire, G. (1987). Tillering and leaf area index in grasses in the vegetative phase. *Grass and Forage Science*, **42** (4): 373-380.

Simon, J. C., Decau, M. L., Avice, J. C., Jacquet, A., Meuriot, F., and Allirand, J. M. (2004). Effects of initial N reserve status and residual leaf area after cutting on leaf area and organ establishment during regrowth of alfalfa. *Canadian Journal of Plant Science*, **84** (4): 1059-1066.

Sinclair, T. R., and Horie, T. (1989). Leaf nitrogen, photosynthesis, and crop radiation use efficiency: a review. *Crop Science*, **29** (1): 90-98.

Sinclair, T. R., and Seligman, N. G. (1996). Crop modeling: from infancy to maturity. *Agronomy Journal*, **88** (5): 698-704.

Sinclair, T. R., and Muchow, R. C. (1999). Radiation use efficiency. *Advances in Agronomy*, **65**: 215-265.

Singh, Y. (1974). Environmental factors affecting the utilization of ^{14}C-labelled organic reserves after defoliation of alfalfa. *Dissertation Abstracts International - B*, **35** (5): 2010.

Skinner, R., Morgan, J., and Hanson, J. (1999). Carbon and nitrogen reserve remobilization following defoliation: nitrogen and elevated CO_2 effects. *Crop Science*, **39**: 1749-1756.

Stoskopf, N. C. (1981). Understanding crop production. 433 p., Reston Publishing Co. Inc, Reston, Virginia.

Szeicz, G. (1974). Solar radiation for plant growth. *Journal of Applied Ecology*, **11** (2): 617-636.

Ta, T., Macdowall, F., and Faris, M. (1990). Utilization of carbon and nitrogen reserves of alfalfa roots in supporting N_2 fixation and shoot regrowth. *Plant and Soil*, **127** (2): 231-236.

Tait, A., and Hik, D. S. (2003). Is dimethylsulfoxide a reliable solvent for extracting chlorophyll under field conditions? *Photosynthesis Research*, **78** (1): 87-91.

Taiz, L., and Zeiger, E. (2002). Plant physiology. 792 p. 3rd Ed, Sinauer Associates, Sunderland, U.S.A.

Tardieu, F., Granier, C., and Muller, B. (1999). Modelling leaf expansion in a fluctuating environment: are changes in specific leaf area a consequence of changes in expansion rate? *New Phytologist*, **143** (1): 33-43.

Thornley, J. H. M., and Johnson, I. R. (2000). Dynamic modelling. *In* "Plant and crop modelling: a mathematical approach to plant and crop physiology", 669 p., The Blackburn Press, Caldwell, New Jersey.

Thornton, B., and Millard, P. (1997). Increased defoliation frequency depletes remobilization of nitrogen for leaf growth in grasses. *Annals of Botany*, **80** (1): 89-95.

Tjoelker, M. G., Oleksyn, J., and Reich, P. B. (2001). Modelling respiration of vegetation: evidence for a general temperature-dependent Q_{10}. *Global Change Biology*, **7** (2): 223-230.

Travis, R. L., and Reed, R. (1983). The solar tracking pattern in a closed alfalfa canopy. *Crop Science*, **23** (4): 664-668.

Trimble, M., Barnes, D., Heichel, G., and Sheaffer, C. (1987). Forage yield and nitrogen partitioning responses of alfalfa in two cutting regimes and three soil nitrogen regimes. *Crop Science*, **25** (5): 909-914.

Vale, F. X. R., Fernandes, E. I. F., and Liberato, J. R. (2003). QUANT - A software for plant disease severity assessment. *In* "8th International Congress of Plant Pathology", pp. 105, Christchurch, New Zealand.

Vance, C. P., and Heichel, G. H. (1981). Nitrate assimilation during vegetative regrowth of alfalfa. *Plant Physiology*, **68** (5): 1052-1056.

Varella, A. C. (2002). Lucerne crop responses to continous and intermittent light under artificial and agroforestry regimes. Ph.D. Thesis, 268 p. Lincoln University, Lincoln.

Volenec, J. J. (1985). Leaf area expansion and shoot elongation of diverse alfalfa germplasms. *Crop Science*, **25** (5): 822-827.

Volenec, J. J., Cherney, J. H., and Johnson, K. D. (1987). Yield components, plant morphology, and forage quality of alfalfa as influenced by plant population. *Crop Science*, **27** (2): 321-326.

Volenec, J. J., Ourry, A., and Joern, B. C. (1996). A role for nitrogen reserves in forage regrowth and stress tolerance. *Physiologia Plantarum*, **97** (1): 185-193.

Volenec, J. J., Cunningham, S. M., Haagenson, D. M., Berg, W. K., Joern, B. C., and Wiersm, D. W. (2002). Physiological genetics of alfalfa improvement: past failures, future prospects. *Field Crops Research*, **75** (2-3): 97-110.

Watson, V. (1947). Comparative physilological studies on the growth of field crops. I. Variation in net assimilation rate and leaf area. *Annals of Botany*, **11**: 41-76.

Watt, J. P. V., and Burghan, S. J. (1992). "Physical properties of eight soils of Lincoln area, Canterbury. Derived data and hydraulic character statements." Department of Scientific and Industrial Research, Lower Hutt, New Zealand.

Whitfield, D. M., Wright, G. C., Gyles, O. A., and Taylor, A. J. (1986). Growth of lucerne (*Medicago sativa* L.) in resposnse to frequency of irrigation and gypsum application on a heavy clay soil. *Irrigation Science*, **7** (1): 37-52.

Wilson, D. R., Muchow, R. C., and Murgatroyd, C. J. (1995). Model analysis of temperature and solar radiation limitations to maize potential productivity in a cool climate. *Field Crops Research*, **43** (1): 1-18.

Woolley, D. J., Karno, Nichols, M. A., and Uragami, A. (2001). Effects of daylength on dry matter partitioning in asparagus. *In* "Proceedings of the 10th International Asparagus Symposium", Vol. 589, pp. 243 247. Acta Horticulturae, Niigata, Japan.

Yan, W., and Wallace, D. H. (1998). Simulation and prediction of plant phenology for five crops based on photoperiod x temperature interaction. *Annals of Botany*, **81** (6): 705-716.

Ziska, L. H., and Bunce, J. A. (1994). Direct and indirect inhibition of single leaf respiration by elevated CO_2 concentrations: Interaction with temperature. *Physiologia Plantarum*, **90** (1): 130-138.

Appendices

Appendix 1 Relationship between crown and taproot concentration of (*a*) soluble sugars, (*b*) starch and (*c*) nitrogen of lucerne crops subjected to four contrasting defoliation regimes in the 2002/03 and 2003/04 growth seasons at Lincoln University, Canterbury, New Zealand.

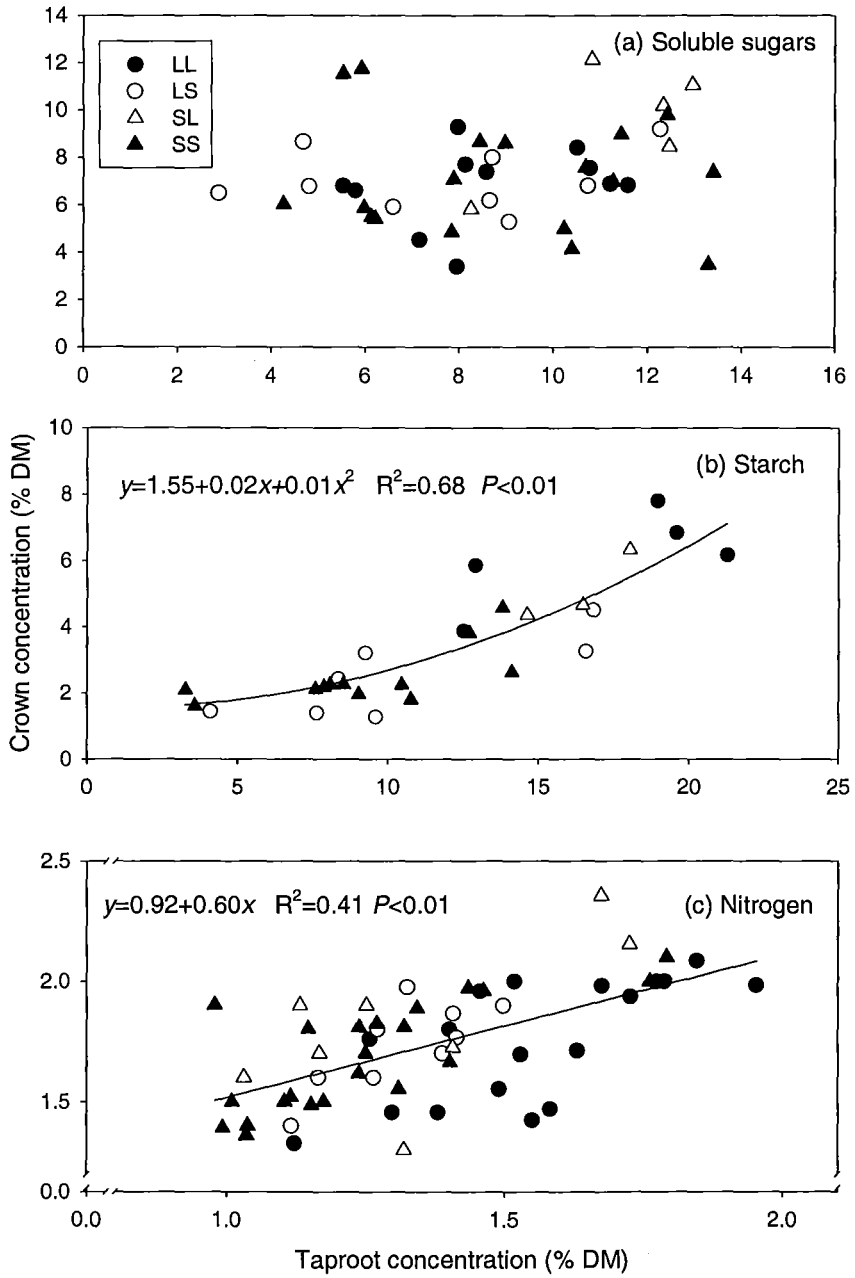

Appendix 2 Parameters of sigmoid curves that represent the seasonal accumulated PAR_i (Figure 6.2) of lucerne crops subjected to four contrasting defoliation regimes in the 2002/03 and 2003/04 growth seasons at Lincoln University, Canterbury, New Zealand.

	a	*b*	*x0*
2002/03 growth season			
LL	1665 (29.9)	44.4 (2.3)	122 (2.9)
LS	1471 (23.4)	40.2 (2.2)	110 (2.6)
SL	1163 (14.4)	42.1 (1.5)	125 (2.0)
SS	1078 (14.7)	39.2(1.6)	118 (117.7)
2003/04 growth season			
LL	1431 (20.0)	44.4 (1.9)	480 (2.3)
LS	1196 (7.2)	37.1 (0.8)	473 (1.0)
SL	985 (10.9)	40.3 (1.2)	497 (1.6)
SS	775 (4.3)	33.3 (0.6)	485 (0.8)

Note: Sigmoid equations are $a/(1+\exp(-(x-x0)/b))$. Values in brachets are one SEM for the respective coefficient. All $R^2>0.99$.

Appendix 3 Canopy specific leaf weight (g DM/m^2 leaf) for lucerne crops subjected to long (42-day cycle, ●) and short (28-day cycle, Δ) defoliation regimes in the 2003/04 growth season at Lincoln University, Canterbury, New Zealand.

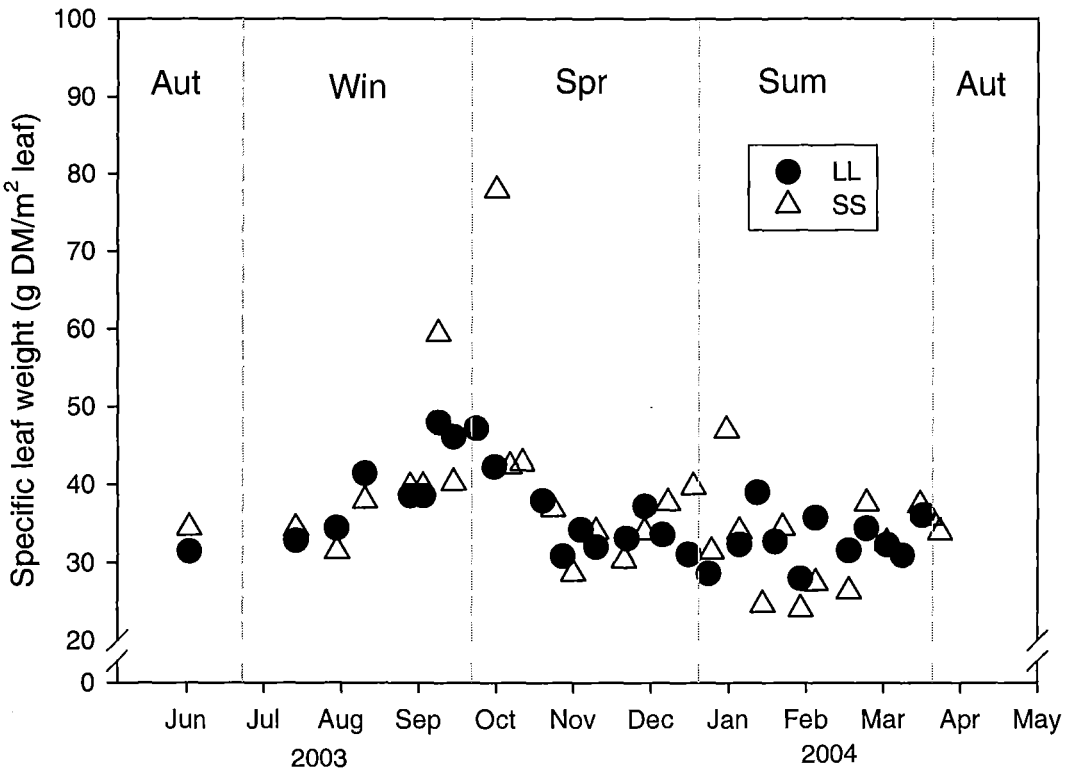

Appendix 4 Estimated fractional partitioning of dry matter to roots for lucerne crops subjected to 28-day regrowth cycles (SS crops) in the 2002/03 and 2003/04 growth seasons at Lincoln University, Canterbury, New Zealand.

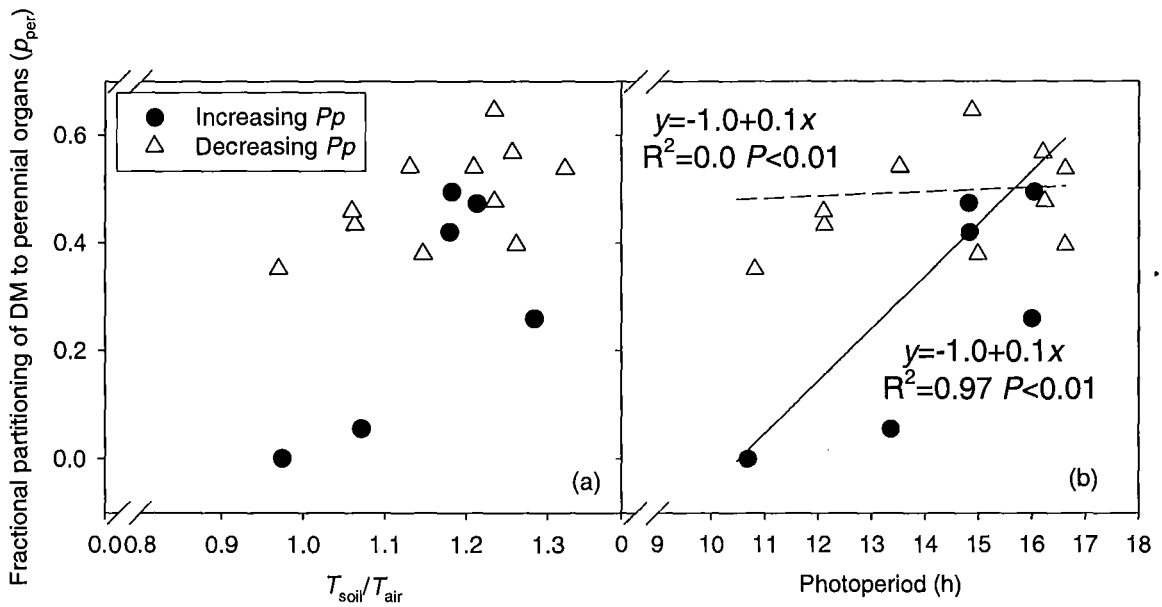

Note: The calculation of p_{per} was done assuming RUE_{total} adjusted for temperature (Figure 2.5.1.4) and without accounting for the potential decline in RUE_{total} in SS crops (Section 7.3.3).

Appendix 5 Leaf photosynthesis at 1000 μmol photon/m^2/s (Pn_{1000}) of lucerne crops subjected to 28-day (SS crop) and 42-day (LL crop) regrowth cycles in the 2002/03 and 2003/04 growth seasons at Lincoln University, Canterbury, New Zealand.

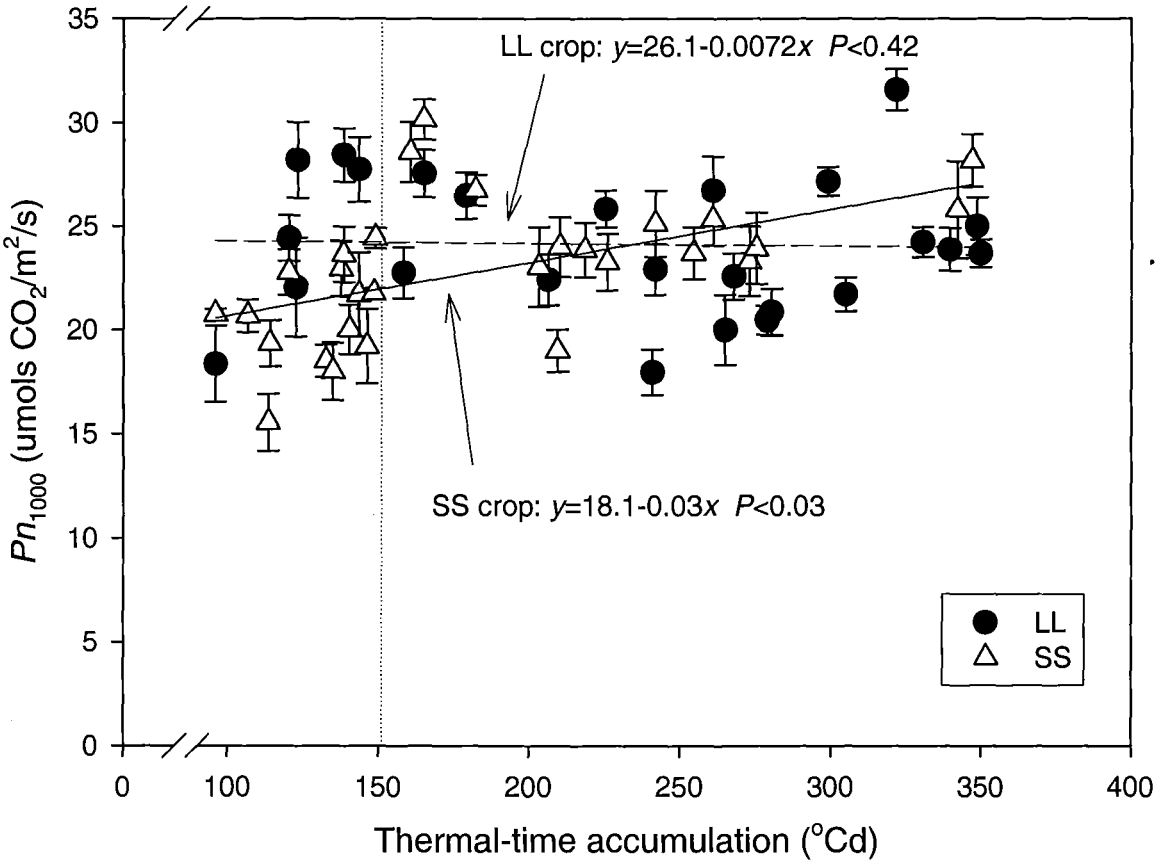

Note: Vertical dotted line indicates a $\sum Tt_{b5}$ 150°Cd which defined the two periods for analysis of variance to compare LL and SS crops (Section 7.3.4.2).

There was no systematic influence (P<0.42) of the period of regrowth (*e.g.* $\sum Tt_{b5}$) on the leaf photosynthetic rates (Pn_{1000}) of LL crops. In contrast, there was a significative increase (P<0.03) in the Pn_{1000} of SS crops at 0.03 μmol/m^2/s/°Cd. At $\sum Tt_{b5}$ greater than 150°Cd Pn_{1000} of SS crops approached the values observed for LL crops and this criterion was used to segment the period in two for a comparison using ANOVA (Section 7.3.4.2).

Appendix 6 Relationship between shoot yield and shoot nitrogen concentration used to calculate the critical concentration of nitrogen (N_{crit}) in Section 7.3.6.

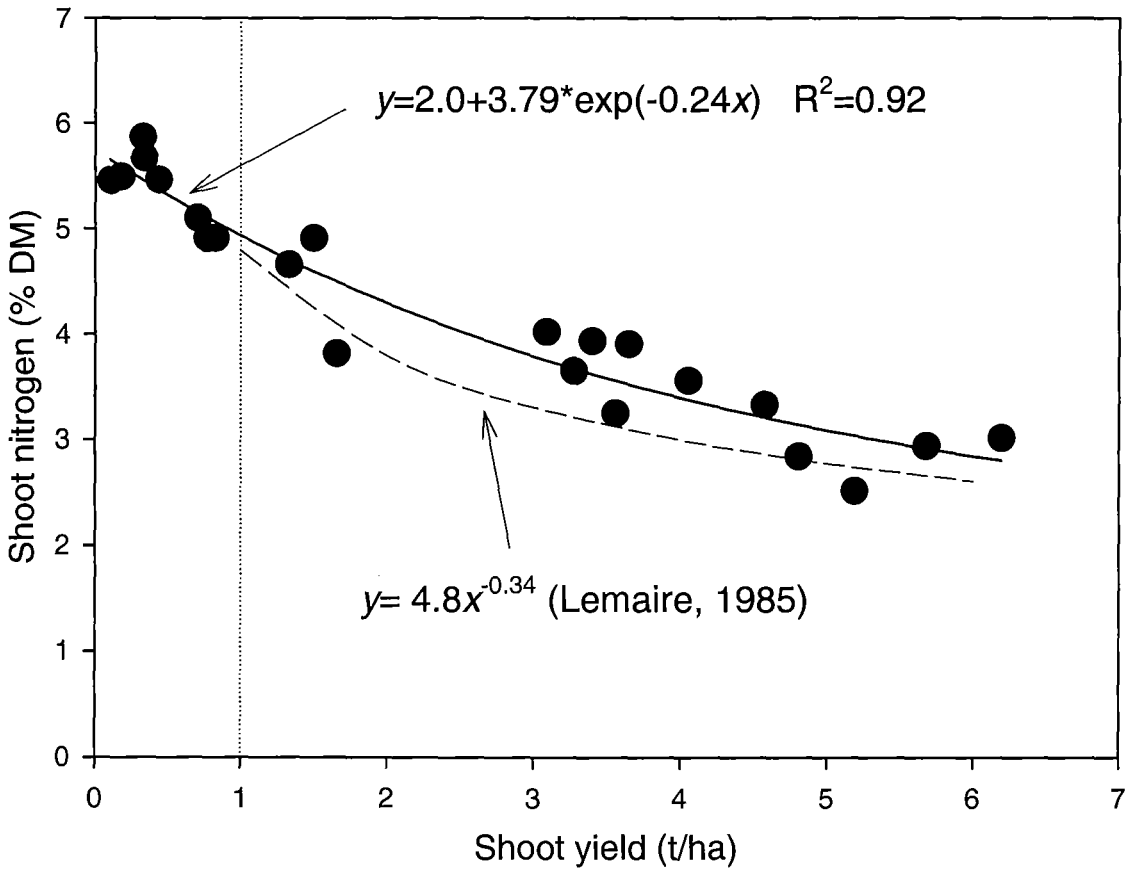

Note: Dashed line represents model proposed by Lemaire (1985) for shoot DM<1t/ha. Solid line is the exponential model found for LL crops. Dashed line indicates yield of 1t/ha where the model for LL was used to calculate critical N.

Appendix 7 Seasonal differences in nitrogen concentration of leaves and stems at harvest for lucerne crops subjected to four regrowth cycles in the 2002/03 and 2003/04 growth seasons at Lincoln University, Canterbury, New Zealand.

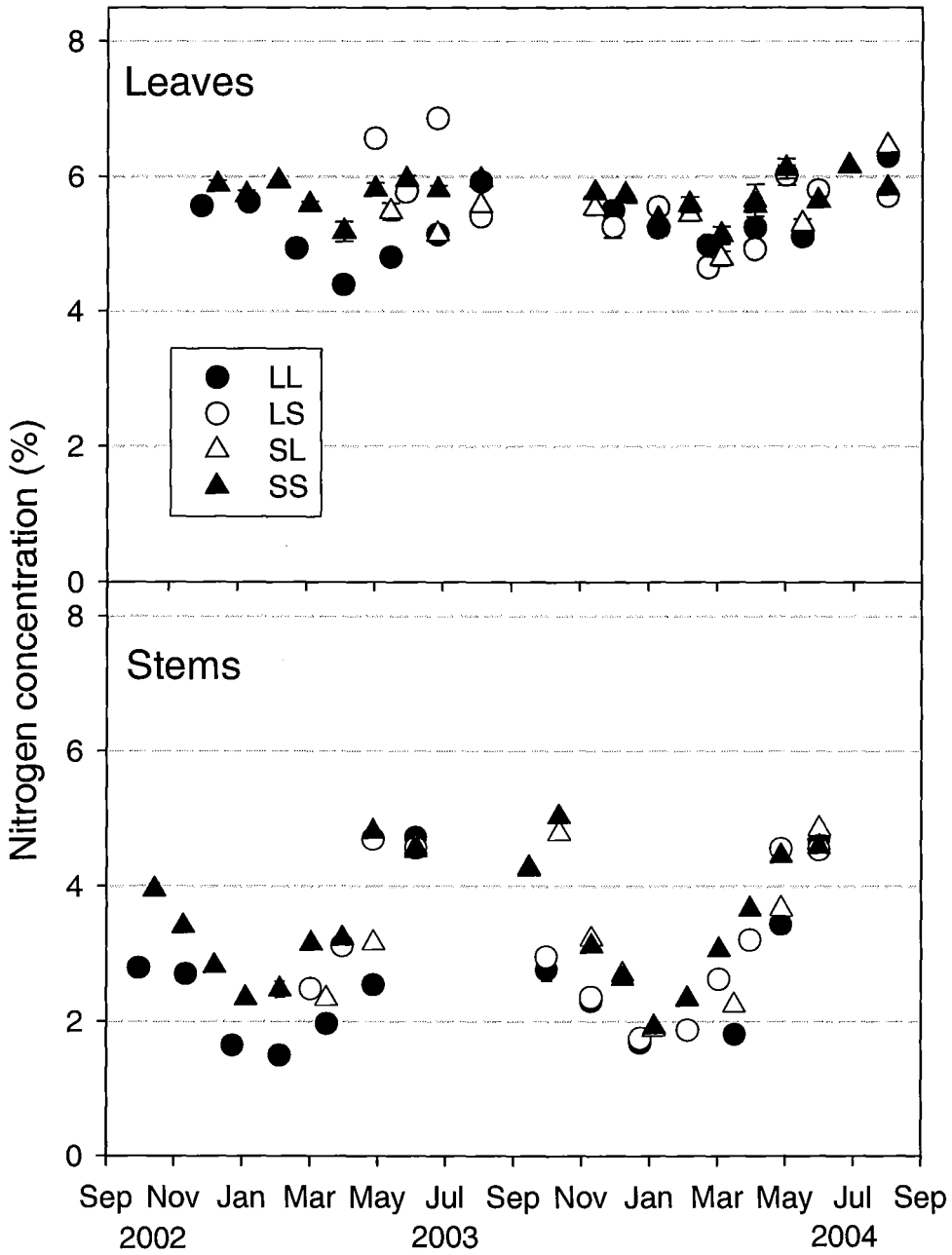

Appendix 8 Relationship between days after grazing and the number of primary leaves in LL crops.

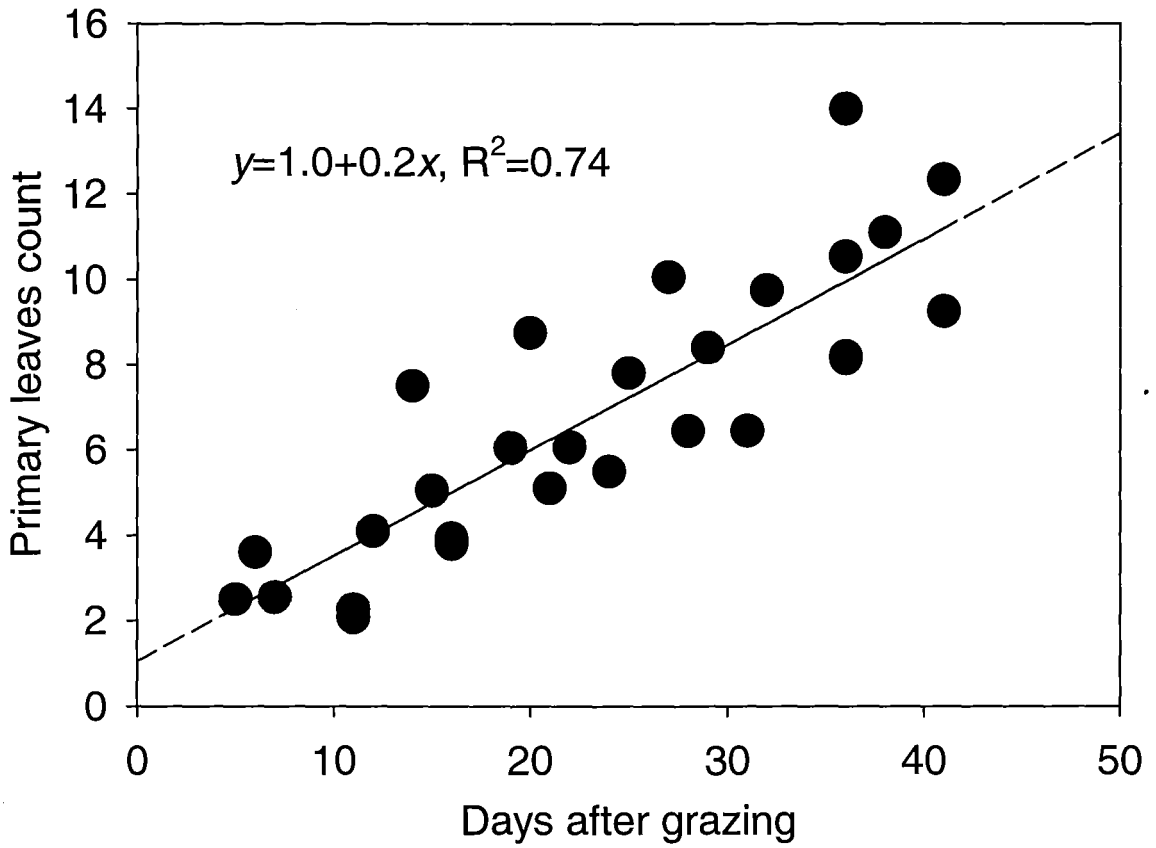

The relationship between the count of primary leaves and the days after grazing indicated that LL crop had one primary leaf left at the start each regrowth cycle. This was incorporated in the lucerne model (8.2.6).

List of publications

Part of the results related to this study were published in:

Moot, D. J., Brown, H. E., Teixeira, E. I., and Pollock, K. M. (2003). Crop growth and development affect seasonal priorities for lucerne management. In "Legumes for dryland pastures" (D. J. Moot, ed.), pp. 201-208. New Zealand Grassland Association, Lincoln, Canterbury, New Zealand.

Moot, D. J., and Teixeira, E. I. (2005). Autumn root reserves of lucerne affected shoot yields during the following spring. In "20th International Grassland Congress" (J. J. Murphy, ed.). Wageningen Academic, Cork Satelite Workshop, Ireland.

Teixeira, E. I., Moot, D. J., and Brown, H. E. (2004). Spring regrowth of lucerne is affected by the level of winter perennial reserves. In "4th International Crop Science Congress" (T. Fischer, N. Turner, J. Angus, L. McIntyre, M. Robertson, A. Borrell and D. Lloyd, eds.). The Regional Institute Ltd, Brisbane, Australia.

Teixeira, E. I., Moot, D. J., Brown, H. E., and Mickelbart, M. (2005). Seasonal variation of taproot biomass and N content of lucerne crops under contrasting grazing frequencies. In "20th International Grassland Congress" (F. P. O'Mara, R. J. Wilkins, L. Mannetje, D. K. Lovett, P. A. M. Rogers and T. M. Boland, eds.). Wageningen Academic, Dublin, Ireland.

Teixeira, E. I., Moot, D. J., and Fletcher, A. L. (2005). Lucerne crown and taproot biomass affected early-spring canopy expansion. In "20th International Grassland Congress" (J. J. Murphy, ed.). Wageningen Academic, Cork Satellite Workshop, Ireland.

Acknowledgements

To my father, my mother and grandmother Isabel. You gave me the basic support, the education and the conditions to live this experience. I humbly dedicate this thesis to you.

I sincerely thank my dear wife Carmen. God knows how greateful I am for your support and love in different aspects of my life. The experience of being by your side in this life is a blessing. You gave me the balance and the strength to accomplish this thesis.

To the Bowers. You are our kiwi family. Thank you for giving us the best possible environment to live and for taking care of us. God bless you all.

To the Varellas. Thank you for making our arrival in New Zealand possible and for guiding our first steps in this beautiful country. You are a wonderful family.

To Dr. Andrew Fletcher. I am thankful for the knowledge you shared with me and the unconditional support that only a true friend can give. I deeply value our friendship.

To Dr. Hamish Brown. I have learned so much from you my friend. I sincerely admire you for your competence, knowledge and your great character. I trust our friendship will last forever.

To Dr. Keith Pollock. Your assistance was beyond my highest expectations. It was a privilege to work and to learn so much from you. Thanks for being my friend.

To Dr. Michael Mickelbart. Thanks so much for your patience and professionalism in teaching me about all the plant physiology part of this project and for the correction of numerous drafts.

To Anna Mills. Thank you so much for helping me and having patience with your office mate, mainly during the last days of the thesis writing. Now it is your turn. I hope to be able to reciprocate the help you gave to me.

To Dr. Nancy Irlbeck. For your friendship, support and inspiration. Thanks for giving us the confidence and encouragement to continue our studies.

To my good friends from the FSC at Lincoln: Alex, Pablo, Al Black, Anthony, Emma, Serkan, Dave, Ben and Jenn. I learned and gained so much from you all. Each one of you helped me at some stage of this Ph.D. It was a privilege to study by your side.

To Dave, Don, Malcolm, Merv and Christina. Many thanks for the professional and precise technical assistance in the field experiment. You made things happen even during the most challenging times.

To the excellent team of professional that assisted me with the laboratory work: Stu, Stephen, Mace, Jeff, Peter, Lucy and Ioshi.

To the FSC team that helped me in different stages of the project: Dick Lucas, Bruce Mckenzie, Mark Bloomberg, Roy Edwards, Alan Marshall, Jenny Lawrence, George Hill, Warwick Scott and Grant Edwards.

To the researchers that contributed with constructive discussions and inspiration for the improvement of this study: Dr. Jean Louis Durand, John Hargreaves, Dr. Peter Jamieson and Dr. Michael Robertson.

To my Brazilian teachers: Professors Wilson R. S. Mattos, Sila C. da Silva, Moacyr Corsi, Vidal P. de Faria who first inspired me to start my Ph.D. studies and created the conditions for this dream to come true.

To the NZODA scholarship programme for providing financial support for the study. Thanks to the New Zealand embassy staff in Brazil especially to Mrs. Heloisia Fontes.

Finally, I am immensely thankful to my supervisor Dr. Derrick J. Moot. Your great respect and care for your students is inspiring. I have great admiration for your knowledge and especially for your ability to impact so positively in the professional and personal development of your students. I sincerely thank you for everything that you taught me and for helping me beyond your duties, in order to encourage me to complete the Ph.D. and have the most awesome experience in New Zealand.